A HYBRID SYSTEM OF MICROBIAL ELECTROLYSIS CELL AND ANAEROBIC DIGESTION FOR BIOMETHANE PRODUCTION

BY

NIBEDITA DEB

A dissertation submitted in fulfillment of the requirement for the degree of Doctor of Philosophy of (Engineering).

Kulliyyah of Engineering
International Islamic University Malaysia

September 2023

ABSTRACT

Food waste (FW) poses a significant global challenge due to the increasing population. Anaerobic digestion (AD) was a commonly used process to convert organic waste into biogas, primarily methane (CH_4). However, CH_4 production in AD was often low. To upgrade CH_4 production, a hybrid microbial electrolysis cell (H-MEC) system combining AD was used. In this study, two types of fungal strains (TNAF-1 to TNFA-3 and TNBC-1 to TNBC-3) were isolated from animal feed and compost. The enzyme activities such as cellulase, and amylase of 300U/mL and 400U/mL, respectively were produced by the selected strains. Optimization using the face centered central composite design (FCCCD) under the response surface methodology (RSM) was conducted to increase the reducing sugar production to 162 mg/mL under the optimized conditions of pH 5, Total solids (TS) of 12.5%, and enzyme loading of 80 U/mL. The biogas production was optimized using one factor at a time (OFAT) method with the parameters of inoculum of 25%, pH 7, digestion times of 29 days, 500mL of hydrolysate food waste, and temperature at 30°C (±2), resulting in a biogas composition of 3% H_2, 57% CH_4, and 40% CO_2. To address energy efficiency and sustainability, the H-MEC system was designed based on electromethanogenic microbes (EMMs) for enhanced biogas upgrading. EMM strains (TNFW-1 to TNFW-3 and NTAS-1 to NTAS-3) were isolated from AD using food waste and anaerobic sludge samples, respectively. The EMMs demonstrated the efficient CO_2 conversion in a dual-chamber method. The strain, TNFW-2 produced supernatants with a 92% BioM (biomethane) production rate from the direct gas phase (CO_2/H_2). Optimal growth conditions were determined, yielding a 92% BioM yield with substrate dose of 100mL, inoculum dose of 10mL, flow rate of 5L/hour, H_2/CO_2 ratio of 50:50%, pH 7, applied potential of 900mV, and 36 hours of incubation. The SEM (spell out) images revealed irregular EMM structures with netted texture, and their activity was associated with a recorded potential value of 900mV. The strain, TNFW-2 was identified as the same species and the chemical composition of the extracellular EMMs was *Methanobacterium formicicum* of 98% sequence similarity. EMMs exhibited stability within a pH range of 4.5-8, with maximum CH_4 production at a temperature of 28±2ºC and pH 7 for at least 36 hours. The optimized H-MEC system demonstrated 92% CO_2 conversion at an organic CO_2 flow rate of 5 L/h and 36 hours of incubation time. The optimal H-MEC conditions for EMM-based biogas upgrading included two chambers with stainless steel (SS) with graphite (SS+GF) electrodes, an applied voltage of 900mV, pH 7, and an EMM dose of 10mL. Under these conditions, 92% CO_2 removal in terms of CH_4 production was achieved. Kinetic analysis revealed growth-associated BioM production, with an estimated specific growth rate (μ) of $0.207h^{-1}$ and maximum specific rate of product formation of approximately $0.239h^{-1}$. These findings highlight the potential of the new EMMs for non-toxic and biodegradable biogas upgrading, which may show a potential solution for future applications in the wastewater treatment plants.

ملخص البحث

يشكل هدر الغذاء تحدياً عالمياً كبيراً نظراً لزيادة عدد السكان. تعتبر عملية الهضم اللاهوائي هي العملية المستخدمة بشكل شائع لتحويل النفايات العضوية إلى غاز البيوغاز، وبشكل رئيسي البيتان (CH_4). ومع ذلك، كان إنتاج غاز البيتان في الهضم اللاهوائي غالبًا ما يكون منخفضًا. لتحسين إنتاج غاز البيتان، تم استخدام نظام الخلية الكهروكيميائية المختلطة (H-MEC) الذي يجمع بين الهضم اللاهوائي وميكروبات إلى TNBC-1و TNFA-3 إلى TNAF-1) في هذه الدراسة، تم عزل نوعين من الفطريات. كهروالهضمية لترقية إنتاج غاز البيوغاز من أعلاف الحيوانات والسماد. تم إنتاج الإنزيمات مثل السيلولاز والأميليز بنسبة 300 وحدة / مل و 400 وحدة / مل على (TNBC-3 ضمن منهجية سطح الاستجابة (FCCCD) تم إجراء عملية الأمثلة باستخدام التصميم المركز المركب للوجه.التوالي من السلالات المحددة (TS) لزيادة إنتاج السكر المختزل إلى 162 مجم / مل تحت الظروف المحسنة والتي تشمل درجة الحموضة 5 والمواد الصلبة الكلية (RSM) (OFAT) تم تحسين إنتاج غاز البيوغاز باستخدام طريقة عامل واحد في كل مرة. بنسبة ٪12.5 وتحميل الإنزيم بنسبة 80 وحدة / مل باستخدام المعايير التالية: نسبة العزل بنسبة ٪25، درجة الحموضة 7، أوقات الهضم لمدة 29 يومًا، 500 مل من نفايات الطعام المحلولة، ودرجة ، و٪40 ثاني أكسيد (CH_4) بيتان ، ٪ 57 (H_2) الحرارة عند 30 درجة مئوية (±2)، مما أدى إلى تركيبة غاز البيوغاز بنسبة ٪3 هيدروجين لتحسين (EMMs) بناءً على ميكروبات كهروالهضمية H-MEC لتحسين كفاءة الطاقة والاستدامة، تم تصميم نظام.(CO_2) الكربون من الهضم اللاهوائي (NTAS-3 إلى NTAS-1و TNFW-3 إلى TNFW-1) EMMs ترقية غاز البيوغاز. تم عزل سلالات بكفاءة باستخدام (CO_2) تحويل ثاني أكسيد الكربون EMMs أظهرت. باستخدام عينات نفايات الطعام والطمي اللاهوائي على التوالي محاليل فوق السائل بمعدل ٪92 من إنتاج البيوم (البيوغاز) من الطور الغازي المباشر TNFW-2 طريقة الغرفتين المزدوجتين. أنتجت السلالة تم تحديد ظروف النمو المثلى والتي أدت إلى حصول معدل ٪92 من البيوم بوزن 100 مل من المادة الأساسية، و 10 مل من (CO_2/H_2) ، ودرجة الحموضة 7، والجهد المطبق 900 مللي فولت، و36 ساعة من ٪50:50 H_2/CO_2 العزل، ومعدل تدفق 5 لتر / ساعة، ونسبة غير منتظمة مع نسيج مشبك، وتم ربط نشاطها بقيمة جهد مسجلة بقيمة 900 مللي EMMs عن هياكل SEM كشفت صور. التحضير *Methanobacterium* الخارجية هو EMMs كنفس النوع، وكان التركيب الكيميائي لل TNFW-2 فولت. تم تحديد السلالة استقراراً في نطاق الحموضة من 4.5 إلى 8، مع أقصى وكانت أقصى EMMs أظهرت. بتشابه متسلسل بنسبة ٪ 98 *formicicum* المحسن H-MEC أظهرت نظام. إنتاجية لغاز البيتان عند درجة حرارة 28±2 درجة مئوية ودرجة الحموضة 7 لمدة 36 ساعة على الأقل بمعدل 5 لتر/ساعة وزمن التحضير 36 (CO_2) عند معدل تدفق عضوي لثاني أكسيد الكربون (CO_2) تحويل٪92 من ثاني أكسيد الكربون ، (SS+GF) والجرافيت (SS) تشمل غرفتين بقطبين من الصلب غير القابل للصدأ EMMs ساعة. الظروف المثلى لترقية غاز البيوغاز بناءً على بمعدل 10 مل. تحت هذه الظروف، تم تحقيق إزالة ٪92 من ثاني EMM وجهد مطبق بمعدل 900 مللي فولت، ودرجة الحموضة 7، وجرعة بمعدل (μ) أظهر التحليل السينوبسيني نمواً مرتبطاً بإنتاج البيوم، مع معدل نمو محدد تقديري . بالنسبة لإنتاج غاز البيتان (CO_2) أكسيد الكربون الجديدة EMMs تسلط هذه النتائج الضوء على إمكانات . 0.207 ساعة^-1 وأقصى معدل محدد لتكوين المنتج بمعدل 0.239 ساعة .في تحسين ترقية غاز البيوغاز بشكل غير سام وقابل للتحلل، مما قد يمثل حلاً محتملاً لتطبيقات المستقبل في محطات معالجة مياه الصرف الصحي

APPROVAL PAGE

The dissertation of Nibedita Deb has been approved by the following:

Md. Zahangir Alam
Supervisor

Mohammed Saedi Jami
Co-supervisor

Mariatul Fadzillah Bt. Mansor
Co-supervisor

Husna Binti Ahmad Tajuddin
Co-supervisor

Nassereldeen Ahmed Kabbashi
Internal Examiner

Luqman Chuah Abdullah
External Examiner

Akram M Z M Khedher
Chairman

DECLARATION

I hereby declare that this dissertation is the result of my own investigations, except where otherwise stated. I also declare that it has not been previously or concurrently submitted as a whole for any other degrees at IIUM or other institutions.

Nibedita Deb

Signature……  Date…19-02-2023……

INTERNATIONAL ISLAMIC UNIVERSITY MALAYSIA

DECLARATION OF COPYRIGHT AND AFFIRMATION OF FAIR USE OF UNPUBLISHED RESEARCH

A HYBRID SYSTEM OF MICROBIAL ELECTROLYSIS CELL AND ANAEROBIC DIGESTION FOR BIOMETHANE PRODUCTION

I declare that the copyright holder of this thesis/dissertation are jointly owned by the student and IIUM.

No part of this unpublished research may be reproduced, stored in a retrieval system, or transmitted, in any form or by any means, electronic, mechanical, photocopying, recording or otherwise without prior written permission of the copyright holder except as provided below

1. Any material contained in or derived from this unpublished research may only be used by others in their writing with due acknowledgement.

2. IIUM or its library will have the right to make and transmit copies (print or electronic) for institutional and academic purpose.

3. The IIUM library will have the right to make, store in a retrieval system and supply copies of this unpublished research if requested by other universities and research libraries.

By signing this form, I acknowledged that I have read and understand the IIUM Intellectual Property Right and Commercialization policy.

Affirmed by Nibedita deb

…… ……19-02-2023……..

Signature Date

ACKNOWLEDGEMENTS

In the name of Allah, the most Gracious, the most Merciful. All praises are indeed due to the Almighty Allah SWT, Lord of the world, Sustained, Protector, and Provider, who enabled me to complete this thesis successfully. May the blessing and peace of Allah be upon the Prophet Muhammad SAW (PBUH) and his entire household.

I would like to express my profound gratitude and appreciation to Professor Dr. Md. Zahangir Alam, the main supervisor of the supervisor committee for providing invaluable advice, untiring assistance, encouragement, guidance and motivation that enabled me to accomplish the Ph.D program smoothly and timely. I am deeply indebted to Professor Dr. Mohammed Saedi Jami, Assistant Professor Dr. Mariatul Fadzillah Bt. Mansor, and Assistant Professor Dr. Husna Binti Ahmad Tajuddin, members of the supervisory committee and Assistant Professor Dr. M Sultana Alam for their constructive suggestions, proper guidance and encouragement throughout my study period. May Allah reward them abundantly, Jazakallah Khair.

I wish to sincerely thank the staff members of all laboratories (Bioenvironmental, Biochemical, Molecular & genetic, Analytical), Haji Sukiman, brother Nasa, Hafizul, Azlan, Iznan for their gently assistance in the research of the study. I am grateful to Associate Prof. Dr. Mohamed Elwathig Saeed Mirghani, INHART, IIUM, for helping me to data analysis during my research. I am also grateful to Prof. Dr. Misni Misran and brother Fateh, Department of Chemistry, University of Malaya, for helping me to use their equipment toward the completion of my study.

In addition, I wish to express my love and offer my deep sense of gratitude to my parents, family members and to my husband (Dr. Tawfikur Rahman) for his love, patience, encouragement and moral support throughout my studies and thesis completion. Express my heartfelt gratitude to my brothers, sisters, brother-in-law, a sister-in-law who always encouraged and inspired me during the study period. I would also like to special thanks to my respected sister Mala Khan, Bangladesh Reference Institute for Chemical Measurements, BRiCM for their cooperation and encouragement during my staying and study period in Bangladesh.

I would like to express my gratitude to the Ministry of Education (MOE) Malaysia for granting a Fundamental Research Grant Scheme FRGS 2019-1 for the financial support. Thanks also due to IIUM through RMC for financial management and monitoring the progress of the project.

My heartfelt appreciation goes to all my colleagues and friends in IIUM especially Sr. Amal for her time, continuous guidance and supports, Sr. Jebunessa and Bro. Qabas for their kind assistance, support and accompany during my laboratory time. I will always be grateful.

TABLE OF CONTENTS

LIST OF TABLES

LIST OF FIGURES

LIST OF ABBREVIATIONS

2D	Two Dimensional
3D	Three Dimensional
ANOVA	Analysis of Variance
A	Ampere
AD	Anaerobic Digestion
BOD	Biochemical Oxygen Demand
BEC	Bioelectrochemical Cell
BFC	Bioelectrochemical Fuel Cell
BioM	Biomethane
C.V.	Coefficient of Variation
C/N	Carbon Nitrogen Ratio
CCD	Central Composite Design
CMC	Carboxymethyl Cellulose
COD	Chemical Oxygen Demand
CPO	Crude Palm Oil
DNS	Dinitrosalicylic Acid
DOE	Design of Experiments
DNA	Deoxyribonucleic Acid
et al.	(Et Alia): and Others
EMM	Electromethanogenesis Microbes
ECP	extracellular polymers
EPS	Extracellular polymeric substances
FCCCD	Face Centered Central Composite Design
FPA	Filter Paper Assay
FW	Food waste
g	Gram

g/L	Gram Per Liter
GC/MS	Gas Chromatography–Mass Spectrometry
H-MECAD	Hybrid Microbial Electrolysis Cell Anaerobic Digestion
HRT	Hydraulic Retention Time
kJ	Kilojoule
kWh	Kilowatt Hour
kW	Kilowatt
LSF	Liquid State Fermentation
MEC	Microbial Electrolysis Cell
MES	Microbial Electrolysis Synthesis
MDC	Microbial Desalination Cell
mScm^{-1}	Microsiemens/Centimeter
mV	Millivolts
min	Minutes
mm	Milimolar
mm/s	Milimolar Per Second
mg/mL	Milligram Per Mililiter
OFAT	One Factor-At-A-Time
PBD	Plackett—Burman Design
PDA	Potato Dextrose Agar
PPM	Parts Per Million
PCR	Polymerase Chain Reaction
pNPP	Para-Nitrophenyl Palmitate
rpm	Revolution Per Minute
RSM	Response Surface Methodology
SEM	Scanning Electron Microscopy
TDS	Total Dissolved Solids
TSS	Total Solids
TEM	Transmission electron microscopy
VFA	Volatile Fatty Acids

VS	Volatile Solids
V	Voltage
U/G_{ds}	Unit Per Gram Dry Substrate
U/ml	Unit Per Milliliter
UV	Ultraviole
v/v	Volume Per Volume
w/v	Weight Per Volume
w/v	Weight Per Volume
w/w	Weight Per Weight
YM	Yeast Malt Extract Medium
YPD	Yeast Extract Peptone Dextrose

LIST OF SYMBOLS

-	Minus Sign
%	Percentage
+	Plus Sign
<	Less than Sign
>	Greater than Sign
±	Plus or Minus Sign
µ	Mu
°C	Degree Celsius
ß	Beta
α	Alpha
γ	Gamma

CHAPTER ONE

INTRODUCTION

1.1 BACKGROUND OF THE STUDY

Wasted food was a significant challenge within the global food system. It pertains to edible nourishment that was created for human use but remains unconsumed and was discarded at various points in the food supply chain, including farming, processing facilities, and both household and commercial kitchens (Riccaboni et al., 2021). Different terms like food wastage, biowaste, and kitchen refuse were frequently used interchangeably to depict this problem (Sharma et al., 2022). As per the Food and Agriculture Organization, roughly one-third of all food generated for human consumption goes to waste, totaling about 1.3 billion tonnes every year (Boliko, 2019). This wastage happens across the entire supply chain, starting from production and continuing through to household consumption.

Food wastage posed a substantial worldwide concern, especially widespread in more advanced nations. In the United States, the combined food waste from retail and consumers stands at a concerning 188 kg per person annually, equating to an estimated worth of $165.6 billion. Likewise, in Europe and North America, the annual per-person food wastage can climb to levels as high as 280-300 kg (Garrone, Melacini, & Perego, 2014). Southeast Asia also experiences substantial food waste, estimated at 33% of total food produced in the region. Malaysia, specifically, faces the challenge of household food waste, with an average of 0.5-0.8 kg of uneaten food discarded per day per household (Abd Ghafar, 2017). Anticipated to deteriorate in the upcoming years, this issue is set to intensify

due to economic progress, population expansion, and urban development. Malaysia's population was estimated to achieve 33.4 million by 2020 and is projected to grow even more, reaching 37.4 million by 2030.

The social influence of FW was substantial as well. With millions of people suffering from hunger and malnutrition, reducing food waste could help alleviate food insecurity and improve access to nutritious food (Paritosh et al., 2017). Food waste also exacerbates inequalities and inequities in food distribution and access. Efforts to tackle the global food waste issue include implementing sustainable food production practices, improving storage and transportation infrastructure, promoting efficient food processing and packaging, educating consumers about food waste reduction, and developing innovative solutions for food recovery and redistribution (Zhang et al., 2014). Addressing food waste was crucial not only to ensure food security and sustainability but also to make more efficient use of the planet's limited resources and reduce the environmental impact of food production (Kiran et al., 2015). Food waste contains valuable components such as sugars (55-67%), starch (40-55%), and cellulose (2-3%), which can be converted into biogas, ethanol, and lactic acid (Wang et al., 2005; Zhang et al., 2014; Yang et al., 2021). Enzymatic hydrolysis methods have been explored as viable solutions for recovering fermentable sugars from food waste and unsorted MSW (Chandrasekhar et al., 2018).

AD-based MEC technology was a more complex method where the conversion of different kinds of the organic substrate takes place by resources of microbes in the presence of oxygen. Under anaerobic circumstances, the breakdown of an organic molecule may be divided into four primary steps: hydrolysis, acidogenesis, acetogenesis, and methanogenesis. Advance AD system was produced more than 40 to 60% CO_2 and other

gas (Molino et al., 2013; Zhang et al., 2014; Stoknes et al., 2016; Arelli et al., 2020; Qu et al., 2021; Bywater et al., 2022). The first stage, hydrolysis, was already identified as the essential to creating a good digestive process. Various treatment approaches designed to enhance hydrolysis were conducted such as mesophilic and thermophilic treatment in the temperature about 25 to 220°C, physical deterioration including high-pressure, ultrasonic, homogenization, and other refining processes, chemical treatments like acid, ozone and alkali and biological treatments, which demonstrated that approaches shown in optimizing the hydrolytic step consequence in improved biogas conversion due to breakdown and release of organic material, making each other more stable (Salihu & Alam, 2016). The second step of the acidogenesis processes was carried out by a consortium of commonly dependent on microbes with hydrolytic-fermentative microorganisms, proton-reducing acetogenic microorganisms, hydrogenotrophic methanogens and acetoclastic methanogens (Zabranska & Pokorna, 2018). However, AD-based MEC technology was strongly connected to the microbial structure groups present in the bioreactor additionally to the operating conditions employed (Barbosa et al., 2019). Consequently, the introduction of biogas as a co-substrate into an AD may cause modifications in microbial groups, and these modifications may, in turn, result in changes in the main degradation ways. Finally, the methanogenesis steps were severely anaerobic archaea communities into acetoclastic and hydrogenotrophic methanogenesis. The most commonly hydrogenotrophic methanogenesis substrates were hydrogen (H_2), carbon dioxide (CO_2) and format (HCO_2^-), while the acetate was the major organic matter for acetoclastic methanogens making methane via acidogenesis and acetogenesis though insufficient other different elements such as CH_2OH (methanol), C_2H_5OH (ethanol) and $C_3H_4O_3$ (pyruvate) can also be used

(Martínez et al., 2019). Due to the limited breakdown of the methanogenesis process, the organic elements present in food waste were degraded in an anaerobic condition by acetogenic bacteria and relationship with fermenting. This syntrophic connection was continued by the interspecies hydrogen transfer process. Particularly, H_2 was used up by hydrogenotrophic methanogens which was a significant transitional in the AD of organic waste. Interspecies H_2 and H_2 levels transfer optimizes the breakdown of the perfect bacteriological groups present in biomethane creating consortia (Rozenfeld et al., 2019).

Hybrid microbial electrochemical systems (H-MES) were an effective technique to generate energy in a stable and ecologically friendly approach (Leung et al., 2022). Simply said, H-MES generates by chemical energy converting electrical energy derived from cellulosic materials via the catalytic reaction utilizing a biological electrocatalyst. H-MES technology was a multidisciplinary discipline that combines electrochemical processes, nanotechnology, microorganisms, and analytical chemistry (Bajracharya et al., 2016). In H-MES, the liquid was oxidized at the anode chambers, producing the electrons or protons that were then transferred to the cathode chamber under the influence of (external) voltage differential. Redox processes occur at the cathode chamber area in the existence of electrochemically active microorganisms. Based on the reactor structure, ambient conditions, and intended outputs, MESs will be further categorized as MECs (Park et al., 2022), MDCs (Cao et al., 209), MFCs (Strik et al., 2011), and microbial solar cells (Ali et al., 2018). These MECs are powered by electro-microbiology concepts, which were employed to investigate the diverse potential of electrochemically active microorganisms. MFCs can generate energy from aerobic wastewater, but MECs needed an electrical source to produce hydrogen from natural wastewater. MECs were a

significant MES for producing cost-effective and ecologically friendly energy, but they cannot match with other forms of energy including ethanol, methane, hydrogen, and other significant organic chemicals. MECs were a proficient method for creating fuel and electricity from organic substances such as agricultural waste (Escapa et al., 2016; Liu et al., 2010).

Biomethane (BioM) was a sustainable fuel that was formerly created by the decomposition of organic matter of bio-waste. Furthermore, the procedure requires many days to accomplish. The appearance of anaerobic microorganisms in the MES bacterial community facilitated the collection of CH_4 from the cathode chamber of MECs via CO_2 electromethanogenesis (Gunaseelan et al., 1997). BioM was commonly discovered in MECs during the hydrogen generation stage related to methanogen development. Chae et al., discovered that BioM production fluctuates with changes in reactor design, substrate, inoculum, and catalyst loading. Methanogens occur during the hydrogen generation step, reducing the H_2 output. Several ways were explored to reduce the formation of methanogens bacteria in MECs, but still, the majority of these have shown to be energy intensive and ineffectual (Lu et al., 2011). As an alternative to suppressing methanogens, generating methane immediately via MECs has several benefits over anaerobic digestion. Methane generation and food waste material degradation were two distinct mechanisms in MECs that lead to a high methane concentration in biofuels (Jadhav et al., 2019).

This research aimed to advance environmental sustainability by leveraging microbial electrolysis cells (MEC) within bioelectrochemical cells (BEC), an emerging green technology renowned for its efficiency in reducing CO_2 emissions and increasing biomethane (BioM) production without the need for additional mechanisms (Vu et al.,

2019). To optimize BioM production from food waste, a hybrid system called H-MECAD was proposed, which involved capturing CO_2 within a single reactor. Microorganisms derived from renewable sources like anaerobic sludge, food waste, tannery sludge, and sewage sludge were employed in this process, ensuring cost-effective production of electrolytic bacteria compared to commercial alternatives (Alam et al., 2009a). By utilizing electrolytic microbes, the breakdown of complex organic compounds was enhanced, leading to accelerated conversion into biomethane.

1.2 PROBLEM STATEMENT

The global reliance on fossil fuels has led to the depletion of non-renewable resources and increased carbon dioxide (CO_2) emissions, resulting in environmental hazards such as global warming and water acidification (Dianat et al., 2022). With these concerns in mind, there was a need to explore carbon-free renewable technologies that can provide sustainable electricity generation while minimizing environmental impact (Pham et al., 2022). Additionally, the management of organic waste, particularly food waste, has become a pressing issue due to population growth and its associated environmental and economic challenges (Long et al., 2022). Current treatment methods, such as anaerobic digestion (AD), require additional upgrading systems to remove CO_2 from biogas for increased biomethane production (Oconnor et al., 2022). However, this incurs extra costs and limits the economic and environmental sustainability of the process.

To address these challenges, researchers have turned to bioelectrochemical cells (BEC) employing microbial electrolysis cells (MEC) as a potential solution for synthesizing biomethane (BioM) from CO_2. However, there was a lack of understanding

regarding the effective utilization of complex substrates, the optimization of microbial interactions within the electrolytes, and the stability of the process. Moreover, the current research on MEC with AD primarily focuses on pure substances, while the potential of microorganisms and their roles in electromethanogenesis, enzymatic reactions, and biofilm formation remain unexplored. In light of these existing challenges, there was a need to develop an efficient and effective process to address the high yield of biomethane, CO_2 capture, and utilization, as well as the stability of the process (Arvin etal., 2019; Guo et al., 2017; Moreno et al., 2016). A hybrid system of MEC and AD (H-MECAD) in a single or duble reactor has the potential to overcome these challenges, leading to increased biomethane production and improved management of food waste (Deena et al., 2022; Hong et al., 2022; Park et al., 2018). Further research was necessary to explore the fundamental aspects of this approach and optimize the process for sustainable and high-rate biomethane production. Base on literature review, there were many challenges in the AD and MEC systems; the main challenges were focused as:

1. Environmentally, it contributes to greenhouse gas discharges and as decomposing FW in landfills generate CH_4 gas.
2. The most attractive approach was anaerobic digestion (AD) for food waste treatment. which considered being a source of biogas that can be used in heat and electricity generation.
3. The biogas contains approximately 60% CH_4 and 40% CO_2 which was required to biogas upgrading by removing the CO_2 for increased biomethane production in the conversion of heat to the high efficiency of thermal and electric energy.
4. MECs face challenges in terms of slow reaction rates.

1.3 RESEARCH PHILOSOPHY

Cost-effective processes were desired in the industry. Reducing energy consumption by conducting the process at mild conditions was one of the most important approaches. Therefore, this study proposed a two-stage MEC and AD system capturing the CO_2/CH_4 for high yield of biomethane production at a high rate to meet the demand for biofuels as well as using environmentally friendly treatment. The study involves the production of several electrochemically active microorganisms with different properties and selecting the best either mono or mixed bacteria for biomass dissolution. The potential electrochemically active microorganisms would be effective in the high content of BioM production using the hybrid system of H-MECAD system. The H-MECAD system/method will enhance the high content of BioM production by more than 90%. Food waste can be a suitable feedstock for high yield of BioM production as it has high organic content towards the suitability of anaerobic digestion. The main goal was to achieve maximum BioM production with low-cost processes with an environmentally friendly approach.

1.4 RESEARCH OBJECTIVES

The main objective of this research was to design a H-MECAD for high content of BioM production from FW. Hence, the goals of the suggested research endeavor, derived from the primary aim, were as follows::

1. To identify and characterize the potential hydrolytic strain through isolation and screening from several bio composts and animal feed for hydrolysis of FW.
2. To optimize the process parameters of AD of FW with pre-treatment (hydrolysis) strategy by potential isolated strain for the enhanced BioM production.
3. To identify, evaluate, characterize the potential electromethanogenesis microbes (EMMs) through isolation and screening from anaerobic sludge of the FW and anaerobic sewage sludge and optimize the CO_2 to CH_4 conversion process of the selective potential strain that has capability by H-MECAD.
4. To design and optimize the operational factors of the H-MECAD system for enhancing BioM and evaluate the process kinetics for growth and production.

1.5 RESEARCH METHODOLOGY

This study was comprised of laboratory-based experimental work in a single chamber AD and two chamber H-MEC system, and the procedures adopted were designed to enhance biomethane production from food waste by using potential hydrolytic enzyme and electromethanogenesis bacteria system. In the first step, the potential hydrolytic enzyme and electromethanogenesis bacteria strains were isolated and purified from several composts and AD of the FW sample by spread plate method. The screening of pure strains was cultured in the shake flask to test their entrapment potentiality to increase the biogas

and convert CO_2 to CH_4 of food waste. Furthermore, hydrolytic enzyme and electromethanogenic microorganisms (EMMs) were used to test their biogas yield to upgrade biogas by AD based H-MECs. After the selection of potential hydrolytic enzyme and electromethanogenic microorganisms (EMMs), screening of suitable nutrient, optimization of hydrolytic enzyme and electromethanogenic microorganisms culture conditions, single and compatible mixed culture were carried out to produce maximum biomethane production based on H-MECAD. Subsequently, the potential EEMs strain was characterized by identification, scanning electron microscopy (SEM), chemical and elemental analysis to comprehend the nature of the electromethanogenesis and its electron transfer mechanisms in converting BioM. The methanogenesis process was optimized by electromethanogenesis microbes to reduce CO_2 and convert CH_4. Then electron transfer process was investigated by using the electromethanogenesis microbes in a lab scale two chamber MECs to calculate particles settling gas flow rate. Finally, electromethanogenesis microbes' dosage and flow rate were optimized for rapid bio methane production of food waste by a lab scale MEC system. The summary of the main steps of the research methodology was illustrated in Figure 1.1

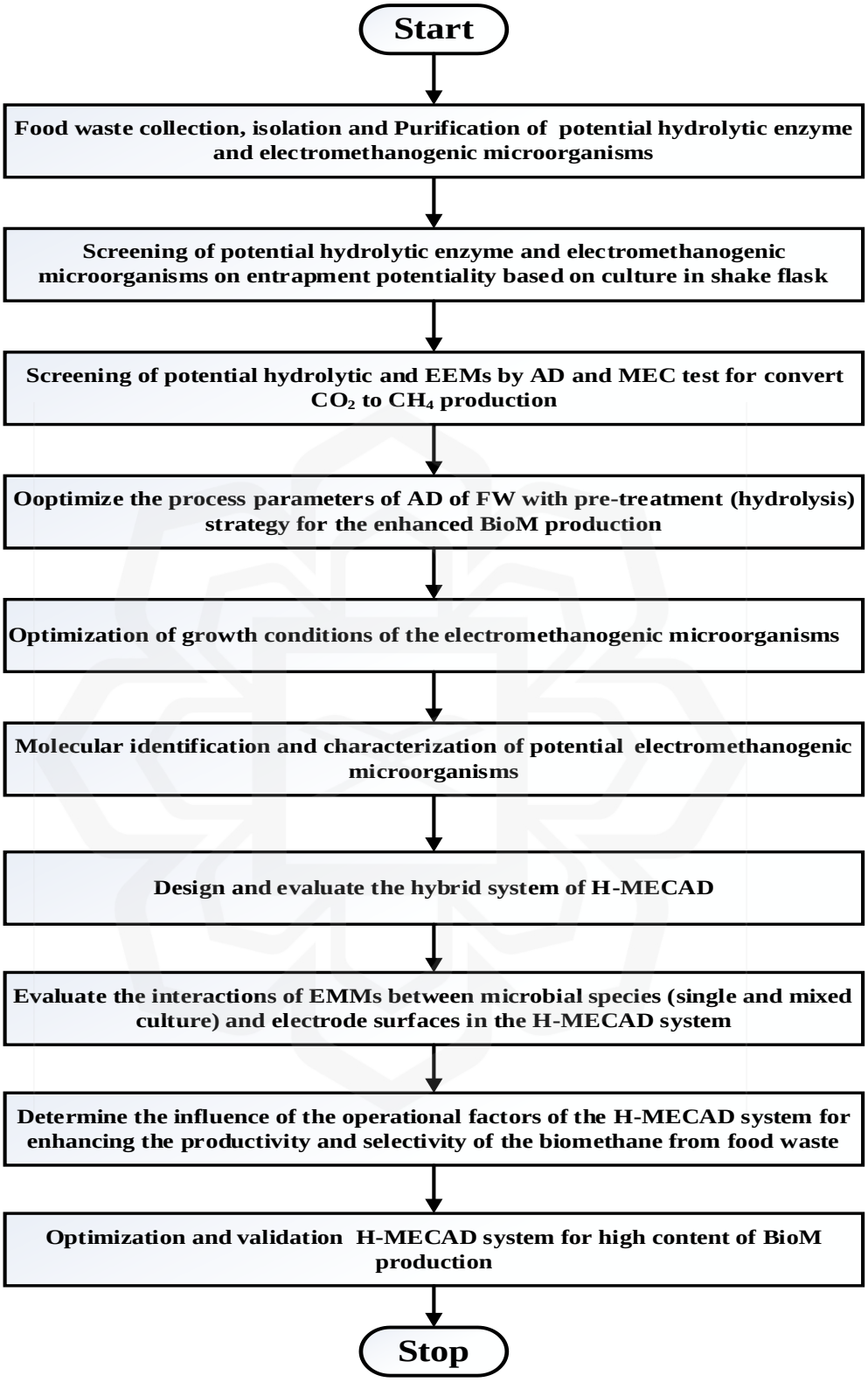

Figure 1.1: Flowchart depicting the operation process of the research study

1.6 RESEARCH SCOPE

The scope of this study was the isolation, identification and characterization of potential hydrolytic and electromethanogenic bacteria to reduce CO_2 from AD based FW which could be a new replacement for chemical conversion. The specific scopes were as follows:

- Several characterizations of FW like total suspended (TS), volatile solids (VS), total dissolved solids (TDS), moisture content, COD, total sugar, reducing sugar, hemicellulose, cellulose, lignin and pH were performed as a preliminary study to improve the hydrolysis process for biogas production.
- Isolation of filamentous fungi and screening of potential hydrolytic strain to breakdown lignocellulosic biomass from FW for AD system.
- Evaluation and characterization of the potential hydrolytic strain produced *Trichoderma ressi* and *Aspergillus niger* by SEM, TEM, chemical and elemental analysis in order to find out their mechanisms in terms of breakdown lignocellulosic biomass.
- The quantitative analyses to achieve optimum biogas production were carried out using OFAT and statistical analysis through response surface methodology (RSM).
- Optimize the AD system which were digestion time, pH, and AD inoculum dose of the VS reduction to enhance biogas production.
- Isolation of EMMs and screening of potential electromethanogenesis bacteria to reduce CO_2 from biogas composition for H-MEC system.
- Optimize the growth conditions which were substrate concentration, pH, and inoculum dose of the electromethanogenesis bacteria to enhance production.

- Evaluation and characterization of the electromethanogenesis bacteria produced *Methanobacterium formicicum* by SEM, chemical and elemental analysis in order to find out their convesion mechanisms in terms of CO_2 reduction.
- To find the optimum conversion conditions which were substrate concentration, inoculum dose, pH, incubation time, gas flow rate and high & low gas flow rate and long & short time to achieve maximum CO_2 reduction by the electromethanogenesis bacteria.
- To study the f H-MECAD process in a dual chamber with membrane and optimize the conversion process parameters which were electron transfer mechanism, current density, CV substrate loading, pH and applied voltage to observe the effect of conversion capability in a dual chambers model on H-MECAD process.
- Subsequently, a process validation was carried out to verify the consistency of the medium components and process conditions between the planned and executed experiments.. Lastly, kinetic study was done to determine the BioM production in a specific conversion time.

1.7 THESIS ORGANIZATION

The dissertation was divided into five chapters; where Chapter One covers the background of the study, statement of problems associated with the study, research philosophy, research objectives and research scope. Chapter Two reviews the literature regarding AD based H-MECs, different chemical and electron transfer mechanism, electroactive bacteria, H-MECs working principal, hydrogen growth response, selection of cathode and anode material, electromethanogenesis chemical reaction and their applications on CH_4 Yield.

The methodology of the investigation was described in Chapter Three in which the detailed description of materials, design, simulation analytical and experimental procedures adopted in the research have been clearly described. The results of the investigation were presented and discussed in Chapter Four. Specifically, the isolation and screening of potential electroactive bacteria to CO_2 reduction, optimization of growth conditions, characterization of electroactive bacteria and optimization of AD-based H-MECs based CO_2 to CH_4 process were clearly presented. This chapter further discussed the H-MECAD system for BioM conversion process in a settling single or two chamber and optimization of parameters by lab scale production. Finally, Chapter Five presents the conclusions of the findings and recommendations for further improvement of the studies.

CHAPTER TWO

LITERATURE REVIEW

2.1 INTRODUCTION

Several studies and researches in connection to the current development have been followed up in this chapter. Physical and chemical characteristics, current functions as a microbial Electrolysis Synthesis (MES) with the aid of many other technologies such as nanoparticles and hydrogen evolution reaction and use of FW, existing techniques and hydrolysis methods were reviewed. Electrochemically active microorganisms to convert organic matter into the high rate of BioM by using CO_2 in the hybrid system of MEC and AD in a single reactor or two chamber bioreactors. Prospects for the utilization of raw FW to produce bioM based on its physical and chemical behaviour were discussed as well. A generalized mechanism for electromethanogenesis was described, as well as its electron transport technique. In addition, the characteristics of MECs, such as design, setup, reactor components, microbial species, and process parameters, were thoroughly reviewed. Other than the above-mentioned fundamental topics on FW characterization, cellulase enzyme production, Electromethanogenesis microbes' yield, the conversion process and different kinetic studies have been reviewed.

2.2 FOOD WASTE

Food waste was defined as any edible food material that is discarded, lost, or left uneaten at any stage of the food supply chain. This can include food that was wasted during production, processing, distribution, retail, or consumer levels. Food waste can occur due

to various reasons, such as spoilage, expiration, overproduction, improper storage, and consumer behavior (Yusoff et al., 2022). It encompasses both cooked and uncooked food items, including fruits, vegetables, grains, dairy products, meats, and prepared meals (Taiwo et al., 2011). However, FW treatment was essential due to the significant environmental, economic, and social impacts associated with unmanaged food waste, necessitating comprehensive and efficient strategies to mitigate its adverse effects, reduce greenhouse gas emissions, recover valuable resources, and address the challenges of food security and sustainability. Table 2.1 represents the physical and chemical characteristics of FW used in different studies.

Table 2.1: Characteristics of raw FW

Parameters	Standard	Metal/Chemical	Standard
pH	4.6 -11.80	Phosphorous (g/kg)	2.3
Moisture Content (%)	61.3-85.7	Cadmium (mg/kg)	<0.5
Dry matter (kg/kg)	0.2-0.8	Potassium (g/kg)	3.5
Starch (%)	24-46.1	Iron (mg/kg)	2850
COD (g/L)	44.2-162.2	Manganese (mg/kg)	83
TS (g/L)	14.3-38.7	Copper (gm/kg)	23
VS (g/L)	85-125.5	Zinc (gm/kg)	54
Total sugar (mg/mL)	35.5-69	Chromium (mg/kg)	30
Lipids (%w/w)	6.4-24.1	Nickel (mg/kg)	35
Cellulose (%w/w)	1.6-16.9	Nitrogen (g/kg)	17.9
Protein (%w/w)	3.9-21.8	Phosphorus pentoxide (g/kg)	5.7
Ash (%w/w)	1.2-5.9	Potassium oxide (g/kg)	14.6
Carbon Nitrogen Ratio (C/N)	20-25	Mercury (mg/kg)	<1.0

Source: Paritosh et al., (2017); Zhang et al., (2017); Zhang et al., (2014)

According to the analysis, the global food waste amounted to 931 million tonnes (equivalent to approximately 121 kg per person). This waste was categorized across three

sectors: households accounted for 61%, food service contributed 26, and retail made up 13% of the total food waste (Vida et al., 2022). However, one common way to estimate food waste was by determining the percentage or weight of food that is discarded or uneaten compared to the total food available (Pour and Makkawi, 2021). This was calculated using the following formula:

$$\text{Food Waste Percentage} = \left(\frac{\text{Amount of Discarded Food}}{\text{Total Amount of Food}}\right) \times 100 \quad (2.1)$$

According to Zhang and Cunsheng, (2014), household food waste utilization focuses on a small percentage of the cell walls, which were comparable to lignin, neutral detergent fiber, and cellulose. Table 2.2 provides an overview of various studies on methane production using hydrolytic enzymes.

Table 2.2: Overview of waste treatments using hydrolytic enzymes for BioM production.

Enzyme/ Source	Substrate	Remarks	Reference
Lipase, Protease and Carbohydrase / *Candida rugosa, Aspergillus,*	Food waste	With an enzyme mixture ratio of 1:2:1 at a dose of 0.2% (w/w) and a time of 10 hours, an organic loading rate of 9.1 g/L/d resulted in an observed yield of 0.35 L/g methane and a COD removal efficiency of 95%.	Moon & Song, (2011)
Ultraflo ® L or Aspergillus/ Novozymes	Corn cob	The AD of the raw corn cob yielded of 22.3% methane volume. The total of 264 pretreatments was inadequate to cover the extra expenditures.	Pérez-Rodríguez et al., (2017)
laccase enzyme/ *Pleurotus eryngii*	Corn Stover	The activity was improved by 16%. Untreated waste, BioM production by 20%. Enzyme was increased by 19%.	Wyman et al., (2018)
Cellic® CTec2 and Cellic® HTec2/cellulase enzymes (Novozymes)	Safflower Crop	Treated samples was exposed to 72 hours of temperature at 45°C, and an enzyme loading of 10 FPU/g straw was 14.7%, which was enhanced to 72.9% after 5 hours at 180°C.	Hashemi et al., (2019)

Food waste treatments using hydrolytic enzymes for methane production involve the application of enzymes to break down complex organic compounds in FW. These enzymes facilitate the hydrolysis of carbohydrates, proteins, and lipids into smaller, soluble molecules. Food waste is initially treated with hydrolytic enzymes to initiate the breakdown into simpler compounds like sugars, amino acids, and fatty acids, increasing the availability of substrates for methane-producing microorganisms. The resulting mixture is then transferred to a methane reactor where methanogenic microorganisms convert the organic compounds into methane through anaerobic digestion. Methane is produced as a metabolic byproduct of the methanogens (Zhi et al., 2019; Fazeli et al., 2016).

2.3 ANAEROBIC DIGESTION

Enzymatic hydrolysis was considered as a cost-effective and ecologically beneficial method of dealing with FW. Enzymatic hydrolysis such as cellulase and amylase are locally produced. AD has not been reported in SBR hydrolysis and fermentation. It was a biochemical process that includes the biodegradation of soluble organic active substance into biofuels through four major steps: hydrolysis, acidogenesis, acetogenesis, and methanogenesis (Bo et al., 2014). Biomass is degraded in an anoxic conditions (zero-oxygen) environment to generate bioenergy, a gas combination composed of CH_4 (50-70% volume), CO_2 (25-50% volume), and various trace gases such as H_2, ammonia, hydrogen sulfide, and others gases. This technology offers several quality advantages, particularly in the generation of thermal and electrical power for commercial processes. CH_4 generation from the AD of organic materials has traditionally been planned, and it was being investigated as a sustainable energy source. Furthermore, to improve the sustainable

development of the CH_4 generation process, CO_2 recycle from various biological ways may be incorporated to supply additional biomethane via microorganisms electrosynthesis. Microorganism methanogenesis, also characterized as electromethanogenesis, may occur at lower atmospheric conditions than the AD mechanism (Logan et al., 2012). The investigation of electromethanogenesis utilizing MEC indicates that the organic compounds existing in FW may be handled while also producing BioM. In terms of increased CH_4 output and the utilization of the AD controller's wastewaters, this technique outperforms standard biogas yield (Zhang et al., 2014).

A set of biological pathways related the bacteria emerge in both interrupted and linked microbial community when integrated with the electrocatalytic respondents. Because the MEC technology was an anaerobic electrolysis mechanism that affects a microorganism's species from an acidogenic treatment technique for wastewater. Acetate generation was followed by methanogenesis, which includes H_2 transformation, after glucose acidification to short-chain carboxylic acids (propionic, butyric) (Falk & Benz, 2011). Furthermore, an electrocatalyst microorganism's cell (Xeab) uses the mediator as an electron acceptor to oxidize the acetate, contributing to increased H_2 generation. Figure 2.1 depicts the reaction configuration of biochemical model was based on AD.

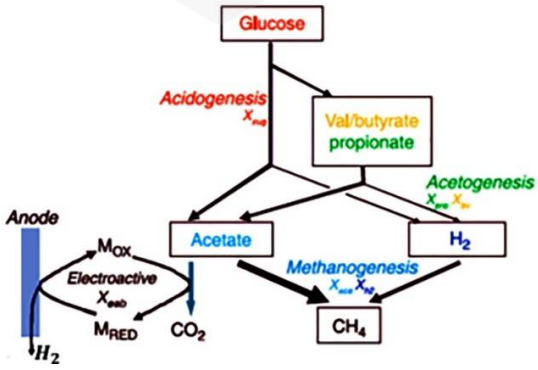

Figure 2.1: The biochemical model based on AD (Picioreanu et al., 2008).

There were many operating conditions that affect the efficiency of feedstock treatment. Type of carrier to enzyme plays a great role to degrade the feedstock, particularly FW. A study was done using polyvinyl-alcohol gel beads on agro-industrial feedstock has found a 28% increase in biogas yield when compared to the controlled bioreactor.

2.3.1 Parameters Affecting the AD of Food Wastes

According to Ukonu (2011), numerous parameters impact biogas yield including such inoculum, loading rate, digester design, substrate type, pH, volatile fatty acids, feedstock biofuel capacity, hydraulic retention time, temperature, C: N ratio and other trace gases as stated below (Kavuma, 2013).

2.3.1.1 Substrate Concentration and Enzyme Dosing

The organic loading rate was a determinant of the AD system's biomass conversion capability. It establishes the volume of material that may be used as an intake in the AD system. A system increase might lead to a low biogas production. This occurs as a result of the buildup of inhibitory chemicals in the digestion sludge, including fatty acids. The processes that will also arise if the mechanism was overloaded would result in the expansion of acidogenic bacteria, significantly lowering the pH in the medium and disrupting the congregation of methanogenesis. Furthermore, there were a clear link between biofuels yield and loading rate. The loading rate was optimal for acidogenesis, preventing ch4 formation while boosting VFA synthesis in it (Dhanariya et al., 2014).

The first obstacle faced in production of biogas from food waste was the difficulty to hydrolyze the polymers because of the complex structure. For food waste conversion to

biogas, the big polymers must be broken down to their monomers in order for the microbes to utilize them. Several studies were revealed that a wide range of various pretreatment approaches were proposed over the past 50 years (Carlson, 2005; Huang et al., 2015; Song et al., 2022). They were categorised as physiochemical, physiological, chemically, or physico-chemical processing conditions based on the pressures or energy consumed during the transesterification process (Deb et al., 2019). Biocatalytic hydrolysis was its greatest option for overcoming this barrier since it has minimal capital costs, low thermal efficiency, no reagents required, and comforting environmental conditions Alvira, (2019).

2.3.1.2 pH

The pH of a medium was an indication of the strength of its basic or acid state, and it was an estimate of its acidity (Cookson, 1974). Anaerobic bacteria in wastewater treatment processes were often particularly effective in the neutral pH range of 7.0. The dosage level acceptable used by most organisms was 6.0-to-9.0; digesting will continue further than this level, although with substantial reduction (Deb et al., 2023). The organic matter negatively impacted at pH 9.0 was allowed to reactivate once the pH was adjusted to stability, however the organic matter negatively impacted at pH 5.0 was not useable. Generated in acidic circumstances will become extremely harmful to CH_4 microorganisms. As a result, it was critical that sometimes pH not go below 6.2 for an extended length of time. The pH measures the strength of the basic or acidic cation. So, this component was critical, the process must regulate the pH. The pH maintains between 7.2 and 8.2 when methane gas generation stabilizes. The ideal pH range for anaerobic procedure was at 7.0 to 7.2, although it will work just well with a pH ranging from 6.6 to 7.6 (Holl et al., 2022).

2.3.1.3 Agitation

As mentioned before, mixing may result in a washout of biomass in a continuous process. However, mixing was good to have uniform contact of feed to the biomass (Poh & Chong, 2010). Mixing can be done with slurry recycle, mechanical or biogas recirculation (Karim et al., 2005). They also have found that mixing can greatly improve biogas production however not efficient at vigorous mixing method that can inhibit methanogenesis. He also mentioned that mixing should be made after starting up as it may cause pH to increase thus disturb the methanogenesis and the microbial community growth. Suitable mixing optimization has yet to be done on FW (Poh & Chong, 2010).

2.3.1.4 Temperature

Mesophilic and thermophilic operating temperature was feasible due to the temperature of POME when released was 80 – 90°C (Zinatizadeh et al., 2006). Temperature also has impact on biogas generation. The temperature at which the steps of biogas generation occur was critical and must be kept consistent (Kavuma, 2013). Physiological and biochemical variables (including such temperature and pH) have a greater influence on the hydrolysis and acidogenesis processes than biological factors (Kobayashi et al., 2017). Temperature was commonly categorized into three ranges: psychrophilic (12 to 16°C), mesophilic (35 to 37°C), and thermophilic (55 to 60°C). Mesophilic and thermophilic environments were chosen in most anaerobic studies because greater temperatures may result in a faster rate of hydrolysis, creating more biogas, and methane generation in thermophilic conditions was nearly identical as in mesophilic conditions. Greater temperatures were thought to induce

system destabilization, and also another drawback was a higher energy need (Huo et al., 2022).

2.3.1.5 Organic Loading Rate

A high organic loading rate will improve biogas production. However, COD removal was low. The opposite situation happens with low organic loading rate (Ahmad et al., 2012). On the other hand, another study has found that high organic loading rate contributes to both high COD removal and biogas production when biomass in the system was retained without maintaining the pH (Basri et al., 2010).

2.3.1.6 Hydraulic Retention Times

The maximum duration that solids and liquids were kept in the digestive mechanism was measured by hydraulic retention times. All factors were strongly connected to anaerobic processes (hydrolysis, fermentation, and methangenesis) and anaerobic reactor capacity. Each anaerobic digestion reaction necessitates a specific hydraulic retention time to perform, and if the specified hydraulic retention time was smaller, the digestion mechanism will stop (Sharma et al., 2022). Hydraulic retention times were similar in a totally mixed reactor with no recycling. In reality, Hydraulic retention time levels for slightly elevated digestion vary from 10 to 20 days. Hydraulic retention time, also defined as hydraulic residence time, was the amount of time it takes for a hydrophilic component to remain in a bioreactor. From the economical aspect, low HRT was desired because it can reduce operational time and thus save money and electricity. However, retaining suspended microbes seems farfetched due to washout (Chen et. al, 2001; Oh et. al, 2004).

2.3.2 The Stages of Anaerobic Digestion based on Microbial Electrolysis Cells

AD was a biological progression that happens in the absence of oxygen to break down organic matter into biogas and digestate. The biogas contains methane and carbon dioxide and was utilized as a renewable energy source for electricity generation and heating. The digestate was a nutrient-rich fertilizer for agriculture. The process takes place in anaerobic digesters, which were sealed containers that control temperature, pH, and other conditions to optimize the digestion process. The stages AD system were as follows: (a) pretreatment: raw materials were prepared for digestion by grinding, mixing, or homogenizing to increase surface area for microbial action. (b) hydrolysis: enzymes break down complex organic compounds into simpler sugars and organic acids. (c) acidogenesis: bacteria convert the organic acids into acetic acid, hydrogen, and carbon dioxide. (d) acetogenesis: acetic acid was further converted into methane and carbon dioxide by methanogenic bacteria. (e) methanogenesis: The final stage of anaerobic digestion, in which methanogenic bacteria convert the acetic acid and hydrogen into methane. (f) solids separation: the solid and liquid fractions were separated to allow for further treatment or disposal of the residual solids. (g) gas cleaning: the biogas produced was cleaned of impurities such as sulfur, moisture, and carbon dioxide before it can be used as a fuel. Overall, the anaerobic digestion process was a controlled biodegradation of organic material that results in the production of biogas, which was utilized as a sustainable energy source.

AD generates biofuel, decrease organic compounds, moderate's sludge, and minimizes pathogens, but it was primarily related by a number of operational concerns, including slow progress of biogas microbes, high initial digestive performance, short or medium hydraulic retention time, the need for a relatively high heating rate, and volatile

fatty acid (VFA) intensification in the reactor. Table 2.3 reviews the studies concerning the AD of different types of FW.

Table 2.3: Anaerobic digestion processes of food waste for methane production.

Types	Reactor Capacity	Waste	Inoculum	HRT (days)	Times (days)	CH_4 %	H_2 %	CO_2 %	Reference
Two phase Bioreactor	5L	FW	Cow manure	1	29	70	7.3	22.7	Bo et al., (2014)
Single Bioreactor	5L	FW	Anaerobic solid sludge	16	30	52	3.1	40	Deb et al., (2019)
Bioreactor	12L	FW	Anaerobic solid sludge	20	60	68.8	9.3	21	Youn & Shin, (2005)
Bioreactor	4.5L	FW	Solid sludge	27	200	62.6	1.9	37.4	Banks et al., (2011)
Tank	900m^3	FW	Granular sludge	80	426	75	1.9	22	Moon & Song, (2011)
CSTR	3L	FW	Anaerobic solid sludge	16	225	50	10	40	Dai et al., (2013)
Digester	800ml	FW	Activated sludge	Batch	30	55.2	9.7	25	Zhang et al., (2013)
Batch	5000 mL	FW	Anaerobic solid sludge	28	28	73	0.9	26	Forster et al., (2008)
CSTR	10L	FW	Solid sludge	5	150	80	2.1	16	Kim et al., (2010)
Batch	5L	FW	Landfill soil & cow manure	60	60	68	3.5	28	Kim et al., (2008)

AD based MECs were subsequently presented as a technological advance for the effective generation of biofuels from organic substances to address these constraints. Electroactive microbes on the electrode materials transform organic materials in AD based MECs into CO_2, H^+, and e^-. The generated e passes through the electrical supply to the

electrodes and was utilized in the generation of CH_4 and H_2. Furthermore, by combining hydrogen with carbon dioxide, CH_4 was produced, resulting in stronger methanogenesis and quicker stabilized processes than standard AD. AD based MECs can also reduce sulfate, nitrobenzene and NO_3, maintaining significant organic carbon decolorization efficiency and disintegration rates. Based on the findings of current AD based MECs research, oxidation reactions provide quick stabilized and CH_4 output at the start of an operational. Metabolic pathways, on the other hand, have a bigger influence on methane generation during the stabilizing period than redox processes. As a result, research on AD based MECs has focused not only on oxidation and reduction (improvement of low-cost anode and cathode materials and high efficiency, electrochemical reaction analysis, novel reactor design for practical utilize and electrochemical efficiency calculation), in addition to the impact of MECs on microorganisms.

2.3.2.1 Microorganism for Bio (degradation)

According to the biogas production via anaerobic method was a suitable solution for food waste management. The method has less significant cost and low residual waste production and the use of FW as a green power source (Nasir et al., 2012; Morita & Sasaki, 2012). Microorganism cooperation in organic matter degradation based anaerobic digestion involves almost three stages such as enzymatic hydrolysis, acid formation, and gas production as shown in Figure 2.2 the digestion process.

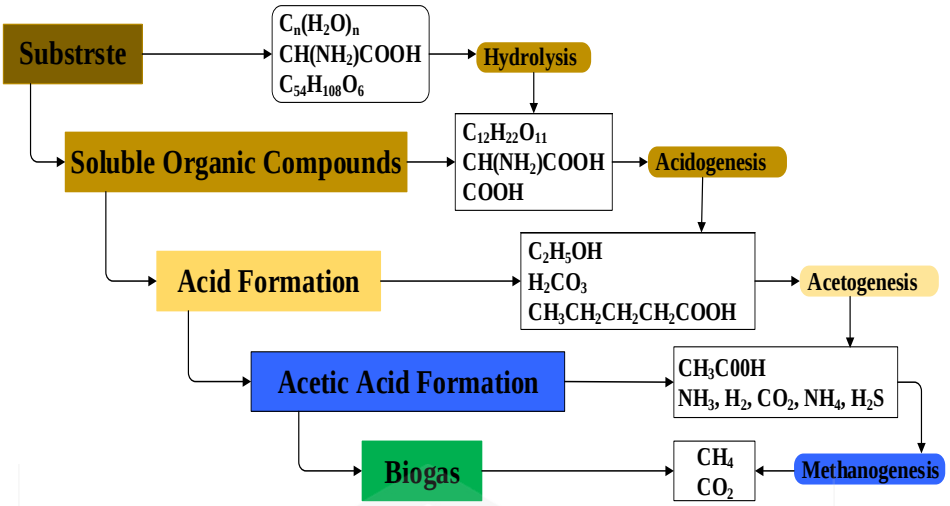

Figure 2.2: Anaerobic digestion Stages (Paritosh et al., 2017).

2.3.2.2 Hydrolysis

In the initial phase, a nonpathogenic anaerobic bacterium inhibits the biomass biologically active components (lipids, proteins, starch, and cellulose) to produce small molecular mass solubility molecules and several inorganic compounds. Hydrolysis was its preliminary step of the fermentation system. Because microbial fermentation microbes unable directly consume polymers, that phase was critical for the AD process (Adekunle et al., 2015). As a result, non - soluble biologically active materials like cellulose was converted into simple sugars like sugars, amino acids, and fatty acids. Hydrolytic enzymes (lipases, cellulases, amylases, proteases, etc.) hydrolyze diverse polymeric materials to monomers, such as cellulose to sugars and amino acids, which were released by germs and made accessible to all other microorganisms. Enzymatic hydrolysis breaks down the polymers into monomeric units or oligomer. Polysaccharides were broken down into monosaccharides and oligosaccharides. Equation (2.2) shows the production of glucose molecules by starch hydrolysis. Proteins were broken down into amino acids and lipids and peptides were rehabilitated into fatty acid and glycerol.

$$nC_6H_{10}O_5 + nH_2O \rightarrow nC_6H_{12}O_6 \quad (2.2)$$

Mital, (1997) described that, in the AD, the hydrolysis rate was comparatively slower than the acid formation rate and depends on the bacterial concentration, the nature of substrate, temperature, and pH of the bioreactor.

2.3.2.3 Acidogenesis and acetogenesis

The monomers produced by the hydrolysis process permeate into the molecules of some of the other microorganisms (i.e., acidogenic microorganisms) across the membrane and may be destroyed further by those microbial species during the acidogenesis procedure. VFAs, alcohol, ketones, CO_2, H_2, NH_3, H_2S, and other chemicals were commonly found in the compounds. During the acetogenesis pathway, the methanol and simple volatile acids were further degraded into acetic acid and H_2. Because the end result of these two reactions was acid, some scientists refer to them as acidogenesis (Wainaina et al., 2019). Because these two mechanisms were so quick, a dramatic pH decrease was possible, particularly if the reactors were saturated. The situation was exacerbated by anaerobic digestion of food waste, which entails a significant hydrolysis rate, which means that much material was accessible for acidogenesis microorganisms. When the acidogenesis rate was too rapid and the pH decrease was considerable, methanogens (methane-forming microorganisms) were severely inhibited (Leung & Wang, 2016). Acetogenic bacteria be appropriate to genera *Syntrophobacter and Syntrophomonas* (Schink, 1997) convert the acid phase produces into acetates as shown in Equation (2.3) and hydrogen. A small number of acetate molecules were also produced by the reduction of CO_2 utilizing H_2 as an electron source. Acetates will further be used by methanogens in the following steps.

$$nC_6H_{12}O_6 \rightarrow 3nCH_3COOH \quad (2.3)$$

Also, acetogenesis was the stage, which illustrates the biogas production efficiency because 70% of methane develops when acetate decreases. Simultaneously, 11% of hydrogen was also formed during the method (Schink, 1997).

2.3.2.4 Methanogenesis

Methanogenesis was the process by which methanogenic microbes transform soluble materials into CH_4. Two-thirds of the total CH_4 generated was sourced from acetic acid conversion or digestion of ethanol synthesized in the second phase, including such methyl. The remaining one-third of CH_4 created was caused by the replacement of CO_2 by H_2. Given methane's great ability for influencing global warming, the objective was to discover a way to minimize the environmental impact of biological treating wastewater. As a result, this step was skipped, instead of generating CH_4, the formation of volatile fatty acids was prioritized (Karakashev et al., 2005). The following activity in response throughout this phase:

$$CH_3COOH \rightarrow CH_4 + CO_2 \quad (2.4)$$

Methane can be produced in two approaches by two forms of methanogens: (a) acetoclastic methanogens which make methane from acetic acid and (b) hydrogenotrophic methanogens which was used hydrogen to decrease carbon dioxide. Table 2.4 summarizes the studies concerning active genera in anaerobic digestion and microbe collaboration in organic substance degradation.

$$CO_2 + 4H_4 \rightarrow CH_4 + 3H_2O \quad (2.5)$$

Table 2.4: Bacteria collaboration in organic substance degradation.

Type of Reaction	Hydrolytic Enzymes	Active Genera	Product	Reference
Hydrolysis	Cellulases	*Gluconacetobacter, Sarcina, Agrobacterium, Sporobacterium*	Simple sugars, peptides, fatty acids	Lo et al., (2009);
	Lipases	*Bacillus, Lactobacillus, Pseudomonas, Propionibacterium, Sphingomonas*		Tongco et al., (2020);
	Proteases	*Bacillus, Lactobacillus, Penicillium, Virgibacillus pantothenticus,*		Caresani et al., (2019);
	Amylases	*Aspergillus niger, Sphingomonas Bacillus, Lactobacillus, Aspergillus, Penicillium fellutanum, Saccharomyces kluyveri*		Balaban et al., (2018); Tabssum & Ali, (2018);
	Phytase	*Bacillus, Lactobacillus, Cellulosimicrobium, Achromobacter, Tetrathiobactor*		
	Pectinases	*Bacillus, Pusillimonas, Staphylococcus, Bifidobacterium, Aspergillus niger, Megasphaera*		
Acidogenesis	Syntropic bacteria	*Clostridium, Paenibacillus, Ruminococcus*	Volatile fatty acids	Hao et al., (2020).
Acetogenesis	Acetogenic bacteria	*Acidaminococcus, Aminobacterium, Desulfovibrio,*	CH_3COOH	Fu et al., (2019)
Methanogenesis	Methanogens	*Methanolobus, Methanogenium, Methanohalophilus, Methanosaeta, Methanohalobium, Methanococcoides, Methanosalsus, Methanoculleus, Halomethanococcus, Methanolacinia,*	CH_4	Zhang et al., (2019)

Table 2.4 shows to carry out a thorough analysis of hydrolysis, acidogenesis, acetogenesis, and methanogen microbes to present the origin for detecting the most promising species for further study. The database contains environmental influence that factors the growth of each species in subterranean environments expected to be aimed for CO_2 storage.

2.3.3 Electromethanogenesis Chemical Reaction

Every raw material within a species was the outcome of a metabolic process or route. Different physiological stages may be required to break, change, or develop biological structures and molecules. Various metabolic process byproducts can function as reactants in some other route. In this section, we detail the specific mechanisms for CH_4 anaerobic metabolism, also known as methanogenesis. Methane was produced by three metabolic pathways such as hydrogenotrophic methylotrophic, and acetoclastic, CO_2 reduction as demonstrated in Figure 2.3. Regarding these, the CO_2 reduction route was thought to be the primary engine of methane yield. While engaging with starter cultures, therefore, alternative paths become more important.

Besides the *M. barkeri* that utilize all three routes, mostly all methanogens utilized in CH_4 electrochemical conversion processes utilize the CO_2 reduction route. On the other hand, microbes such as *M. hollandica* and, *M. thermophila* can exclusively use methylotrophic and acetoclastic routes. The CO_2 reduction process was almost four times more common than the acetoclastic and methylotrophic routes mixed. This was due to the ease with which CO_2 and hydrogen were supplied throughout hydrogenotrophic methanogenesis. CO_2 was decreased and catalyzed to create formylmethanofuran, with

decreased ferredoxin (Fdred) serving as an electrophile. The formyl set was relocated to tetrahydromethanopterin in the second phase (H_4MTP). The dehydration process generates methylene-H_4MTP, which was then decreased to methyl-H_4MTP using decreased F420 as an electron acceptor. Subsequently, methyl-CoM was concentrated to CH_4 with coenzyme B (HS-CoB) both as an electron acceptor after the methyl set was relocated to coenzyme M (HS-CoM). To regenerate the coenzymes, the resultant CoM-S-S-CoB was decreased using H_2. It needs to be emphasized that certain methanogens can employ formic acid as an electron acceptor for CO_2 reduction rather than H_2.

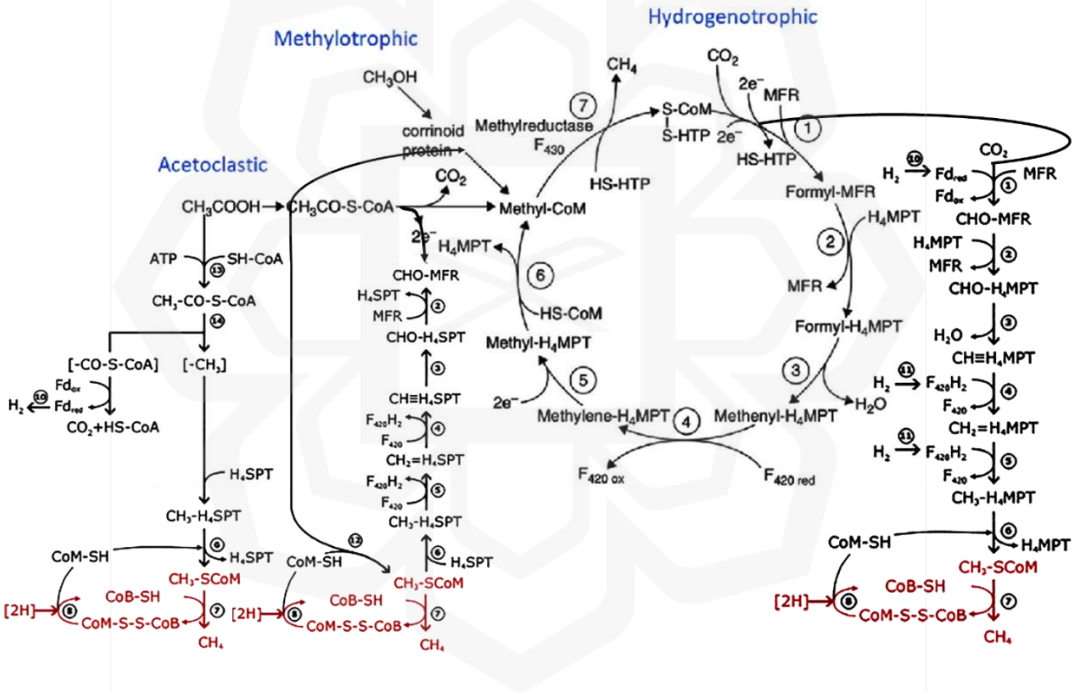

Figure 2.3: Three metabolic microbes for electromethanogenesis. (a) Acetoclastic, (b) Hydrogenotrophic and (c) Methylotrophic methanogenesis (Sadhukhan et al., 2016).

The species *Methanosarcina* and *Methanotrix* synthesize CH_4 using acetate. Acetate should always be released for acetoclastic methanogenesis to emerge. This was accomplished by the synthesis of ATP and coenzyme A into acetyl-CoA, which was then divided by the CODH/acetyl-CoA polymerase combination. According to the

hydrogenotrophic CH_4 generation process, the CH_3 group was converted to tetrahydrosarcinapterin (H_4SPT) and then transformed into CH_4. The final method of producing organic CH_4 use substituents materials such as dimethyl sulphide, methanol, methanethiol, or methylamines. *Methanosarcinales* were a community of several methylotrophic microorganisms. At the initial stage, appropriate methyltransferases convert the methyl group from the material to a corrinoid protein, which was then converted to HS-CoM again by methyltransferase to generate methyl-CoM. Similarly, one methyl-CoM was converted to CO_2 through the opposite way hydrogenotrophic route, providing sufficient hydrogen to convert three methyl-CoM to CH_4 as a byproduct of proton motive force (Sadhukhan et al., 2016).

2.3.4 Biogas

Biogas was a biofuel produced from the anaerobic fermentation of biological materials (known as feedstock) through bacteria. Furthermore, biogas was mainly composed of CH_4, with some CO_2 and other trace gases such as carbon monoxide (CO), nitrogen (N_2), hydrogen (H_2), Sulphide (H_2S) and oxygen. The average composition of biogas components was represented in Table 2.5. However, the proportion of methane within biogas varies between 55% and 75%, depending on the quality of treatment process or technique used to enhance it and the nature of sources which will be explained in the following sections. Discharging large amounts of food waste without control causes severe pollution to the environment. Therefore, it was proven that anaerobic digestion was an effective solution to treat and valorize food waste among other treatment techniques.

Table 2.5: Average compositions of biogas

Matter	%
Methane (CH_4)	55-75
Carbon dioxide (CO_2)	25-75
Carbon monoxide (CO)	0-0.03
Nitrogen (N_2)	1-5
Hydrogen (H_2)	0-3
Sulphide (H_2S)	0.1-0.5
Oxygen (O_2)	0.1-0.8

Source: Acién et al., (2012)

The enhancement of AD performance was important field that many researches have been conducted on and have shown the promising way for enhancing performance of AD was the pretreatment, co-digestion of FW with other organic waste and the optimization of some AD digestion parameters. A clear explanation of these enhancement methods was discussed on the subsequent section.

2.3.5 Biomethane

The biomethane (BioM) was a source of energy that was obtained through the digestion of organic content by the microorganism. Animal waste, plant waste, municipal wastewater waste, sewage sludge, and any other biodegradable matter can be utilized as biological feedstock (Wellinger, et al., 2013). AD was the most often utilized biodegradable waste treatment method for converting trash into alternative fuels. As shown in Figure 2.4, four main steps of reaction were associated with the process of decomposing FW into CH_4, CO_2, and freshwater during the biogas production: hydrolysis, acidogenesis, acetogenesis, and methanogenesis. In an anaerobic digestion system that produces biofuels, raw FW was

transformed into volatile fatty acids with the help of acid-forming microorganisms. The volatile fatty acids were subsequently broken down into methane and carbon dioxide. As a result, this step was skipped, rather than methane, the formation of volatile fatty acids was prioritized. The following responses occur throughout this phase (Dhanariya et al., 2014).

- Acetate conversion: $2CH_3CH_2OH + CO_2 \leftrightarrow 2CH_3COOH + CH_4$

Followed by: $CH_3COOH \leftrightarrow CH_4 + CO_2$

- Methanol conversion: $CH_3OH + H_2 \leftrightarrow CH_4 + H_2O$

- Carbon dioxide reduction by hydrogen $CO_2 + 4H_2 \leftrightarrow CH_4 + H_2O$.

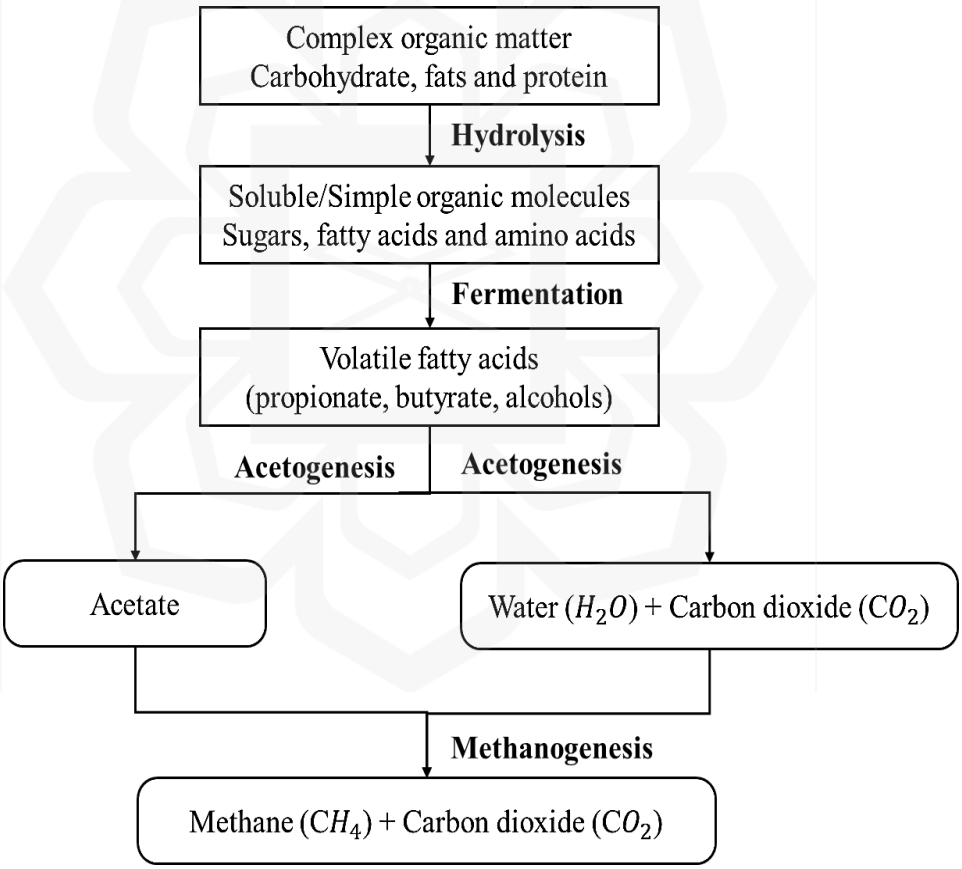

Figure 2.4: Process diagram of methane production (Bharathiraja et. al, 2016)

In the extended aerobic process to produce biogas, FW was treated in a way to meet the standards of the Department of Environment. There were many ways to treat the complex matter in order to convert them into a simple matter. AD has not been reported in SBR hydrolysis and fermentation. These methods of pretreatment will be discussed in the next section. Despite the benefit of the BioM production from various wastes including food waste, still, the low methane content (50-70%) with more than 40% of CO_2 mixture limits the high efficiency in the conversion of thermal heat or electricity generation to make economically feasible for industrial applications (Cerrillo et al., 2018). Therefore, upgrading of BioM to increase the pure methane as clean energy as well as utilization of CO_2 into methane was required for high efficiency of thermal and electric heat generation and safe of the environment by capturing CO_2.

2.4 CONVENTIONAL MICROBIAL ELECTROLYSIS CELL SYSTEMS

Carbon dioxide (CO_2) levels in the atmosphere were rising and threatening ecosystems of human beings. Therefore, efficient technologies need to be developed to decrease CO_2 emissions and to sustainably produce carbon-neutral bioenergies. Nowadays, carbon capture, utilization, and storage were applied to mitigate CO_2 emissions in the atmosphere by different CO_2 transformation technologies, such as chemical, photochemical, electrochemical and biological were being investigated. Figure 2.5 shows a two-stage BEC system capturing the CO_2/CH_4 for high yield of biomethane production. In this case, BEC represents a novel promising approach, by which CO_2 can be reduced to the renewable bioenergy (CH_4) in a process known as MEC whereas, in the past, BEC was applied in the MFC for the generation of electricity from various waste without considering the emission

of the CO_2 to the atmosphere (Santoroa et al., 2017; Tee et al., 2017). Considering the environmental issue as well as upgrading of biogas (removal of CO_2 and high content of biomethane), MEC could be more attractive to overcome the current problem. In this system, the main gape was low reaction rate using EMMs. Bo et al., (2014) discovered that through combining the MEC with AD in a single-chamber, cylinder shape, stainless-steel reactors, CH_4 concentration was enhanced by 2.3 times when comparing to typical AD process.

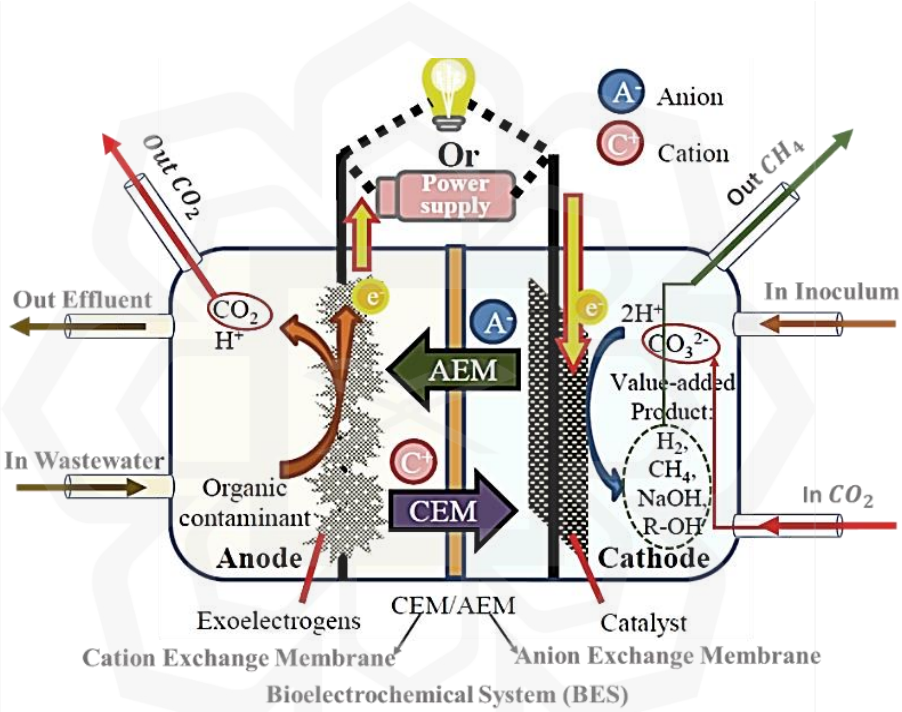

Figure 2.5: Schematics of two stages bioelectrochemical system (Lu et al., 2015)

Moreover, the efficiency of COD removal has been quadrupled, and carbon recapture has been raised by 56.2%. Guo et al., (2013) discovered that the biocatalytic method increased hydrogen and CH_4 yield from AD of sewage sludge in single-chamber MEC, and that when as particularly in comparison to controls,, H_2 fuel was increased 1.7-5.2-fold and CH_4 yield was increased 11.4-13.6-fold with Ti/Ru electrodes at applied

potential of 1.4 and 1.8V, combined particularly in comparison to controls, H_2 fuel was increased 1.7-5.2-fold and CH_4 yield was increased 11.4-13.6-fold with Ti/Ru electrodes at applied potential of 1.4 and 1.8V, combined. In Malaysia, the performance of the MEC biocathode with sulfate-reducing microorganisms for the reason of hydrogen generation was tested, and it was discovered that the procedure increased by 6 times when compared to a control without MEC (Jafary et al., 2017). According to Kadier et al., (2015), the most crucial issue for MECs to evolve into a commercially viable H_2 production method was the advancement of low-cost, high-efficiency cathode catalysts.

In comparison to the AD that produced hydrogen from OW, the MEC had improved hydrogen extraction and a larger feedstock combination (Sun et al., 2009). However, concerning microbial fuel cells (MFCs) where a range of substances are investigated (Pant et al., 2010; Keller, 2010), most microbial electrolysis cell (MEC) investigations have heavily relied on the usage of pure chemical compounds as the input material. When alternative sources like animal and household wastewaters were introduced, the production of H_2 was limited, yet there was an increase in CH_4 synthesis (Ditzig & Logan, 2007; Wagner et al., 2009). A comprehensive inventory of materials employed in MEC research is furnished in Table 2.6. Research demonstrated hydrogen synthesis from cellulose in a two-chamber MEC, yielding 63% hydrogen, which was akin to the 64% derived from glucose but lower than the 82% attained with acetic acid. This suggests that complete hydrogen retrieval was not achieved during the fermentation stage of the process.

Table 2.6: Overview of some studies on hydrogen and methane production using MECs

MEC	Substrate	Source of Inoculum	Remarks	Reference
MEC has two chambers, an anode of graphite granules (1320 m^2/m^3) and a cathode of platinized carbon fabric.	Cellulose	Bacteria derived from a soil used to start up the cell in MFC mode.	Substrate concentration was used by 1 g/L. Maximum H_2 recovered was 0.11 m^2 $H_2/m^3/d$ at a set voltage of 600 mV.	Cheng & Logan, (2007)
A solitary graphite fiber brush anode and multiple carbon cloths were utilized in both single and two-chamber MEC setups.	Anaerobic Sludge	Methane electromethanogenesis even with an abiotic anode with cathode.	High voltage of 1.23 and 1.05 V. Methane was produced at the overall energy efficiency of 80%	Cheng et al., (2009)
Single-chamber MEC membrane-free. The anodes and cathodes (4.0 × 5.0 × 0.2 cm) were constructed from Ti/Ru alloy mesh plates.	Sewage sludge	Each MEC received 148 mL of sludge and 2 mL of mineral medium.	The electrode gap was 2 cm. H_2 increased by 1.7-5.2 times, and CH_4 by 11.4-13.6 times at voltages of 1.4 and 1.8 V.	Guo et al., (2013)
Single-chamber membrane-less. Anode (carbon brush) and cathode (carbon cloth with Pt).	Glucose	Household sewage was employed to initiate the cell under MFC operation.	1 g/L glucose was used. At applied voltages of 0.9 Vdc. 1.87 m^2 H_2 $/m^3/d$ of maximum H_2 was recovered.	Selembo et al., (2009)
Membrane less single chamber MEC. Anode (carbon fiber brush) and cathode (carbon cloth).	Waste from an ethanol type fermentation CSTR.	Household sewage was utilized for MFC operation.	6500 mg/L of COD. Used in 600 mV. Maximum H_2 was recovered of 1.41 m^2 H_2 $/m^3/d$.	Lu et al., (2009)

2.4.1 Hybrid Microbial Electrolysis Cells

Liu et al., (2005) designed MECs as the key consideration for chemical compound reduction. Since, the literature of MEC was used partially purposed but it was more efficient system to remove, reuse and recycling systems (Kadier et al., 2016; Lu & Ren, 2016). Technically, exoelectrogen microorganisms that could also interchange electrons via the intracellular apparatus in MECs use electrodes device as an electron sink to oxidize organic substances and provide H^+ ions. Protons diffuse via a polymer electrolyte layer to the negative electrode and were reduced by ions exchanged through the external electrical circuits to form H_2. Because of the metabolic impediment, the MEC system cannot function abruptly, and an additional electrochemical reaction was necessary to drive the lowering reaction (Kadier et al., 2015; Kumar et al., 2017). Figure 2.6 shows a standard schematic depiction of hybrid MECs.

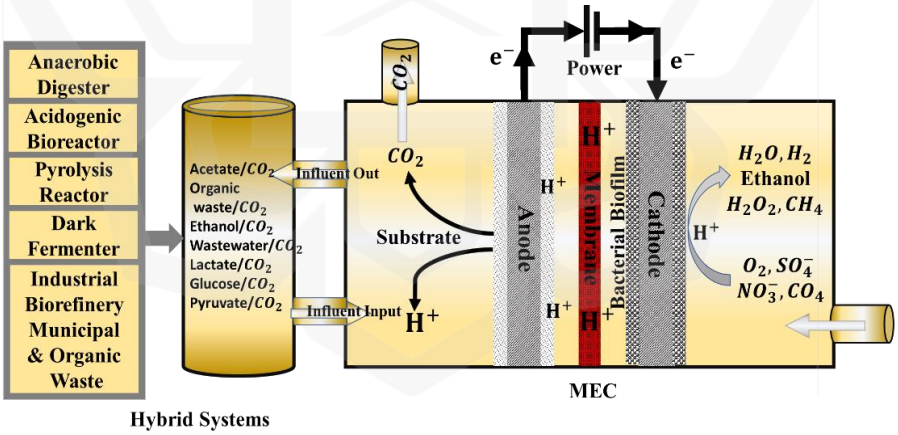

Figure 2.6: Schematics of two stages hybrid MEC system (Kadier et al., 2015).

In the hypothesis of hybrid MECs, any carbon compounds that were processed by the bacteria exoelectrogens were utilized in the anode chamber of MECs. This has driven to a huge assortment of organics sources considered in MECs, ranging from characterized

unadulterated chemicals to mix of real wastewaters (Kadier et al., 2014; Escapa et al., 2016). With various carbon sources, the anode electrical potential can operate minimum voltage 200mV to 1V. The normal values of a few commonly utilized carbon sources have appeared in Figure 2.6. The half-reaction at the cathode terminal was the decreasing of protons to H_2 gas. Based on the Nernst conditions, the cathode electric potential will be influenced by the concentration of free protons like partial pressure of H_2, pH of electrolyte, and temperature. As demonstrated in Figure 2.6, the cathode electric potential reduces with rises in the partial pressure of H_2, pH value, and temperature. Concerning the impact on cathode electric potential, pH was the important parameter (Rozendal, et al., 2006). The input energy was important for MECs because of the thermodynamic limits (Liu et al., 2005; Call & Logan et al., 2008). Under standard conditions such as H_2 halfway weight (pH), pH and temperature, the cathode electric potential for H_2 improvement comeback was almost -410mV which was more negative than the anode electric potentials utilizing most of the carbon sources. Hypothetically, it ought to be conceivable to form the response happen suddenly with glucose as substrate, but glucose, in that case, should be completely oxidized to CO_2 which dose not happen in anaerobic fermentation (Wünschiers & Lindblad, 2002). Another method to diminish or expel the energy prerequisite of MECs was to reach the cathode electric potential by modifying the pH or pH. This seems feasible because the cathode electric potential would be high enough on the off chance that the cathodic electrolyte pH can be decreased to lower than 5 or keep up the pH at lower than 0.001 bar. In any case, keeping up a low pH in cathode would square the proton movement through the membrane, along these lines coming about in diminished pH in anode terminal which

was destructive to the bacteria. On the other hand, keeping up a greatly low pH was illogical during the operations.

2.4.2 Benefits and drawbacks of hybrid MEC technology

Compared with other hydrogen creating methods, one of the essential points of MECs was mild working conditions. In the rule, as it where 0.11 V input was required to drive the hydrogen generation from acetate (Liu et al., 2005; Kadier et al., 2016), and this was often less than 10% of the normal power range from 1.23V – 2.0 V required for water electrolysis. In this way, the energy cost of hydrogen generation in MEC was approximately 1-3 kWh/m^3, whereas the ordinary mechanical electrolyzers would raise to 4.5 - 5.0 kWh/m^3 (Kadier et al., 2016).

In Addition to the cost, the H_2 yield was much higher within the MEC method, compared with the fermentation-based forms. Due to the energy obstruction examined over, the stoichiometric H_2 yield was the dark fermentation method was as it were 4 mol H_2/mol of glucose (Wang et al., 2011; Mohan et al., 2007) and the normal values detailed in real studies were 2.5-3 mol H_2/mol of glucose (Mohan et al., 2012). Several by-products such as acetate and butyrate were moreover generated during this method and their conversion into hydrogen gas was not thermodynamically possible. These by-products generation dark fermentation also shows the degradation of the incomplete organic during these methods. All the same, on the off chance that those substances can be oxidized, the yield of H_2 seem at that point be drastically increased. Stoichiometrically, this would include up 4 mol H_2/mol of acetate and might bring up the entire H_2 yield from glucose near to its hypothetical constrain of 12 mol H_2/mol of glucose. Moreover, MECs were prevalent in

terms of the immaculateness of H_2 as well. Due to the spatial partition of H_2 generation and organic degradation in MECs, it was likely to have other gasses such as carbon dioxide and other fermentation gasses in minor extents (Ren et al., 2011).

The H_2 purity was important for its different downstream applications, for illustration, it should be sulfur-free to be utilized in proton exchange membrane fuel cell systems. Therefore, MECs appear to be more appropriate as decentralized frameworks for the yield of H_2 at residential destinations. Hybrid MECs with other existing procedures to produce additional benefits seem moreover possibly be a productive approach to progress their industrial achievability within the future.

2.4.3 Production of chemicals in hybrid MECs

A hybrid MEC with AD system, named here as H-MECAD was studied to estimate the energy recovery from pretreated wastewater. Figure 2.7 shows the important physical mechanisms of H-MECAD that consist of an AD, an anode, a cathode, electrochemically active microbes, a membrane, and a power supply. To build a novel CO_2 bioconversion and bio-electrolysis response utilizing a microbials system based on the electromethanogenesis mechanism and to establish a microbiological method to generate CO_2 into biofuel. Based on the methanogen, biofuel may be produced electromethanogenically without the need for external hydrogen. The methanogen utilized hydrocarbons produced by the inorganic electrolytic cell in the reaction mechanism for hydrogenotrophic methanogenesis.

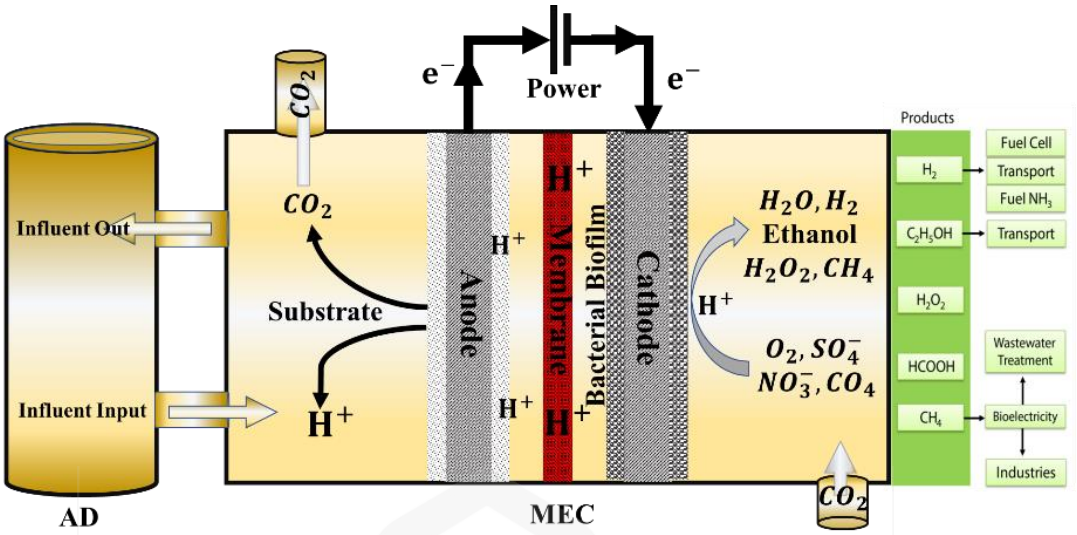

Figure 2.7: Schematic diagrams of a typical H-MECAD (Ren et al., 2011).

2.4.3.1 Bio-Methane

In practice, hydrocarbon synthesis from the AD of organic material had also remained complicated, and it was being researched as a sustainable approach. Furthermore, in order to establish a sustainable hydrocarbon manufacturing method, reuse CO_2 generated from biochemical systems processes may be coupled to give additional hydrocarbon via advanced oxidation synthesis. Advanced oxidation hydrocarbon synthesis, commonly known as electro-methanogenesis, could indeed operate at lower ambient temperature than AD. The advantage of electro-methanogenesis using the integrated MEC technique was that organic material present in wastewater may be treated while also producing byproducts. In terms of enhanced bio fuel output and the utilization of AD industrial effluent, this approach was more essential than standard methanogenesis. The precise substance of H_2 and CH_4 based on the modify in Gibbs free power which was 2119 kJ mol^{-1} electrons or COD equivalent of 4.12 kWh kg^{-1} and or 2101 kJ mol^{-1} electrons or

COD equivalent of 3.52 kWh kg^{-1} respectively. Whereas the energy demand of electrical was 3.35 kWh kg^{-1} of COD per Volt entailing that H_2 and CH_4 generation becomes dynamically unfavorable at applied voltages >1.23 and >1.05 V respectively (Logan et al., 2008; Pant et al., 2012).

Clauwaert and Verstraete (2009) appeared BEC methane generation utilizing MEC with a single chamber operation, utilizing plain graphite as anode and cathode electrode. In this case using an applied voltage of 0.8V, reporting a higher biomethane production rate of 0.75 ± 0.12 L $L^{-1} - MEC\ d^{-1}$ from 4.13 kg $m^{-3} - MEC\ d^{-1}$ COD loading with 86 ± 14% of acetic acid derivation to biomethane conversion, while without voltage condition the biomethane production rate of 0.17 ± 0.06 L $L^{-1} - MEC\ d^{-1}$ of methane were produced at a COD nourishing of 1.38 kg $m^{-3} - MEC\ d^{-1}$ with acetic acid derivation to methane conversion which was 47 ± 17%. The benefit of biomethane was that it can effortlessly be transported or stored. Compression, transport in storages and pipes includes develop innovations and seem quickly be coordinates into an existing infrastructure (Cheng et al., 2009). CH_4 yield in the bioelectrochemical system as described in the literature was summarized in Table 2.7. In terms of power composition, H_2 generation was chosen over CH_4 generation because the methanogenic transition of H_2 to CH_4 results in a 15% kinetic loss of efficiency. Nonetheless, unavoidable CH_4 formation, H_2 can also be provided as high oxidation H_2 in MECs, making it unsuitable as a biochemical for specific uses. H_2 detoxification may also be energy inefficient, increasing power and production costs. Because high membrane costs, sustained pH functioning, and high dielectric breakdown cell reactance may be eliminated easily by deleting the nanoparticle membrane in MECs, several analysts have focused on (Tartakovsky et al., 2009).

Table 2.7: Methane production in different BECs.

Types of MEC	Types of Electrodes	Methane Recovery	Remarks	Reference
Single- and two-chamber MEC	a single electrode was used. Anode and cathode use graphite fiber brush and carbon cloth.	Overall energy efficiency of 70% Of CH_4. Supply voltage was –1 V.	CO_2 was converted to methane by electromethanogen esis. Abiotic archaea covered by both sides.	Cheng et al., (2009)
Membrane less. High surface area	Granular graphite electrodes in both side	The methane was produced of 0.33±0.07L $CH_4\ L^{-1}$ MEC day^{-1}. Convert methane of 65%. Applied cell voltage -0.8 V.	223 A m^{-3} of maximum current density. Acidified condition. Limited continuous systems.	Clauwaert, & Verstraete (2009)
Single chamber	Anode and cathode use graphite fiber brush and carbon cloth with Pt.	The methane of 28%. Voltage was 0.2 V and needed longer retention time.	Current density of 292 A m^{-3} . 87% of hydrogen and used 28 mL.	Call & Logan, (2008)
Single chamber	Anode and Cathode make graphite fiber brush and carbon cloth with Pt.	Found 3.1% of methane. Used 0.7 V of supply voltage. CH_4 higher than H_2 gas production.	Methane yield principally occurred. Acetate concentrations were highest.	Wang et al., (2009)

A two-chamber MEC with a membrane dividing the anode and cathode can experience intriguing concentration diminishment because of the accumulation of H^+ or OH^- in one chamber, given that they aren't generated through half reactions at the electrodes (Lee & Rittmann, 2010).

2.4.3.2 Biogas Upgrading

Biogas inferred from the AD of natural waste was a combination of CO_2 (25–50%) and CH_4 (50–75%). The most chemical condition for the biogas generation was: CH_3 - COOH $\rightarrow CH_4 + CO_2$. It was well known that the undesirable CO_2 will decrease the biogas quality and harm biogas compression. Biogas, once filtered by removing the impurities, basically CO_2, can be utilized as sustainable energy and low carbon fuel replacing conventional gas for power era and normal gas vehicle transportation. Strategies for biogas updating was centered on the CO_2 removal accompanied by a small CH_4 loss (Persson, 2003). However, the procedure for updated biogas generation by in situ changing over CO_2 into extra CH_4 and expanding CH_4 yield at the same time has never been reported. Quickly developing BEC innovation has been demonstrated to be a promising stage for CO_2 conversion and capture comparing with other techniques (Logan & Rabaey, 2012). With a little expansion of voltage at the MEC, electromethanogens can utilize hydrogen or electrons formed at the cathode to change over CO_2 into CH_4 straightforwardly (Cheng et al., 2009; Van et al., 2012). In the current operation, a novel method, i.e., coupling MEC and AD, for in situ changing over CO_2 into CH_4 and improving CH_4 generation at the same time was presented. In this modern prepare, the chemical condition for the biogas generation can be modernized as takes after: $CH_3COOH \rightarrow 2CH_4$, which has never been recorded.

Several endeavors were being affected to enhance the normal CO_2: CH_4 the ratio of around 2:3 within the biogas in arranges to increase the product quality for novel applications which was biomethane. Among the current biological biogas upgrading technologies, MEC with AD based innovation has newly developed as a promising alternative (Muñoz et al., 2015). A verification of theory carried out by Muñoz et al., (2015)

and it comes about in an enhanced biogas content CO_2<10% (v/v) with a recovering performance of the upgrading method when the electrodes were set inside the AD and the framework was worked in continuous mode. Besides, some current studies also demonstrated that the integration of AD and BES may fulfill biogas upgrading (Sravan et al., 2021). For example, Dou et al., (2018) embedded an anode and cathode in an AD reactor growing the methane content up to 98% (v/v), basically due to the in situ CO_2 reduction by the hydrogenotrophic methanogens which utilized the H_2 created within the anode and cathode as an electron donor. Other studies contributed to developing information on the electron exchange instruments for gas updating to BioM inside use hybrid biocathode, moreover announcing hydrogenotrophic methanogenesis by *Methanobacterium sp.* as the most mechanism for methane generation within the biocathode instead of coordinate electromethanogenesis (Dou et al., 2018). In any case of the need for long-term operation studies in bigger digesters, the promising results demonstrated in the lab-scale show the requirement to concentrate the attempts in a further up-scaling of the method.

2.4.3.3 Other bio-chemicals

Current research on bioelectrochemical systems (BESs) primarily focuses on the production of various fuels and chemicals beyond hydrogen, acetic acid, and methane (Rabaey & Rozendal, 2010). By applying additional electricity, the MEC's iron electrode facilitates the production of sodium carbonate and molecular oxygen, leading to improved overall productivity in wastewater treatment. While the electrolytic reduction of CO_2 using metals as electrocatalysts has been extensively studied for fuel synthesis, it has faced challenges in terms of sustainability and resource utilization. In contrast, microbial

electrosynthesis (MES) offers a more efficient and electron-rich alternative for electricity-driven biochemical and fuel synthesis. Recent investigations have reported the supplementary production of butyrate and ethanol through CO_2 reductions using lithoautotrophs in MES. Additionally, the formation of methanol from acetate as a substrate has been demonstrated at the electrode of BES. Most studies on microorganism capabilities for CO2 reduction have focused on hydrogen production at the cathode as a facilitating factor (Li et al., 2012). Strains such as *Ralstonia eutropha* have been genetically engineered to produce liquid fuel and methanol by modifying the traditional poly-hydroxybutyrate synthesis pathway. Xafenias et al., (2015) have successfully enhanced 1,3-propanediol production using glycerol as a material and a combined electrocatalyst. Furthermore, alternative mechanisms have been proposed for the creation of acetone, butanol, and succinate through bacterial pathways.

2.5 H-MECs MICROBIAL PATHWAY

H-MECs were a concept established from MES with an AD system in which an external voltage was utilized to exceed the metabolic potential barrier in order to drive biological processes. During AD, organic substances were decomposed in an oxygen-free environment, resulting in the creation of a gas blend termed biogas. This biogas is composed of methane (constituting 50–70% by volume), carbon dioxide (making up 25–50% by volume), and trace amounts of hydrogen, hydrogen sulfide, ammonia, and other minor gases. Electromethanogenesis produces BioM in two different ways: directly through the uptake of electron density from an electron beam as represented in Equation 2.6, or indirectly through the production of hydrogen as well as other molecules including

acetate and formic acid, which were then mixed with CO_2 to form BioM and water as shown in Equation 2.7 & 2.8 (Ai L et al., 2022).

$$CO_2 + 8H^+ + 8e^- \rightarrow CH_4 + 2H_2O \quad (2.6)$$

$$\rightarrow 240mV \text{ (Direct electromethanogenesis)}$$

$$2H^+ + 2e^- \rightarrow H_2 \rightarrow 400mV \text{ (Indirect electromethanogenesis)} \quad (2.7)$$

$$CO_2 + 4H_2 \rightarrow CH_4 + 2H_2O \quad (2.8)$$

Hydrogen-consuming microorganisms possess the capability to transfer electrons from the cathode, enabling direct electromethanogenesis, while methanogenic microorganisms present in the biocathode play a significant role in both direct and indirect electromethanogenesis (Guo et al., 2013). H-MECs used for BioM production consist of four essential components: anode, biocathode, ion exchange membrane, and voltage supplier, as shown in Figure 2.8. Additional components depicted in Figure 2.8 include a water storage tank, microbial storage tank, electrodes, connecting pipes, ball valves, methane gas chamber, pump, and gas measuring meter, among others. The anode initiates the oxidation process to generate electrons required for carbon dioxide reduction on the biocathode's surface. The biocathode, on the other hand, is crucial in facilitating the creation of methane by utilizing electrons supplied through the anode's oxidation process with the assistance of bacteria.

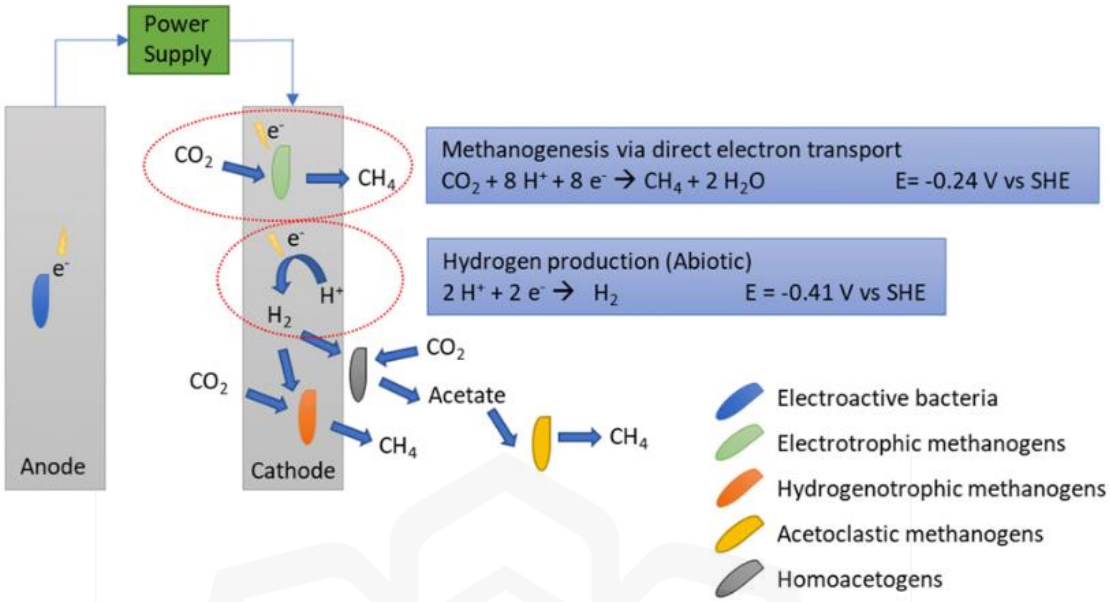

Figure 2.8: Schematics of a typical H-MEC with AD for electromethanogenesis (Buitrón et al., 2019).

An ion exchange membrane was required for ions with positive charges such as H^+ to migrate from the anodic chamber to the cathodic chamber of the H-MEC system. Finally, external power electrical energy was required to thermochemical drive the process. For the electrochemical conversion process to create BioM, a modest voltage source such as a range of 100mV – 1000mV was required (Buitrón et al., 2019). Bacterial constructions in microbiological storage tanks comprise mainly negative bacteria and escherichia coli species. The bacteria's normal metabolism was used to make CH_4. Bacteria turn the substrates to create electrons. This method was an innovative and promising technique for converting CO_2 into sustainable biofuel (CH_4). Charged particles and ions were used by cathode oxygen such as O_2 and create water at the cathode. To address the current issue, MFC may be more appealing. AD connected H-MEC-based electroactive microorganisms as shown in Table 2.10.

Table 2.8: Electroactive microorganisms utilized in H-MECs for BioM yield.

Substrate	Electrogenic bacteria	Electroactive Microbes Shape	MEC	Applied Voltage	Reference
Food waste and Sewage sludge	*Methanobacterium sp.,*	Gram-negative, nonmotile, rod and shaped, obligately aerobic, and facultatively.	Two chamber MEC-AD, and single AD	0.4 V	Zhi et al., (2019)
	Methanosaeta sp.	Gram-negative, rod-shaped and non-motile, occurring singly.			
Anaerobic digester sludge	*Methanobrevibacter sp.*	Gram-positive organisms form pairs, straight rods, helical chains and coccobacillus shapes.	Two chamber MEC	0.7V	Siegert et al., (2015)
Leachates Industrial waste	*Desulfuromondales sp.,*	Strictly anaerobic, rod-shaped, laterally flagellated and Gram-negative.	Two-chambered MEC-AD	0.7 V	Gao et al., (2017)
	Pseudomonas sp	Gram-negative, rod-shaped, asporogenous, and mono-flagellated.			
Metro polytan wastewater	*Methanobacterium sp.*	Rod, curved, crooked, or straight rods, long to filamentous and gram-positive in electron micrographs.	Two-chambered MEC-AD	0.8 V	Cai et al., (2016)
Waste activated sludge	*Geobacter sp.*	Rod-shaped, motile, gram-negative, and anaerobic bacterium	Single-chamber membrane-(MEC) and non-MECs	0.6V	Guo et al., (2013) Sun et al., (2015) Yin et al., (2016)
	Methanosarcina sp.	Irregularly shaped cocci were gram negative and occurred singly.			
Acetate	*Geobacter sulfurreducens sp.*	Gram-negative metal and sulphur reducing proteobacterium.	Two chamber reactors.	0.85 V	Villano et al., (2011)
Alkaline pretreated sludge	*Methanosaeta Sp.*	Gram negative, rod-shaped, non-motile, and usually found singly.	Two identical MEC-AD	0.8 V	Xu et al., (2020)
MR-1 Acetate	*Shewanella oneidensis sp.*	Gram-negative proteobacteria that were typically rod shaped.	Double chamber MFCs	0.14V	Xio et al., (2020)

Exoelectrogenic microorganisms metabolize organic materials in a MEC, producing CO_2, ions, and protons. The microorganisms deliver charged particles to the anode and produce protons into solutions. In principle, producing hydrogen at a MECs cathode requires just approximately 0.1 V of independent power. Therefore, due to over-potentials at the electrodes, a potential of 0.3 V or more was required. This electrical supply was far lower than the 1.8 to 2.0 V typically needed for water oxidation.

2.6 H-MECS HYDROGEN GROWTH RESPONSE

Because of the rising global energy demand, existing power-producing methods may degrade the environment. Power generation that was both environmentally benign and sustainable was a problem for future civilizations. The environmental issues generated by energy sources have shifted emphasis to sustainable, reduced, and low-carbon-emitting technologies (Guo et al., 2013). Hydrogen (H_2) was a compelling alternative to fossil fuels in the coming years. Due to its recovery and recycling and lack of toxic byproducts, hydrogen was an environmentally friendly and safe alternative to conventional carbon fuels. In today's environment, hydrogen was produced by converting hydrocarbons, a process that isn't feasible and results in large carbon dioxide (CO_2) releases. H_2 might be created by electrical and chemical hydrogen growth response in the context of a reduced catalyst that connects sustainable energy sources including wind, photovoltaics, hydroelectricity, and biofuels, increasing the rate of hydrogen synthesis. It was also the most effective and viable way for producing high purification and huge quantities of hydrogen. Since the 22^{nd} century, hydrogen growth response was one of the most researched electrocatalysts. In spite of its substantial cost, photocatalysis provides an

efficient technique for producing extremely pure protons. Hydrogen growth response ($2H^+ + 2e^- \rightarrow H_2$) was a form of electrical and chemical reaction process that may also create H_2 (Benck et al., 2014). Hydrogen growth response was a classic single catalytic step two electron transfer reaction that yields H_2 as shown in Figure 2.9. Hydrogen growth response (HGR) may lead to the long-term viability of hydrogen fuel, which was transferable, reusable, and adaptable in zero-emission conventional combustion fuel cells. The creation of hydrogen from H-MECs were a sustainable technology for producing H_2 from natural materials such as food waste under the influence of an electric charge. An external power supply in the form of the applied voltage was necessary to push the negative free energy of the reaction, resulting in the production of hydrogen in the cathode chamber.

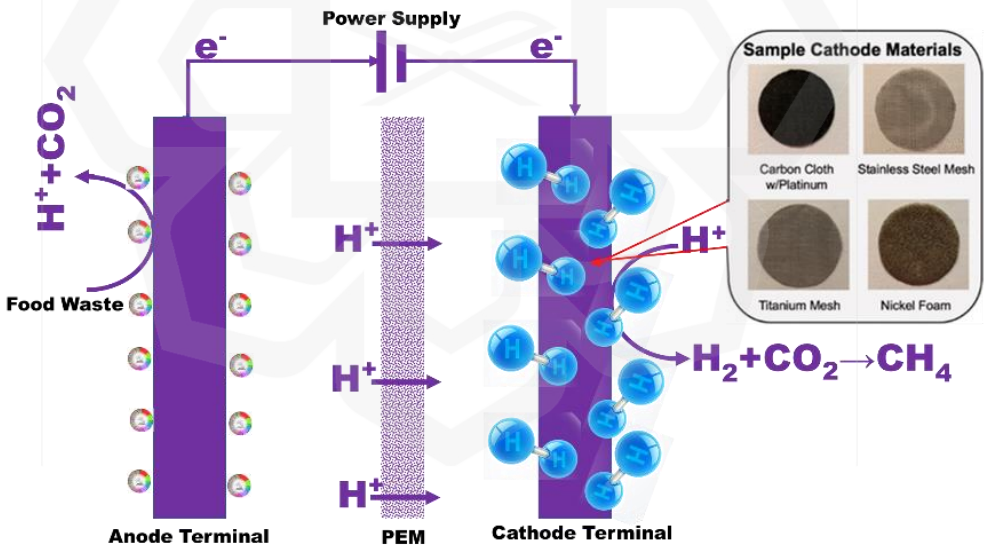

Figure 2.9: Summary of MEC catalysts used in novel material for hydrogen growth response (Zhou & Gu, 2013).

The feedstock in this H-MEC mechanism was oxidized by microorganisms, which creates ions, protons, and CO_2. The external power supply transfers electrons to the

cathode, whereas the membrane for proton exchange transports ions (H^+) to the cathode chamber. Protons diffuse to the cathode side, where they interact with electrons to form H_2 (Zhou & Gu, 2013).

2.7 SELECTION MATERIALS USED IN H-MECs

The materials utilized to design the MECs device were crucial in determining the overall system performance. By analyzing the type of content, one may determine whether it creates value and a competitive advantage for commercial applications. When going to put up a MEC device, the overall price of the conductors and membranes was measured. Material minimization in a MEC was crucial and must be taken seriously for an efficient model.

2.7.1 Anode Chamber Materials

In the realm of MECs, there's a strong demand for anodes possessing specific attributes including superior electrical conductivity, biocompatibility, chemical stability, corrosion resistance, scalability, low resistance, resistance to fouling, robust mechanical strength, and ample surface area. These qualities are deemed crucial for enabling acidogenic bacteria to effectively utilize anodes for aerobic metabolism. Carbon-based electrode materials are prevalent due to their high electrical conductivity, strong biocompatibility, cost-effectiveness, stability, and minimal overpotentials. Various carbon-based anodes, such as carbon sticks, graphite felt, carbon paper, carbon cloth, carbon fiber, graphite granules, and porous graphite felt, have been employed for CO_2-to-CH_4 conversion, as outlined in Table 2.9.

Table 2.9 Anode types utilized in double chamber MECs

Reference	Anode Terminal	Types of MEC	External Voltage	Methane Yield
Zhen et al., (2015)	Carbon  Sticks	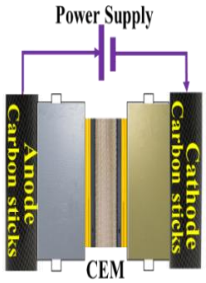	Applied −900V. Anode chamber was filled 100-mM NaCl.	CO_2 flushing was effectively improved. 2.30 ± 0.34 mL of CH_4
Cerrillo et al., (2018)	 Carbon Felt	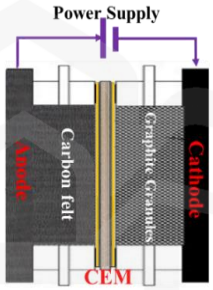	Used −800 mV. Anode 14.46 g N-NH_4 586 + m^{-2} d^{-1}.	79 L CH_4 m^{-3} d^{-1} conversion of CO_2
Huang et al., (2014)	Porous  Graphite Felt	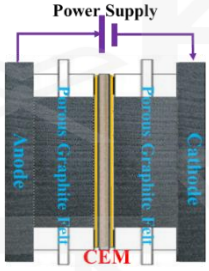	200 mV and Sodium acetate (12.2 mM) in the anode.	0.113 mol/mol of CH_4 Current was normalized in the cathode.
Van et al., (2013)	 Graphite Felt	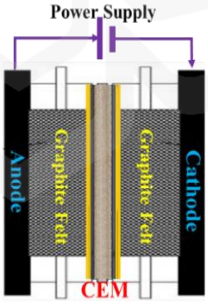	−700 mV and the cathode current density was 0.60 ± 0.16 A/m2 projected cathode.	5.1 L/m^2 projected per day. Hydrogen (35.7% H_2 (v/v)) was detected in the cathode

MFC frequently creates a low operational voltage in relation to the electrical potential of the cell, which was typically referred to as unsustainable kinetically determined possibilities. Energy dissipation can occur in a variety of directions, including

initiation loss, microorganism metabolism loss, charge transport loss, and leakage currents due to a number of factors, the most widely accepted of which was additional mycelium and the chemical molecules created by the starter culture, which can cause bacterial growth of the anode, minimizing the transfer of electrons from the bacterium to the anodic substance. The use of nanoparticles in anodic transformation was one such technique. The nanoparticles increase electron transport by facilitating the development of electroactive bacterium. Different nano-metal or oxide metals, including Mno_2, iron oxides, and Tio_2, were utilized to modify the anode outer edge in order to maximize the inoculum's retaining capacities and increase the electron's electricity transfer rate. Iron oxide can induce EET via two mechanisms: as an electrical conductor inside the biofilm or as interaction by developing on the cell membrane (Nakamura et al., 2013).

2.7.2 Cathode Chamber Materials

Cathode chamber materials were critical in both electrohydrogenesis and electromethanogenesis. Electromethanogenesis requires less electricity than electrohydrogenesis which was used in a range of 0.23 V to 0.41 V versus SHE. Therefore, more power was often needed to eliminate cathodic ionic conductivity. Cathode chamber material parameters, such as porous structure, high conductivity, and cytocompatibility, will now performance a significant role in the MEC impact of development. According to Rozendal et al., (2008) the cathode provides for 47% of the overall cost savings for constructing MECs. The total quality of MECs were determined by the electrodes and materials used to create devices. Methane was produced via CO_2 conversion on both electrodes: anode and cathode, using directly transferred electrons or

oxidation reactions. For the construction of CO_2 to CH_4, different carbon-based cathodes including carbon stick, nickel steel, carbon cloth, carbon fiber, graphite granules, and carbon felt were utilized as shown in Table 2.12. Nonspontaneous responses often occur in the cathode area, which necessitates the use of a particular material to catalyze oxidation and reduction. Platinum, for example, demonstrated its catalytic capability by optimizing oxidation and reduction. It was a valuable metallic element with excellent biocompatibility. However, there were other drawbacks, such as negative environmental effects and expensive costs. Because of their ease of access, cheapness, consistency in alkaline conditions, and low activities, materials including stainless steel alloys and nickel have been found to be efficient options. Stainless steel has been used in the development of anaerobic digesters paired with single-chamber MECs to increase methane output (Moreno et al., 2016). In addition to stainless steel, electrocatalysts dependent on alloys including iron-graphite and Ti/Ru have developed to increase CH_4 generation in the sudden appearance of sewage sludge (Guo et al., 2013). Carbon-based cathodes made of parietal graphite and porous carbon could also be advantageous for methane generation. Siegert et al., (2015) studied the generation of CH_4 in valuable metals such as platinum, nickel, and stainless steel and nonprecious carbon-based materials like carbon black, plain graphite, and carbon brush. Also, the author discovered that a simple graphite cathode generated more methane than a precious metal-based cathode. Cathodic materials made of carbon sticks and graphite felts had the best methane output and cathode conversion efficiency.

Table 2.10: Cathodes types utilized in double chamber MECS

Reference	Cathode Surface	Types of MEC	Voltage (mV)	Bacteria and Methane Yield
Zeppilli et al., (2015)	Graphite Granules	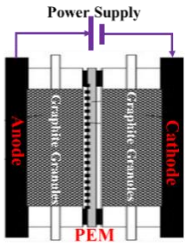	−200. 70–81 % of current converted into CH_4 cathode.	*Methanobrevibacter arboriphilus and Methanosarcina mazei.* 47.7 ± 4.8 (meq/d) of CH_4.
Ding et al., (2016)	Carbon Felt	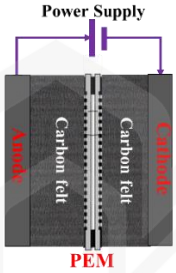	−800. Cathode 46- 66 % of current converted into CH_4.	Phosphofructokinase and alters fructose-6-phosphate to fructose-1,6-bisphosphate. 62.8 mL of CH_4
Sugnaux et al., (2017)	Nickel Steel	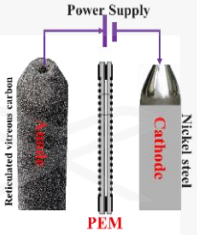	+2000. Cathode 67–75 % of current converted into CH_4	*Methanothermobacter marburgensis and M. thermautotrophicus*. 68.7% of CH_4
Villano et al., (2011)	Graphite Granules	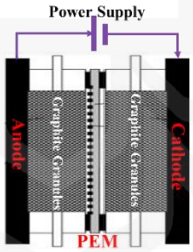	+500. Cathode 67–81 % of current converted into CH4	*G. sulfurreducens* 6.4 meq L^{-1} d^{-1} of CH_4
Zhen et al., (2016)	Carbon stick	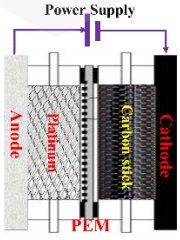	−1400. Cathode 36-58% of current converted into CH_4.	*Methanomicrobiales* 80.9 mL/L of CH_4

Carbon nanotubes having many walls that have been modified with catalytic compounds like as s platinum, ammonia, iron phthalocyanine, nickel, and manganese

oxide was utilized as replacements for cathodic material to improve the rate of methanogenesis (Siegert et al., 2015).

2.7.3 Membrane Materials

Membranes were MEC components that were utilized to spatially separated the cathode and anode into sections. This separator was crucial in the construction of any two-chambered MEC. Membranes inhibit substrates, hydrogen gas, hydrocarbons, and microorganisms from mass diffusing between the anodic and cathodic chambers. These only enable protons to move across electrodes. It was essential to consider pH fluctuations in Table 2.13. These also serve as a separator to prevent short circuits in MECs. MECs used a variety of membranes, including the widely utilized proton exchange membrane Nafion. In MEC reactors, ion exchange membranes like AMI-7001 (Cheng et al., 2009), CSO monovalent-cation-selective exchange membranes (Zhen et al., 2015), Nafion membrane (Siegert et al., 2015), Ultrex CMI-17000 (Hou et al., 2015), Ultrex CMI-7000 (Xafenias & Mapelli, 2014), None-woven fiber (Park et al., 2018) and Tubular anion exchange membrane Zeppilli et al., (2020) have been tested. Types of membrane used in two-chambered MEC. It was important to observe the variations in pH gradient throughout the membrane caused by cation exchange instead of proton exchange, which results in lower pH at the anode and increased pH at the cathode. This pH shift can have a deleterious impact on microbial load in both the anodic and cathodic chambers (Sun et al., 2009).

Table 2.11: Membranes types utilized in double chamber MECS

Reference	Anode and Cathode of MEC	Membrane	Applied Voltage	Methane Production
Park et al., (2018)	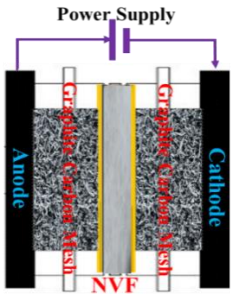		300 mV and 0.45-µm membrane filter was used.	Final steady state (290 –365d). Start (1 – 69 d). Midway steady state (70–289d).
Zeppilli et al., (2020)	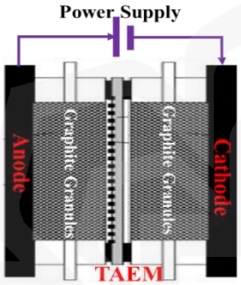		200 mV and the inner anodic of 3.14 L was separated	300 meq/d when HCO_3^- ion from AEM membrane.
Siegert et al., (2014)	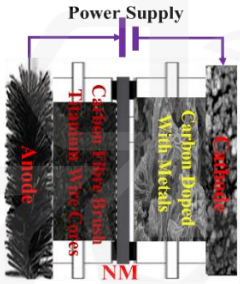		−600 mV. Length of 3.8 cm. Diameter of 2.4 cm Separated by a NM.	Molar hydrogen production rates of 247 ± 87 nmol cm^{-3} d^{-1}. .
Siegert et al., (2015)	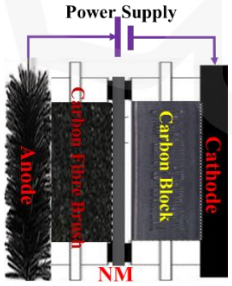		−600 mV. Length of 3.8 cm. Diameter of 2.4 cm. Separated by a NM.	250 ± 30 nmol cm^{-3} d^{-1}. Carbon fiber brushes of (4×4cm, 740 m^2). Graphite blocks of (2×2×.32cm)

2.8 MECS ELECTRON TRANSFER MECHANISMS

The electron transfer methods appropriately seen in MESs appear close to the mechanisms studied for dissimilatory metal decreasing microbes (Louro et al., 2019). The different recommended electron transfer mechanisms in the MESs were demonstrated in Figure 2.10.

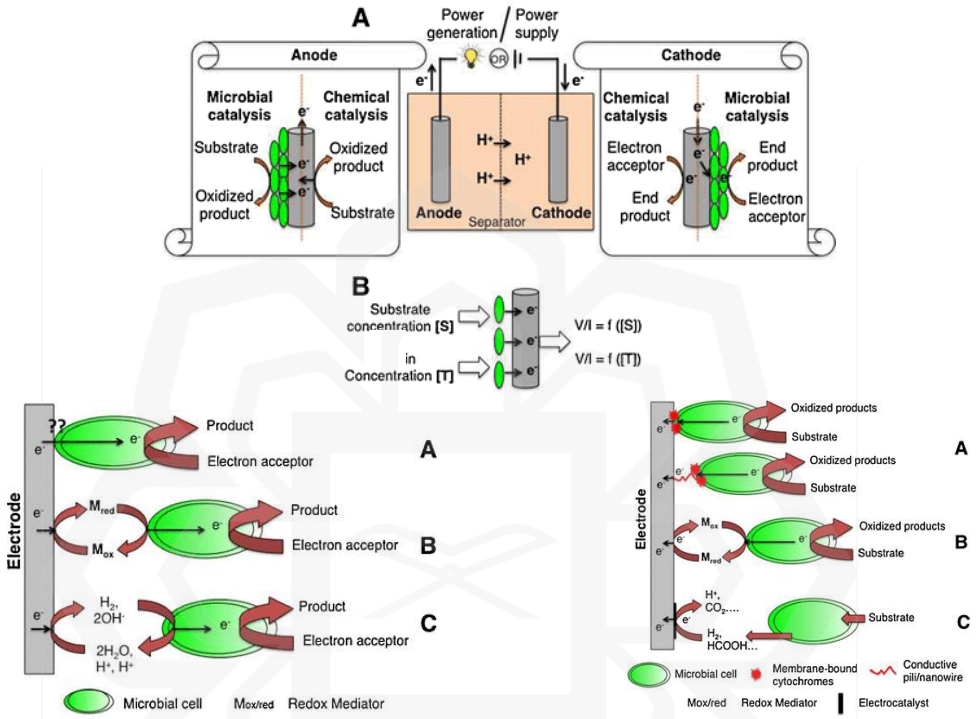

Figure 2.10: Microorganism–electrode transfer based bacterial MES. It appears via (A) electrically conductive pili (nanowires), (B) mediators exogenous redox, and (C) primary metabolites via oxidation of reduced (Pant et al., 2012)

Several other bacterial structures which include both side of Gram-negative and Gram-positive microorganisms, such as *Bacillus subtilis* (Nimje et al., 2009), *Corynebacterium sp.* (Liu et al., 2010), *Escherichia coli* (Weld et al., 2011; Veer Raghavulu et al., 2011), *Klebsiella pneumoniae* (Xia et al., 2010; Zhang et al., 2008), *Pseudomonas sp.* (Venkataraman et al., 2010; Timur et al., 2007), and *Proteus vulgaris* (Yuan et al., 2011; Kim et al., 2000), were also used to verify their applicability in MECs. Groups of different microbial phyla like *acidobacteria, bacteroides, deltaproteobacteria, firmicutes*

sphingobacteria, and *alpha-*, *beta-*, *gamma-*, developed from various natural sources of inoculum fed in the cathode chamber with pure substrates (Logan 2009; Chae et al., 2009). Similarly, the capability of such yeasts as *Arxula adeninivorans* (Haslett et al., 2011), *Saccharomyces cerevisiae* (Raghavulu et al., 2011; Walker & Walker, 2006) and *Hansenula polymorpha* (Shkil et al., 2011) to operate as anode catalysts was shown (Prasad et al., 2007; Babanova et al., 2011). Within MECs, a novel concept emerged known as electromethanogenesis, where methanogenic bacteria employ an electrochemical process at the cathode, using electrical current as a reducing power to produce CH_4. As per equation (1), it was observed that the efficiency of converting consumed electrons at the cathode into methane reached up to 96%. However, the underlying molecular mechanism of this reaction remains unexplained thus far. Some investigations have supported the theory that methanogenic archaea might directly generate protons and electrons (as shown in Equation 2.9) (Van Steendam et al., 2019).

$$C0_2 + 8\,H^+ + 8\,e^- \rightarrow CH_4 + 2\,H_2O \quad (2.9)$$

During the electromethanogenic method, a large number of hydrogen growth was not found (Perona et al., 2019). Nevertheless, there was still a probability that the procedure requires the *de novo* structure of molecular hydrogen in Equation (2.10), which was then directly used for hydrogenotrophic methanogenesis in Equation (2.11) by methanogens. The structure of molecular hydrogen as shown in Equation (2.10) will occur as an abiogenic electrochemical reaction (Vladimirov et al., 2004).

$$2\,H^+ + 2\,e^- \rightarrow H_2 \quad (2.10)$$

$$C0_2 + 4H_2 \rightarrow CH_4 + 2\,H_2O \quad (2.11)$$

2.8.1 Electroactive Bacteria Electron Transfer Mechanism

According to the findings, electroactive microorganisms do not have a single evolutionary path. Significantly more electroactive microorganisms were likely to exist in the environment as well as established strain collections, however, their EET capability was being underutilized due to present culture procedures as established in Figure 2.11.

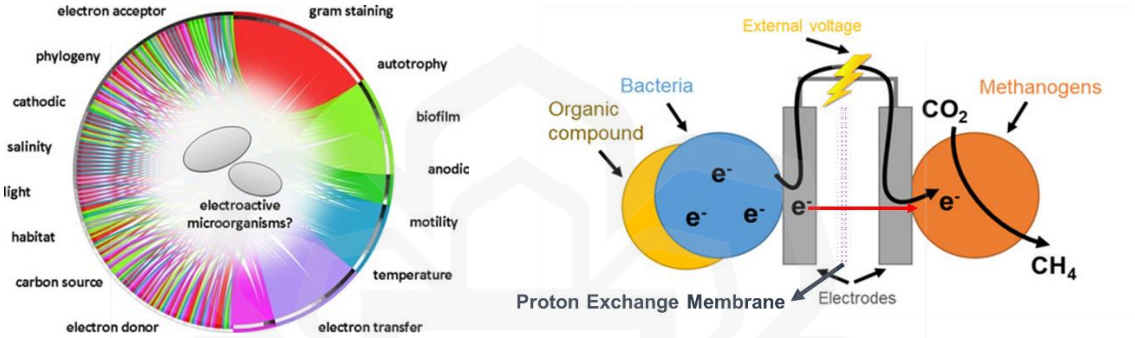

(a) (b)

Figure 2.11: H-MEC for (a) electroactive bacteria (Koch & Harnisch, 2016) and (b) electron transfer mechanism (Jones & Solomon, 2015).

The inner-sphere process involves the sharing of a crossing molecule between two different metals, while the outer-sphere method involves the direct exchange of electrons between two different metals without the utilization of a crossing molecule.

2.8.1.1 Anode Chamber Electron Transfer Mechanism

Different types of bacteria can grow in H-MECs on either the anode terminal or the cathode terminal. Gram-negative bacteria including *Geobacter spp.* and *Shewanella spp.* were commonly found on the anode terminal, which also oxidizes organic materials and generates an electron flow as shown in Figure 2.12. H-MEC-based AD systems were electrochemical conversion devices that convert the molecular type of energy held in the

feedstock to high-value-added compounds like methane, acetate, hydrogen, and others. The substrate concentration of specific species of bacteria that can create electrons or decrease CO_2 was used for this biodegradation process. Electroactive microorganisms were the name given to these microbes (Kadier et al., 2016). The development of volatile byproducts like methane in MEC was greatly influenced by the interaction of microorganisms with other elements. Transfer of electrons from organic substances (or substrate) to the electrodes was crucial for the efficient operation of MECs. The ability to effectively design H-MECs can be improved by having a better understanding of this microbial extracellular electron transfer mechanism.

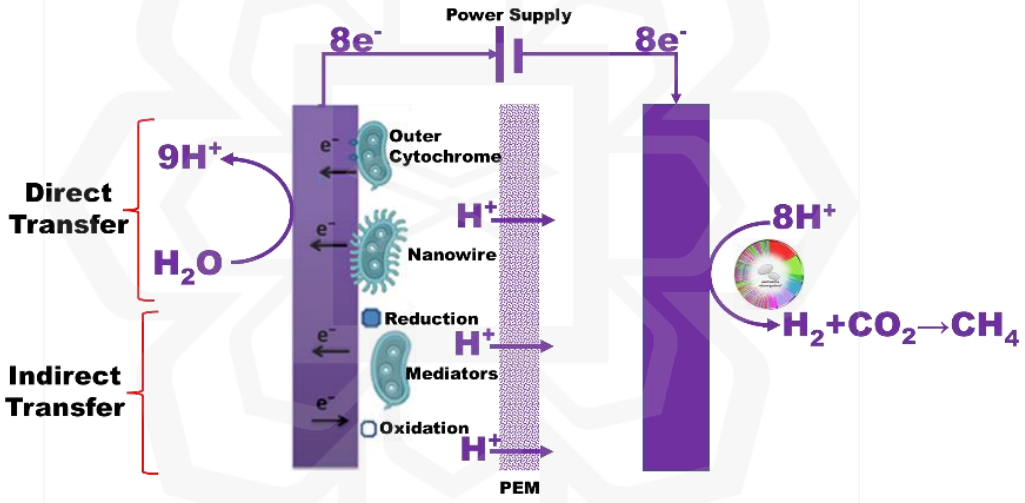

Figure 2.12: A schematic of electron transfer from exoelectrogen to anode and pathway in *Shewanella* (Kadier et al., 2016).

Electrotrophic microorganisms were those that can take electrons, whereas exoelectrogens were those that can transmit electrons to cell membranes. Electroactive microorganisms have been discovered in a number of settings, including, anaerobic sewage sludge, residential wastewater, and ocean and sea sediments.

2.8.1.2 Electron Transfer Mechanism at Cathode Terminal

Protons and electrons produced through catalytic oxidation were used on the cathode surface to reduce CO_2 both directly and indirectly. Direct electromethanogenesis occurs in the biocathode via redox outside cell membranes in the presence of isoenzymes in interaction with the negative electrode (Blasco-Gómez et al., 2017). In contrast to cytochrome, other outer membrane enzymes implicated in electron transport include ferredoxin, rubredoxin, hydrogenase, and/or base-catalyzed dehydrogenase. Conducting biofilm participates in EET of electromethanogenesis in the same way as bioanodes do as show in Figure 2.13.

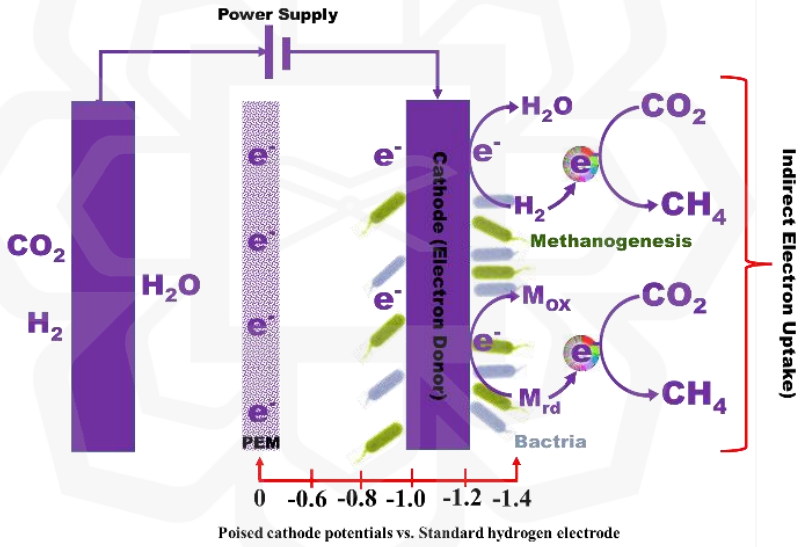

Figure 2.13: Indirect microbial electron transfer scheme for the methane production at the cathode (Blasco-Gómez et al., 2017).

Additional electron shuttlers or intermediaries, such as riboflavins, phenolic acid, and 40 % of the total released by bacteria, can increase electron transport and, as a result, indirect electromethanogenesis. Transfer electrons organisms that convert CO_2 to CH_4 such as *Methanosaeta* and *Methanosarcina* may be exoelectrogenic directly from

elemental iron (Rotaru et al., 2014). A higher proportion of methane was produced by the carbon dioxide reduction process depicted in Figure 2.14. The metabolic pathway methanogenic microorganisms can develop including both anode surfaces and cathode surfaces, although they prefer the cathode. *Methanospirillum, Methanobacterium, Methanosarcina, Methanocorpusculum Methanoculleus,* and *Methanobrevibacter* have been discovered to develop on anodes surface, implying the capability of methane production (Gao et al., 2017). On the other hand, *Methanosarcina* may generate methane via the hydrogenotrophic and acetoclastic pathways. On the cathode chamber, *Methanobrevibacter, Methanospirillum* and *Methanoregula* have been seen developing (Siegert et al., 2015).

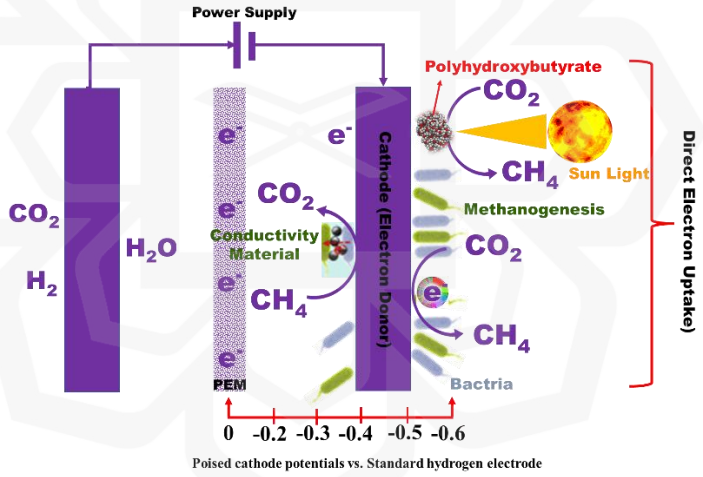

Figure 2.14: Direct bacterial electron transfer system for the BioM yield (cathode side) (Gao et al., 2017).

Microbes also including *Methanosaeta* and *Methanobacterium* employ electrons to directly create CH_4 using carbon dioxide reduction. Increased CH_4 generation was observed while different based on recommendations of methanogens congregate to a certain amount and become linked with the electrode. Electromethanogen

hydrogenotrophic interactions play a significant role in CH_4 generation by forming on the cathode side (Baek et al., 2018). In contrast, methanogens including *Methanocorpusculum* were ineffective at arresting negative electrons and rely on the cross-species transfer of electrons performed by electroactive bacteria including *Geobacter or Acetobacterium* (Buitrón et al., 2019). The electro syntropy of specific bacterial communities for CH_4 yield was affected by the type of electrocatalyst used and the microorganisms existing in the experiment. To improve CH_4 synthesis in H-MECs, it was critical to comprehend the concept of electron transport between electroactive bacteria and an electrode. The precise process for electron transport has yet to be determined. Conversely, three recognized routes explain the production of CH_4 by H-MECs. Firstly, the electron transfer mechanism process relies on direct electron transfer from microorganisms to an interconnection via external membrane proteins like cytochrome. Another method occurs in the presence of soluble electron shuttles (compounds such as quinones, flavins, melanin, and phenazines which move electrons between microorganisms and the electrode via diffusive transport. Whereas the third consideration emphasizes a characteristic that was part of the intracellular periplasmic space which was referred to as nanomaterials and was accessible for the transfer of electrons from microorganisms to the cathode as an electrophile (Reguera et al., 2005).

2.9 CONFIGURATION OF AD BASED H-MEC SYSTEM

The layout of the chamber in MECs was critical in selecting the method to make or convert CO_2 to CH_4. The design of MEC has a direct impact on CH_4 output, overall fuel efficiency, and operational costs. Reactor operating designs, including single-chamber

and double-chamber options, have been proposed. The existence or absence of proton or ionic exchange membranes in the system determines the chamber structure, which normally divides the structure into one or two chambers.

2.9.1 Configuration of Single-Chamber H-MEC

Decoupling membranes from double-chambered systems results in single-chambered MECs. As a result, the anode and cathode stay inside the same liquid of the single chamber, reducing both the electromotive force voltage difference and the pH imbalance. This lessens the particular risk caused by the membrane barrier. It also reduces the reactor's high initial investment and streamlines its construction. Manufacturing and purification were simplified as a result of this benefit. Because it doesn't entail membrane-related problems such as contamination and impedance, single chamber reactors were simple to build and maintain (Selembo et al., 2009). Furthermore, the single-chamber MEC structure promotes the growth of hydrogenotrophic methanogens, which create CH_4 by consuming H_2. Materials were reported to be used in the construction of single chamber reactors. Materials including polypropylene, acrylic, and stainless steel have been described to be used in the construction of single chamber reactors. Several MEC prototypes with single-chamber configurations have been used to create CH_4. A single chamber MEC with a flat stainless-steel cathode and a graphite block anode was one such configuration as shown in Figure 2.15. From Figure 2.15 shown that the cathode was built of a stainless-steel-based proton exchange membrane which was positioned vertically and anode fabricated of graphite block which was placed at the bottommost of the reactor plumb. At an applied protential range of 100mV- 700mV, the reactor realized methane

yield of around 0.028 $m^3/m^3/d$. On the other hand, the anode terminal was constructed from graphite fiber brushes the volume of $0.8m^3$.

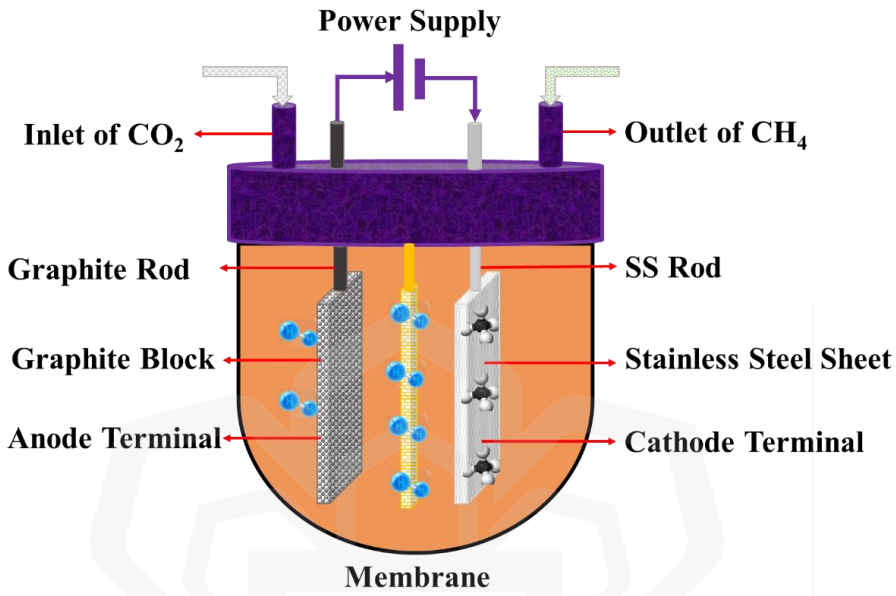

Figure 2.15: Single-chambered H-MECs block diagram

Stacked cathodes terminal diameter of 0.05 m and 60 mesh were produced and placed in classification by titanium wires with a 5 mm abaxial surface using diverse layers of round shape stainless-steel materials. The relatively high area was created, and when the ratio of cathode porous structure volume was more than 2.5, it was effective in increasing CH_4 yield. Concentric electrodes in a tubular design were utilized as a substitute MEC preparation for improving CH_4 yield during anaerobic digestion.

2.9.2 AD based H-MEC of Two-Chamber Configuration

The two-chamber design was the most common kind of MEC, because the cathode and anode function independently in two compartments separated by a membrane. The

cathode and anode were linked via an electrode surface to which amount of electricity was provided by a source of energy throughout this setup as show in Figure 2.16.

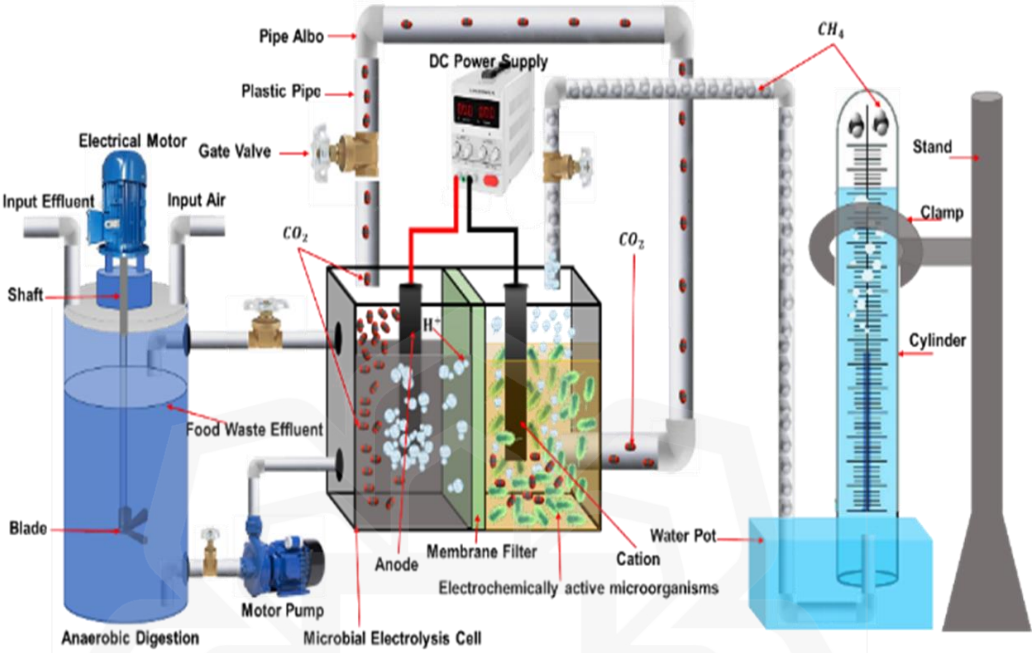

Figure 2.16: Block diagram of the two chamber AD based H-MEC system

Several membranes have been utilized in two-chamber design MECs, with the most popular being a proton exchange membrane created utilizing structural features and allowing only free protons (H+) to flow through (Torres et al., 2007). Charge-mosaic membranes, bipolar membranes and anion-exchange membranes such as AMI-7001 were also utilized in two-chamber MECs. At terminal voltage ranging from 200mV to 1200mV, CH_4 yield reached 656 mmol/m^2/d. The constructed two-chamber MEC process to creation CH_4 from acetate using *Geobacter sulfurreducens* as a microbial bioanode connected to a methanogenic microbial biocathode (Varanasi et at., 2019). The two-chamber MEC design was more sophisticated than the single-chamber reactor setup.

However, the negatives impact includes expensive membrane rates, membrane susceptibility and degradation, and pH imbalance created by the membrane's use.

2.10 MEMBRANE AND SEPARATOR MECHANISMS FOR MECs

The primary role of the MEC membrane was to segregate the anode and cathode reactions while obstructing the transfer of hydrogen from the anode to the cathode chamber. Concurrently, it permitted selective ion transport between the anode and cathode. The materials employed for MEC membranes can be categorized based on their degree of fluorination, including acid-base blends, perfluorinated ionomers, nonfluorinated hydrocarbons, nonfluorinated membranes with aromatic backbones, and partially fluorinated polymers (Yasri et al., 2019). The efficacy of ionomer membranes as ion-conducting materials stemmed from the hydrophilic nature of sulfonate groups that attract water. When these membranes became hydrated, protons gained high mobility in the hydrophilic regions formed by the sulfonic acid groups, effectively forming channels through which H+ ions could move freely under an increase in potential (Gatto et al., 2019).

Nonetheless, the paramount role of a membrane was the segregation of the anode and cathode chemistry. Three critical parameters determined the behavior of separator materials: ion exchange capacity, porosity, and pore size (Ahamed & Asiri, 2019). These separators were broadly categorized into semipermeable and permeable types. Semipermeable separators selectively allowed specific species to pass based on molecular charge. In electrochemical contexts, these were labeled as "membranes" and the separation was contingent upon the molecule's charge. Conversely, permeable separators permitted bulk liquid flow but lacked selectivity, allowing neutral molecule transport. In

electrochemical contexts, these were also referred to as membranes. The simplest form of separators was porous separators that hindered the combination of gaseous products due to appropriately sized pores, usually in the range of 1–50 μm (Yasri et al., 2019).

2.11 FACTORS AFFECTING PARAMETERS IN MECs

Various elements impact the performance of microbial electrolysis cell (MEC) systems. These factors include the type of electrode substance, pH level, electrode surface area, temperature, solution conductivity, internal losses within the system (like concentration and ohmic losses), and the quantity of catalyst loaded into the system (Khan et al., 2017). The essential parameters that influence the generation of methane and the energy recuperation in MEC systems were explained.

2.11.1 Substrate

Industrial, municipal and household wastewaters have all been tested for methane generation. Using all these waste items as a substrate for methane production also aids in pollutant removal, indicating that the MECs technique for manufacturing CH_4 was ecologically beneficial. The average methane production and the substrate consumption dynamics during the incubation time. The most commonly was used in CH_3COONa substrate for CH_4 production of MECs.

During the first operation time, the bio-reactor was injected range 0.2 g/L to 0.5 g/L CH_3COONa. For the second step of this process, the operating condition was changed to 0.4 g/L to 0.9 g/L, followed by increases in CH_3COONa to 1 g/L and 1.8 g/L in succeeding stages. In one litter of solution, the following elements of synthetic

wastewater were formulated: 0.116 g NaCl, 0.31 g NH_4Cl, 4.4 g KH_2PO_4, 0.1 g $MgCl_2$ $6H_2O$, 3.4 g KH_2HPO_4, and 0.13 g KCl.

2.11.2 pH

The pH level of the medium in MEC systems plays a pivotal role since it impacts the kinetics and thermodynamics of the reactions (Khan et al., 2017). The pH inversely correlates with the cell potential (E-cell), with the anodic reduction potential decreasing by 0.059V for each pH unit increase. Liu et al., (2014) identified an optimal pH of 9 for the reduction of chemical oxygen demand (COD) and hydrogen (H_2) production in MEC systems. Any deviations from this optimal pH, whether higher or lower, can influence the production of gases. Furthermore, alkaline pH conditions were found to be favorable for microorganisms, while acidic pH conditions were more suitable for fungi. Nimje et al., (2011) observed heightened electrochemical activity when the anolyte pH was elevated from 7 to 9. The rationale behind the increased electrochemical activity at higher pH values was that exoelectrogenic populations exhibit a preference for higher pH to facilitate electron transfer to the anode (Khan et al., 2013).

2.11.3 Temperature

Temperature served as a critical factor impacting the efficiency of energy and the power density within MEC systems. The dominant aspect of the MEC configuration was anaerobic, where the mobility of bacteria was influenced by temperature, such as within the mesophilic range of 35–40°C (Khan et al., 2014). A study conducted by Di Lorenzo et al., (2009) explored the performance of MEC systems at three distinct temperatures: 20°C,

25°C, and 30°C. This investigation revealed that the highest levels of chemical oxygen demand (COD) removal and Columbia efficiencies were achieved at 30°C. Furthermore, akin to methanogenic reactors, MEC systems could operate even at temperatures slightly above 20°C (Pham et al., 2006).

2.11.4 Solution Conductivity

The rate of H_2 production was also impacted by the solution's conductivity, although the influence was relatively minor. A higher level of solution conductivity benefits the transfer of ions, leading to an enhancement in the performance of the MEC setup (Khan et al., 2017). The solution's conductivity demonstrates an inverse correlation with the resistance of the system. Call and Logan (2008) noted that elevating the solution's conductivity from 7.5 to 20 mS/cm^{-1} resulted in an overall improvement in the production rate. Similarly, Logan et al., (2006) indicated that employing solutions with higher conductivity could significantly reduce ohmic losses in the MEC system. Hutchinson et al., (2011) established that by reducing the solution's conductivity from 7.8 to 1.8 mS/cm^{-1} and increasing the electrode spacing from 0.4 to 1.4 cm, the internal resistance of the system was enhanced.

2.11.5 Catalyst

The catalyst was employed to mitigate the kinetic hindrance associated with proton reduction and to accelerate the reaction for hydrogen generation (Chen et al., 2015). It was widely recognized that introducing a catalyst onto the cathode surface amplifies the rate of hydrogen production. Diverse types of catalysts were used to alleviate the activation energy and reduce the reaction overpotential in microbial electrolysis cell (MEC) systems. In their

research, Liu et al., (2014) deduced that an optimal catalyst loading rate should be approximately 0.2 mg/cm², while not dipping below 0.1 mg/cm². Conversely, lower loading rates correspond to diminished energy efficiency and power output. The commonly employed catalysts for electrodes were metal-based catalysts, which came with several drawbacks such as susceptibility to poisoning and high cost. A solution to these issues lay in the advancement of biocathodes, where microbial organisms catalyzed the cathode reactions. This approach was more economical, sustainable, and environmentally friendly (Khan et al., 2017).

2.11.6 Applied Potential

One of the required physical criteria for the functioning of MECs to generate CH_4 was the electric potential or additional voltage. Changes in electric potential have a considerable influence on the growth and dispersion of electroactive microbes, as well as CH_4 formation. It was critical to remember that excessive amounts of supplied electron density may be harmful to the bacterium. This study suggested the necessity to examine utilized potentials to maximize bacterial growth and promotes the activation. Gram-positive microorganisms were discovered to be the most often employed electroactive microbes in MECs paired with anaerobic digesting processes in several studies.

The three-dimensional design of their peptidoglycan cell wall affords substantial resilience to external shocks (Varanasi et al., 2019). As a result, suitable external voltage must be considered for diverse materials in order to produce high rate CH_4 production. The technique of voltage supply and adequate utilization were required to calculate the process cost. Direct current power supplies were commonly employed in lab-scale

reactors, but they fail when the methane generation mechanism was scaled up (Guo et al., 2017). Standard voltage control and real-time control were required for the operation to be industrialized. Thus, several aspects like as substrate type, cell layout, electrode composition, and microbes determine the appropriate potential difference in MECs. This reliance on many parameters highlights the necessity for voltage tuning for each MEC for improved system fuel efficiency.

2.11.7 Current Density

The design process of MEC units that could significantly contribute to biomethanation, underutilizes supplied current density. By raising the current density, bunched MECs can bypass the inherent drawbacks caused by a low oxide layer ratio. Additionally, many research found that using different electrode topologies can improve power density production as well as wastewater treatment.

2.12 OPTIMIZATION OF H-MECs

Optimization was a computable industrial choice making tool. It uses particular methods to decide the most cost effective and productive solution for a particular issue by shifting the concerning parameters. The Complicated nature of the connection of chemical factors and physical components during bioconversion of production process does not allow suitable complete designing. Therefore, to gain the optimum or maximum industrial outcome, the operating condition should be optimized. There were different strategies used in research design either statistical or non-statistical approach (Alam et al., 2008). A brief review of these two methods was given below:

2.12.1 One-Factor-At-A-Time (OFAT) Method

One factor at a time (OFAT) was established on non-statistical approach. OFAT was utilized while the small number of parameters was to be considered. For the reason that it was not only difficult, time consuming and impossible for the one-dimensional search to achieve a suitable optimum condition in a finite number of experiments (Xu et al., 2003) but also can lead to misreading of results not due to the consideration of the relations between various factors (Haltrich et al., 1994). Nevertheless, still it was being used in several researches for bioethanol production. Either it was utilized alone (Niranjane et al., 2007), where the different parameters were evaluated or it was utilized together with the statistical method (Alam et al., 2008b).

2.12.2 Statistical Approach

This method has been included to overcome the single factor problems. It was utilized to look for the optimum condition and screen the factors of the maximum response (Box and Behnken, 1960). Bioconversion optimization should be possible considering the interaction, quadratic, and linear effects in the treatment. In bioprocess designing, it has been generally refined and optimized through various studies and research efforts (Beg et al., 2003; Dutta et al., 2004). Response surface methodology and fractional factorial design were two key methods of statistical optimization.

Central Composite Design (CCD) and Plackett—Burman Design (PBD) were the two effective and efficient methods for systematic analysis on the target factors. However, PBD was a positive screening design, which significantly decreases the number of experiments, and provide more information as expected for the assessment of the target

factors. Only the best effective factors were chosen out for further optimization studies, others with less significance to response value may be absent in further experiment (Plackett and Burman 1946). PBD has been generally used in numerous fields, for example, the formulation of multicomponent, mediaum optimization and so on (Naveena et al., 2005; Loukas, 2001). After focusing on specific parameters via the process of Plackett-Burman Design (PBD), the optimization of these parameters was carried out using Central Composite Design (CCD), taking into account linear, quadratic, and interaction effects in the treatment. Numerous scholars have employed these optimization techniques to determine the highest achievable yield of bioethanol production (Alam et al., 2009; Salihu et al., 2011; Maryam et al., 2007; Wen et al., 2005).

2.13 KINETIC STUDY OF BIOMETHANE PRODUCTION

Kinetic study plays and important role to determine of some important parameters such as process yield, process control criteria, specific growth rate, heat evolved, process productivity, strategy for the production of a specific product (Oliveira et al., 2016). Complete quantitative investigation of the kinetics conduct of a response system requires not just mathematical expressions representing the time course of each essential factors like enzyme concentration and substrate biomass, but also, critical parts of fungal cell physiology, chemical adsorption, and substrate reactivity should be incorporated also. Basically, few studies on the kinetic model of BioM production, though the whole model of bioethanol growth has not been revealed yet. Most of the cases, a few numbers of factors were considered to describe the kinetic behaviour of growth of the BioM during convertion process by the reason of complexity of consideration of numerous parameters during the

simulation calculation and modelling and complications of accessibility of the particular data (Andrade et al., 2021).

Type of substrate and its concentration (Aguilar et al., 2002; Chanal et al., 1992), oxygen supply (Brown and Zainudeen, 1977), pH of the medium (Chanal et al., 1992), and type of the MECs operation (Mitra and Wilke, 1975; Ghose and Sahai, 1979; Najafpour et al., 2004) were studied to define the kinetic behaviour by several models. Oliveira et al., (2016) where it was considered cell concentration, substrate concentration, and product concentration vs. time of the batch BioM process to evaluate the kinetic behaviour. Andrade et al., (2021) to study the kinetic behaviour of growth during fermentative production of BioM on EAB using FW where cell mass and substrate concentration were considered.

2.14 CHAPTER SUMMARY

The major problems associated with food waste treatments using hydrolytic enzymes for methane production include complexity and variability of food waste composition, cost and availability of suitable enzymes, influences on enzyme stability and activity, and logistical challenges in scaling up. Food waste can have a wide range of organic compounds with different compositions, making it challenging to achieve consistent and efficient hydrolysis using hydrolytic enzymes like cellulase and amylase. Enzymes used in food waste treatments can be expensive, especially for large-scale applications. Finding commercially available enzymes specifically effective for food waste hydrolysis may be limited, adding to the overall cost and feasibility of the process. In addition, factors such as temperature, pH, and inhibitory substances present in food waste can influence the stability and activity of hydrolytic enzymes, requiring careful monitoring and control to maintain optimal

conditions for enzyme activity. On the other hand, scaling up the food waste treatment process using hydrolytic enzymes for methane production can pose logistical challenges, including efficient mixing of enzymes with food waste, managing large waste volumes, and designing suitable reactor systems for optimal hydrolysis and methane production at a larger scale. Addressing these challenges requires ongoing research and development to optimize enzyme formulations, improve process efficiency, and find cost-effective solutions for large-scale implementation. Additionally, efforts are needed to screen other microorganisms from food waste, sewage sludge, and nature that may produce positive results in terms of CO_2 removal in food waste treatment applications. Furthermore, the optimization of hybrid microbial electrolysis cell (H-MEC) based biomethanation processes and kinetic studies are essential for achieving maximum performance in reducing CO_2 emissions from food waste treatment.

CHAPTER THREE

MATERIALS AND METHODS

3.1 INTRODUCTION

This chapter includes detail of experimental procedures, equipment's, materials and methods employed in order to accomplish the set objectives. It involves the methods used in the isolation, purification and screening of potential hydrolytic microorganisms and electromethanogenesis microbes to reduce CO_2 and upgrade biogas from food waste. The production, characterization, electron transfer mechanisms, design and operation process, settling characteristics and conversion performance of potential electromethanogenesis microbes were discussed in detail. The entire experimental procedure was shown in Figure 3.1.

Majority of the experimental methods were of international standards supported such as APHA and protocols which were published in reported journals. The equipment, setup, samples, chemicals and reagents, microorganisms and media composition were designated in detail in this chapter. Throughout the experiment, microbiological protocols were strictly followed in order to put contaminations to the barest minimum.

3.2 RESEARCH FLOWCHART

The following flow diagram describes the experimental process of BioM convertion. The detailed descriptions of the experimental flowchart were given in the following sections.

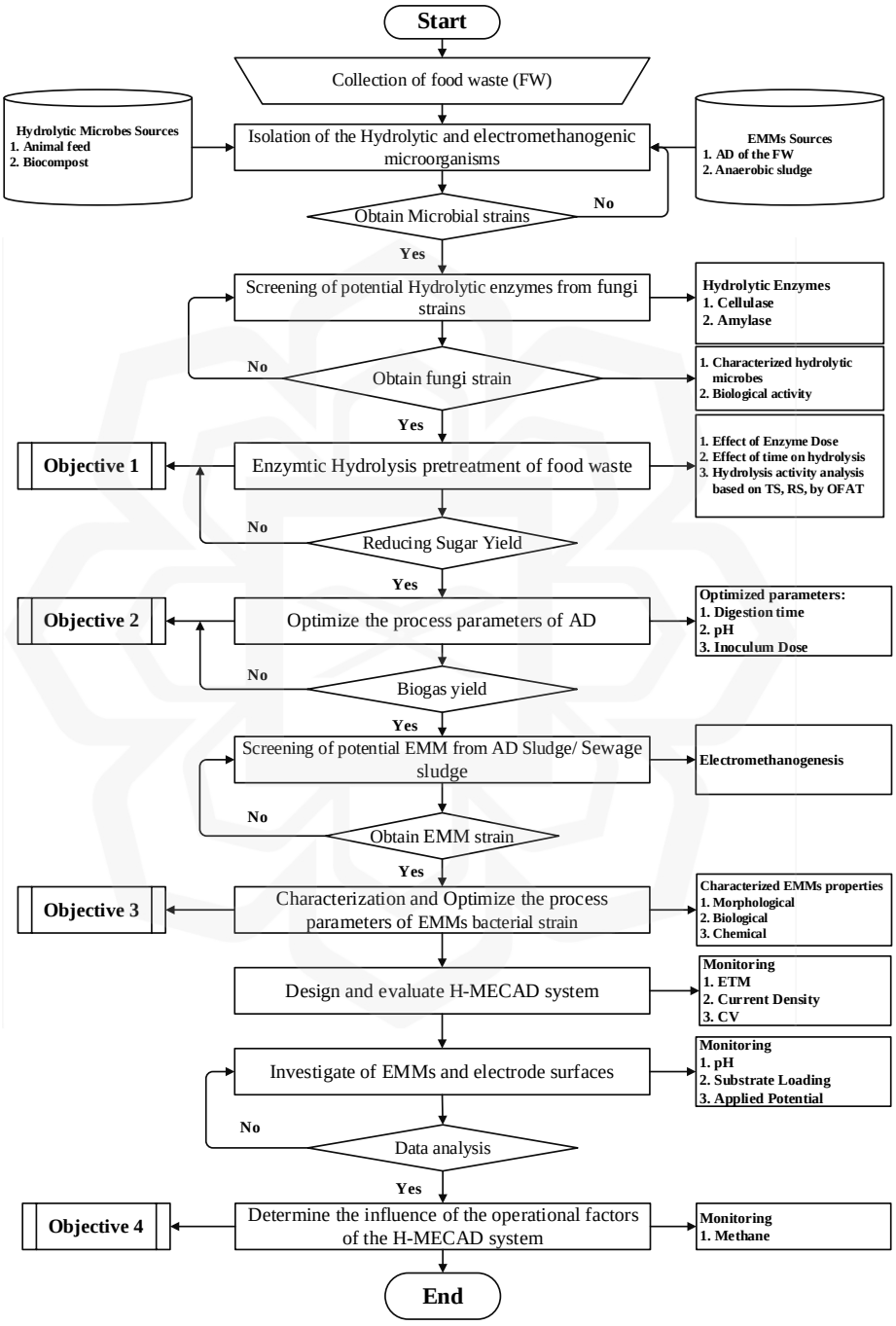

Figure 3.1: Flowchart depicting the overall activities of the research study

3.3 MATERIALS

3.3.1 Sample (FW) Collection and Characterization

Restaurant and supermarket food waste was procured from Bangladesh. To prevent fungal growth, the food waste sample was stored in a cold room at 4°C. The primary material under investigation in this research comprised household food waste gathered from various cafeterias in Dhaka, Bangladesh. The accumulated food waste consisted of approximately 30 kg, comprising 10 kg of mixed vegetables, 5 kg of assorted fruits, 5 kg of cooked rice, 5 kg of leftovers, 3 kg of meat and fish, and 2 kg of peels and other components. The second material employed was anaerobic sludge acquired from the Dasherkandi Sewerage Treatment Plant in Dhaka, Bangladesh, and it was used as the inoculum for the anaerobic digester. To account for differing dietary practices leading to variations in food waste composition, a reliable source of food establishments was selected for consistent collection and characterization of food waste. The primary parameters assessed for high BioM (biomethane) production included pH, volatile solids, carbohydrates, protein, fat and oil, total solids, and mineral compositions. Standard methods established in APHA (1989) were used for the analysis of all these parameters.

3.3.2 Chemicals and Reagents

All the chemicals and reagents were obtained from ROnex International, Labtex Bangladesh, Jonaki Sientific Store, Bangladesh. The list of the chemical and reagents were referred to the Appendix A.

3.3.3 Equipment and Apparatus

A pH meter and a total dissolved solids (TDS) meter were used to measure the pH and TDS respectively. A vacuum pump, an oven and desiccators were used in total suspended solids (TSS) measurement. A 10-mL cylinder, 100 mL cylinder, 250 mL filter flask and a magnetic filter holder were used in the FW characterization experiment. The equipment used was sterilized in an autoclave. 500 mL Erlenmeyer flask was utilized to carry out the pre-treatment, hydrolysis and fermentation steps of the experiment. An orbital shaker incubator was needed to incubate the Erlenmeyer flasks operating at 150 rpm. To transfer liquid volume pipettes was used. For analysis, a spectrophotometer and curvets were utilized. To mix reagents together, labelled test tubes were used. Petri dishes were used for culture preparation, followed by transferring the culture into a Erlenmeyer flask was utilized in 250 mL. A shaker incubator utilized also being used here. A brief description and the specification of these equipment's and instruments were referred to the Appendix B.

3.3.4 Microorganisms for AD system

The potential hydrolytic microorganisms utilized in the present study were isolated from bio composts and animal feed. Every strain was upheld on potato dextrose agar (PDA) with a concentration of 3.9% w/v. Subcultures were performed on a monthly basis, and the strains were preserved in a refrigerator at 4°C. Additionally, one strain was stored at ambient room temperature (28±2°C) for later utilization.

3.3.5 Electromethanogenesis Microorganism's for H-MECAD System

The electromethanogenesis microorganisms were isolated from anaerobic sludge of the FW and anaerobic sewage sludge. All strains were preserved on Basal Medium, sub cultured once in a month and stored in the chiller at 4ºC and a strain kept at room temperature (28±2ºC) until required for further use.

3.3.6 Consumable Items and Instruments

Aluminium foil was used to cover the Erlenmeyer flasks and to make aluminium dishes for characterization of FW. Filter papers were used in the TS, TV and so on experiment. As a safety precaution, gloves were needed at all times. Glass rod was used for stirring solutions, whenever needed (Appendix C). The equipment employed include autoclave, orbital shaker, thermal shaker, laminar air flow chamber, laboratory incubator, chiller, US-VIS spectrophotometry, freeze dryer (LABCONCO), Portable gas detectors (China and India), Field Scanning Electron Microscopy- FSEM, compound microscope with digital camera, maffle furnace, vacuum pump, desiccator, centrifuge, measuring balance, pH meter, gel electrophoresis apparatus, PCR machine, hot plate and MEC chamber constructed lab scale.

3.3.7 A Set Up of the H-MECAD System for BioM Production

A 1000 mL capacity of an integrated bioelectrochemical system for microbial electrolysis cells and anaerobic digestion was fabricated, installed and tested for evaluation of the upgraded biogas production from food waste as shown in Figure 3.2. The chambers used in this setup had dimensions of H=254mm, L=228.6mm, and r=38.1mm, resulting in a volume of 1389999.93 cubic mm, as illustrated in Figure 3.2. Both the anode and cathode

chambers were equipped with two ports on the left, two on the right, and two ports on the top side. Each inlet and outlet had a diameter of 12.7mm, and a 12.7mm gate valve was used. By fixing one 12.7mm inlet and one 12.7mm outlet in a specific configuration, the effective volume was achieved to be approximately 1389999.93 cubic mm.

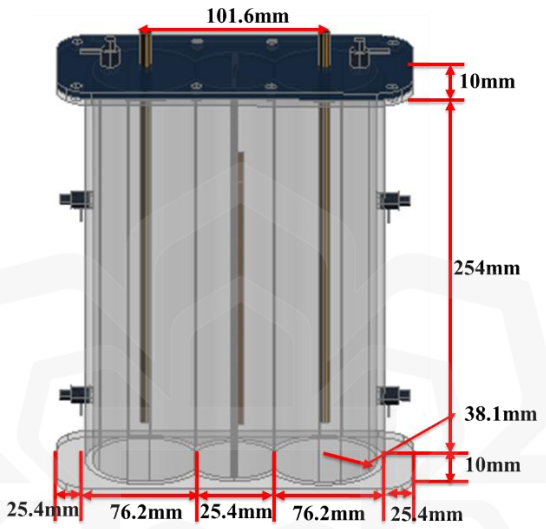

Figure 3.2: AD based H-MEC 3D diagram.

The set up was constructed with a two-chamber reactor, anode and cathode chambers, membrane, monitoring of pH, temperature and mixing with all standard specifications were to be provided by the local manufacturer.

3.4 ANALYTICAL METHOD

The analytical analysis of all parameters such as total suspended solids, dissolved solids, total volatile solids, pH (Instruction's manual supplied by Hanna Instruments), reducing sugar (Zhao et al., 2009), total sugar (Rambla et al., 1997), fatty acids (Véras et al., 2011), chemical oxygen demand, protein (Tang et al., 2008), microbial growth (Madigan et al., 2003), electricity (Logan, 2006), biogas (Weiland, 2010), H_2 (Logan et al., 2008), CO_2 (Li

et al., 2018)) etc. involved in this research will be conducted according to the standard methods. The biodegradation rate was monitored in each step of the process to evaluate the effective bioconversion.

3.4.1 Food Waste Characterization

To characterize food waste, total suspended solids, total dissolved solids pH and others were measured. Thus, food waste was characterized according to the following procedures.

3.4.1.1 Moisture Content

The assessment of moisture content in FW involved measuring the weight of an evaporating dish and noting the initial weight (W1) of a 100 g sample using a balance. Subsequently, the dish containing the sample was subjected to drying in an oven set at a temperature of 103°C to 105°C for approximately 24 hours. After cooling the dish and sample in a desiccator, the final weight (W) of the dish with the dried sample was recorded. Moisture content was done by considering the loss in weight and converted to percentage and the formula used was presented in the Equation 3.1. The moisture content of a material can be determined using various methods including: drying the sample in an oven at a specific temperature to remove moisture (APHA, 2012; Zhang., 2007).

$$\%\ \text{Moisture content} = \frac{initial\ Wt(\ g) - oven\ dry\ Wt(g)}{initial\ \ Wt(g)} x100\% \qquad (3.1)$$

3.4.1.2 Determination of Total Solids (TS)

The term "total solids" denotes the quantification of all solids, regardless of whether they are suspended or dissolved. In essence, it signifies the residue that remains after the process

of evaporation (Abbassi-Guendouz et al., 2012). To start with, aluminium or evaporating dish was prepared by heating it at 103 to 105 °C for about 1h and recording its weight after making it cool down in desiccator. After that, 2 mL of food waste sludge was poured on the prepared dish and dried at 103 to 105 °C with the oven for 1h. The weight of evaporated dish was recorded after being cooled down in desiccator. Therefore, total solid was calculated by the formula as followed by APHA, (2012) (Equation 3.2).

$$TS\ (\%) = \frac{Weight\ of\ dried\ solids\ (mg)}{Sample\ volume(mL)} \times 100 \quad (3.2)$$

In this formula, the weight of dried solids refers to the weight of the sample after it has been dried to remove all moisture. The weight of the sample is the initial weight of the sample before drying.

3.4.1.3 Determination of Total VS measurement

The residue obtained from total solid analysis was ignited in a furnace and heated at 550 °C for 1h. After being cool in the desiccator, the weight of the residue will be recorded. Thus, total volatile solid was calculated as follow (Equation 3.3):

$$\text{Total Volatile Solid}\ (\%) = \frac{Weight\ of\ Volatile\ Solids(mg)}{Weight\ of\ Dry\ Solids} \times 100 \quad (3.3)$$

3.4.1.4 Determination of Total Dissolved Solids (TDS)

Total Dissolved Solids (TDS) were described as solid substances capable of traversing a filter featuring a pore size of 0.45 µm. TDS serves as a means to gauge the quantity of substances dissolved within food waste. The process to assess TDS involved filtering the food waste sample, followed by evaporating the filtrate (the portion of the food waste that passes through the filter) within a pre-weighed dish. Subsequently, the dish with the

evaporated material was subjected to drying in an oven at 180°C for a duration of 6 hours. The alteration in the dish's weight represented the cumulative amount of dissolved solids, a value expressed in milligrams per liter (mg/L) and computed as outlined in Equation (3.4) (APHA, 2012).

$$TDS\ (mg/L) = \frac{\text{Weight of dried residue (g)}}{\text{Sample volume(mL)}} \times 1{,}000{,}000 \quad (3.4)$$

3.4.1.5 Determination of Chemical Oxygen Demand (COD)

The COD was determined to evaluate the organic content in FW by Standard Methods (APHA, 1989).

Procedure: The COD value of the treated sample was determined using a Hach DR 2400 spectrophotometer. Because the spectrophotometer's range was 1500 mg/L, each sample must be diluted before being evaluated. Because the concentration of COD in food waste was quite high and needs to be diluted, the high range COD vial was utilized in this research. Before placing the vial in the Hach DBR 200 COD digestion reactor, it was warmed to 150°C. A prepared sample was defined as 2 mL of diluted material pipetted into a COD vial. In the meantime, another vial was filled with 2 mL of deionized water to serve as a blank. Cap both vials firmly and rinse with deionized water before wiping with a clean paper towel. Both vials were gently inverted to mix before being placed in the reactor and heated for 2 hours. The vials were then allowed to cool to room temperature before the COD concentration was measured using a Hach DR 2400 spectrophotometer.

3.4.1.6 Determination of pH

1 mL of the prepared sludge of food waste that was stored in 4 °C was mixed well and dilute with 50 mL of distilled water. 20 mL of the diluted sample was poured into 50 mL conical flake and the pH was taken and read with the pH meter, Mettler Toledo FiveEasy Benchtop Meter once the sensor of pH was immersed in the solution. In the case of adjustment sodium chloride (NaOH) of 4 N was used.

3.4.1.7 Determination of Reducing Sugars

DNS reagent will be used to measure the amount of reducing sugars. In order to prepare 100 ml of the DNS, 1 g of the reagent will be dissolved in 50 mL of water. Then, 30 g of ($KNaC_4H_4O_{654}H_2O$) will be added slowly to the solution followed by the addition of 20 mL of 2N NaOH. Dilution to a final volume of 100 mL will be done by adding distilled water. To detect the reducing sugars amount, 0.3 mL of the hydrolyzed sample will be added in a test tube to 0.3 mL of the previously prepared DNS reagent. The test tube was to be stood in boiling water for 5-10 minutes. The test tube should be covered with a paraffin film to avoid liquid loss due to evaporation. Finally, 3 mL of water will be added to the test tube and the tube was to be left to cool down then absorbance will be read with green light (540nm) calibration will be done with water (Zhao et al., 2008).

3.4.1.8 Determination of Total Sugars

Sample and water of 1 ml will be taken in a test tube. Then, phenol reagent (5%) of 1 mL will be added in a series of tubes. Afterward, Sulfuric acid (98%) of 5.0 mL will be added from the fast-flow pipette. The solution will be mixed immediately and allowed for cooling

before the absorbance was read at 490 runs. Finally, absorbance values will be translated into total sugar using a standard curve (Rambla et al., 1997).

3.4.1.9 Determination of Cellulases Enzyme Activity

There was a different category of enzymes found in cellulase systems which were breakdown crystalline cellulose for instance exo-1, 4-ß-D-glucanases, endo-1, 4-ß-D-glucanases and cellobiose. The cellulase enzyme activity by the DNS method (Miller, 1959) was carried out to know the degradation capacity of cellulose of FW. its preparation process was discussed in Appendix E.

3.4.1.9.1 Determination of Endo-1, 4-ß-D-Glucanase

The liquefiable derivative of cellulose, carboxymethyl cellulose (CMC), was commonly employed for the assay of endo-cellulase activity. Activity on CM-cellulose can be defined by measuring the significantly raise in power reduction of the solution or the drop-in viscosity (Ghose 1987).

Reagents: DNS reagent and 2% (w/v) CMC in .05 M sodium citrate buffer pH 4.8.

Procedure: In a test tube, a volume of 0.5 mL of the enzyme sample was diluted using citrate buffer. Several dilutions of the enzyme were created, with one yielding slightly more than 0.5 mg of glucose and another producing significantly less. Following an incubation period of 5 minutes at 50°C in a water bath, a mixture of 0.5 mL of CMC was prepared and thoroughly mixed. This mixture was allowed to incubate at 50°C for a duration of 30 minutes. To terminate the reaction, 3 mL of DNS solution was introduced to the mixture, which was subsequently heated precisely for 5 minutes. Finally, 20 mL of

distilled water was added, and the mixture was agitated by gently tilting the tube at various intervals. At 540 nm, the absorbance was determined. Translation of the absorbance after the deduction of enzyme and reagent blanks was prepared using a linear glucose standard curve, which was made by plotting glucose used against absorption at 540 nm.

Calculation:

$$\text{CMC Unit} = \frac{0.185}{Enzyme concentration\ to\ release\ 0.5\ mg\ glucose} \times \frac{U}{mL} \qquad (3.5)$$

3.4.1.9.2 Determination of Exo-1, 4-ß -D-Glucanases Activity

The activity of exo-1, 4-ß -D-glucanases was determined using Filter Paper (Ghose 1987). The test works by calculating a set quantity of glucose (2 mg) from 50 mg of filter paper.

Reagent: Citrate buffer was 0.05 M used to prepare 4.8 pH by 210g of dissolving citric acid monohydrate in 750 mL deionized water and to obtain a pH of 4.3, 50-60 g of NaOH was added. Then, up to 1liter of deionized water was additional to the solution to create 1M of citrate buffer and by adding NaOH the pH was fixed at 4.5. This 1 M citrate buffer was diluted using 0.05 M and 4.8 of pH was increased.

Procedure: This process's identification of glycosidic bond cleavage entails the same and simultaneous preparation of 3 kinds of test tubes (pitches and controls, glucose standards, and assay mixes), as described below. A Whatman No. 1 filter paper strip measuring 1.0 × 6.0 cm, with a weight of 50 mg, was utilized as the medium. The experiment tube was filled with an extended filter paper strip. The sample solution was introduced with 1.0 mL of 0.05 M Na-citrate (pH 4.8), ensuring that the filter paper strip became saturated with the buffer. Subsequently, 0.5 mL of enzyme solution (sample)

concentrated within citrate buffer was added. Each enzyme sample was subjected to four-fold dilution, with one dilution yielding a slightly greater than 2.0 mg quantity of glucose (absolute measurement), and another dilution producing a slightly lesser than 2.0 mg amount of glucose (absolute value). These specific dilutions were anticipated to release around 2.1 and 1.9 mg of glucose, respectively. Various assays based on enzyme concentration were performed to achieve these goals. All buffered samples were incubated at 50°C for around 60 minutes. After 60 minutes, each test tube was withdrawn from the 50°C bath and 3.0 mL DNS reagent was added immediately to terminate the enzyme process. Enzyme blanks, glucose standards, all samples, and Spectro zero were heated for about 5 minutes before adding 10 ml distilled water. At 540 nm, the color generated was tested against by the Spectro zero.

Spectro zero and enzyme blank:

- Spectro zero: citrate buffer was 1.5 mL.
- Enzyme control: citrate buffer of 1.0 mL + enzyme dilution of 0.5 mL (For each dilution examined, a separate control was generated)
- DNS was 3.0 mL added and boiled 5 mints.

Glucose standard: Anhydrous glucose stock solution (10 mg/mL) was prepared and kept at - 20°C. After melting, the norm was a vortex to guarantee proper mixing. The appropriate dilutions were created from the stock solution:

1.0 mL + 0.5 mL buffer = 1:1.5 = 6.7 mg/mL

1.0 mL + 1.0 mL buffer = 1:2 = 5 mg/mL

1.0 mL + 2.0 mL buffer = 1:3 = 3.3 mg/mL

1.0 mL + 4.0 mL buffer = 1:5 = 2 mg/mL

Calculations: The concentration of glucose (mg/0.5 ml) was plotted against absorbances at 540 nm to construct a linear glucose standard curve. After subtracting the enzyme blank, the quantity of glucose released in each sample tube was determined using this standard curve. A plot of glucose liberated versus the logarithm of enzyme concentration predicted the enzyme concentration that released just 2.0 mg of glucose. To determine the needed enzyme concentration, two data points extremely close to 2.0 mg were picked and a straight line was drawn between them, using this line to insert between the two spots to get the enzyme dilution that generated closely 2.0 mg glucose equivalents of reducing sugar. The equation was used to compute the activity.

$$\text{FPU} = \frac{0.37}{Enzyme concentration\ to\ release\ 2.0\ mg\ glucose} \times \frac{units}{mL} \qquad (3.6)$$

3.4.1.10 Determination of amylase Activity

The DNS method (Miller, 1959) was employed to evaluate glucoamylase activity, utilizing soluble potato starch (1% w/v) as the substrate (Riaz, et al., 2012). A mixture of 1 mL of 1% w/v soluble potato starch in 50 mM Mcllvaine buffer (pH 5) was combined with 100 µL of extracellular enzyme supernatant and then incubated at 60°C for a duration of 30 minutes. The enzymatic reaction was halted by introducing 1 mL of DNS reagent. After being heated at 100°C for 5 minutes, the reaction mixture was subsequently cooled for 2 minutes on ice. Absorbance was measured at 540 nm using a spectrophotometer, comparing it against a blank. The blank mixture was prepared by adding DNS before introducing the enzyme, while an enzyme that was included in the mixture was denatured through boiling.

This entire procedure was conducted in triplicate. Enzyme activities were quantified using the same methodology outlined above, relying on a calibration curve constructed with D-glucose as the standard. In the experimental conditions, one unit of enzyme activity represented the quantity of enzyme necessary to release 1 mol of glucose from soluble starch within a minute. All the reagents employed in this study were detailed in this description.

Reagents used for enzyme assay (DNS method)

i. At 20°C and sodium phosphate buffer pH was 6.9; consists of 20 mM sodium dihydrogen phosphate (NaH_2PO_4) and 6.7 mM Sodium chloride (NaCl), pH was attuned to 6.9 using 1M NaOH. Fresh Sodium Phosphate buffer was prepared prior to assay conduction.

ii. Mcllvaine buffer (pH 5) at 20°C; consists of 0.2M Na_2HPO_4 and 0.1M citric acid. Fresh Mcllvaine buffer was prepared prior to assay conduction.

iii. Soluble starch solution was 1% (w/v), prepared by dissolving potato soluble starch of 1% (w/v) in each of the previously mentioned buffer solutions. The solubilization of starch in each of the buffers was achieved by heating on the hot plate with continuous stirring. The fresh soluble starch solution was prepared prior to assay conduction.

iv. Dinitrosalicylic acid (DNS) color reagent, 100mL of DNS color reagent was prepared by mixing 50 mL of 96 mM dinitrosalicylic acid solution with 50 mL of sodium potassium tartrate solution, the later was made by dissolving 30 gm of sodium potassium tartrate in 20 mL of 2M NaOH at 70°C and the size was made

up by addition of 30 mL distilled water. The DNS color reagent was stable for six months and was stored at room temperature in an amber bottle.

Standard curve preparation: A spectrophotometer with a wavelength of 540 nm was used to measure the volume of the colored combination. The undetermined sample's sugar content will then be read off a calibration graph (standard curve) built utilizing confirmed sugar contents. Different concentration of a defined solution concentration were utilized to calculate the unknown solution's concentration. A stock solution of 0.2% (w/v) D-glucose was prepared; a standard curve was made by pipetting (in milliliters) the following reagents into test tubes as described in Table 3.1 below.

Table 3.1 Illustration of standard curve preparation protocol

	Std 1	**Std 2**	**Std 3**	**Std 4**	**Std 5**	**Std 6**	**Std 7**	**Blank**
0.2% (w/v) D-glucose (stock solution) (mL)	0.05	0.2	0.4	0.6	0.8	1	2	0
Distilled water (mL)	1.95	1.8	1.6	1.4	1.2	1	0	2
(DNS) colour reagent (mL)	1	1	1	1	1	1	1	1

Following that, the experiment tubes were immersed in a boiling water bath for 5 minutes, and the intensity of the color was measured at 540 nm in comparison to a blank contain only deionized and (DNS) color solution. The spectrophotometer data were plotted against the dosage of D-glucose to create a standard graph.

Calculations: Determination of amylase activity:

$$\text{Reducing sugar released } (\mu\text{mol}) = \frac{\text{Absorbance (sample)- Absorbance (blank)}}{0.068} \quad (3.7)$$

$$\text{Enzyme activity } \left(\frac{\text{U}}{\text{mL}}\right) = \frac{\text{Change in substrate concentration}}{\text{Reaction time}} \times \frac{1}{\text{Enzyme volume}} \quad (3.8)$$

3.4.1.11 Determination of Hydrogen

Since hydrogen gas was widely utilized as a green energy source, hydrogen gas sensing technology was frequently utilized. The exponential nature of H_2 gas necessitates detection at extremely low concentrations. As a result, ppm level sensing of H_2 gas leaks seems to become critical in order to minimize highly unsafe circumstances. There were several methods for detecting H_2 gas, that have all been thoroughly investigated. Each method has benefits and disadvantages, allowing the individual to select the most appropriate technique based on its implementation. The effective improvement methods allow detection systems to actually function in a wide range of temperatures, humidity levels, and concentration levels. Detection limit has been a problem for all types of different sensors, but with the progress of nano - materials, several more scientists have mentioned detection limits for hydrogen gas. Biosensors sense the presence and composition of specific gases, such as hydrogen.

The MQ8 hydrogen gas sensor was a type of metal oxide semiconductor sensor. This sensor detects hydrogen gas in the air, detects gas leakage, and detects the existence of hydrogen gasses. This detector was very easy to utilize and able to detect hydrogen gas concentrations ranging from 100 to 10,000 ppm somewhere else. The MATLAB code can be found in Appendix H.

3.4.1.12 Determination of Carbon dioxide

The evaluated CO_2 levels values will be demonstrated on the OLED module, and the Arduino MQ-135 sensor readings will be compared with the ultraviolet CO_2 sensor data.

Aside from CO_2, Arduino was used to evaluate the concentrations of biogas, smoke and other gas. At the conclusion of the document, the complete code as shown in in Appendix A for interfacing the MQ-135 Sensor with Arduino. In this section, some key components of the MQ135 Arduino code.

3.4.1.13 Determination of Methane

The analysis of bioMethane was carried out to determine the biogas content after conversation using by Arduino MQ-135 sensor and gas chromatography method (Korytár ert al., 2002).

3.4.1.13.1 Determination by Arduino MQ-4 sensor

The MQ-4 log-log scale curve for gas concentration in parts PPM was used to display the sensitivity characteristics of the MQ-4 as shown in Figure 3.3. The MQ-4's sensitivity to gases was shown by the curve in the gadget documentation. Its sensitivity to methane's chemical formula, CH_4, may be shown here. Propane and butane gases, which were both recognized LPG components, were not included in the curve (Yang et al., 2019).

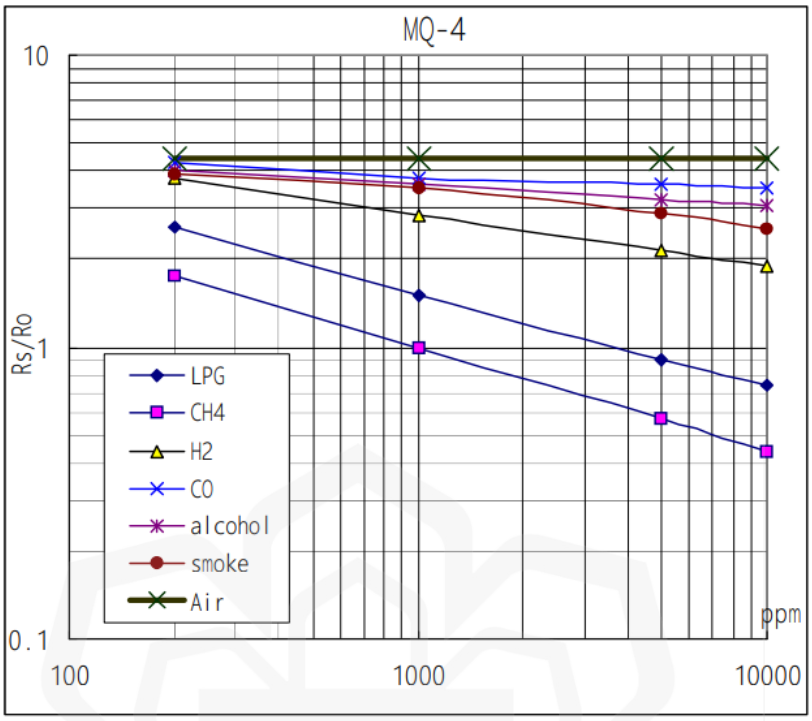

Figure 3.3: MQ 4 log-log scale curve for gas concentration in parts-per-million

The graph illustrates the relationship between the R_S/R_0 ratio and gas absorption in parts per million (PPM) on a logarithmic scale. Here, R_0 represents the sensor resistance in clean air, and R_S denotes the measured sensor resistance. The R_S/R_0 ratio provides a measure of gas concentration, allowing us to calculate the gas concentration in PPM. This calculation will be incorporated into our Arduino program. The point of maximum clarity was observed when R_S/R_0 equaled 1 and PPM reached 10,000. Another notable observation occurred at an R_S/R_0 value of approximately 0.58, corresponding to a PPM level of around 5,000. The formula (3.9) is employed to initiate this analysis.

$$\log Y - \log Y_1 = \frac{\log Y_1 - \log Y_1}{\log X_2 - \log X_3} (\log X + \log X_1) \tag{3.9}$$

From the first point will be assign $Y_1 = 1$ and $X_1 = 10000$, and from the second point will be assign $Y_2 = 0.58$ and $X_2 = 5000$. Substituting the following numbers into the equation (3.10) above:

$$\log Y = -0.339 \log X + 1.071$$

Changing Y to R_S/R_0 and X to PPM and solving for PPM:

$$PPM = 10000 \left(\frac{R_S}{R_0}\right)^{-2.95}$$

3.5 EXPERIMENTAL METHODS

The primary experimental resources, including food waste, chemicals, reagents, machinery and equipment, glassware, and assorted consumables, are elaborated upon in the subsequent sections.

3.5.1 Preparation of Hydrolytic Fungi Growth Media

This study was performed use of Potato Dextrose Agar (PDA), which was produced based on the manufacturer guidelines. Thus, 39 g of PDA was diluted in 1000 mL of distilled water and sterilized (autoclaved) for 15 minutes at 121°C at 15Pa pressure. The sterilized PDA was then poured aseptically in to disposable petri dishes in a UV sterilized laminar air flow cabinet. The PDA plates were then left almost open for solidification for immediate or otherwise stored in a chiller (4ºC) for further use.

3.5.1.1 Isolation and Purification of Hydrolytic Fungi

The fungi strains were extracted from several resources like animal feed and bio compost and using the spread plate technique (Sakthi et al., 2012). The solid sample of 10g was taken in Erlenmeyer flask using 250mL capacity and dissolved in 100mL sterilized distilled water. After that the raw sample was mixed in 150 rpm for 60 minutes and centrifuge 5000 rpm at 4ºC of temperature. The raw sample of 1mL was liquefied in 9 mL water (sterilized distilled). The raw suspension sample was mixing up to 10^9. Two different fungi strains such as one fungi strain, the diluted samples were transplanted on PDA plates that had been previously prepared while another fungi strain was inoculated on prepared starch agar plates such as pH 7.0, starch agar (g/L), 15.0g agar, 10.0g soluble starch and 3.0g beef extract. The inoculation plates were cultured at room temperature (30±20°C) for 5-7 days before being removed. Following an incubation time, colony formation was noticed. On generate bacterial cultures, the immature fungal colonies were petri dish scraped up and placed to fresh sterile PDA and starch agar plates. Pure cultures of fungi strains were obtained after successive transfer of individual colony in PDA and starch agar plates which was incubated at 37 ± 2ºC for 5-7 days. Finally, pure fungal strains were obtained and then kept it in a chiller at 4ºC temperature and a strain at room temperature (30 ± 2ºC).

3.5.1.2 Fungal Strains Sub-culture

Fungi stains were sub-cultured by using flamed scalpel to scrape or cut small part of fully grown fungi and transferred to inoculate sterile petri dish and sealed with parafilm to prevent contamination with unwanted microbes. The culture plates were then subcultured at 37ºC for 12 days to complete mycelial growth for inoculum preparations.

3.5.1.3 Inoculum preparation

The technique outlined by Alam et al., (2003) was employed to generate a starter culture for enzyme synthesis. To maintain the uniformity of colony proportion, fungal cultured plates aged seven days were rinsed using approximately 25 mL of sterilized distilled water, achieved with a curved glass rod. To segregate mycelia from the extract solution, the extracted fungal samples underwent filtration using Whatman No. 1 filter paper. The supernatant was then quantified (1.5×10^8 to 3×10^8 spores/mL) using a Hemocytometer, and it was transferred to a 150 mL Erlenmeyer flask for use as the spore suspension. The procedure for inoculum preparation of both fungal strains is detailed in Appendix I. Similarly, the processes for enzyme production media and the steps involved in cellulase and amylase production were provided in Appendix I.

3.5.2 AD based Enzymatic Hydrolysis Process

Enzymatic hydrolysis was conducted within a 10L plastic container, the same location where the pretreatment took place. The study employed cellulase and amylase enzymes with an activity level of 326 CMC U/mL and 400 U/mL, respectively. These enzymes were utilized across a range of doses, varying from 20U to 200U per 50mL of pretreated food waste, to assess the enzymatic hydrolysis rate. This stage of experimentation involved observing the initial cellulase enzyme dose over 5 days (ranging from 40U to 140U), enzyme pH (ranging from 4.5 to 7), hydrolysis duration (ranging from 0 to 5 days), and enzyme dose (ranging from 40U to 200U) to optimize the process conditions. The flasks containing the samples were subjected to agitation at 150 rpm under ambient temperature conditions of 30°C (±2). After 24 hours, samples were taken and subjected to centrifugation

at 5000 rpm for 20 minutes, with the supernatant subsequently analyzed for parameters including total solids (TS), volatile solids (VS), and chemical oxygen demand (COD). Alongside the optimization of substrate concentration, the optimal cellulase and amylase enzyme doses were also determined using a fractional factorial central composite design (FCCCD) approach.

3.5.3 Statistical Analysis for Enzymatic Hydrolysis

In two steps, the operating parameters for enzymatic hydrolysis of food waste were determined. In the initial process, the variables were validated using the OFAT technique to determine likely optimal levels. On the second approach, a FCCCD optimized procedure was used under the RSM to characterize the nature of the response surface in the experimental setup and illustrate the ideal circumstances of the most relevant predictor factors.

3.5.3.1 One-Factor-At-A-Time (OFAT) For Hydrolysis

OFAT analysis process was utilized to further evaluate the most contributing factors affecting the optimum reducing sugar production. The following Table 3.2 summarized the OFAT design for hydrolysis to increase reducing sugar production.

Table 3.2: OFAT factors designed considering the range under consideration and the fixed variables

Factor	Range tested	Fixed parameters
TS (%)	5 - 15	Enzyme dose 20U/mL, Time 5 days, pH 5, Room temperature 30°C (±2).
pH	4.5 - 7	TS 12.5%, Time 5 days, Room temperature 30°C (±2).
Hydrolysis time (Days)	0 - 7	TS 12.5%, Room temperature 30°C (±2), Enzyme dose 80U, Enzyme pH 5.
Final enzyme dose (U)	40 - 140	TS 12.5%, Room temperature 30°C (±2), Enzyme pH 5, Hydrolysis time 5 days.

The objective of this study was to identify the most effective combinations of parameters that result in optimal production of reducing sugars while minimizing resource requirements. This was achieved by altering individual components while keeping the rest constant. The selection of factors for investigation was based on their significant influence, including factors like time, total suspended solids (TSS), pH, hydrolysis duration, and the ultimate enzyme dose.

3.5.3.2 Response Surface Methodology (RSM) for Hydrolysis

For the optimization and validation of the experiments, the statistical software Design Expert 12.0 (Stat-Ease Inc., Minneapolis, USA) was utilized. RSM was employed to fine-tune the hydrolysis parameters for achieving the most favorable production of reducing sugars. The specific RSM approach employed in this study was executed in the FCCCD

format. Following the OFAT results, the data were subjected to analyze the RSM. Factors that produced maximum reducing sugar at specific points and demonstrated a clear optimum level were further chosen for FCCCD, while other parameters with comparatively small differences were fixed at the level where they produced highest reducing sugar production. Two factors were analyzed for FCCCD such as substrate concentration and enzyme dose. The layout of the FCCCD model's experimental design is presented in both Table 3.3 and Table 3.4. This design encompasses a total of 13 experimental runs, incorporating 5 center points (runs 1, 2, 4, 5, 8). Every individual factor was evaluated at three distinct levels represented by the codes: low (-1), medium (0), and high (+1).

Table 3.3: The Parameters employed in the FCCCD, along with the different factor levels for the hydrolysis process

Factor	Units	Low	High
TS	%	10	15
Enzyme dose	U	60	100

Table 3.4: FCCCD experimental design for hydrolysis

	Factor 1	**Factor 2**	**Factor 1**	**Response 2**	
Run	A: TS %	B: Enzyme Dose U/mL	pH	RS (Actual) g/L	RS (Predicted) g/L
1	12.5	80	5.5		
2	12.5	60	5		
3	10	100	4.5		
4	**12.5**	**80**	**5**		
5	15	80	5		
6	**12.5**	**80**	**5**		
7	12.5	80	4.5		
8	**12.5**	**80**	**5**		
9	15	60	5.5		
10	15	100	4.5		
11	**12.5**	**80**	**5**		
12	10	60	5.5		
13	15	60	4.5		
14	**12.5**	**80**	**5**		
15	**12.5**	**80**	**5**		
16	15	100	5.5		
17	10	100	5.5		
18	10	60	4.5		
19	10	80	5		
20	12.5	100	5		

3.5.3.3 Validation of the Model for Hydrolysis

A various experiment was carried out to confirm the optimal results in order to certify the developed model. It was conducted by repeating the experiment at various design conditions that generate high, medium and low response. Whereas, the experimental results were related with the predicted values as made by the Design Expert software. The variance between predicted and experimental findings indicated that the approach was reliable.

3.5.4 Preparation of EMMs growth media for methane production

The collected different sample of EMMs were cultivated in a solid medium using a petri dish. Suspend 28 g of nutrient agar powder in 1000mL of purified water with pH adjusted at 7.4. Later, it was autoclaved at 121 °C for 15 minutes by using autoclave and once the media was chilled to room temperature, each of the two strains was cultured in the media and incubated for overnight in the shaker with 150 rpm and 37° C (Djordjevic, 2002).

3.5.4.1 Isolation and purification of electromethanogenesis bacteria

The bacteria were isolated from different sources such as AD based FW effluent and anaerobic sludge and using the spread plate technique (Sakthi et al., 2012). One mL raw food waste and anaerobic sludge sample were liquified in 9 mL deionized water. The both raw sample solution was degraded up to 10^{-1} to10^{-7}. The diluted samples were immunized on prepared nutrient agar plates. The immunized plates were incubated at 37±2ºC of temperature and allowed to grow for 3-7 days. Following an overnight incubation, bacterial colonies formation was seen. To isolate pure cultures, the young microbe's colonies were inoculated picked up and placed to fresh sterile enriched dishes. Pure cultures of filamentous bacteria were obtained after successive transfer of individual colony in nutrient agar plates and incubated at 37±2ºC for 3-7 days. Finally, pure filamentous bacteria strains were obtained and then kept it in a chiller at 4ºC temperature and a strain at room temperature (30 ± 2ºC).

3.5.4.2 Electromethanogenesis bacteria Sub-culture

Electromethanogenesis microorganisms were subcultured by scraping or cutting a small portion of fully grown electromethanogenesis microorganisms with a flamed scalpel and transferring to inoculate a sterile Petri dish sealed with parafilm to prevent contamination with unwanted microbes. The plates were then incubated at 37ºC for 7 days to complete mycelial growth for inoculum preparations. The medium composition was shown in appendix J.

3.5.4.3 Inoculum preparation

Inoculum preparation for filamentous EMMs was performed by using nutrient agar plates (Wagner, 2012) and each plate were washed with around 10 mL sterile distilled water using bent glass rod. After that, 10 mL of culture inoculum was transferred in 90 mL of nutrient in the 250 mL Erlenmeyer flask, place the liquid culture media. The inoculated solution was incubated for 3 days at 37±2°C room temperature and also at 150 rpm shaking for their growth. The concentration of the cell in the inoculum was determined for future use in bioconversion (10^8 cells/mL).

3.5.4.4 Effect of single and compatible mixed culture

The objective of the experiment was to evaluate methane production through the cultivation of both individual and combined bacterial cultures. A production medium of 100 mL enrichment liquid media was subjected to sterilization through autoclaving at 121°C for 15 minutes. This sterilized medium was then inoculated with 2% (v/v) EEMs for the purpose of introducing single and mixed culture inoculants. EMMs inoculum was generated from

culture plates that were ten days old, and this culture was nurtured in a rotary shaker at a speed of 0 rpm within a 250 mL Schott Duran glass container. Throughout a period of 6 days, the culture was maintained at a constant temperature of 28±2°C. To establish an initial pH of 7.0±0.1, either 1M NaOH or 2M HCl was employed for pH adjustment. Post the 6-day treatment period, both the individual and mixed cultures were collected and subjected to centrifugation to segregate the biomass from the supernatant (centrifugation at 10000 rpm for 10 minutes at 25°C). The supernatants were subjected to methane production assessment.

3.5.5 Screening of Potential EMMs to produce methane by MEC Test

3.5.5.1 Cultivation of EMMS strains

The EMMs cultivation media was prepared with enrichment liquid media. 100 mL culture broth was poured in to each 250 mL schott duran glass bottle. The medium was sterilized after autoclaving it for 15 minutes at 121°C. Then, 5% (v/v) EMMs inoculum was added to liquid medium. Each beaker was cultured with inoculum for 14 days on a shaking incubator set to 150 rpm at ambient temperature and in the darkness. The pH of the organism was initially regulated to 7.0±0.1 utilizing 6.4% aqueous solution. After 14 days of culture, all EMMs were extracted and their tubes were centrifuged and organic matter were collected using Whatman No.1 filter paper. The harvested supernatants and biomass after dried were used as conversion to produce methane.

3.5.5.2 Physiological characteristics of strain EMM

The physiological properties of strain EMM-TN were studied in terms of substrate consumption, pH range, growth, antibiotic tolerance, NaCl meditation range, and DNA G+C content. The light sensitive density at 660 nm was measured utilizing a spectrophotometer and the percentage of CH_4 in the gas phase was measured utilizing a gas chromatograph. All physiological investigations were carried out twice. Under N_2, acetate and format were eliminated from the enrichment medium, which was then employed for substrate use tests. Anaerobic stores of filter decontaminated substances were created and sequentially applied at 50 mM final concentrations. A newly developed frish culture was injected at 10% (v/v) and cultured in 250mL of schott duran glass bottle for 14 days at 30°C. The control was medium under AD based gas phase.

The growth optimal temperature in the enrichment medium at the ideal pH was established. schott duran glass bottle containing 10% (v/v) sample was co–cultured at temperatures ranging varied from 25°C to 55°C. Every other day, the schott duran glass bottle were compressed with AD based gas phase to provide an adequate supply of substratum. At the ideal temperature, the pH needed in the enrichment solution was determined and modified to pH varied from 4.0 to 9.0. To get findings above pH 4.0, pure Na_2CO_3 was added to a pH 4.0 solution until the optimal response was attained. By eliminating the $NaHCO_3$ from the basal medium and freezing it in a CO_2 atmosphere, the pH 4.0 solution was created.

The sensitivity of the EMM-TN strain to various antibiotics, including *ampicillin, penicillin G, spectromycin, kanamycin, tetracycline,* and *chloramphenicol,* all at concentrations of 100μg/mL, was assessed. New culture media containing each of the four

antibiotics were prepared, and 5 mL portions of the EMM-TN culture were introduced into these media. The EMM-TN culture with antibiotics was then incubated at a temperature of 37°C for a week. The impact of the antibiotics was gauged by comparing the growth of cultures exposed to the antibiotics with that of a control culture. To evaluate the isolate's tolerance to varying salinity levels, NaCl concentrations ranging from 0.5% to 3.0% NaCl were used at intervals of 0.5%. This range of NaCl concentrations was achieved by incorporating a sterile anoxic stock solution of NaCl (58.44 g/L) into the medium.

3.5.5.3 Microscopy

Cells were frequently seen using an Olympus phase-contrast microscope. A conventional Gram-stain kit was utilized to determine the Gram characteristics. The hanging-drop method was used to measure motility using a glass cavity slide.

3.5.5.4 Deoxyribonucleic Acid (DNA) extraction and (G+C) content

DNA was isolated from culture samples of strain EMM-TN cultivated in the enrichment medium using a Fast DNA SPIN kit and the subsequent producer's directions. On a 1% agarose gel, DNA integrity was examined, and DNA concentration was quantified utlizing Nanodrop. Thermal denaturation characteristics were used to calculate the Guanine (G) and Cytosine (C) (G+C) content of DNA (Sly et al., 1986). The procedures for DNA extraction and G+C content of strain EMM-TN were repeated multiple times until unambiguous findings were obtained.

3.5.5.5 PCR amplification of 16S rRNA genes

In a polymerase chain reaction (PCR) thermal cycler, the forward and reverse primers employed to amplify the 16S ribosomal RNA (rRNA) sequence (~1,350 bp) were Ar109f (5'-ACKGCTCAGTAACACGT-3') (Großkopf et al., 1998) and Ar1383r (5'-CGGTGTGTGCAAGGAGCA-3') (Shlimon et al., 2004). The reaction mixtures, assembled in a 200 µL PCR reaction tube, had the following components, totaling a final volume of 20 µL: 2 µL of PCR reaction buffer, 2 µL of dNTP mix (35 mM), 0.5 µL of each primer (10 µmol/µL), 0.1 µL of Taq DNA polymerase, 1.0 µL of template DNA sample (100 ng), and 13.9 µL of molecular grade water. The PCR reactions were initiated by promptly placing the reaction tubes into a preheated thermal cycler set at 94°C. Following an initial denaturation step (94°C, 4 min), a total of 30 cycles of denaturation (94°C, 30 s), annealing (55°C, 30 s), and extension (72°C, 90 s) were conducted. Subsequent to a concluding extension phase (72°C, 6 min), the samples were maintained at 4°C until further analysis.

3.5.5.6 PCR amplification of mcrA genes

Amplicons of 490 bp were generated using the MLf (5'-GGTGGTGTMGGATTCACACARTAYGCWACAGC-3') and MLr (5'-TTCA TTGCRTAGTTWGGRTAGTT-3') primer combinations (Luton et al., 2002), whereas the ME1 (5'-GCMATGCARATHGGWATGTC-3') and ME2 (5'-TCATKGCRTAGTTDGGRTAGT-3') primer pairs yielded products (Simankova et al., 2003). The denaturation, annealing, and extension steps were carried out at 96°C (15 s), 55°C (30 s), and 72°C (90 s) for the MLf/MLr primers. Meanwhile, for the ME1/ME2

primers and MR1/ME2 primers, the temperature conditions were set at 94°C (40 s), 50°C (45 s), and 72°C (90 s) during denaturation, annealing, and extension, respectively.

3.5.6 Characterization of the Selected EMMs

3.5.6.1 Morphological and Molecular Identification

To examine the morphology of the EMM-TN strain, external growth was utilized, and observations were made using a light microscope along with a digital camera (National DC5-163 Digital, National Optical & Scientific Instruments, Inc., Schertz, USA). For molecular identification, DNA was extracted from pure cultures of EMM-TN strains that had been cultivated on enrichment medium for 14 days. Genomic DNA extraction, PCR amplification, purification of PCR products, and sequence determination were carried out by DNA Solution Ltd (Dhaka, Bangladesh). In each PCR cycle, a positive control using DNA from pristine cultures as the template and a negative control using molecular grade water were included.

To assess the DNA product, electrophoresis was performed on a 1.2% w/v agarose gel, which was colored and run at 100 V for 30 minutes in 1 Tris-acetate-ethylene-diamine-tetraacetic acid (EDTA) buffer. The TAE buffer contained 40 mM Tris base and 0.5 M EDTA (pH 8.0). A 2.5 µL Ladder I DNA quantification marker was employed during gel electrophoresis. The gel was captured using the Bio Imaging System and WiseCapture II software. PCR cycles included a 5-minute initial denaturation at 95°C, followed by 30 cycles of denaturation at 95°C for 30 seconds, annealing at 57°C for 1 minute, extension at 72°C for 3 minutes, and a final extension at 72°C for 10 minutes. The amplified DNA was

analyzed using gel electrophoresis. The 16S rDNA sequence was evaluated and compared to other sequences in the GenBank database using the online tool BLAST.

3.5.6.2 Separation and Purification

Following a 14-day incubation period, EMMs were isolated through the process of centrifuging the culture broth at 10,000 rpm, at a temperature of 25°C, for a duration of 10 minutes. The resulting supernatant was collected. To precipitate insoluble constituents, a mixture consisting of two volumes of cold ethanol (maintained at 4°C) was introduced to the supernatant in a ratio of 2:1. The combination was allowed to stand for 10 minutes, after which the upper phase was examined for any precipitated substances. The particulate matter was then extracted, subjected to washing with deionized water, and subjected to pneumatic treatment. This procedure was performed to acquire purified EMMs, following the approach outlined by Deng et al., (2005).

3.5.6.3 Chemical and Electrode Analyses

The phenol-sulfuric acid method was applied to calculate the total carbs and sugar content, with glucose serving as the reference solution (Nielsen, 2010). The total protein content was determined using the Folin-phenol reagent technique, with bovine serum albumin serving as the control (Lowry et al., 1951). The approach of Chen and Johnson was used to estimate chitin using glucosamine as a benchmark (1983).

Gas chromatography was employed to quantify the quantities of CH_4 and H_2 gas produced. In order to standardize hydrogen gas production rates to a methane-based molar scale, the rates were divided by four, considering the stoichiometric conversion of four

moles of hydrogen gas to one mole of methane. Concentrations of acetic, formic, propionic, and butyric acids were determined using high-performance liquid chromatography. Electrodes were prepared and analyzed through environmental scanning electron microscopy. More comprehensive data regarding these procedures can be found in the Supporting Data section.

3.5.6.4 EMMs Performance

The mechanism of Carbon dioxide reduction to CH_4 performed by methanogenic bacteria utilising cathode directly as a source of electrons or indirectly via hydrogen was known as electromethanogenesis. Understanding the impact of various controlling cathode potentials on the operational characteristics of electromethanogenic organisms was critical for efficient cathode design techniques. Different potentials (0.3V and 1.4V) were applied to replicate enhanced electromethanogenic groups, and the potential-induced alterations were examined utilizing a metagenomic and metatranscriptomic method.

3.5.6.5 Stability of EMMs

In this experiment, pH, temperature and time were investigated for stability of the EMMs. The pH of EMM was adjusted to 4,5, 6,7, 8 and 9 with 1M NaOH and 2HCl. EMM was kept at different temperature of 20, 25, 30, 35, 40, 45 and 50ºC for 7 days. The EMM was kept in room temperature (28±2ºC) and low temperature (25ºC) for 14 days. And gas phase tests were conducted to observe EMM activity in terms of reduce CO_2 from enrichment medium suspension. Enrichment medium suspension was used 10mL of EMMs. The medium was prepared with gas phase H_2: CO_2 (4:1) and pressurized to 100KPa. Gas

samples were connected Arduino Uno based gas sensor which was measure volumetric content in terms of CO_2, CH_4, O_2 and H_2 was determined.

3.5.7 Statistical Analysis

Optimization of AD based enzymatic hydrolysis, EMMs and H-MEC process were carried out using statistical software package-Design Expert 12.0.0 (Stat Ease Inc., Minneapolis, USA). FCCCD by RSM was used for process optimization.

3.5.7.1 One-Factor-At-A-Time (OFAT)

The most influential parameters were studied to determine EMMs such as pH, temperature, conversion time (days) and inoculum (% v/v). Table 3.5 shown the summarized OFAT design for to increase BioM production. All the experiments were conducted in triplicate. The CH_4 yield was measured by followed previous section (3.4.3.5).

Table 3.5: OFAT factors designed for fermentation

Factor	Range tested	Fixed parameters
pH	4 - 8	Basal Media 10mL/100mL, CO_2:H_2 ratio 20:80, Time 36 hours, gas flow rate 5L/hour, temperature 30°C, inoculum 10mL, applied voltage 0.9V.
Substrate (g/L)	10-100	pH 7, CO_2:H_2 ratio 20:80, Time 36 hours, gas flow rate 5L/hour, temperature 30°C, inoculum 10mL, applied voltage 0.9V.
EMM Inoculum (% v/v)	1 - 6	Basal Media 10mL/100mL, CO_2:H_2 ratio 20:80, Time 36 hours, gas flow rate 5L/hour, temperature 30°C, pH 7, applied voltage 0.9V.
Gas flow rate	1-11	Basal Media 10mL/100mL, CO_2:H_2 ratio 20:80, Time 36 hours, pH 7, temperature 30°C, inoculum 10mL, applied voltage 0.9V.
Time (Days)	1 - 7	Basal Media 10mL/100mL, CO_2:H_2 ratio 20:80, pH 7, inoculum 10mL, applied voltage 0.9V.

3.5.7.2 Response Surface Methodology (RSM) for Hydrolysis

For the purpose of optimizing and validating the studies involving EMMs activity, the statistical software package Design Expert 10.0 (Stat-Ease Inc., Minneapolis, USA) was utilized. The aim was to enhance the methane (CH_4) output, and thus, the parameters of EMMs were optimized using RSM. The specific type of RSM employed in this context was a FCCCD. Within this approach, two variables were investigated: inoculum dose and gas flow rate. The layout of the FCCCD model, outlined in Table 3.6, consisted of a total of 30 experimental runs, including 6 center points. Each individual factor was examined at three different levels, represented by the codes: low (-1), medium (0), and high (+1).

Table 3.6: FCCCD experimental design for EMM activity

Run No.	Factor 1 A: High Flow rate (L/hour)	Factor 2 B: Short Time (Hours)	Factor 3 C: Low Flow rate (L/hour)	Factor 4 D: Long Time (Hours)	Response % CH4 Conversion (Actual)	Response % CH4 Conversion (Predicted)
1	**5**	**24**	**5**	**24**		
2	5	24	1	36		
3	8	18	3	30		
4	11	18	3	30		
5	11	12	5	24		
6	11	12	1	24		
7	8	18	3	30		
8	**5**	**12**	**5**	**24**		
9	5	18	3	30		
10	**11**	**24**	**5**	**24**		
11	8	18	3	30		
12	11	24	1	36		
13	**11**	**24**	**5**	**36**		
14	**5**	**24**	**5**	**36**		
15	8	18	1	30		
16	8	18	3	36		
17	8	12	3	30		
18	8	24	3	30		
19	11	24	1	24		
20	8	18	3	30		
21	5	12	1	36		
22	11	12	5	36		
23	8	18	3	30		
24	8	18	5	30		
25	11	12	1	36		
26	5	24	1	24		
27	8	18	3	30		
28	5	12	1	24		
29	**5**	**12**	**5**	**36**		
30	8	18	3	24		

3.5.7.3 Validation of the experimental model

The model was confirmed by using dissimilar combinations of four variables with in the design space. The six set of experiments were selected by the point prediction process of the Design Expert software 12.0.0, to achieve the maximum turbidity reduction. The predicted results were compared with experimental results by calculating error percentage (Table 3.7).

Table 3.7: Model validation experiment

Experiment No.	High gas flow rate (L/hour)	Short Conversion Time (Hours)	Low gas flow rate (L/hour	Long Conversion Time (Hours)	CH_4 Conversion%	
					Predicted	Experimental
1	8	22.48	5	36		
2	8	14.76	1.07	28.52		
3	8	12.18	4.22	25.33		

3.5.8 Design, Fabricate and Characteristics of H-MECAD system

3.5.8.1 Design procedure of AD based H-MEC system

The key development in MEC technology was the cost-effective and customizable design MEC configuration. Moreover, innovative and cost-effective metals or microbial cathodes were urgently needed to overcome electrode potential and inner resistance within the chamber. Besides, the usage of membranes or membrane pH variations in design method must be avoided in order to save manufacturing costs. More expertise with actual biofuels including various biological substrates like particulate and polymeric compounds was also still necessary for the usage of diverse biofuel in MEC processes. Furthermore,

methanogenic H_2 utilization must be avoided in MEC methods with biocathodes or without membrane MEC methods. New advancement, paired with further financing and research in MEC structures, would enable for the commercialization of this novel biomethane system to occur shortly (Lv & Wang, 2017; Otero et al., 2018). The proposed design hybrid system consists of a two chamber MEC such as anode and cathode chamber, AD connected input and output port which were connected in anode side of MEC chamber, membrane filter slot chamber which was divided in four slots, electrode, electrical motor and motor pump ports, plastic pipe, pipe albo, clamp, measuring device connecting port, EMMs input port was connected in cathode chamber input port, etc. Figure 3.4 shows the proposed model of H-MECAD. In this design, two electrode port was used which was connected electric potential supply system. From Figure 3.4 shown that different view angle such top, bottom, left, right and isometric views were design by using Auto Cad 2019 software. In addition, the proposed design was used unique design each chamber was divided into five sub chambers for small and large volume purposed. In addition, the operational factors of the H-MECAD system such as temperature was an significant factor that influences their concert because it was progress the collection and action of electrogene. The proposed design was designed low and medium temperature and pressure. However, the use of metal body can also use high temperature and high pressure. BioM production of H-MECAD was simultaneously influenced by the hydrodynamic force and cathode EEMs, where the consequence of the hydrodynamic force for creating H_2 was better than that of the anode EEMs.

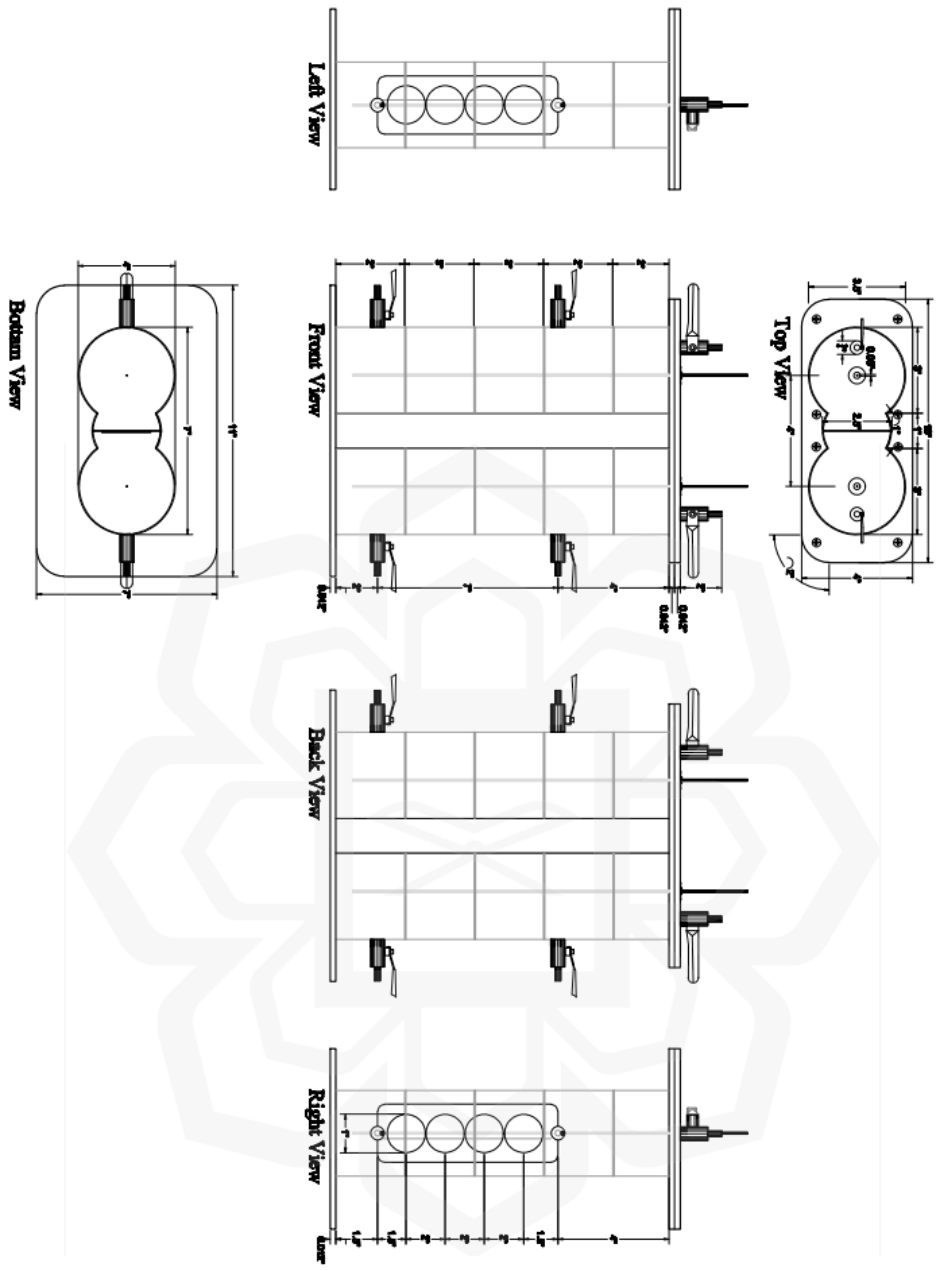

Figure 3.4: AD based H-MECs 2D diagram.

Design of the surface properties electrode, like size of the electorde, electrode distance, conductivity and surface morphology, also will be considered. Finally, the operational factors of the H-MECAD system for enhancing the productivity and selectivity of the H_2, CO_2, and CH_4 will be determined by the SEM analysis.

3.5.8.2 Fabrication of AD based H-MEC system

Two chamber anode and cathode were fabricated in the IUBAT electrical and electronic laboratory using 3mm of transparent plastic sheet using leakage resistant sealing gam. The chambers dimension of MEC duel chaber systems were H=10″, L=3″ and r=1.5″ which volume was 84.823in^3 as shown in Figure 3.5. In anode and cathode chamber using to two ports on the left, two on the right and two port on the top side each inlet or outlet diameter of ¼ inch hole and using ¼ get valve. one inlet of ¼ inch and one outlet of ¼ inch were static in such a technique that actual volume originated around 84.823in^3. Additionally, the top and bottom side of both chambers were proporly sealed by using top and bottom cover which were around L=10″, W=4″ and H=3mm of thickness, screw and sealing gam to circumvent any source of air enable the development of acidogenic microorganisms temporarily preventing the progress of methanogenic microorganisms. Using both chambers were four sub chambers each circular hole of around 3inch in height and 1.5 inches in diameter was made and each circular was attached to three flat electrodes which were around 1.4 inches in diameter, 1mm in thickness, and 1inch distance. In this chamber graphite sheet of dimension 1.4 inch of diameter and thickness of 1 mm was utilized electrode and was used with stainless-steel round bar of dimension hight of 14inch, thickness of 8mm. In anode chamber one inlet gate valve was connected of 1.5 mm diameter PVC pipe between anode chamber inlet get valve and 6V to 12V DC electric motor pump output or delivery outlet and another one inlet of the motor pump was connected in AD system outlet gate valve. In this gate valve was used to make effective volume of around 1000mL (water and gas). However, anode chamber outlet gate valve was connected by using 1.5 mm diameter PVC pipe to ADs inlet gate valve (bypass line). In

this chamber the top portion gate valve was placed in cathode chamber in inlet gate valve by connected 1.5 mm diameter PVC pipe there would be proper supply of CO_2 throughout the cathode chamber.

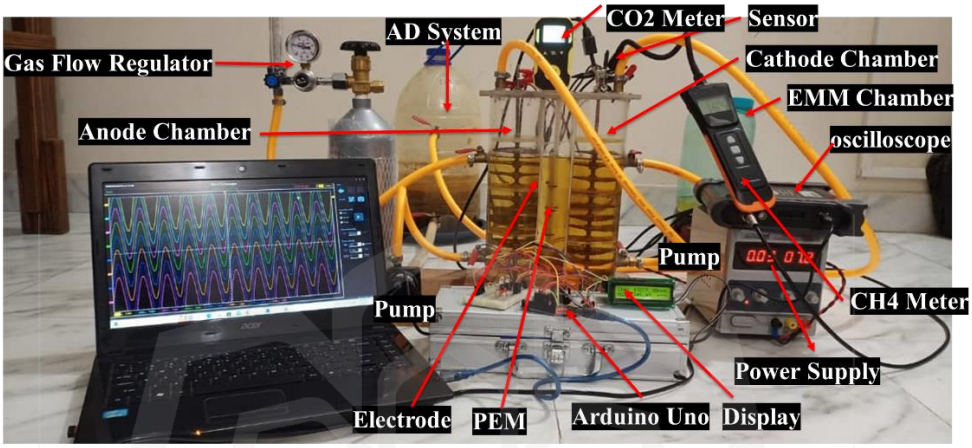

Figure 3.5 AD based H-MECs experimental setup.

Whereas in cathode chamber one outlet gate valve was attached to EMMs chamber which was dimension of 11inch x 4.5inch x 2inch make inject effective volume of EMMs. In this chamber the top portion was connected different types of gas measure meters in such a way that there would be proper measure throughout the experimentation. These two chambers were separated by membrane filter which acts as the proton exchanger. Dimension of membrane chamber was 12inch x 2inch x 3inch and distance between anode and cathode around of 1inch. Using membrane slot was four different membrane or same membrane depend on volume capacity of anode and cathode chamber. In addition, each membrane filter dimension was diameter of 1inch and thickness of 0.5mm.

3.5.8.3 Operation of AD based H-MEC system

Bioelectrochemical systems were extraordinary systems that use the potential energy of waste products and cellulosic to transform it into electrical energy or hydrogen/chemical compounds in MECs. MECs use an electric current to partially reverse the process of generating hydrogen or methane from biological material. Figure 3.6 depicts the suggested H-MECAD model.

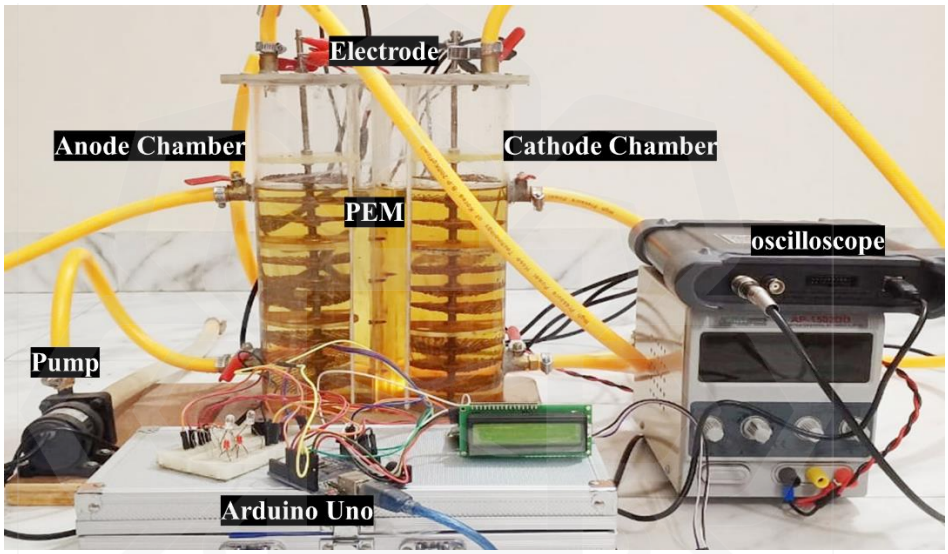

Figure 3.6: Experiment model of H-MECAD

The microbial electrolytic cell and anaerobic digestion were beneficial in the proposed hybrid system for producing a high concentration of BioM from FW. The food waste was suitable for high yield of biogas production. Therefore, the upgrading of biogas to increase the pure methane as clean energy as well as utilization of CO_2 into methane was required for high efficiency of thermal and electric heat generation and safe of the environment by capturing CO_2. FW was taken from the AD system and pretreated by using enzymatic hydrolysis and ready hydrolytic substrate with biogas contains loaded into the anode chamber. Whereas cathode chamber was filled basal or enrichment media. The

hydrogen-producing microbial electrolysis cell (H-MEC) integrated with anaerobic digestion (AD) was operated under fed-batch conditions at a consistent temperature of approximately 30°C. The anode chamber was constructed in a sealed manner to prevent the entry of air and thereby inhibit the growth of electro-methanogenic microorganisms. The experiment was conducted both with and without the addition of a 5% dextrose solution within the anode chamber. Gas meter was used to measure biogas, CH_4 and H_2 the top cathode side gate valve. Figure 3.18 shows the essential components of H-MECAD, which consists mostly of a cathode and an anode terminal. It also includes electrocatalyst suitable microorganisms, a membrane, and an additional power backup. Parameters impacting the functioning of H-MECAD in electrochemical conversion systems also include separator, substrate, microorganism, operational factors, reactor configurations, anode, and cathode. The aforementioned parameters should be examined in order to increase BioM generation in H-MECAD and realized its practical use.

3.5.9 Optimization of H-MEC Systems Parameters

The optimization of the conversion process was achieved through the utilization of RSM, specifically employing the approach of a FCCCD. The experiments detailed in this investigation were executed employing the OFAT method, which allowed for the assessment of potential optimal levels. The FCCCD approach was employed to delineate the response surface nature in the experimental setup, elucidating the optimal conditions for both critical independent and dependent variables. The data provided represents the mean values obtained from three separate replicates. Subsequently, ANOVA was

conducted, followed by a least significant difference test, as determined by the statistical software employed in the study.

3.5.9.1 One-Factor-At-A-Time (OFAT) for H-MEC

OFAT analysis method was described in the section 3.4.2. The most influential parameters were studied to determine fermentation process such as H-MEC pH, anode and cathode substrate, applied potential, current density and CV. Table 3.8 shown the summarized OFAT design for H-MEC to increase bioM production.

Table 3.8: OFAT factors designed for H-MEC

Factor	Range tested	Fixed parameters
Substrate Loading (g/L)	50-100mL	pH 7, Time 36 hours, temperature 30°C, inoculum 10mL, applied voltage 0.7V, gas flow ratio 5l/hour, CO_2:H_2 ratio 20:80 and Current density 600mWm^{-2}.
Applied potential (V)	0.1-1.5	pH 7, Time 36 hours, temperature 30°C, inoculum 10mL, substrate loading 100mL/500mL, applied voltage 0.7V, gas flow ratio 5l/hour, CO_2:H_2 ratio 20:80 and Current density 600mWm^{-2}.
pH	4.5 - 8	Time 36 hours, temperature 30°C, inoculum 10mL, applied voltage 0.7V, substrate loading 100mL/500mL, gas flow ratio 5l/hour, CO_2:H_2 ratio 20:80 and Current density 600mWm^{-2}

3.5.9.2 Response Surface Methodology (RSM) for H-MEC

The design of experiments (DOE) for this study was done using Design-Expert version 10. A FCCCD was used to optimize the independent variables such as pH, substrate loading

applied voltage and BioM as shown in Table 3.9. The effect of those variables was studied by measuring the amount of BioM production. The six center points were employed to model the surface response function of the manipulated variable. RSM was a collection of mathematical and statistical techniques that prove valuable for the development, enhancement, and optimization of processes.

Table 3.9: FCCCD experimental design of H-MECAD

Run	Factor 1 A: Substrate Loading (mL)	Factor 2 B: pH	Factor 3 C: Applied Potential (mV)	CH_4 Conversion (%)	
				Experimental	Predicted
1	100	6.5	900		
2	100	7	1100		
3	150	6.5	1100		
4	**100**	**7**	**900**		
5	50	6.5	1100		
6	150	7.5	700		
7	50	7.5	1100		
8	150	6.5	700		
9	**150**	**7**	**900**		
10	50	7	900		
11	**100**	**7**	**900**		
12	100	7.5	900		
13	50	7.5	700		
14	**100**	**7**	**900**		
15	100	7	900		
16	**100**	**7**	**900**		
17	**100**	**7**	**900**		
18	100	7	700		
19	50	6.5	700		
20	150	7.5	1100		

RSM was applied where several variables (independent variables) impact almost concert measure or excellence characteristic of the progression (response of interest) and the objectives was to optimize this response (Bradley, 2007). It was a powerful technique for the modelling and analysis the problems. According to the FCCCD for the three variables, response surface of the central composite design with one response and three levels (High, medium and Low) denoted by +1, 0 and -1 gave 20 runs of experiments as shown in Table 3.9.

3.5.9.3 Validation of the experimental model

The statistical approach was evaluated in terms of all 2 factors in the design process. A set of four trial configurations, chosen as predicted by the Design Expert software's point prediction tool, were used to investigate the optimum conversion activity under specified conditions (Table 3.10). All of the tests were done in triplicates.

Table 3.10: Experimental model validation

Substrate Loading (mL)	**CO_2/H_2 flow ratio**	**Applied potential (mV)**	**CO_2 to CH_4 Conversion**		**Error (%)**
			Experimental (%)	**Predicted (%)**	
100	50:50	900			
100	60:40	900			
100	70:30	900			
100	80:20	900			
100	90:10	900			

3.5.9.4 Studies of the Kinetic Parameters of the H-MEC

An experiment was conducted with optimum media and H-MEC based CO_2 to CH_4 conversion conditions to determine the effect of conversion time on BioM production as well as to determine the BioM production and biomass growth kinetics during the conversion. These concerns, the BioM production, growth of biomass in terms of flow of CO_2, hydrogen content was determined from every 3 hours until the 45 hours. The yield of BioM production based on total hydrogen consumption ($Y_{p/s}$), the yield of biomass formation based on hydrogen consumption ($Y_{x/s}$), the yield of product formation from biomass ($Y_{p/x}$), the specific growth rate (μ) and the specific rate of product formation (q_p) was estimated from the experimental results. The specific growth rate (μ) and the specific rate of product formation (q_p) were determined by the Equation 3.10 and 3.11.

$$\ln X = \ln X_0 + \mu t$$

$$X = X_o e^{\mu t} \tag{3.10}$$

Where, X is biomass

X_0 is initial biomass

t is time

$$q_p = Y_{p/x}\mu + m_p \tag{3.11}$$

Where, $Y_{p/x}$ is the true yield of product from biomass

m_p is the specific rate of product formation due to maintenance

3.5.10 Comparison of H_2-CO_2 and EMMs

The experiment has been conducted after completing validation experiment on conversion process. In the experiment, low, medium, high and combination of design level were chosen from validation part (Table 3.11) to compare the EMM and chemical coagulant in the conversion process. The EMM dosages were 6, 8, 10, 12 and 14 mL/L as low, medium & high in the optimization of conversion process. These doses had a corresponding H_2-CO_2 concentration of 1, 5, 8, and 11L/hour respectively. In hydrogen, the H-MEC efficiency was observed at the same percentage of EMM. The H_2-CO_2 and EMM doses were presented in Table 3.11.

Table 3.11 Comparison between EMM and CO_2 on H-MECADs

Experiment No.	Gas flow rate (L/hour)	EMM Dose	BioM %	
		mg/L	CO_2	Biogas
1	5	10		
2	5	10		
3	5	10		

3.6 SUMMARY

This chapter attempted to give detailed step by step descriptions of the analytical and experimental methods employed to achieve all objectives of the research. The study started with different samples collection, isolation, purification and screening and this was followed by entrapment potentiality test of enzymatic microbes, EEMs and eventually potential microbes were screened based on AD based H-MEC test for BioM production from food waste. After selection of potential enzymatic microbes and EEMs, effect of

nutrients, suitable growth conditions were tested and BioM production was conducted for next objective. The characterization by identification and then chemical analysis, zeta potential, SEM and evaluation of EMMs performance were conducted to find out electron transfer mechanisms of the EMMs for BioM production. After achieving the mechanisms, optimization of conversion process was performed by FCCCD and suggested solutions by the model equation were validated. Settling characteristics through a lab scale settling design was used and stability was analyzed to evaluating the BioM performance of the new EMM. Then optimization of H-MECAD process with FCCCD as the method used and suggested model solutions were validated as required and also compare the production capacity with chemical coagulant. Finally, raw and treated biogas qualities were analyzed. In addition, all the experiments were conducted in triplicate.

CHAPTER FOUR

RESULTS AND DISCUSSION

4.1 INTRODUCTION

This chapter describes the entire experimental results obtained to achieve the research objectives. The presentation of the results and discussions was followed sequentially with the objectives of this study described in Chapter One. The first objective was focused on the isolation, purification and screening of potential microbes in terms of BioM. All experimental results for the characterization of Food waste and hydrolysis process to increase biogas and BioM production through liquid state fermentation were presented and discussed. The order of presentation of the results and discussion followed sequentially to cover all objectives those were highlighted in the chapter one (section 1.3).

The first screening was carried out on a number of isolated hydrolytic microbes and EMMs to evaluate the entrapment ability in a schott duran glass bottle for upgrade BioM from AD system biogas contains. The second screening was conducted by using supernatant and hydrolytic microbes and EMMs to upgrade BioM from AD system CO_2 and H_2. The first objective was concluded to optimize the growth conditions for enhancing production of the potential hydrolytic microbes and EMMs. Also, the first objective was focused on identification, characterization hydrolytic microbes and EMMs performance that was conducted for the evaluation of conversion mechanisms. The hydrolytic microbes were identified by both its morphological and phylogenetic characteristics.

On the other hand, the potential EMMs identified as Lentinus squarrosulus EMM-TN was selected EMM for production of BioM. The EMMs was characterized by FTIR, SEM, zeta potential, chemical and elemental analysis to understand the electron transfer mechanisms for convert CO_2 to CH_4. The second objective was focused on hydrolysis process, optimization and validation of model suggesting optimum values of process conditions necessary for high biogas production from food waste. However, the third objective was focused design and fabricate H-MEC system which was locally available. In addition, the third objective was focused on H-MEC operation process, optimization and validation of model suggesting optimum values of process conditions necessary for high BioM production from AD system CO_2 and H_2. Three optimization studies were carried out by using design expert software version 10.0.0. Response surface methodology (RSM) was implemented through FCCCD to achieve at optimum levels of investigated parameters. After obtaining the optimized H-MEC operating conditions, the fourth objective to evaluate the interactions of EMMs between microbial species (single and mixed culture) and electrode surfaces in the H-MECAD system for high content of BioM production in a lab scale settling H-MECAD. Finally, the objective five to determine the influence of the optimization of operational factors process conditions was optimized of the EMMs to reduce CO_2 from food waste-based AD in a hybrid model. Then, the result was followed by the validation study in order to verify the optimized process conditions for CO_2 reduction by a flowing environment. The results were also examined to compare the system efficiency between the H-MECAD and EMMs. Finally, H-MEC based AD system was used to reduce the CO_2 of AD system and upgrade CH_4 quality standard in World, to show the potential EMMs of using the new proposed methods and design.

4.2 CHARACTERIZATION OF FOOD WASTE

Table 4.1 provides an overview of the properties of the FW composition employed in this research. After the removal of bones and shells, the remaining waste was mixed with distilled water in a 1:1 (w/w) ratio. Thoroughly characterizing the FW was of paramount importance before embarking on the optimization process, as it served as the substrate during both media and process optimization for BioM production. Given the variances observed among different production units and other factors, this study undertook the essential task of characterizing the FW. Results from the analysis revealed that the raw sample contained 15.6% (w/v) total solids (TS), with 30.23 mg/mL of total sugar, 16.5 mg/mL of reducing sugar, 3.37% (w/w) cellulose, and a pH of 5.35. Notably, the characterization of the FW in Table 4.1 aligns with the composition of actual household food waste samples reported in existing literature (Garca et al., 2005; Matsakas et al., 2014; Alibardi & Cossu, 2016). Strazzera et al., (2018), despite collecting their sample from the same household food waste, observed a COD value of 111 mg/mL. In the context of waste management practices, Lin et al., (2013) highlight that a significant portion of biodegradable waste is either directed to landfills or utilized for primary recycling and reuse, such as organic manure, biofuels, or livestock feed when feasible. Unfortunately, this approach leads to environmental and social consequences, including emissions of pollutants into soil, air, and water. Notably, each ton of biodegradable waste deposited in landfills results in the emission of approximately 4.2 tons of carbon dioxide (CO_2), contributing to about 3% of the overall global greenhouse gas (GHG) emissions (Segrè and Falasconi, 2011). Furthermore, to improve its effectiveness, the waste was mixed with water at a 1:1 (v/v) ratio and mechanically broken down into smaller particles. This treated

mixture was subsequently subjected to digestion at a temperature of 55°C for a period of 12 hours, resulting in the production of a hydrolysate rich in sugars, with a concentration of 164 g/L (Choi et al., 2017; Cremonez et al., 2020; Brown et al., 2020; Michelin et al., 2020).

Table 4.1: Characterization of the food waste

Parameters	**Units**	**Concentration**
Total Solids (TS)	(% w/v)	15.6
Total Suspended Solid (TSS)	(%w/v)	13.2
Total Dissolved Solids (TDS)	(%w/v)	2.4
Volatile Solids (VS)	(%w/v)	13.62
Volatile Suspended Solids (VSS)	(%w/v)	11.47
Volatile Dissolved Solids (VDS)	(%w/v)	2.09
Moisture Contain	(%)	79.53
Reducing Sugars	mg/mL	16.5
pH	-	5.05
Proteins	(%w/v)	9.7
Chemical Oxygen Demand (COD)	g/L	89.2
Carbohydrates	(%w/v)	25.4
Cellulose	% (w/w)	3.7
Hemicellulose	% (w/w)	1.19
Lignin	% (w/w)	0.57

4.3 ISOLATION, PURIFICATION AND SCREENING OF ENZYMETIC MICROBS

Six fungi strains such as TN-AF1, TN-AF2, TN-AF3, TN-BC1, TN-BC2 and TN-BC3 were isolated from animal feed and bio compost as shown in Figure 4.1 and Figure 4.2.

From Figure 4.1, based on external appearance, colour and colony texture, TN-AF1 to TN-AF3 colonies were velvety in textures having blue greenish to moderate bluish green and powder aspect. Also, the TN-AF1 to TN-AF3 showed white colonies of cotton texture and colonies diam of 36~52mm after separation or single colonies. However, the surface colonies observation showed that the strain TN-AF1 to TN-AF3 were under mesophilic and filamentous fungi. Several scholars have been described the morphological identification of mesophilic and filamentous fungus (Pinto et al., 2012; Fakhru'l-Razi et al., 2002; Awadalla et al., 2017). The clear zone of inhibition was observed after the enzymatic utilization of the cellulose (Khokhar et al., 2012). The study was set about to isolate, purify and screen the mesophilic and filamentous fungus from animal feed for the degradation of food waste and increase the Biogas.

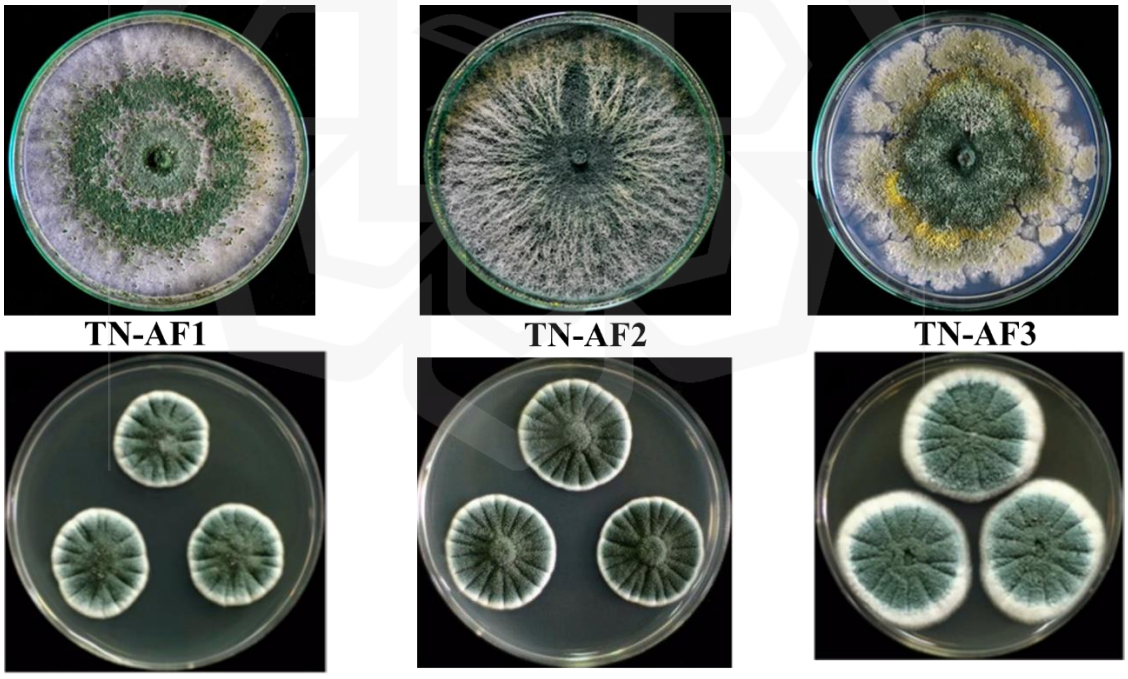

Figure 4.1: Isolated filamentous fungus from animal feed.

The colonies of TN-BC1 to TN-BC3 were net like texture and the surface colony colour was initially sometime becoming crustose, yellow greyish to blue green and powdery, colour changed to black at maturity strain TN-BC2. According to Figure 2, colonies observed was a mold belonging to the filamentous fungus. The filamentous fungus was made up of specific molds that may be detected on plants, in soil, and in water. This strain a haploid filamentous fungus and used for food waste management and biotransformations purposed.

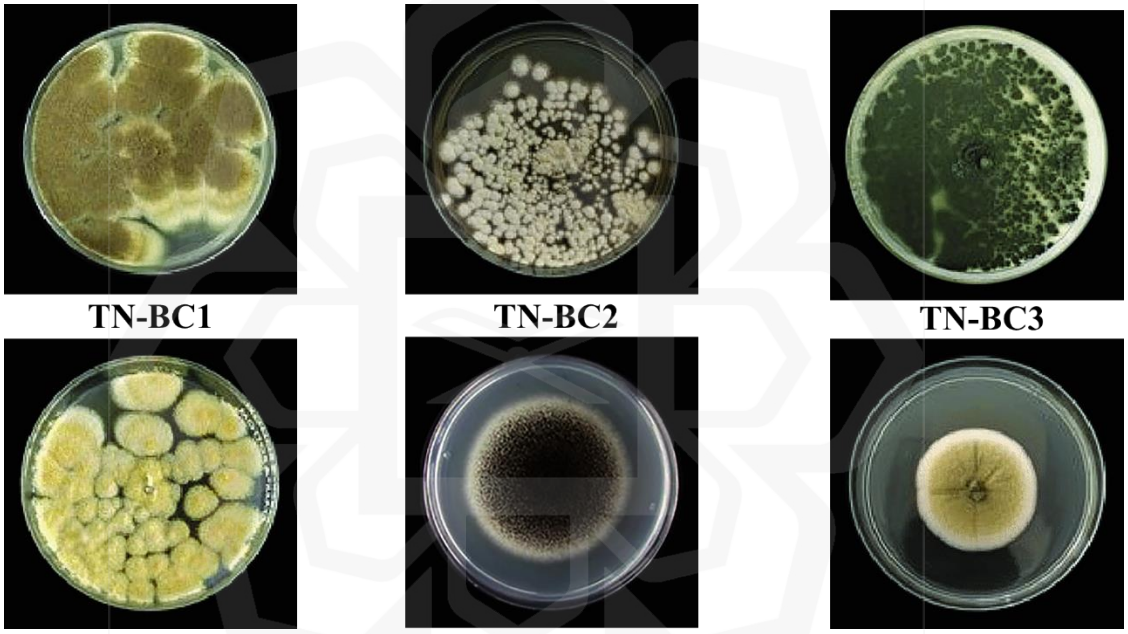

Figure 4.2: Isolated filamentous fungus from bio compost.

The haploid filamentous fungus isolates were screened to check their ability to degrade food waste through the Congo red plate screening method. The clear zone of self-consciousness was detected after the enzymatic use of the amylase (Khokhar et al., 2012). The study was set about to isolate, purify and screen the mesophilic and haploid filamentous fungus from bio compost for the degradation of food waste and increase the Biogas.

4.3.1 Morphological Characteristics Potential Fungus

The differences in morphological characteristics among potential fungus strains were summarized in Table 4.2, focusing on the physical appearance, color, and macromolecular properties of 7-day-old fungal cultures plated on PDA. Among the six strains studied, three exhibited green to dark green coloration, one showed yellow to greenish hues, and two displayed light yellow to blackish shades. After three days, all fungal strains matured and developed conidia, with their colors shifting from white to greenish during the initial incubation period. None of the three strains (TNAF1, TNAF2 and TNAF3) exhibited *T. reesei* concentric rings, but three strains (TNBC1, TNBC3 and TNBC3) formed filamented hyphae resembling small plants of *A. Niger*. Additionally, TNAF1 and TNBC3 strains produced extracellular green pigments, which turned greenish after 7 days of incubation at 28°C. Notably, TNBC3 and TNAF1 showed a significant level of morphological similarity. Through morphological examination, it was determined that both strains belonged to separate species, TNAF1 (Peciulyte et al., 2014; Akli et al., 2022) and NTBC3 (Perrone et al., 2011; Hong et al., 2013; El-araby et al., 2022). According to Table 4.2, TNAF1 was now grouped in a phylogenetic clade with *T. parareesei* and *T. gracile* (Samuels et al., 2012). While *T. reesei*, *T. parareesei*, and *T. gracile* all grow at temperatures between 25-35°C and 35°C on PDA, *T. reesei* produces fewer conidia on PDA and synthetic nutritional agar (SNA) (Samuels et al., 2012). Notably, the conidial features observed in this study were consistent with those reported in previous publications on *A. niger* strains (Hong et al., 2013; El-araby et al., 2022). However, strain TNBC3 exhibited larger metula, a biseriate sterigmata structure, compared to prior investigations (Table 4.2).

Table 4.2: Morphologic characteristics potential fungus

Morphologic	**TNAF1**	**TNBC3**
Gram stains (Abundant)	---	+++
Appearance	Cottony	Cottony
Canidia diameter (μm)	3.4	3.9
Phiulide ($length \times width$; μm)	7.7×2	7.8×3.6
Melula ($length \times width$; μm)	28.8×7.5	35.5×8.1
Vesicle (diameter; μm)	43	45
pH for growth		
Optimum	5.5	9
Maximum	6.5	12
Margins	Round	Entire
Elevations	Convex	Umbonate
Growth	Rapid	Rapid
Temperature for growth (°C)		
Optimum	35	28
Maximum	55	45

This discrepancy might be attributed to the asexual fungus *A. niger's* high amount of genetic diversity (Perrone et al., 2011). In this investigation, strain TNBC3 was the only *A. niger* isolate having amylase enzyme activity out of the total of morphologically recognized *A. niger* isolates, showing the occurrence of various genotypes among *A. niger* strains.

4.3.2 Molecular Identification by Observing Microscopic Morphology

Two potentially promising fungal strains, namely TNAF-1 and TNBC3, were subjected to PDA incubation at a temperature of 28°C for a duration of six days. Notably, both strains displayed a distinctive green colony coloration. In terms of growth characteristics, TNAF-1 isolates exhibited a radial growth pattern and demonstrated faster growth compared to the TNBC3 isolates. Microscopic analysis revealed that TNAF-1 isolates displayed spherical-shaped conidia, whereas TNBC3 isolates exhibited dark-green pigmented conidia. Chlamydospores were identified in two isolates, and branched conidiophores were also observed (Figure 4.3). Further classification was based on the presence of dimitic and amphimitic hyphal systems. The Trichoderma sp (TNAF1 strain) and Aspergilla sp (TNBC3 strain) were categorized under the family Polyporaceae, considering the morphological features and microscopic characteristics (Pegler, 1983; Singer, 1986). These findings were consistent with the generative and skeletal hyphae as well as the round-shaped basidiospores (TNAF1) and entire-shaped basidiospores (TNBC3) described by Karunarathna et al., (2011). The color transformation of the fresh fruiting body, initially whitish and then turning greenish with aging, was also observed.

Molecular identification of the fungal strains relied on the rRNA operon gene sequence, encompassing 18S rRNA, ITS1 spacer, 5.8S rRNA, ITS2 spacer, and 28S rRNA. This analysis revealed the highest matching with the Trichoderma sp (TNAF1 strain) and Aspergilla sp (TNBC3 strain) genera. A sequence-similarity comparison against GenBank's existing gene sequences involved 10 related strains within the Trichoderma sp (TNAF1 strain) and Aspergilla sp (TNBC3 strain) genera. Based on these nucleotide sequences, the isolated filamentous strain exhibited a 99% similarity to the Trichoderma sp (TNAF1

strain) and Aspergilla sp (TNBC3 strain) genera, as indicated by GenBank accession Numbers GTNA02201 and GTNB02202.

Through a combination of morphological and phylogenetic characteristics, the strains (TNAF1 and TNBC3) were conclusively identified as Trichoderma reesei TNAF1 and Aspergilla niger TNBC3. To visually depict the relationship between the strain and comparable sequences from GenBank, a phylogenetic tree was constructed (Figure 4.3). Additionally, the SDS-PAGE analysis and nucleotide sequence of the fractionated DNA bands of TNAF1 were provided in Appendix C.

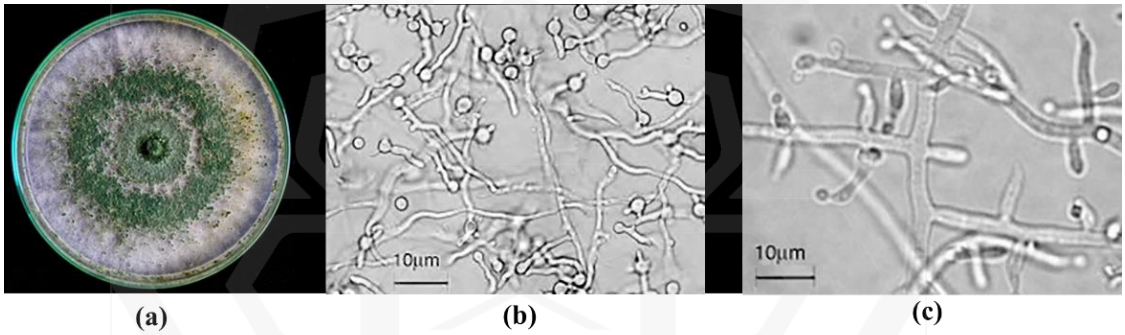

Figure 4.3: Culture of *Trichoderma reesei* TNAF1 (a) Colony morphology of *Trichoderma reesei* TNAF1 grown on PDA plates after 7 days. (b) Microscopic photograph of fungal basidiospore observed under light microscopy 10 µm (c) Sterigmata (metula, phialides) and conidia 10µm.

Figure 4.4 depicts a phylogenetic tree based on known representatives of the *Aspergillus niger* strain (TNBC3). Strain TNBC3 exhibited considerable similarities to strains from the *Aspergillus niger* genus, with the maximum similarity of 99% with *Aspergillus niger* strain TNBC3 (GenBank accession Number GTNB02202). TNBC3 was recognized as *Aspergillus niger* and given the name A. niger based on the following features. TNBC3 *Aspergillus niger*.

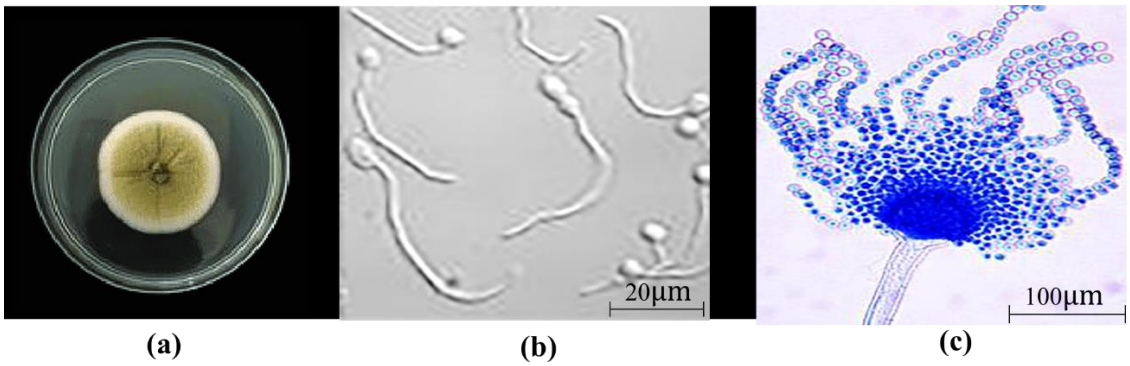

Figure 4.4: Culture of of *Aspergillus niger* TNBC3 (a) Colonies grown for 7 days on PDA plate. Scale bar, 2 cm. (b) Microscopic photograph of fungal basidiospore observed under light microscopy 400 X magnifications and 20 µm (c) Conidial structure displaying vesicle and sterigmata of 100 µm.

4.4 EFFECT OF ENZYMATIC HYDROLYSIS BASED ON AD SYSTEM

Enzymatic hydrolysis was necessary for accelerating the hydrolysis process and make the cellulose, hemicellulose and lignin more accessible. Enzymatic hydrolysis of lignocellulosic material was affected by hydrolytic enzyme like cellulase and amylase enzymes (Elgharbawy et al., 2016; Parthasarathy et al., 2016; Pal et al., 2016). Amylase was utilized to develop the hydrolysis of starch. Whereas cellulase was utilized to progress the hydrolysis of cellulose. Cellulase and amylase were both utilized to development the hydrolysis of food waste as it contains significant volumes of cellulose and starch.

The food waste sample was pre-treated by cellulase and amylase for enzymatic hydrolysis. The hydrolytic enzymes were added to 1000mL plastic jar containing raw food waste. The applied concentration was varied between 40 and 140 U/mL and the optimum dose (40 to 140U/mL) of cellulase and amylase hydrolytic enzymes was determined by measuring reducing sugars. Then, the enzymatic hydrolysis treatment was conducted by adjusting the pH of the food waste by adding different concentration of NaOH or HCL and

subsequently re-adjusted the pH ranges from 5 to 7. The enzymatic hydrolysis treatment of the food waste before hydrolysis was done intensively using OFAT method.

4.5 OPTIMIZATION OF ENZYMATIC HYDROLYSIS

AD house intricate organic substances that comprise complex polymers, which are not directly accessible to microorganisms without undergoing hydrolysis pretreatment or other preparatory steps. Thus, the hydrolysis process serves the purpose of breaking down large organic macromolecules into smaller constituents. These smaller components can subsequently be utilized by acidogenic bacteria, facilitating the subsequent methanogenesis phase. However, it has been previously noted in the literature that the hydrolysis step in food waste anaerobic digestion remains a limiting factor within the biological processes of anaerobic digestion.

To address this rate-limiting aspect, the hydrolysis of food waste was explored using hydrolytic enzymes within a dedicated hydrolysis reactor. Enzymes play a crucial role in converting carbohydrates, lipids, and proteins into simpler components like sugars, long-chain fatty acids, and amino acids, respectively, as elucidated by Li et al., (2011). Following enzymatic breakdown, the hydrolysis products can diffuse through the cell membranes of acidogenic microorganisms, promoting the biodegradation of organic compounds. Thus, incorporating enzymes capable of enhancing hydrolysis and enabling the degradation of complex carbohydrates is essential. Consequently, this study aimed to investigate the impact of enzyme quantities and biodegradation duration on food waste hydrolysis. This exploration sought to assess the viability of employing enzymes in the hydrolysis process as a pretreatment for food waste. It aimed to determine the optimal enzyme quantity and

biodegradation time for the hydrolysis process. The optimization of enzymatic hydrolysis was carried out in two phases. Initially, a OFAT design was employed to evaluate the potential optimum levels of three key parameters: hydrolysis pH, hydrolysis time, and enzyme dosage. This initial phase was executed within the context of the hydrolysis treatment strategy outlined in previous sections. Subsequently, the parameters identified as optimal from the OFAT study underwent further assessment using the statistical optimization technique known as FCCCD.

4.5.1 One-Factor-At-A-Time (OFAT) Experimental Analysis

The One Factor at a Time (OFAT) experimental approach was extended to identify the predominant factors within the hydrolysis treatment process that significantly impacted the proximity of TS and VS values. This endeavor aimed to establish optimal design conditions for TS and VS values before proceeding to the optimization phase, as highlighted by Rashid et al., (2011). The pivotal parameters subjected to the OFAT investigations encompassed enzyme pH, hydrolysis time, and enzyme dosage. The intent was to discern their influences on TS, VS, reducing sugar (RS), and COD values, with a focus on achieving closely aligned results.

4.5.1.1 Effect of hydrolytic time on hydrolysis process

During enzymatic hydrolysis of volatile solids, the solid substrate was broken down by enzymes into smaller compounds. The volatile solids, such as sugars or organic acids, were converted into gases or volatile liquids that can be easily removed by evaporation or distillation. The product of enzymatic hydrolysis of volatile solids may also contain water,

which can be removed through a drying process. This process can be used to produce biofuels, flavorings, and fragrances, among other things (Guilbault, 2013). The optimized process conditions were evaluated by monitoring the degradation of organic compounds over a span of 0 to 7 days during enzymatic hydrolysis. The influence of incubation time on organic compound degradation was investigated, with daily assessments conducted up to 7 days. Results revealed that the incubation time exerted a significant impact on organic compound degradation, with the highest degradation observed after 5 days of incubation, yielding an RS value of 115.64 g/L. Figure 4.5 portrays the outcomes of the hydrolysis time evaluation, indicating that extending the incubation time beyond 7 days did not lead to a further increase in organic compound degradation.

As depicted in Figure 4.5, the RS content was initially 16 g/L prior to hydrolysis, and this value increased to 16.50 g/L, 100.73 g/L, 104.86 g/L, 107.24 g/L, 113.47 g/L, 115.64 g/L, 109.90 g/L, and 105.85 g/L for incubation durations of 0-day, 1-day, 2-days, 3-days, 4-days, 5-days, 6-days, and 7-days, respectively. These results were obtained under a constant enzyme dose of 80 U/mL and a TS content of 12.5%. Additionally, the characteristics of the food waste substrate were determined both before and after digestion. For the substrate initially possessing an RS content of 15.5 g/L prior to digestion, the RS content was significantly increased to 115.64 g/L post-digestion. FW hydrolysis was reduce sugar content by breaking down carbohydrates into simpler sugars through the action of enzymes. The effect of reducing sugar content was influenced by factors such as incubation time of 5 days and total solid content of 12.5% TS. Incubation time refers to the duration of time that the food waste was subjected to hydrolysis, and longer incubation times generally result in greater sugar reduction of 115.64 g/L. Total solid content refers to the

amount of solids present in the food waste, and higher total solid content generally results in greater sugar reduction due to increased availability of carbohydrates for enzymatic breakdown. This implies that varying the duration of hydrolysis time contributes to the degradation of organic compounds, thereby enhancing the hydrolysis of food waste. Conversely, a control group with a hydrolysis duration of 0 days, representing food waste without any duration of treatment, was also investigated to assess the influence of hydrolysis time on food waste hydrolysis (Wang et al., 2022).

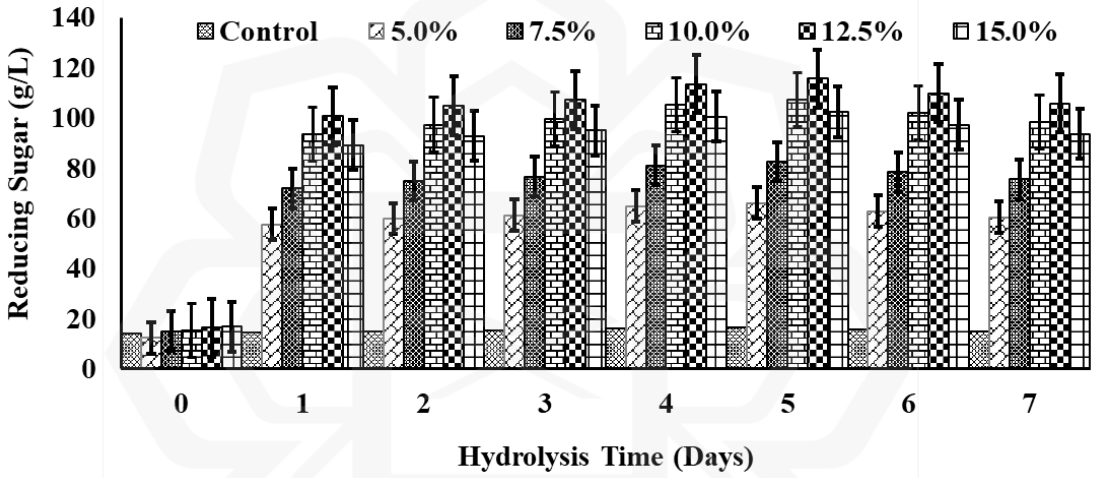

Figure 4.5: Effect in reducing sugar of food waste hydrolysis with different incubation time and %TS. Other factors were fixed enzyme dose 80U/mL, pH 5 and room temperature 30^{o}C (±2).

Following a 7-day period of hydrolytic acidification, the volatile solids experienced a reduction of 48.1%, resulting in the production of 6.8 g/L of volatile fatty acids, 82 g/L of reducing sugars, and 4.7 g/L of acetic acid (Yan et al., 2022; Kiran et al., 2015). In the realm of enzyme digestion studies, it has been highlighted that growth substrates contribute to 40% of the overall manufacturing expenses, a cost that can only be mitigated through the adoption of cost-effective alternative substrates (Reshmy et al., 2022).

4.5.1.2 Effect of hydrolytic pH on hydrolysis process

The influence of hydrolysis pH on the breakdown of organic compounds by the hydrolytic enzyme was examined across a range of pH values from 4.0 to 6.0, as depicted in Figure 4.6. The optimal pH for this enzyme's activity was determined to be pH 5. Under this pH condition, there was a 12.5% solubilization of organic compounds, while the control exhibited a level of 14.79 g/L of RS. Although the most effective organic compound degradation was observed at pH 5, it was noted that the enzyme exhibited significant activity for organic compound degradation across the pH range of 4.5 to 7. Specifically, the degradation of organic compounds at pH 4, 4.5, 5, 5.5, 6, 6.5, and 7 resulted in RS levels of 16.72 g/L, 66.88 g/L, 83.60 g/L, 117.04 g/L, 109.35 g/L, 103.66 g/L, 95.30 g/L, and 76.58 g/L, respectively, all lower than the optimum degradation observed at pH 5. Other variables were held constant, including an enzyme dose of 80U/mL, a 5-day incubation time, a TS of 12.5%, and a room temperature of 30°C (±2). The effectiveness of reducing sugar in food waste hydrolysis through changing the pH level varies. Acidic conditions (low pH) can increase the rate of hydrolysis and sugar production, while alkaline conditions (high pH) can inhibit hydrolysis and sugar production. Optimal pH levels for sugar reduction in food waste hydrolysis typically range from 4 to 7, depending on the specific microorganisms and conditions being used. Nonetheless, the TDS concentration experienced a slight increase after undergoing enzymatic hydrolysis, indicating the progression of hydrolysis and degradation of intricate organic compounds present in the AD system. In this study's hydrolysis process, the VS saw a substantial increase of 68.50 g/L, signifying a noteworthy trend.

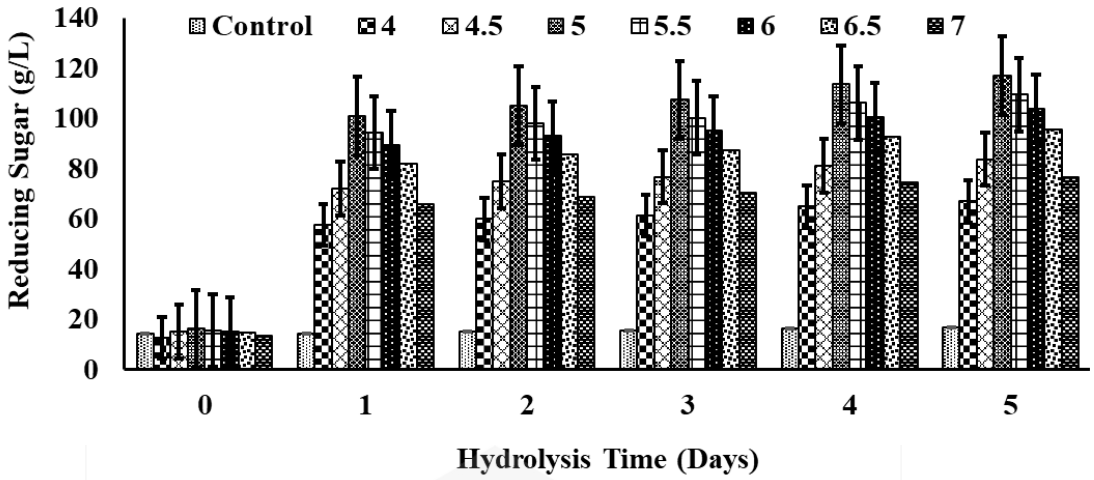

Figure 4.6: Effect in reducing sugar of food waste hydrolysis with different pH. Other factors were fixed enzyme dose 80U/mL, incubation time 5days, TS 12.5%, and room temperature 30^{o}C (±2)

Conversely, TDS exhibited a notable surge during the enzymatic hydrolysis period. This elevation can be attributed to the fact that the breakdown of organic compounds by the hydrolytic enzyme led to an augmented presence of dissolved organic and inorganic solids in the suspended form. pH, which has been highlighted by Cysneiros et al., (2012) and Horiuchi et al., (2002), stands as an operational factor that can be fine-tuned to enhance hydrolysis and acidogenesis rates. Additionally, research has revealed the influence of pH on bacterial species and the biochemical variations it triggers, as shown by Jankowska et al., (2015), Xu et al., (2011), and Ye et al., (2007). Consequently, pH control emerges as a promising in-situ strategy to achieve targeted carboxylate synthesis within leach bed reactors.

4.5.1.3 Effect of hydrolytic enzymes dose on hydrolysis process

The investigation aimed to determine the optimal enzyme dosage for achieving the best conditions for the hydrolysis of the collected FW. To achieve this, varying doses of

enzymes were applied to different masses of FW. TS and RS measurements were taken daily for a span of 5 days, and the outcomes were depicted in Figures 4.7. Diverse concentrations of enzyme doses (comprising 50% cellulase and 50% amylase), specifically 40U, 60U, 80U, 100U, 120U, and 140U, were employed to optimize the enzymatic hydrolysis. As inferred from Figure 4.7, RS content was approximately 15.63 g/L before digestion in the flasks with different enzyme doses. Subsequent to 5 days of digestion, the RS content increased to 16.72 g/L, 76.08 g/L, 91.96 g/L, 117.04 g/L, 100.65 g/L, and 90.29 g/L for enzyme doses of 40U, 60U, 80U, 100U, 120U, and 140U, respectively. Hence, Deepanraj et al., (2015) explored the impact of VS concentration on food waste's biogas production in an anaerobic batch digester by considering various TS concentrations of food waste. The characteristics of the food waste were evaluated both before and after digestion. For a substrate with a TS concentration of 12.5% before digestion, VS diminished to 60.47 g/L post-digestion. In the case of a food waste sample with an RS concentration of 16.35 g/L, the RS content escalated to 117.04 g/L, employing an enzyme dose of 80U/mL. The effectiveness of reducing sugars during food waste hydrolysis, under diverse enzyme dosages, relies on numerous factors, including enzyme type and quality, substrate (food waste) properties, pH, temperature, and reaction duration. Nevertheless, in general, escalating the enzyme dose can accelerate the rate and efficacy of sugar reduction. However, excessive enzyme dosing can lead to diminished efficiency and elevated costs. Determining the optimal enzyme dose necessitates experimentation and optimization.

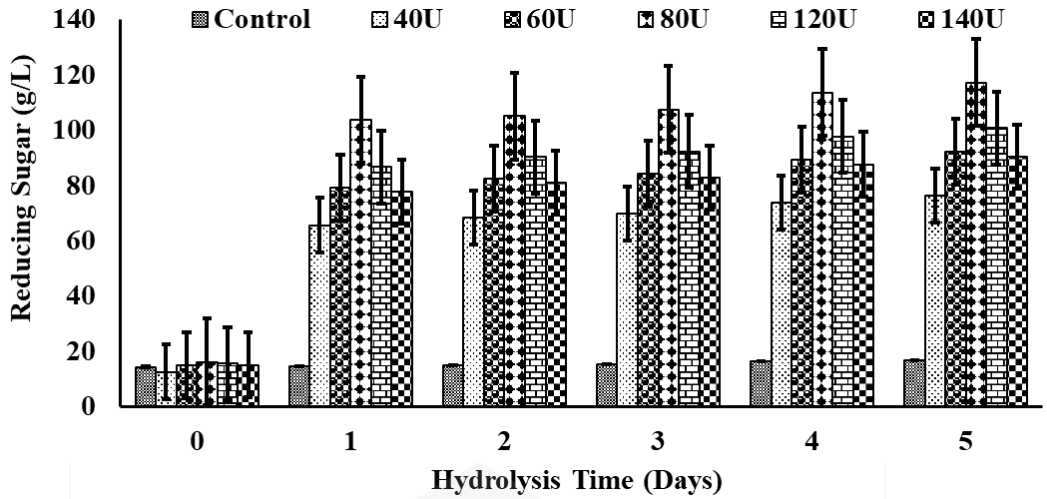

Figure 4.7: Effect in reducing sugar of food waste hydrolysis with different dose of hydrolytic enzyme. Other factors were fixed pH 5, incubation time 5days, TS 12.5%, and room temperature 30°C (±2).

Furthermore, concerning the optimal enzyme dose, it was observed that the dose of enzymes didn't significantly affect the organic compounds' degradation, as different enzyme doses yielded VS values in close proximity. This signifies that even minimal enzyme doses can contribute to organic compound degradation and enhance food waste hydrolysis. Conversely, a control with 0 U/mL of enzyme—indicating food waste without enzyme treatment—was also included to assess enzyme influence on food waste hydrolysis. The control's TS values remained largely unaffected, indicating minimal degradation of organic compounds during FW hydrolysis. In accordance, Confer and Logan (1998) and Confer and Logan (1997) highlighted that microbe-mediated hydrolysis disintegrates recalcitrant insoluble biomolecules such as polysaccharides and proteins, followed by the release of hydrolytic protein molecules into the feed liquid. The enzyme dosage exerted influence over substrate degradation, as seen in studies by Higuch et al., (2005) and Parawira et al., (2005).

4.5.2 Optimization of the Hydrolysis Process FCCCD Under RSM

Through the implementation of OFAT studies, significant factors were identified for subsequent optimization using a FCCCD under the RSM. This approach aimed to establish the optimal conditions for increasing RS content through enzymatic hydrolysis. In the FCCCD design, the interplay between various factors could be explored, with a focus on enhancing the statistical methodology to better comprehend the intricate relationships among these factors that contribute to RS enhancement. This strategy also aimed to minimize the number of experiments required, thus reducing costs. Within the FCCCD framework, two primary factors were examined: TS within the range of 10 to 15% (g/L), enzyme dose spanning 60 to 100 U, and pH range of 4.5 to 5.5. The remaining factors, which had shown less impact on RS enhancement in the OFAT studies and were optimized for that context, were maintained at their respective optimum concentrations. The obtained results, outlined in Table 4.3, showcased both actual and predicted reducing sugar values for each experimental run. These values were derived from the regression equation established for the 20 runs conducted. Notably, the center point of the design yielded the highest RS increase at 118.02 g/L, while the lowest RS outcome was observed in the 11th experimental run.

The regression coefficients for the equation were computed through diverse regression analyses conducted on the experimental data. This derived equation was then employed for projecting the increase in RS. The quadratic polynomial equation depicted the trends in RS enhancement based on the interaction of TS and enzyme activity. This equation was expressed in terms of coded factors, as illustrated in the following equation. The utilization of coded factors in the equation allowed for making predictions regarding

the response under specific levels of each factor. In this coding scheme, the high levels of the factors were represented as +1, while the low levels were denoted as -1.

Table 4.3: FCCCD experimental design for selection of medium components and process conditions for RS production.

	Factor 1	**Factor 2**	**Factor 1**	**Response 2**	
Run	A: TS	B: Enzyme Dose	pH	RS (Actual)	RS (Predicted)
	%	U/mL		g/L	g/L
1	12.5	80	5.5	101	101.11
2	12.5	60	5	86	89.67
3	10	100	4.5	59	59.05
4	**12.5**	**80**	**5**	**117.56**	**115.86**
5	15	80	5	92.01	88.12
6	**12.5**	**80**	**5**	**116.25**	**115.86**
7	12.5	80	4.5	102	102.19
8	**12.5**	**80**	**5**	**114.26**	**115.86**
9	15	60	5.5	54.71	54.59
10	15	100	4.5	54	55.62
11	**12.5**	**80**	**5**	**118.01**	**115.86**
12	10	60	5.5	35	33.31
13	15	60	4.5	40	40.31
14	**12.5**	**80**	**5**	**116.12**	**115.86**
15	**12.5**	**80**	**5**	**113.56**	**115.86**
16	15	100	5.5	62.9	64.99
17	10	100	5.5	43	42.61
18	10	60	4.5	47	44.84
19	10	80	5	75	79.19
20	12.5	100	5	105.34	101.97

*Bold indicates center points

This coded equation proved valuable in ascertaining the relative impact of the factors by evaluating the coefficients associated with each factor.

$$RS = 115.86 + 4.46A + 6.15B - 0.54C + 0.2738AB + 6.45AC - 1.23BC - 32.20A^2 - 20.04B^2 - 14.21C^2 \quad (4.1)$$

Where, RS was the (g/L) as a function of the coded levels of %TS (A) and enzyme dose (B) and pH (C) respectively.

The ANOVA results for the response surface analysis of the quadratic polynomial model applied to Response 1, which corresponds to the increase in RS, are presented in Table 4.4. The considerable F-value of 220.51 for RS and the associated p-value of less than 0.0001 for the RS model clearly signify the significance of the selected quadratic model. The p-value was also utilized to assess the significance of each coefficient and to evaluate the strength of interaction between the independent coefficients. Lower p-values indicate higher coefficient significance. A p-value of less than 0.0001 indicates that the model terms were indeed significant, while values exceeding 0.1 indicate insignificance of the model terms. In this context, terms such as A, B, AB, A^2, and B^2 were determined to be significant in the model, significantly influencing the overall production of reducing sugar. Furthermore, considering the F-values associated with the main factors studied, it was observed that the substrate concentration exhibited the highest value, signifying its substantial impact on the improvement of RS. Conversely, the enzyme dose exerted the least pronounced effect. The lack of fit F-value of 4.67 for RS suggests that the lack of fit was not significantly different from the pure error. A lack of significant lack of fit implies that the model fitting was satisfactory.

The results from the ANOVA analysis involve comparing the calculated p-values to a predetermined significance level, typically set at 0.05, to determine the statistical significance of the observed relationships. In the current context, the p-value of 0.5781 surpasses the significance level of 0.05, indicating that the relationship between pH and the

outcome variable is not statistically significant at the chosen significance level. The ANOVA analysis further reveals that the factors "enzyme" and "pH" did not yield significant results, implying that these factors lack a statistically significant effect on the outcome variable under analysis.

Table 4.4: Analysis of variance (ANOVA) of the polynomial model for Response 1: RS

Source	Sum of Squares	df	Mean Square	F-value	p-value	
Model	17451.70	9	1939.08	220.51	< 0.0001	significant
A-TS	199.09	1	199.09	22.64	0.0008	
B-Enzyme Dose	378.59	1	378.59	43.05	< 0.0001	
C-pH	2.91	1	2.91	0.3304	0.5781	
AB	0.5995	1	0.5995	0.0682	0.7993	
AC	332.95	1	332.95	37.86	0.0001	
BC	12.03	1	12.03	1.37	0.2693	
A^2	2851.63	1	2851.63	324.29	< 0.0001	
B^2	1104.05	1	1104.05	125.55	< 0.0001	
C^2	555.04	1	555.04	63.12	< 0.0001	
Residual	87.93	10	8.79			
Lack of Fit	72.41	5	14.48	4.67	0.0581	not significant
Pure Error	15.52	5	3.10			
Cor Total	17539.63	19				

R^2 = 0.995, Adjusted R^2 = 0.9905, C.V.= 3.59, Predicted R^2= 0.9665, Adequate precision= 39.3691

The coefficient of determination (R^2) close to unity confirms a strong correlation between the actual and predicted values. Moreover, the model's effectiveness is underscored by the notably high values of R^2 = 0.995, adjusted R^2 = 0.9905, predicted R^2

= 0.9665, and adequate precision = 39.36 for the RS response. The adequacy of the model's signal-to-noise ratio was assessed through adequate precision, where a ratio exceeding 4 indicates a favorable model performance. In this investigation, the model under study exhibited a substantial RS ratio of 39.3667, thus meeting the criteria for a good model. Additionally, the coefficient of variation (C.V.) characterizes the extent of data distribution. For the RS response, the C.V. was measured at 1.39%, falling within the acceptable range. Smaller C.V. values, approaching zero, denote enhanced reproducibility. Conversely, higher C.V. values suggest increased variability in the mean value and do not yield a satisfactory response model (Rashid et al., 2011; Akinfalabi et al., 2020; Rashid et al., 2019).

The mathematical equation of regression served as a model to delineate the connection between a reliant factor (in this instance, the generation of reducing sugar) and one or more autonomous factors (total solids, enzyme dose, and pH). This regression equation was harnessed to construct graphical representations like contour and response surface plots. The motive was to visually portray the association between these variables and pinpoint the most favorable amalgamation of total solids, enzyme dose, and pH that leads to the highest output of reducing sugar (Aswathy et al., 2010; Jeya et al., 2010). The contour plot, a two-dimensional portrayal, manifested how the production of reducing sugar alters as a function of total solids and enzyme dose, all while maintaining a constant pH. On the other hand, the response surface plot, rendered in three dimensions, demonstrated the fluctuation in reducing sugar production with variations in total solids, enzyme dose, and pH. These graphical representations were instrumental in recognizing the ideal amalgamation of elements that result in optimal reducing sugar yield. The plots also

unveiled that augmenting total solids, enzyme dose, and pH led to an escalation in RS removal. The contour plots' shapes were indicative of the extent of interactions among these variables (Aswathy et al., 2010; Jeya et al., 2010).

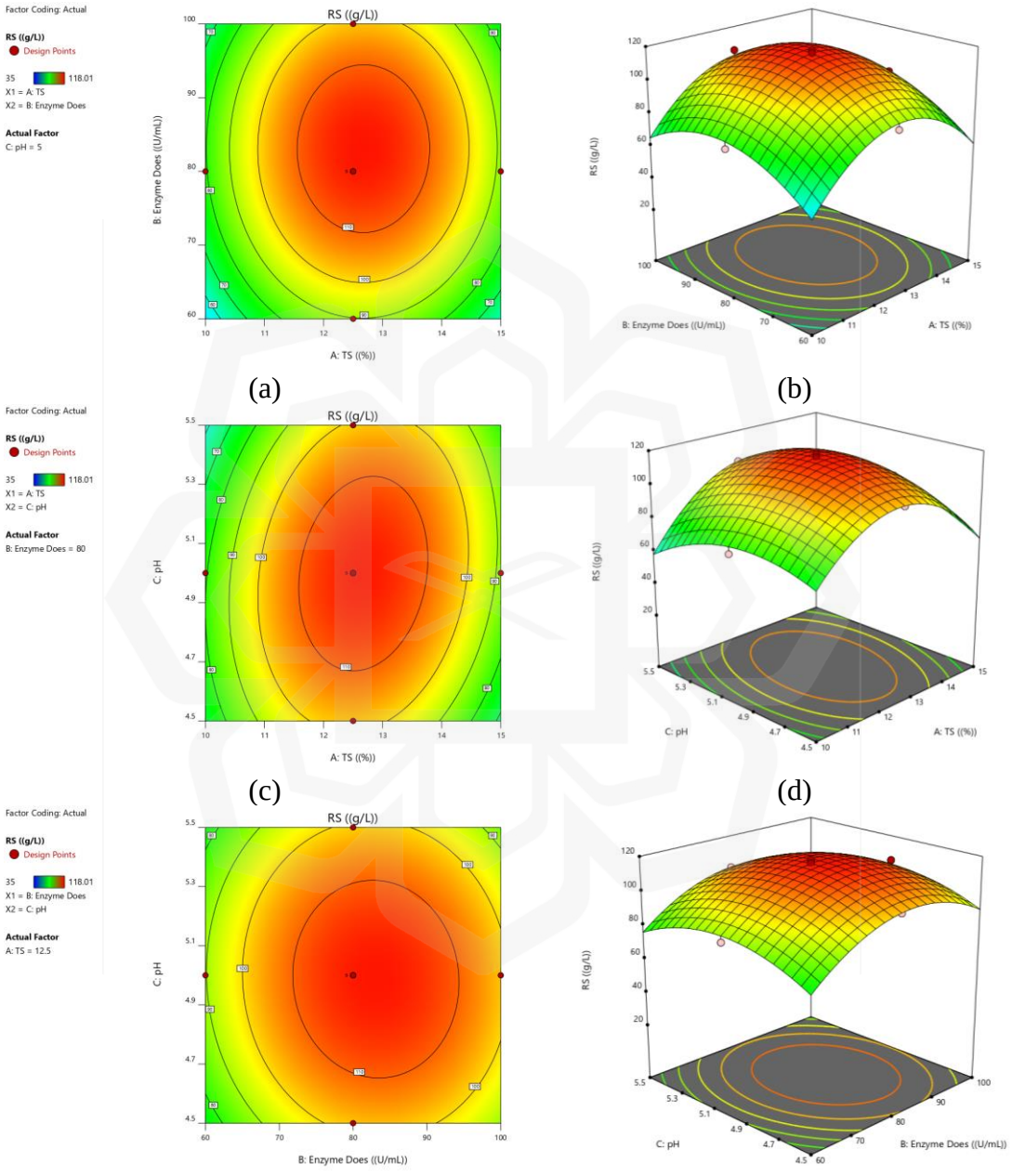

Figure 4.8: Interaction of food waste (TS), enzyme dose and pH on hydrolysis (g/L of RS): (a, b) 2D and 3D contour plot of TS and enzyme dose; (c, d) 2D and 3D contour plot of TS and pH; (e, f) 2D and 3D contour plot of enzyme dose and pH.

Figure 4.8 illustrates the graphical representation of the interplay among TS (food waste), enzyme dose, and pH through a three-dimensional (3D) response surface and a two-dimensional (2D) contour plot. The findings revealed a noteworthy outcome: diminishing the enzyme dosage bolstered the reduction of VS, whereas elevating the enzyme dose stifled the yield. This phenomenon could be attributed to the saturation effect, as elucidated by Aswathy et al., in 2010. The pinnacle achievement in RS production, as depicted in Figure 4.8, was marked by a utilization of 118g/L of food waste, along with an enzyme dose of 80U/mL and a pH of 5, showcasing an optimal configuration.

4.5.3 Validation of the Model Developed: Hydrolysis of FW

The validity of the suggested model was confirmed using the statistical framework, which involved cross-referencing the optimal outcomes. Employing the established model, a range of projected parameter values was computed. The arrangement and fusion of self-reliant variable elements for the food waste hydrolysis were itemized in Table 4.5. Comparisons between the projected and actual process conditions for the food waste hydrolysis revealed that they deviated by no more than 1% in terms of RS content.

Table 4.5: Validation of the developed model enzymatic hydrolysis of food waste

Experiment Number	TS (%)	Enzyme Dose (U)	pH	RS (g/L)		
				Predicted Value	Experiment Value	Error (%)
1	12.66	82.42	4.9	116	114.98	1.023
2	11.21	91.83	5.1	100	98.75	1.25
3	12.67	83.08	4.99	118	116.49	1.022

Consequently, it can be deduced that the proposed model possessed the capability to foresee the reduction in FW hydrolysis. The investigation of the newly developed enzymatic hydrolysis process yielded clear evidence of achieving the highest removal rate of 116.49 g/L of RS. This accomplishment was attributed to the degradation of the lignin and hemicellulose layers of the food waste during the pretreatment stage, along with the intricate interplay of other significant variables, such as the percentage of T), enzyme dose (83.08U/mL), and pH (4.99), as demonstrated in Figure 4.9. The exploration of enzymatic hydrolysis spanned various lignocellulosic sources, including rice hulls (Saha & Cotta, 2008), waste paper (Van et al., 1999), food waste (Kim et al., 2011), sunflower stalks (Sharma et al., 2002), water hyacinth (Aswathy et al., 2010), and rice straw (Ma et al., 2009).

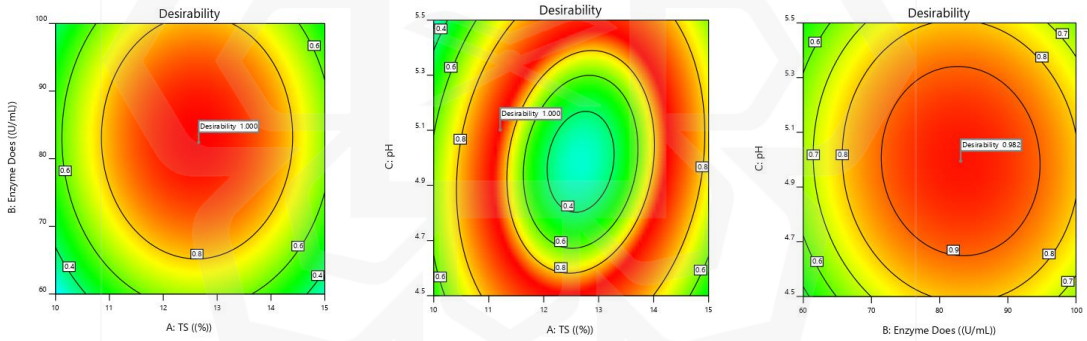

(a) (b) (c)

Figure 4.9: 2D contour plots of predicted value three replications for desirability using (a) TS and enzyme dose, (b) TS and pH and (c) enzyme dose and pH.

Within this context, notable outcomes were observed in related studies. For instance, Ma et al., (2009) documented a reduction of 30.3% during the saccharification process involving rice straw. Likewise, sunflower stalks demonstrated a hydrolysis removal of 57.8%, as reported by Sharma et al., (2002), while rice hulls displayed a removal rate of 32%, according to Saha and Cotta (2008).

4.6 SUMMARY OF THE FIRST OBJECTIVE FINDINGS

The initial objective's findings underscored the significance of employing hydrolytic enzymes in the pretreatment of food waste through hydrolysis, thus highlighting the potential for subsequent anaerobic digestion. This, in turn, highlighted the importance of determining the optimal quantity of hydrolytic enzyme dosage and digestion time for the effective hydrolysis of food waste. To address this, the impact of varying hydrolytic enzyme quantities and digestion times was systematically evaluated using a OFAT approach. The study employed food waste with a notably high concentration to generate diverse methogenesis compounds through the utilization of cellulase and amylase enzymes, employing both OFAT and FCCCD methodologies. Notably, the traditional OFAT investigations indicated that parameters like hydrolysis pH, duration, and enzyme dosage were interconnected with the degradation of lignocellulosic biomass and the production of distinct biodegradable organic compounds. Based on these insights, a second-order regression model was devised, optimizing the interactions of hydrolytic enzyme amount and digestion time using the FCCCD method. This optimization led to a noteworthy enhancement in the reduction of sugar output. The outcomes revealed that while varying enzyme quantities were effective in biodegrading organic matter and augmenting food waste hydrolysis, the optimal digestion time was comparatively extended, as long as 5 days. This can be attributed to the composition of food waste, which consists of sizable polymers necessitating an extended period for degradation. The collective conclusion drawn from this study underscores that introducing hydrolytic enzymes into the hydrolysis process significantly enhances the breakdown of organic matter within FW.

4.7 STUDY OF ANAEROBIC DIGESTION PROCESS OF FOOD WASTE

4.7.1 Characteristic of Anaerobic Inoculum

Various types of starter cultures have been historically employed in the anaerobic digestion process of food waste, with investigations aiming to comprehend the impact of different sources of these starter cultures on the digestion process. This underlines the significance of understanding the attributes of the starter culture used, as it directly influences the outcomes of the anaerobic digestion. In this context, the current study opted for the application of anaerobic sludge sourced from the Dasherkandi Sewerage Treatment Plant as the starter culture. The selected inoculum underwent a series of analyses to establish its characteristics and properties, thereby ensuring its appropriateness for the anaerobic digestion process.

Table 4.6: Characterization of inoculum

Parameters	Values
TS (g/L)	99.58
VS (g/L)	85.54
pH	5.21

The subsequent examination was carried out following the procedural techniques outlined in the methodology section, encompassing measurements of total solids (TS), volatile solids (VS), and pH. These analytical assessments, as outlined in Table 4.6, provided insights into the characteristics of the utilized inoculum. The starter culture displayed a total solid content of approximately 100 g/L and a total volatile solid content in the vicinity of 90 g/L.

4.7.2 One-Factor-At-A-Time (OFAT) Experimental Analysis for AD system

4.7.2.1 Digestion time on AD system for biogas production

The objective of the experiment was to determine the optimal anaerobic digestion (AD) retention time for the given food waste and to subsequently apply these findings to a pilot-scale setup to maximize energy recovery from the waste. The AD system was operated with varying AD retention times, specifically 0 days and 30 days. Biogas production, quantified in parts per million (ppm) using an Arduino Uno based biogas sensor, was monitored daily for a span of 30 days. The trends in daily biogas production and cumulative biogas over each AD retention time were visualized in Figures 4.10. The depicted graph revealed that gas production exhibited a gradual increase from the outset until day 5, after which it experienced a significant upturn between days 4 and 9, resulting in biogas volume ranging from 110 mL/g RS to 288 mL/g RS. Thereafter, a steep surge was observed, particularly between days 9 and 15, reaching around 390 mL/g RS. During this period, other factors were held constant, including a biogas inoculum of 25%, a pH of 7, 500 mL of hydrolysate (with an incubation time of 5 days), the food waste content, and a room temperature of 30°C (±2). Subsequent days, spanning 15 to 20, displayed a slight alteration with a volume of approximately 439 mL/g RS. The highest biogas production was observed within AD retention times of 25 to 27 days. Notably, even at an AD retention time of 27 days, a substantial biogas yield of 484 mL/g RS was achieved. These findings unequivocally validate the efficacy of the methanization process and underscore the pivotal role of hydrolytic enzymes in enhancing biogas volume. As per the researchers' observations, it's generally understood that under mesophilic conditions, significant biogas production can be achieved within a timeframe of 20 to 30 days for anaerobic digestion (AD) retention

time. Between days 20 and 25 in this study, there was a notable increase in biogas production, reaching an almost 484 mL/g RS, which saw a minor increase of only 25 mL/g RS before experiencing a decline.

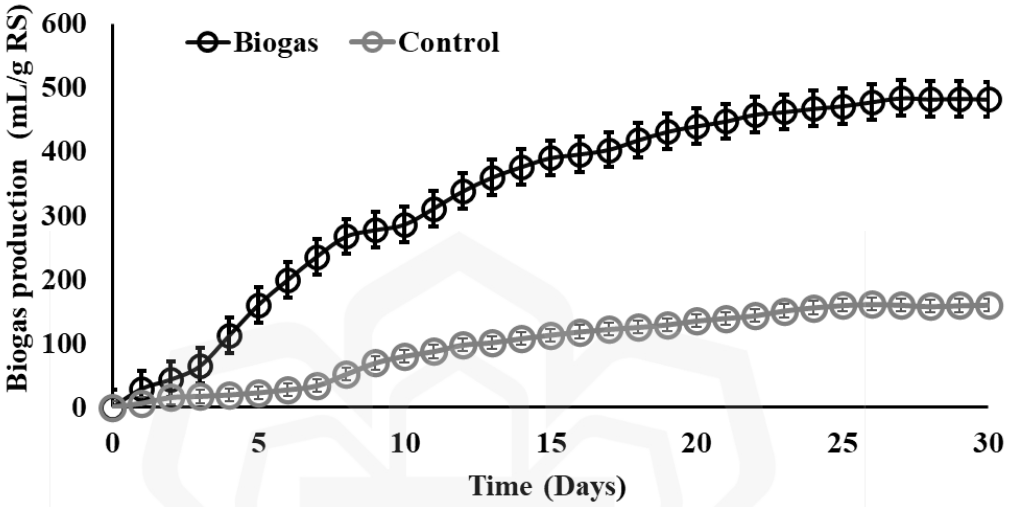

Figure 4.10: Biogas production for different AD digestion times. Other factors were biogas inoculum of 25%, pH of 7, 500mL of hydrolysate (incubation time 5 days) FW and room temperature at 30°C (±2).

Haryanto et al., (2018) conducted a study involving anaerobic digestion with varying AD retention times, specifically 7, 14, 21, 28, and 35 days. The substrate concentration was set at 16% (g/L) of total solids (TS), and the digestion was carried out at a mesophilic temperature of 37°C. Interestingly, they observed that the biogas volume for an AD retention time of 14 days was quite comparable to the volumes achieved with AD retention times of 21, 28, and 35 days. In another study by Kim et al., (2006), the effects of temperature and hydraulic retention duration on AD using food waste as feed were investigated. They found that at a temperature of 50°C and a hydraulic retention duration of 12 days, both AD capacity and the efficiency of food waste digestion were notably improved.

4.7.2.2 pH on AD system for biogas production

The pH parameter bears immense significance in the anaerobic digestion process. The microbial ecosystem within the anaerobic digestion (AD) system is intricate, necessitating careful pH regulation using strong bases like NaOH or HCl. The primary objective behind pH control lies in its evaluation during the hydrolysis stage, where maintaining a lower pH is crucial to prevent the accumulation of volatile fatty acids, which could negatively impact the microbial population. In the broader context of the AD system, the optimal pH range typically falls between 6 and 8, with many studies concurring on the ideal range being around pH 7 (Zhang et al., 2015; Wang et al., 2022; Liu et al., 2023). The production of biogas was most pronounced at a pH of 7, as illustrated in Figure 4.11. The graph portrays fluctuating pH levels, which required daily adjustments due to the sensitivity of microbial survival and its direct influence on gas production in the AD. Initially, the pH began at an acidic level (pH 4.5) and gradually ascended to a pH of 9. Between the pH range of 4 to 6, a progressive increase in biogas yield was observed, ranging from approximately 220 mL/g RS to 366 mL/g RS. This was achieved with specific conditions including a 10% inoculum, an AD digestion time of 27 days, 500 mL of hydrolysate (with a 5-day incubation time), food waste content, and a room temperature of 30°C (±2). However, the biogas yield increase was less pronounced within the pH range of 6 to 6.5. This could be attributed to pH's influence on the chemical stability of compounds like NH_3, H_2S, and volatile fatty acids, which have the potential to hinder bacterial activity. In contrast, the pH of 7 resulted in the highest biogas yield, reaching approximately 377 mL/g RS. These findings clearly demonstrate that biogas volume and degradation efficiency were notably superior within

the pH range of 6 to 7.5. Furthermore, from Figure 4.11, it's evident that biogas production diminished as the pH increased within the range of 8 to 9.

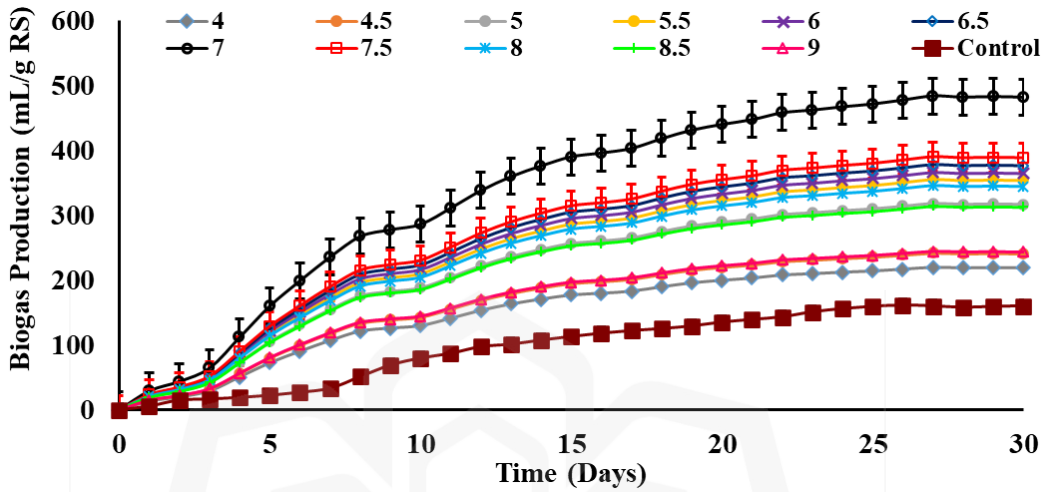

Figure 4.11: Biogas production for different initial pH. Other factors were biogas inoculum of 25%, AD digestion times of 27 days, 500mL of hydrolysate (incubation time 5 days) FW and room temperature at 30°C (±2).

When compared to similar investigations, the current study exhibited an initial acidic pH of 4.5, gradually transitioning to a pH of 9. Over the range of pH 4 to pH 6, the biogas yield demonstrated a gradual augmentation, ranging from approximately 220 mL/g RS to 366 mL/g RS. This was achieved using specific conditions, including a 10% inoculum, a 27-day anaerobic digestion period, 500 mL of hydrolysate (with an incubation time of 5 days) derived from fresh weight (FW), and a controlled room temperature of 30°C (±2). Comparable observations have been reported in previous studies (Zealand et al., 2017; Okeh et al., 2014; Syaichurrozi et al., 2016). However, the increase in biogas yield became relatively marginal from pH 6 to pH 6.5. This phenomenon is attributed to pH's influence on the stability of compounds such as NH_3, H_2S, and volatile fatty acids, which can potentially impede bacterial activity. The apex of biogas yield, approximately 377 mL/g RS, was observed at pH 7. The results strongly suggest that optimal biogas volume and

degradation efficiency were achieved within the pH range of 6 to 7.5. Conversely, the data in Figure 4.11 indicate a decline in production when the pH escalated from 8 to 9, aligning with the observations of other studies (Kiran et al., 2015; Yang et al., 2015). It's noteworthy that these findings are specific to the current study and could differ across other research due to variables such as substrate composition, reactor setup, operational conditions, and the composition of microbial consortia (Pavi et al., 2017).

4.7.2.3 Inoculum dose on AD system for biogas production

The progress of biogas generation resulting from the hydrolyzed food waste (with an incubation time of 5 days) in the presence of hydrolytic enzymes was meticulously examined. The daily biogas outputs from various digesters with differing percentages of inoculum doses and their respective increments in biogas production were graphically illustrated in Figures 4.12. Initially, the daily biogas production was tracked and recorded over a 27-day AD retention period. As indicated in Figure 4.12, the biogas production for varying percentages of inoculum doses became discernible on the initial day, exhibiting gradual growth between days 3 and 7. This gradual increase can be attributed to the nature of the food waste used as a substrate, which was solid in composition and rich in carbohydrates, thereby causing a slower initiation of the anaerobic digestion process. Biogas generation corresponding to distinct AD inoculum doses, including 5%, 10%, 15%, 20%, 25%, 30%, and 35%, was evaluated within the context of a fixed set of conditions: an AD digestion time of 27 days, 500 mL of hydrolysate (with an incubation time of 5 days) from fresh weight (FW), and a controlled room temperature of 30°C (±2). During the initial 7 days, the biogas production for these varying inoculum doses—ranging from 5% to

35%—exhibited comparable trends. This homogeneity in trends can be attributed to the microbial breakdown of the substrate in an oxygen-free environment.

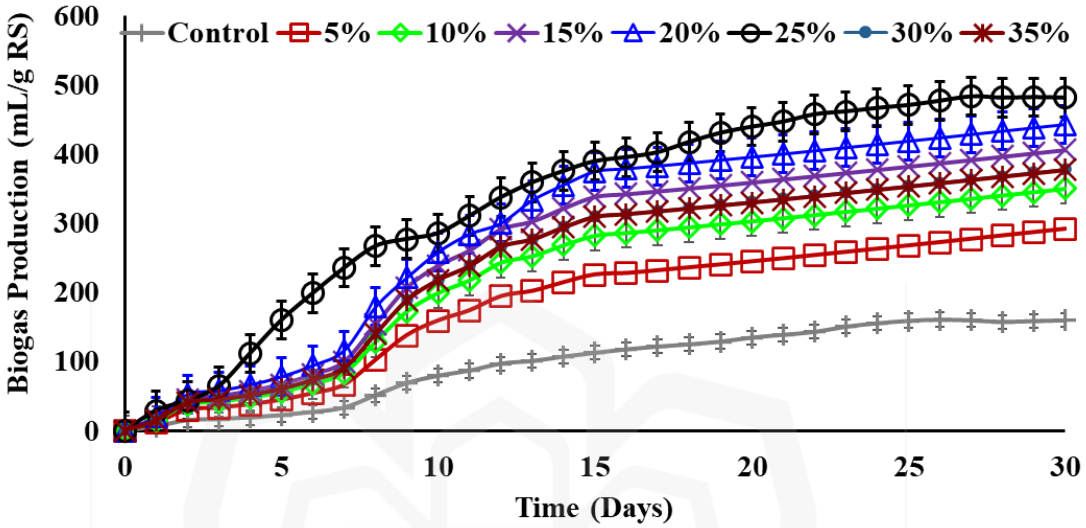

Figure 4.12: Biogas production for different AD inoculum dose. Other factors were pH of 7, AD digestion times of 27 days, 500mL of hydrolysate (incubation time 5 days) FW and room temperature at 30°C (±2).

Between days 8 and 15, the biogas production showed a gradual escalation, attributed to the ongoing breakdown of the food waste substrate, leading to increased sugar production and the conversion of bioenergy into gases by microorganisms. Remarkably, for the AD with 25% inoculum, the peak production occurred around day 29, reaching approximately 485 mL/g RS. Focusing on the daily biogas production for the 25% inoculum, a rapid increase was noted from days 3 to days 10, reaching 64.5 mL/g RS and 285.92 mL/g RS, respectively. Concerning the biogas production from varying inoculum percentages (5%, 10%, 15%, and 20%), a significant rise was observed, with the highest yields ranging from 66.66 mL/g RS to 116.58 mL/g RS at day 7 when the inoculum was set at 20%. Comparing the initial conditions, the 5% inoculum resulted in the lowest biogas volume and slowest startup time. Moreover, the characteristics of the 5% inoculum

combined with hydrolyzed food waste resulted in the lowest volume, even when compared to the control. In contrast, the 15% inoculum combined with hydrolyzed food waste exhibited a notably high gas volume, surpassing the 5% inoculum and control volumes. Ultimately, the digester employing a higher inoculum ratio (25%) achieved the highest biogas volume, as depicted in Figure 4.12. The disparities in biogas production between the control and hydrolyzed food waste underscore the substantial impact of hydrolysis on the anaerobic digestion process, notably enhancing biogas production. Additionally, the variance in biogas volume based on different inoculum ratios highlights the influence of inoculum ratio on biogas production. Put simply, biogas volume increased in tandem with higher inoculum ratios (El Asri et al., 2022). Noteworthy studies include Lopes et al., (2004), who explored the role of inoculated digestion liquid in organic waste breakdown, finding that the quantity of native anaerobic microbes in the digestion process influenced waste efficiency. Neves et al., (2006) revealed that employing particulate sludge as a spore suspension led to increased CH4 yields, suggesting an optimal feed-to-inoculation ratio that maximized CH_4 yields.

4.7.3 Biogas Production using Optimum Parameters

The biogas generation rate exhibited fluctuations, which could potentially be attributed to the presence of methylotroph species within the activated sludge. These organisms utilize CH_4 as both a carbon and energy source for their growth. Throughout the study, the cumulative biogas produced in the system comprised a combination of carbon dioxide, hydrogen, and methane. The composition of the biogas originating from food waste breakdown was as follows: 3% hydrogen, 57% methane, and 40% carbon dioxide, as

illustrated in Figure 4.13. Under the optimal parameters, where fixed factors included a 25% biogas inoculum, pH of 7, AD digestion duration of 29 days, 500 mL of hydrolysate (with a 5-day incubation time) from fresh weight (FW), and a room temperature of 30°C (±2), the biogas production reached its maximum. Using these specified parameters, the total biogas yield amounted to approximately 497.58 mL/g RS. This biogas composition encompassed 18.80 mL/g RS of hydrogen, 299.44 mL/g RS of methane, and 179.33 mL/g RS of carbon dioxide.

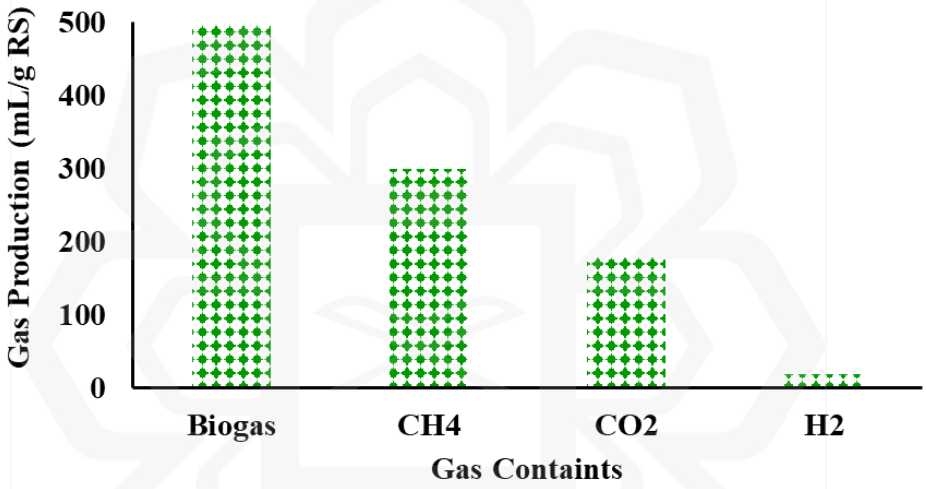

Figure 4.13: Biogas production for optimum AD parameters. The fixed factors were biogas inoculum of 25%, pH of 7, AD digestion times of 27 days, 500mL of hydrolysate (incubation time 5 days) FW and room temperature at 30°C (±2).

Mohan and Jagadeesan (2013) uncovered that the decomposition of FW led to a biogas production consisting of 76% CH_4 and 24% CO_2. Additionally, other research studies have indicated that biogas compositions typically include approximately 55% CH_4 and 30% CO_2, as demonstrated by Bhatia et al., (2020). In the present study, the precise biogas production was determined to be 750.24 ± 34.0 mL/gVS added, achieved within the range of substrate:inoculum ratios from 40% to 80%. This measurement notably surpasses the biogas production values observed in prior investigations, such as the reported 554.0 ±

75.0 mL CH_4/gVS added by Hartmann & Ahring (2005), and the 242.69 mL CH_4/gVS added in the anaerobic digestion of food waste noted by Rabii et al., (2019).

4.8 SUMMARY OF SECOND OBJECTIVE FINDING

The highest biogas production was achieved under optimal OFAT conditions, encompassing a 25% biogas inoculum, a pH level of 7, an anaerobic digestion period spanning 27 days, utilization of 500 mL of hydrolysate (subjected to a 5-day incubation period) obtained from FW, and maintenance at a room temperature of 30°C (±2). These established optimal OFAT parameters demonstrated remarkable potential in enhancing biogas yield within the AD systems. Specifically, the most effective ratio of inoculum to feed was 25%, and the optimal AD digestion duration extended to 29 days. Consequently, the application of hydrolyzed food waste exhibited promising outcomes, with the conversion of nearly 95.96% of the biogas produced from 116 g/L of RS, while only 5.04% of RS remained after a 27-day digestion period. Furthermore, the analysis of the AD system revealed specific biogas constituents, namely 3% hydrogen, 57% methane, and 40% carbon dioxide.

4.9 ISOLATION, PURIFICATION AND SCREENING OF EMMs

Two EMMs strain such as TNFW and NTAS were isolated from AD using food waste and anaerobic sludge sample as shown in Figure 4.14. Based on external appearance, colour and colony texture, TNFW-1, TNFW-2 and TNFW-3 surface colonies were about 2mm in diameter, mixed color such pink, white, yellow and red, circular and concave after three

days incubation. Meanwhile, TNFW-2 and TNFW-3 surface colonies were off white and yellow.

Figure 4.14: Isolated three EMMs from anaerobic digester food waste.

On the other hand, the colonies of NTAS-1, NTAS-2 and NTAS-3 were net like texture and the surface colony colour were almost 1-2mm diameter, yellow, pink, red, brownish, off white, circular and concave after three days incubation as shown in Figure 4.15.

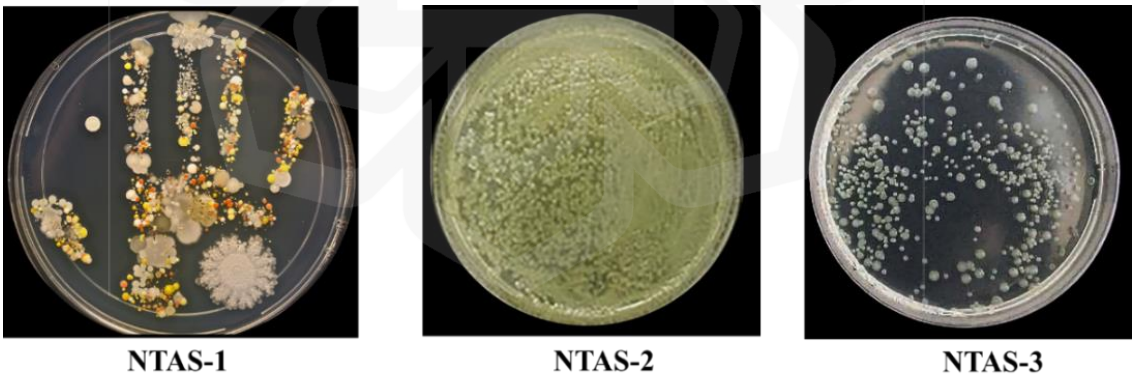

Figure 4.15: Isolated three EMMs from anaerobic sludge.

The surface colonies observation showed that the strain TNFW-1 and NTAS-1 were under different genus of EMMs. The molecular identification of the EMMs strain was described below. Different study was described the morphological identification of circular

and concave EMMs (Pawar et al., 2022; Zakaria et al., 2022; Cheng et al., 2009; Dykstra et al., 2017). The study was set about to isolate, purify and screen the EMMs from food waste and anaerobic sludge for the reduction of CO_2 (Tashyrev et al., 2022).

4.9.1 Morphological Characteristics of Isolated Electromethonogenesis Bacteria

A new EMMs was isolated from AD using FW and anaerobic sludge from Bangladesh. The EMMs enrichment culture conquered by petti dish was attained after one week. Observable colonies in agar plates seemed subsequently three days of incubation at 37°C. Surface colonies were circular and concave, yellow, diameter about 2 mm after three incubations. Only two strain, designated TNWF-2 and NTAS-3, was characterized as demonstrated in Table 4.7. According to Table 4.7 illustrations phenotype and growth characteristics of strain TNWF-2 and NTAS-3 comparing with *Methanobacterium bryantii* DSM 863$^{\mathbf{T}}$ (Bryant et al., 1967; Bryant and Boone, 1987; Boone, 1987) and *Methanobacterium formicicum* DSM1535$^{\mathbf{T}}$ (Boone, 1987). The isolate was genetic differences comparable to the analyzed *Methanobacterium* genus. Both TNWF-2 and NTAS-2 cells were non-motile, straight or crooked rods 3.0 to 15.0 μm long and 0.5 μm broad. They were Gram-positive. Both TNWF-2 and NTAS-2 cells frequently adhered to particulates in liquid cultures, creating clumps. Both TNWF-2 and NTAS-2 like DSM1535$^{\mathbf{T}}$ and DSM 863$^{\mathbf{T}}$, grew across a wide range of temperatures and pH levels. For strain TNWF-2 and NTAS-2, the EMMs optimal pH for microbial growth was pH 7. There was no microbial growth of the both strain below pH 6 or above pH 8.6. The optimum pH for growth of the both strain TNWF-2 and NTAS-2 were pH 7.

Table 4.7: Comparative characteristics of strain TNWF-2, NTAS-2, DSM1535^T and DSM863^T

Characteristics	**TNFW-2**	**NTAS-2**	**DSM1535^T**	**DSM 863^T**
Gram bacteria stains	+	+	+	Inconstant
The shape of cells	Rod	Rod	Rod	Rod
Width Cell (μm)	0.5	0.6	0.4–0.8	0.5–1.0
Length Cell (μm)	3.0–15.0	4.0–15.0	2.0–15.0	10.0–15.0
pH for growth				
Conventional Range	6.0–8.1	6.0–8.6	ND	5.8–8.8
Optimum	7.0	7.0	6.6–7.8	6.9–7.0
Substrate utilization				
Gas phase ratio of H_2/CO_2	+	+	+	+
Harmful impacts (CH_2O_2)	+	+	+	−
$C_2H_3O_2^-$	−	−	−	−
CH_3OH	−	−	−	−
C_3H_9N	−	−	−	−
C_3H_8O	−	−	−	+
$C_4H_{10}O$	−	−	−	+
NaCl for growth range (%)				
Generally using Range	0.5–3.5	0.5–3.5	ND	0.0–1.6
Optimum	2.5	2.5	ND	ND
DNA G+C content (mol %)[1]	41 (T_m)	40.7 (T_m)	41–42 (Bd)	32.7 (T_m)
Tolerance for antibiotics				
Spectromycin	+	+	ND	ND
Penicillin G	+	+	ND	ND
Ampicillin	+	+	ND	ND
Kanamycin	+	+	ND	ND
Tetracycline	−	−	ND	ND
Chloramphenicol	±	±	ND	ND
Temperature for growth (°C)				
Based Range	25–50	25–50	ND	20–50
Optimum	37	37	37–45	37

Whereas the pH was similar to that of *Methanobacterium formicicum* range from pH 6.6 to 7.8 (Bryant and Boone, 1987; Boone, 1987) and *Methanobacterium congolense* range of pH 7.2 (Cuzin et al., 2001), but slightly different from that of *Methanobacterium subterraneum* range from pH 7.8 to 8.8 (Kotelnikova et al., 1998; Patel & Roche, 1990). The pH development range of strain TNWF-2 and NTAS-2 were within the range described for the genus *Methanobacterium* (Krivushin et al., 2010).

BioM was yield by strain TNWF-2 and NTAS-2 using H_2/CO_2 and sodium formate of 50mM. Both of strain TNWF-2 and NTAS-2 could not create CH_4 from 50mM of sodium acetate, 50mM of methanol, 50mM of trimethylamine, 50mM of 2-propanol, and 50mM of isobutanol in a N_2:CO_2 was 4:1 environment. However, both of strain TNWF-2 and NTAS-2 were used the same substrate for methanogenesis as DSM1535^{T} (Bryant and Boon, 1987), but DSM863^{T} were used 2-propanol and isobutanol as hydrogen donors for the reduction of CO to create CH_4 in addition to H_2/CO_2 (Bryant et al., 1967; Bryant and Boone, 1987; Boone, 1987). Both of strain TNWF-2 and NTAS-2 exhibited phenotypic traits with *Methanobacterium formicicum* isolate DSM1535 but had a growth need for yeast extract or sludge fluid, which the type strain did not have. Both of strain TNWF-2 and NTAS-2 were also related to *Methaonbacterium oryzae* DSM11106^{T} (Joulian et al., 2000) and *Methanobacterium beijingense* DSM15999^{T} (Ma et al., 2005), both of which can grow on H_2/CO_2 and formate and require yeast extract. Thus, regarding the strain as chemoautotrophic, the development of both of strain TNWF-2 and NTAS-2 were typical among members of the genus *Methanobacterium* (Boone, 2001).

Both of strain TNWF-2 and NTAS-2 cultivated at NaCl concentrations of 0.5% to 3.5%, with best growth at 2.5% NaCl. The range was characteristic for a halotolerant

bacterium. The strain was resistant to *ampicillin, penicillin G, kanamycin,* and *streptomycin,* but susceptible to chloramphenicol. Tetracycline, on the other hand, entirely stopped cell growth. Tetracycline has been linked to translation inhibition during protein production. Tetracycline decreased the development of *Methanococcus vannielii*, according to Hilpert et al., (1981), although other methanogens examined were insensitive. Chopra and Howe (1978) stated that the methanogens utilized in their investigation were tetracycline insensitive due to the high magnesium content of the growing medium. They discovered that when the quantity of magnesium in a medium grew, the sensitivity of some Gram-negative bacteria to tetracycline reduced, most likely due to the development of antibiotic-cation complexes. The baseline medium for strain TNWF-2 and NTAS-2 development, which contains 3.0 mg $MgSO_4$/L media, may not be sufficient to reduce its sensitivity to tetracycline. Rosenberg et al., (2014) discovered that members of the genus *Methanobacterium* have a chloramphenicol-sensitive particulate dehydrogenase enzyme.

The G+C content of both strain TNWF-2 and NTAS-2 genomic DNA was 41 mol%. This number was comparable to DSM1535^{T} (Bryant and Boone, 1987), but greater than DSM863^{T} (Bryant and Boone, 1987). (Bryant et al., 1967; Boone, 1987). The mol% G+C of the DNA in the *Methanobacteriaceae* family ranges from 23 to 62. (Oren, 2014).

Both strains TNWF-2 and NTAS-2 thrived at temperatures ranging from 25°C to 50°C, with 37°C being the hottest. The majority of Methanobacterium strains were mesophilic, thriving in temperatures ranging from 30°C to 50°C (Krivushin et al., 2010), but not at 55°C (Joulian et al., 2000; Boone, 2001), distinguishing them from the thermophilic genus Methanothermobacter (Wasserfallen et al., 2000).

4.9.1 Molecular Identification of Potential Bacteria

The most potential EMMs strain of TNFW-2 was found belong to the genus *Methanothermobacter sp*. This identification was based on bacteria-colony morphology on basal medium, microscopic images of the phase-contrast and *Methanothermobacter* as shown in Figure 4.16. Based on the existence of dimitic and amphimitic EMMs systems *Methanothermobacter sp* grouped under the four family *Methanobacterium*, *Methanobrevibacter, Methanosphaera* and *Methanothermobacter* (Cersosimo & Wright, 2015; Boone et al., 2015; Balch et al., 1979; Youngblut et al., 2020). Light microscopy image of the bacterial consortium results was agreement with the findings of Karunarathna et al., (2021) which described the rod-shaped (curved, crooked, or straight), ranging between 0.5-1um in width.

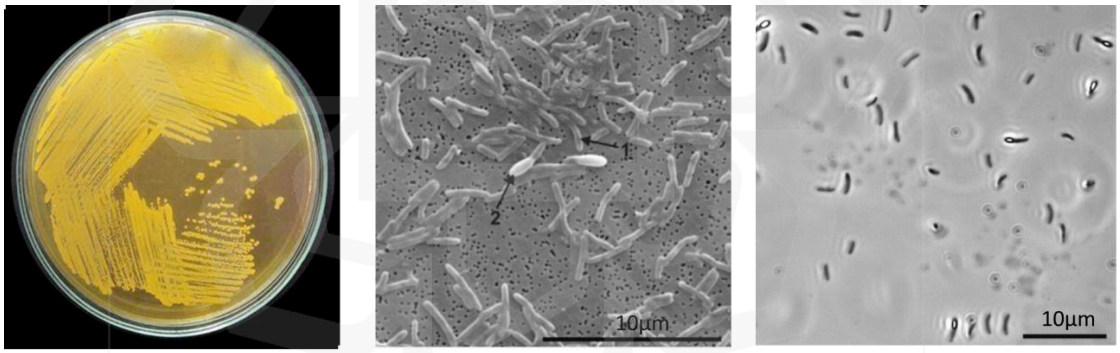

Figure 4.16: Culture of *Methanobacterium formicicum* TNFW-2 (a) Colony morphology of *Methanobacterium formicicum* TNFW-2 grown on basal medium agar plates after 7 days. (b) Images of bacterial basidiospore taken with a light microscope and (c) Phase-contrast structure under light microscopy. Arrows indicate (1) non-sporulated and (2) sporulated cells Bars.

These morphological investigations revealed that the strain belonged to the species *Methanothermobacter sp*. Based on rRNA operon gene (16S rRNA) sequencing, the EEMs strain was most closely related to *Methanobacteriales sp*. The rRNA operon of

Methanobacterium formicicum was compared to available gene sequences in GenBank using 10 related strains of *Methanobacteriales sp*. PCR based on 16S rRNA EMMs strain TNFW-2 identification was additionally confirmed by mcrA gene-based amplification with MLf and MLr primers, resulting in a product size of 440 to 490 bp. The isolation yielded a significant segment of the 16S rRNA gene (1,350 bp) that was analyzed. A comparison of 16S rRNA gene sequences exposed that strain TNFW-2 belonged to the order *Methanobacteriales*. *Methanobacterium formicicum* was 98% sequence similarity, *Methanobacterium bryantii* was 95% and *Methanobacterium ivanovii* was 95% as depicted in Figure 4.17.

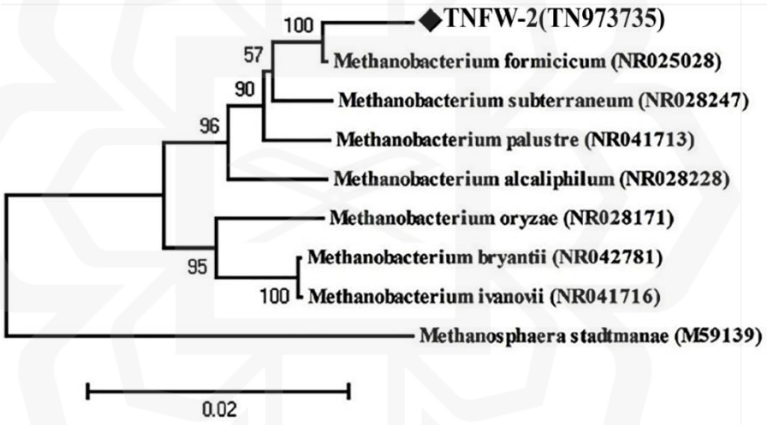

Figure 4.17: Phylogenetic tree constructed utilizing *Methanobacterium formicicum* TNFW-2 rRNA transcription factors gene sequences utilizing basic local alignment search tool pairwise alignments and neighbor-joining technique. Outgroup sources were *Methanosphaera stadtmanae*. The greatest synthesis possibility approach was used to determine the broader development (Tamura et al., 2007). At terminals, the initial parameters were seen (percentages of 500 replicates). The release codes for GenBank were given. Each bar shows 0.02 genetic modifications.

Researchers used primers ME1/ME2 (Hales et al., 1996) and MR1/ME2 (Hales et al., 1996) to get the almost full-length mcrA gene (Simankova et al., 2003). The mcrA gene sequence also revealed that strain TNFW-2 belonged to the order *Methanobacteriales*.

Methanobacterium formicicum of 97% and *Methanobacterium palustre* of 94%, were the nearest cousins based on the bases on the mcrA gene sequence. Furthermore, the sequence component of the mcrA gene from 440 to 490 bp was found, and a molecular phylogenetic tree was constructed based on the methyl-coenzyme M reductase II alpha subunit sequences of the mcrA gene. The mcrA gene sequence-based tree also suggested that strain TNFW-2 was a member of the order *Methanobacteriales*. According to mcrA gene sequence investigation, the closest cousin was *Methanobacterium formicicum* strain of 97% nucleic acid sequence similarity as demonstrated in Figure 4.18.

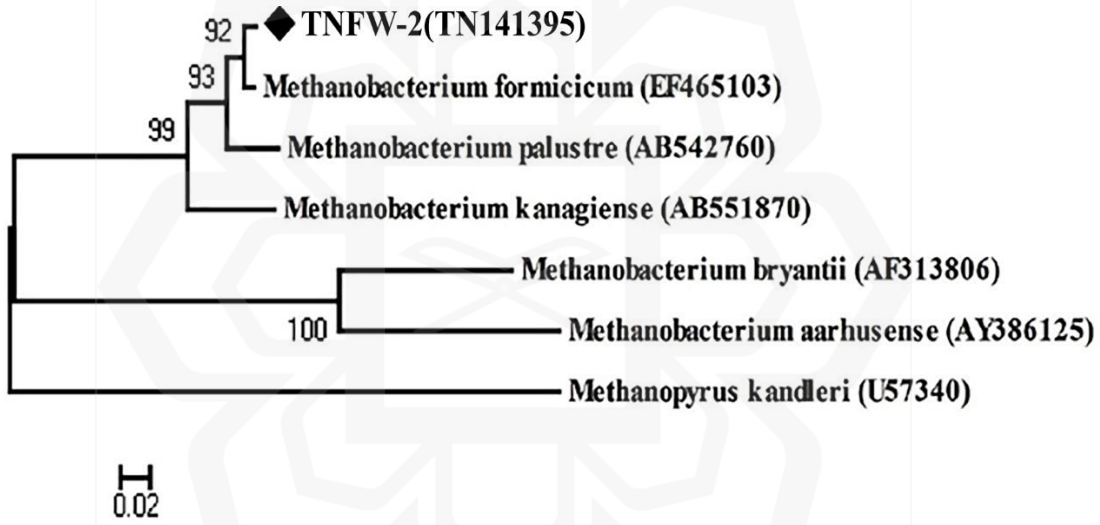

Figure 4.18: Phylogenetic analysis of extracted mcrA gene arrangements revealing the connection of *Methanobacterium formicicum* strain TNFW-2 to other methanogenic archaea and representatives of the genus *Methanobacterium*. Outgroup comparisons were *Methanopyrus kandleri*. The entrance values for GenBank were given. At terminals, the baseline parameters were displayed (percentages of 500 replicates). Each bar shows 0.02 genetic modifications.

There were no substantial variations from DNA versus amino acid sequences, or from the methods utilized (Figures 4.17 to Figure 4.18). The phylogenetic analysis comprising 16S rRNA gene sequences as shown in Figure 4.19 revealed two large groups

that were completely distinct from one another. Cluster 1 had two subclusters, with TNFW-2 in subcluster 1 showing 100% resemblance to *Methanobacterium formicicum* (NR025028).

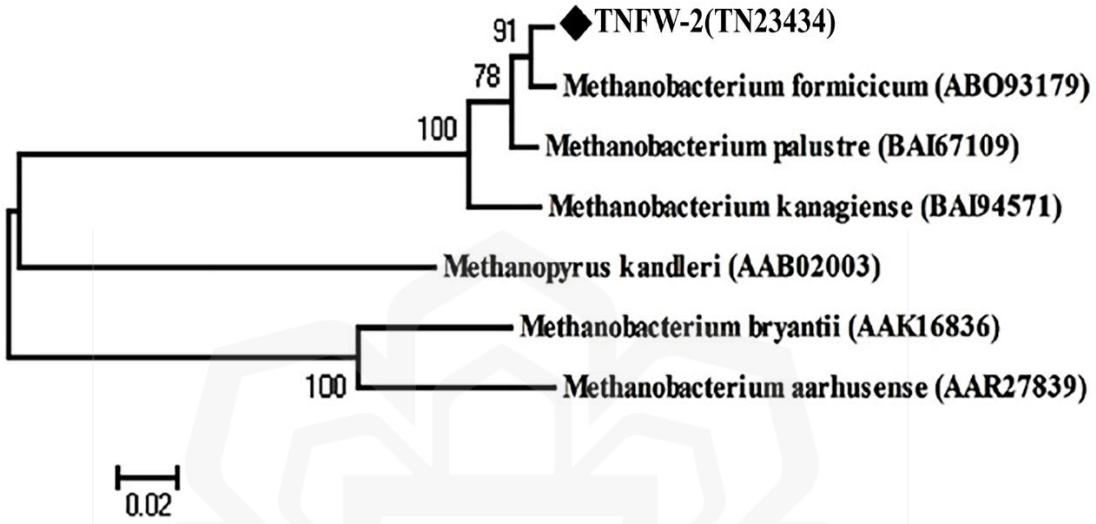

Figure 4.19: Phylogenetic analysis of determined mcrA amino acid sequences illustrating *Methanobacterium formicicum* TNFW-2 connection to kindred methanogenesis. The tree was built utilizing nearest method using similarity matrix (154 amino acid positions; Poisson correction). The *Methanopyrus kandleri* sequence was employed as an outgroup source. Parentheses indicate the authorization code. Each bar shows 0.02 nucleotides modifications.

The mcrA gene as shown in Figure 4.19 and amino acid sequences as shown in Figure 4.19 revealed three primary clusters: cluster 1 had three sub-clusters, one of which included TNFW-2, which exhibited of 99% match to *Methanobacterium formicicum*. All three produced identical phylogenetic findings, confirming the findings of Luton et al., (2002), who suggested that the mcrA gene sequence may be employed as an annotator to 16S rRNA based sequences. *Methanobacterium* formicicum TNFW-1 was proposed as a novel strain within the genus *Methanobacterium* based on physiological and phylogenetic

variations. The fractionated SDA bands of TNFW-1 image by DNS-PAGE analysis and nucleotide sequence were presented in Appendix C.1-C.2.

4.9.2 Chemical Analysis of Potential Bacteria

4.9.2.1 Observation of extracellular polymer by transmission electron microscopy

Transmission electron microscopy (TEM) revealed significant levels of extracellular polymers (ECP) around the cells of methanogens as shown in Figure 4.20. In certain circumstances, polymers stretched from one cell's outer surface to cling to another. Additional polymers were found in *Methanobacterium formicicum* micrographs than in *Methanobacterium sp*. From Figure 4.20, it was mentioned that the TEM structure of *Methanobacterium formicicum* revealed certain features, specifically the CW. The cell wall of *Methanobacterium formicicum* was observed under the TEM with a size of 0.5 pm. This indicates that the cell wall thickness of *Methanobacterium formicicum* is approximately 0.5 pm. Additionally, Figure 4.20 mentions phase-contrast microscopy of strain TNFW2, with an image size of 5μm. Phase-contrast microscopy was a type of microscopy technique that enhances the contrast of transparent or unstained samples by exploiting differences in refractive index within the sample. In the case of strain TNFW2, phase-contrast microscopy was used to observe its characteristics, presumably in terms of cellular morphology or other relevant features. The image captured through phase-contrast microscopy had a size or scale of 5μm, indicating that the observed field of view in the image was 5 micrometers in diameter. These microscopy techniques, such as TEM and phase-contrast microscopy, allow researchers to visualize and study the structures and features of microorganisms at a microscopic level. The *ECP* were found in anaerobic activated sludge, which appeared to

create a robust substrate for cell anchoring in particles (Poi, 1985; Savla et al., 2022). Our findings support the generation of ECP by particles and show that the ECP was produced by the two most common methanogens isolated from the particles (Liu et al., 2003; Bai et al., 2022; Fahimizadeh et al., 2022).

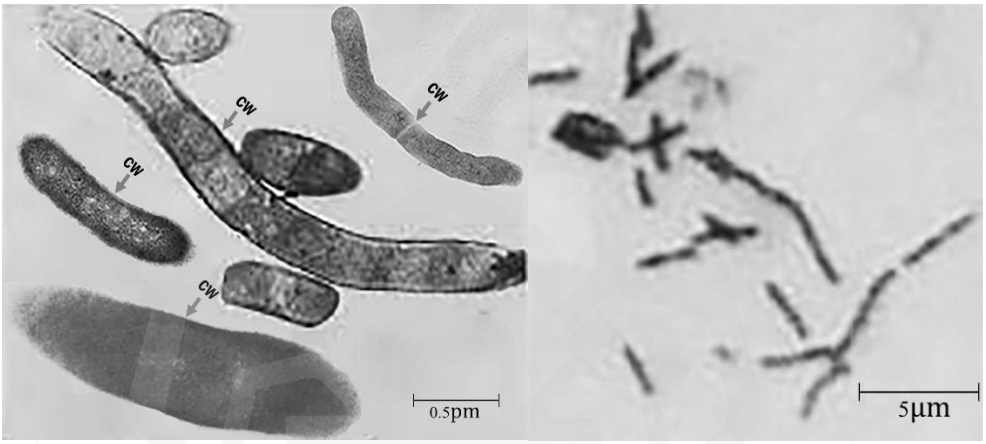

Figure 4.20: TEM structure of *Methanobacterium formicicum* showing CW cell wall, 0.5 pm and phase-contrast microscopy of strain TNFW2 5µm.

According to our TEM analysis, methanogens and other eukaryotic organisms in the particles were enclosed by ECP and held together by fibrous networks (Diaz et al., 2006; Edgcomb et al., 2011; Bang et al., 2012; Kuroda et al., 2022).

4.9.2.2 Chemical composition of the extracellular polymers.

Table 4.8 shows the quantities of total extracellular polymers (ECP) and Extracellular polymeric substances (EPS) recovered from *Methanobacterium formicicum* molecules. Both ECP and EPS were found *in Methanobacterium formicicum* tissues. The anaerobic activated sludge had the same quantity of ECP and EPS as *Methanobacterium formicicum* cells fed on formic acid. Interestingly, *Methanobacterium formicicum* produced less ECP and EPS when cultured on H_2-CO_2. This methanogen generated EPS with a molecular

weight more than 100,000. The polysaccharide content of *Methanobacterium formicicum* ECP was comparable (about 20%) to that of anaerobic activated sludge. For *Methanobacterium formicicum,* the viscosity of the EPS at 0.1% (wt/vol) polymer concentrations was 1 centistoke.

Table 4.8: ECP and EPS in methanogenic anaerobic sludge *Methanobacterium sp.*

Organism	**Growth substrate**	**Amt mg/mL of VSS**		**% of EPS in ECP**
		T-ECP	**T-EPS**	
Anaerobic Sludge	VFA	90.5	18.0	19.9
Methanobacterium	Formate	85	21.8	25.6
formicicum	H_2-CO_2	77	16.2	21.0

The statistics demonstrate the averages of triplicate calculations. VSS stands for volatile solids, and it was utilized to determine the volatile component of feedstock. b Acetate, propionate, and butyrate (2:1:1, mol/mol) were present in the VFA combination.

The EPS of *Methanobacterium formicicum* included 5.3% N, 4.1% H, and 32.1% C, according to chemical analysis. Rhamnose, fucose, mannose, galactose, glucose, glucosamine, galactosamine, and mannosamine were examples of sugars. were the primary sugar contents in the EPS recovered from the anaerobic sludge. Ribose was also found in trace amounts in the EPS. More than half of the sugars generated by *Methanobacterium formicicum* were rhamnose and mannose. Galactose, glucose, mannosamine, and galactosamine were the remaining carbohydrates. Uranic acids and fucose were not found in the EPS of these methanogens, but they were found in the anaerobic sludge EPS. The number of EPS recovered from the methanogenic anaerobic sludge, *Methanobacterium formicicum,* varied from 1.6 to 2.2% of the volatile fraction of the cells in this investigation. These results were comparable to those obtained from many other anaerobic sludges (Veiga et al., 1997; Wu et al., 2020; Morais et al., 2021; liu et al., 2021). The main sugar

concentrations in the EPS from the sludges were equivalent to those discovered by Dolfing et al., (1985) and Harada et al., (1989). These findings back with our prior research on the production of granules by certain cells, in which *Methanobacterium formicicum* functioned as a precursor and a foundation for other species to anchor (Wu et al., 1996). Fucose, on the other hand, was found in the granule EPS but not in the EPS of the single methanogen. Fucose might have been a component of EPS produced by other major anaerobic sludge species.

4.9.2.3 Effect of substrates on the ECP produced by Methanobacterium formicicum

M. formicicum obtains its sustenance from H2-CO2. The formate-grown cells generated larger ECP with a larger polysaccharide composition than the H2-CO2-grown cells as depicted in Table 4.9.

Table 4.9: % Sugars and amino sugars in EPS extracted from *M. formicicum*

Sugar or Amino sugar Contains	**Anaerobic Sludge (mg/mL)**	***Methanobacterium formicicum*** **Formate**	**H_2-CO_2**
Rhamnose	14.85	28.80	25.08
Fucose	11.02	0	0
Ribose	Trace amount	0	0
Mannose	12.35	30.07	24.90
Galactose	15.91	15.86	16.97
Glucose	20.03	9.31	11.97
Glucosamine	7.96	Trace amount	Trace amount
Galactosamine+ mannosamine	7.14	16.93	18.75

The accumulation of yeast extract to the formate-containing solution had no effect on the quantity of ECP in the volatile fraction (data not shown). The sugar contents of EPS isolated from formate and H2-CO2-grown cells were nearly comparable. Rhamnose and mannose were the main sugars as described in Table 4.9. The findings showed that *Methanobacterium formicicum* in the microparticles may create more ECP when cultivated in conditions including formate. Hydrogen and formate were created as byproducts during starter culture and syntrophic breakdown of fatty acids and methanol during anaerobic digestion (Thiele, 1988; Wu et al., 1991). It was difficult to establish the formate-to-hydrogen ratio generated as an advance.

4.9.2.4 EMMs Surface Structure Analysis

From 1.0 L of supernatant, 0.10g pure *Methanobacterium formicicum* TNFW-2 was extracted. The isolated lyophilized *Methanobacterium* was a yellowish color. Figure 4.21 depicts the morphology of isolated *Methanobacterium* using scanning electron microscopes (SEM).

Figure 4.21: SEM images of the purified EMMs produced by *Methanobacterium formicicum* TNFW-1 at magnification ×850

The pure *Methanobacterium* had a circular shape with full borders, was slightly elevated in the middle, and was cream to light yellow in color. The cells were rod-shaped and ranged in size from 0.8 μm to 22 μm. Electron microscopy revealed that the microorganisms were gram-positive, nonmotile, and lacked flagella. The finding was in agreement with Smith et al., (1958) and the configuration result of the *Methanobacterium* molecule may contribute to its high convention of CH_4 production efficiency (Roycroft et al., 2016). SEM images of *Methanobacterium* and the biogas upgrade revealed that polymer bridging can be the CO_2 conversion process (Wang et al., 2020; Zhao et al., 2021).

4.9.3 EMMs Stability

Figure 4.22 shows that *Methanobacterium formicicum* TNFW-2 was stable at wide range, from pH 4 to 9 and optimum growth rate was achieved within the range of 6.5 to 7.5. At pH 7, the growth rate was higher and the growth rate decreased slowly as the pH increased further. Thus, the growth rate was suitable to be applied at neutral condition. This may be due to the growth rate shows different electric charge at different pH and affect the growth rate ability (Pan et al., 2009). At 35°C in basal medium broth, the optimal pH for growth and CH_4 yield seems to be between pH 5.5 and 7.5, as determined by specific growth rates as shown in Figure 4.19 determined from CH_4 yield between 2 and 3 days of culture. The A_{660}, determined at the conclusion of the bacterial culture, confirmed this maximum. At pH 7, the optimum CH_4 yield was 0.078umoL/20mL of growing per day and the optimum growth rate was comparable (0.078 h^{-1}) to that reported from CH_4 records at pH 7. At pH 4, growth was low whereas at pH 4.5 was slight increased per days.

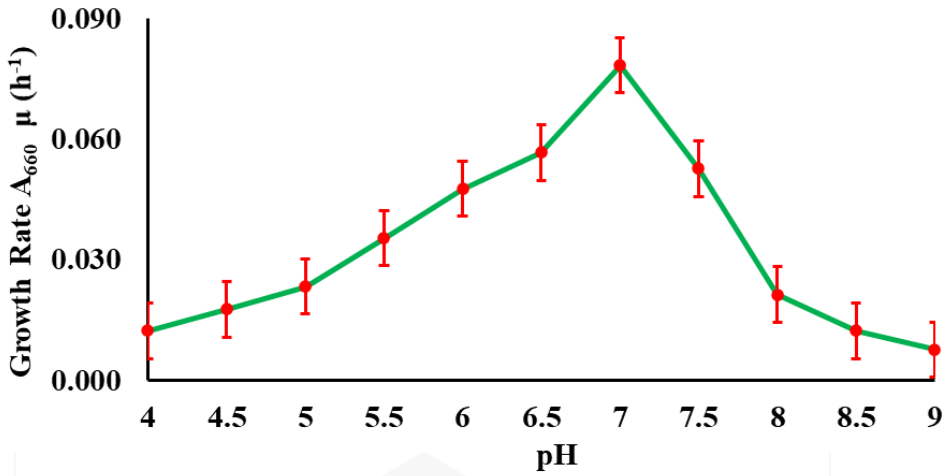

Figure 4.22: Effect of pH on the growth rate of strain TNFW-2.

The effect of temperature on the growth rate activity of EMMs was investigated as shown in Figure 4.23. The results showed that the EMMs was fairly temperature-tolerant and had good CH_4 production activity at wide range of temperature. The growth rate varies and only begins to decrease slightly with further temperature increase from 25°C to 45°C. The highest growth rate of 96% was observed at 30°C and 38°C and the EMMs exhibited temperature stability at 30°C with growth rate activity of more than 92%.

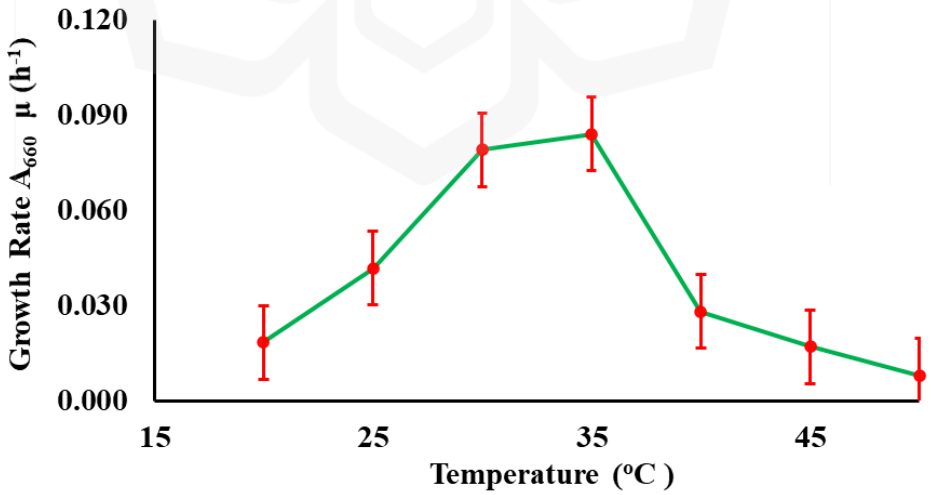

Figure 4.23: Effect of temperature on the growth rate of strain TNFW-2.

The thermal stability of the EMMs content could be a polysaccharide (Oladoja et al., 2017; Haddar et al., 2021). The EEMs may be effective in the room temperature wastewater treatment. Similar work has done by Nguyen et al., (2021), the BioM produced by *Methanobacterium* with a H_2 production activity of about 90% at temperature range from 25 to 50°C. In addition, surface colonies of strain TNFW-2 were 0.3 to 1mm in diameter after 3 to 7 days of incubation in basal agar medium whereas pH of 7 and temperature 35°C. Figure 4.24 depicted that the effect of incubation time on the specific growth rate of strain TNFW-2 based on methane production were plotted. After 2 to 3 days of bacterial culture, the significant colonies were generally detected. The majority of the colonies from the $l0^{-4}$ dilutions were identical, therefore individual colonies were placed into basal broth at pH 7 serially diluted, and plated on agar.

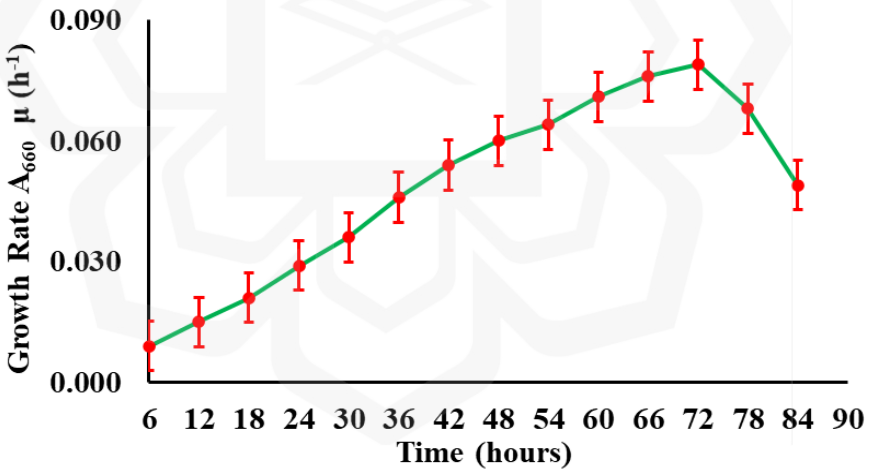

Figure 4.24: Effect of incubation time on the growth rate of strain TNFW-2.

This procedure was repeatedly performed until the structure of cell walls and optical microscopy of colonies transplanted into a synthesized and sophisticated medium containing yeast extract, tryptone, and glucose demonstrated culture purity.

4.10 OPTIMIZATION OF CO_2 TO CH_4 BY USING TNFW-2 STRAIN

Characteristic of the strain TNFW-2 performance can help to understand the behavior of the BioM production in the MECs by using OFAT method.

4.10.1 Effect of Substrates Concentration for CO_2 to CH_4 by using Strain TNFW-2

By substituting H_2 with the alternative substrates at concentrations of 10 mM, strain TNFW-2 capacity to grow on substrates other than H_2-CO_2 was tested such as butyrate, formate, pyruvate, propionate, ethanol trimethylamine, and methanol. When compared to controls with no additional substrate, only sodium formate enabled methanogenesis. The effects on strain TNFW-2 of supplementing 100mL of basal medium, pH 7, incubation at 30°C, under an 80% of H_2-20% of CO_2 gas phase (to gas flow rate of 5L/h) with potential applied voltage at −0.9 V vs SHE and enhancers of methane production were shown in Figure 4.25. In this case, EMMs inoculum was used 10mL/100mL. None of these substance's methane generation in strain TNFW-2 was converted on H_2-CO_2 at the doses tested.

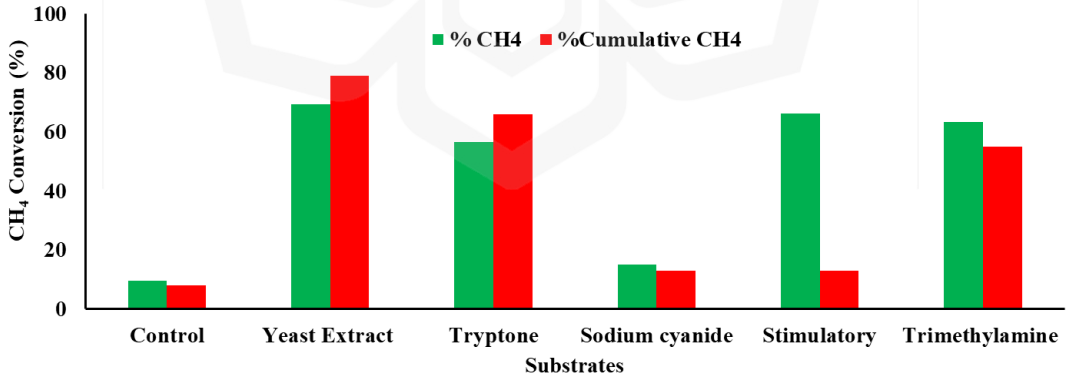

Figure 4.25: Effect of substrates for CH_4 production by using strain TNFW-2. Other factors were fixed EMM dose 10mL, pH 7, gas flow rate of 5L/h, incubation time 24 hours, basal media of 100mL, H_2-CO_2 of 80-20%, applied voltage at −0.9 V and room temperature 30°C (±2).

The maximum CH_2 yields and overall CH_2 levels all validated highly consistent developments in terms of the impacts of different chemicals on growth and methanogenesis, as illustrated by Figure 4.25. Several studies state the abiotic reformation of CO_2/H_2 to CH_4 using heterotrophic bacteria CH_4 production (Savvas et al., 2017; Seifert et al., 2014). Rachbauer et al., (2016), in contrast, demonstrated improved organic biogas compositions, particularly CH_4, with H_2 supplementation and indicated that entire CO_2 generation (> 96%) was achieved with less than 0.1% remaining H_2 by using a basal mix of biochemical H_2 and biogas (36 - 42% CO_2). Similarly, 14 days following the coenzyme M injection, the density of the Mycobacteriaceae species enhanced from 1.05 to 3.34% (peaking at 6.08% at 7 days), as did the prevalence of the gram - positive bacterium phylum, which climbed from 13.2 to 23.92%. MEC was able to boost the synthesis of H_2 from nutrients during microbial digestion (Lu et al., 2010; Nam et al., 2014). While AD, CH_4 was generated through hydrogenotrophic and acetoclastic methanogenesis from degraded simple carbohydrate (Liu et al., 2016).

4.10.2 Effect of Inoculum Dose for CO_2 to CH_4 Conversion

Figure 4.26 shows the optimum EMM inoculum dose to convert CO_2 to CH_4 from basal medium with H_2-CO_2 suspension. The CO_2 reduction of EMM was studied in the dosage range of 0, 1, 2, 3, 4, 5, 6, 7, 8, 9, 10, 11, 12, 13, 14 and 15 mL/100mL. The highest CO_2 convert of 92% was recorded at 10mL/100mL in optimized BioM production. These results showed that over doses from 11 mL to 15 mL/100mL of TNFW-2 caused destabilization of the CO_2, while low dose at 1-5 mL/100mL was insufficient to make bridging between bio-molecules and H_2-CO_2 suspensions. The TNFW-2 showed excessive doses were more

than 11mL/100mL & 15 mL/100mL and low doses less than 1mL/100mL & 7mL/100mL of pH-7 produced by *Methanobacterium formicicum* (Aljuboori et al., 2015). From Figure 4.26, it was clear seen that BioM production strongly depended on the substrates. Considerable CH_4 formation was detected only when the pure CO_2 was used. As a result, more economical methane generation was obtained. The existence of direct electron transfer has initially been mentioned in different catalytic investigations such as electrochemical conversion oxidation process (Comninellis, 1994; Weber & Ramasamy, 2020) and carbon dioxide subsequent decrease to acetate (Hickey et al., 1987; Mohanakrishna et al., 2018), but there were very few proofs to precisely verify the existence of the electron exchange mechanism in the electromethanogenesis technique up to this point (Cheng et al.,2009; Zhang et al., 2019; Zhang et al., 2022), particularly when a more negative potential was attempted.

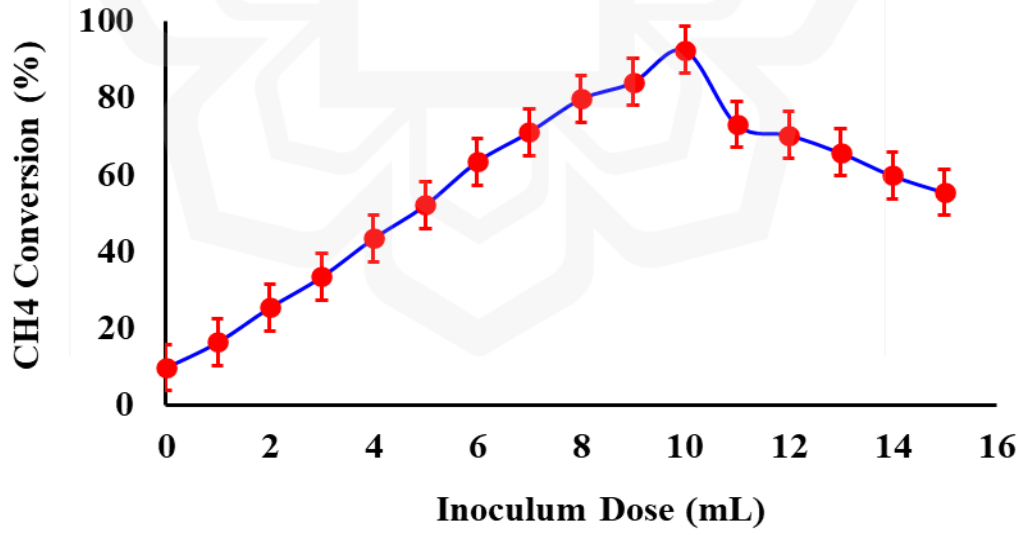

Figure 4.26: Effects on inoculum dose for CH_4 production by using strain TNFW-2. Other factors were fixed the incubation time 24 hours, gas flow rate of 5L/h, pH 7, basal media of 100mL, H_2-CO_2 of 80-20%, applied voltage at −0.9 V and room temperature 30°C (±2).

To demonstrate the presence of direct electron transfer in the electromethanogenesis technique, Fu et al., (2022) increased the cathode potential to 0.9 V vs SHE, but they were still unable to minimize hydrogen as a significant metabolic pathway due to the involvement of the hydrogen evolution reaction (HER) at 0.9 V vs SHE; alternatively, He et al., (2022) adopted a hydrogenase-deletion transformed deficient all catabolic hydrogenases.

4.10.3 Effect of pH

The effect of pH on strain TNFW-2 for production BioM was shown in Figure 4.27. The strain TNFW-2 showed over 92% of BioM yield with broad range of pH at 4 to 9 in the high BioM production initial CO_2 was 20% whereas H_2 was 80% gas phase condition. Result shows that the ionization of the functional groups in the long chain molecules of the strain TNFW-2 was pH 7 dependent which completely ionize at acidic, neutral and alkaline conditions. Therefore, it specifies that the TNFW-2 revelations different electric states at different pH which influence the BioM upgrade process (Li et al., 2017; Lin et al., 2017; Devi et al., 2022). From Figure 4.17, it was shown that the strain TNFW-2 was quite effective in exhibiting BioM production of 55 to 92% at pH 5 to 7. The results revealed that, the formation of electromethanogenesis between EMMs molecules was neutral and basic conditions by adsorbing of proton and hydroxyl ions. At pH 7.0, the equal of OH^- and H^+ ions, the high CH_4 production rate observed was theoretically due to the both control molecules of the functional collections of electromethanogenesis might be qualified to neutralize negative charge atoms completely. At pH 8.0, OH- ions increased and negative charge of EMM atoms could be neutralized by positive charge of functional collections on

electromethanogenesis. On the other hand, lower CH_4 production activity was observed at acidic pH compared to neutral and alkaline conditions at TNFW-2. At pH 4 to 6, H^+ ions increased and positive charge molecules of functional collections may increase the positive charge as compared to negative charge of atoms in the condition, which were imbalance to destabilize the atoms.

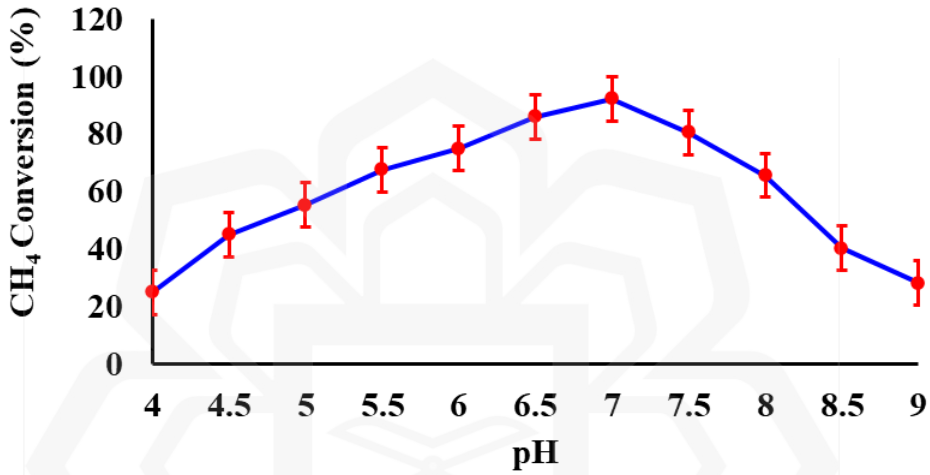

Figure 4.27: Effects on pH for CH_4 production by using strain TNFW-2. Other factors were fixed the incubation time 24 hours, inoculum dose 10ml, gas flow rate of 5L/h, basal media of 100mL, H_2-CO_2 of 80-20%, applied voltage at −0.9 V and room temperature 30°C (±2).

CH_4 synthesis in the anode chamber was a particularly undesired response in this situation because it uses up the H^+ and e that should be utilized to make target electro biofuels at the cathodes (Kumar et al., 2018). The influences of pH on acetogenic amount and microbial community were explored in order to get a new understanding of the mechanism of pH influence on gas bioconversion using acetogen enrichment cultures (Xu et al., 2015; Chakraborty et al., 2020). The highest acetate and ethanol concentrations were obtained at pH 7, with pH 9 coming in second. The effects of pH on acetogenic amount and microbes were explored in order to get a new understanding of the mechanism of pH

influence on gas microbial fermentation using acetogen enrichment cultures. The highest acetate and ethanol concentrations were obtained at pH 7, with pH 9 coming in second (Torino et al., 2001; Ding et al., 2010; Rovira-Alsina et al., 2022).

4.10.4 Effect of Incubation Time

Bacteria that were highly classified such as TNFW-2 and NTAS-2. Introduced in a liquid culture medium that can be used for separating bacteria. Both of them were same genus and species like *Methanobacterium formicicum*. In this type of strain was used to produce high BioM which was around 94% when using directed electron transfer like gas phase of H_2/CO_2 in the ratio of 80:20 at 30°C dual chamber MEC system in the de-oxygenated method. The effects of incubation times like 0, 6, 12, 18, 24, 30 and 36 hours, the results of isolates of bacteria TNFW-2 were shown in Figure 4.28.

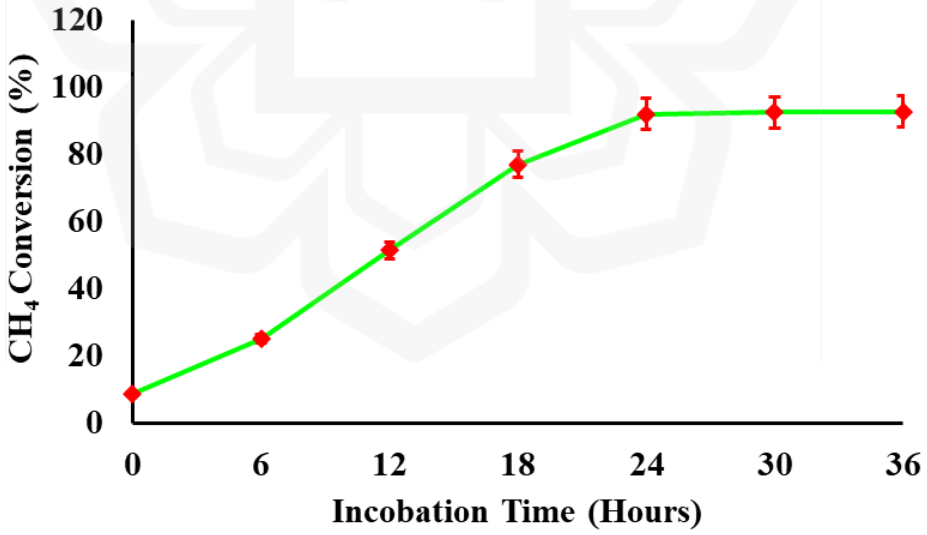

Figure 4.28: Effects on incubation time for CH_4 production by using strain TNFW-2. Other factors were fixed the inoculum dose 10mL, pH of 7, gas flow rate of 5L/h, basal media of 100mL, H_2-CO_2 of 80-20%, applied voltage at −0.9 V and room temperature 30°C (±2).

From Figure 4.28, it was clearly observed that the CH_4 was yield approximately of 92% at incubation time of 24 hours whereas other factors were fixed such as the pH of 7, inoculum dose 10ml, basal media of 100mL, H_2-CO_2 of 80-20%, gas flow rate of 5L/h, applied voltage at −0.95 V and room temperature 30°C (±2). However, the maximum production was slightly increased of 92.5% and 92.7% when incubation time between 30 and 36 hours respectively. Moreover, if the rates of production of hydrogen were substantial, it was expected that microbially mediated translation of H_2 to CH_4 will be time-consuming (Call and Logan, 2008; Bhatia et al., 2022). Both CH_4 generation and fuels efficiency declined greatly, while CO_2 removal fuel utilization dramatically grew. Immobilization or membrane filtration were two methods for separating CO_2 or O_2 from combustion process (Dess et al., 2021; Mohapatra et al., 2022; Spiess et al., 2022).

4.10.5 Effect of Gas Flow Rate

Gas flow rate was a significant influence both on the positive and negative electrode impedance responses. Improved gas flow rate caused a higher magnitude of constant phase element and lower charge transfer and mass transfer associated characteristic impedance, indicating that maximizing gas flow rate was a major beneficial influence on system stability. When the flow rate was increased from 1 to 3 L/hour, the charge transfer resistance dropped significantly, but subsequently rose somewhat when the flow rate was raised to 5 L/hour. This small improvement in resistance to charge transfer at the maximum flow state was much more typically due to a threshold rather than negative effects from the highest flow condition (Aaron et al., 2010). The rise in the constant phase element factor was predictable and consistent with the prior explanation of constant phase element. The

effect of flow on mass transfer susceptibility in both the positive and negative electrode was of significance. The flow rate of medium through the anode chamber, that was isolated from the cathode chamber by a microporous membrane, was directly adjusted under this operation. Under this operation, electrogenic microbes in the positive electrode consumption food wastes in the nonattendance of O_2 and release electrons to the positive electrode in the presence of minimal voltage level, electrographs in the negative electrode can accept and exchange these electrons to the negative electrode via an electrode surface, and CH_4 was produced. Figure 4.29 shows that the different gas flow rate and the strain of TNFW-2 was convert CO_2 to CH_4, the maximum production was 92% when the gas flow rate was used in 5L/hour whereas other factors were fixed such as the inoculum dose 10mL, pH of 7, incubation time of 24 hours, basal media of 100mL, H_2-CO_2 of 80-20%, applied voltage at −0.9 V and room temperature 30°C (±2).

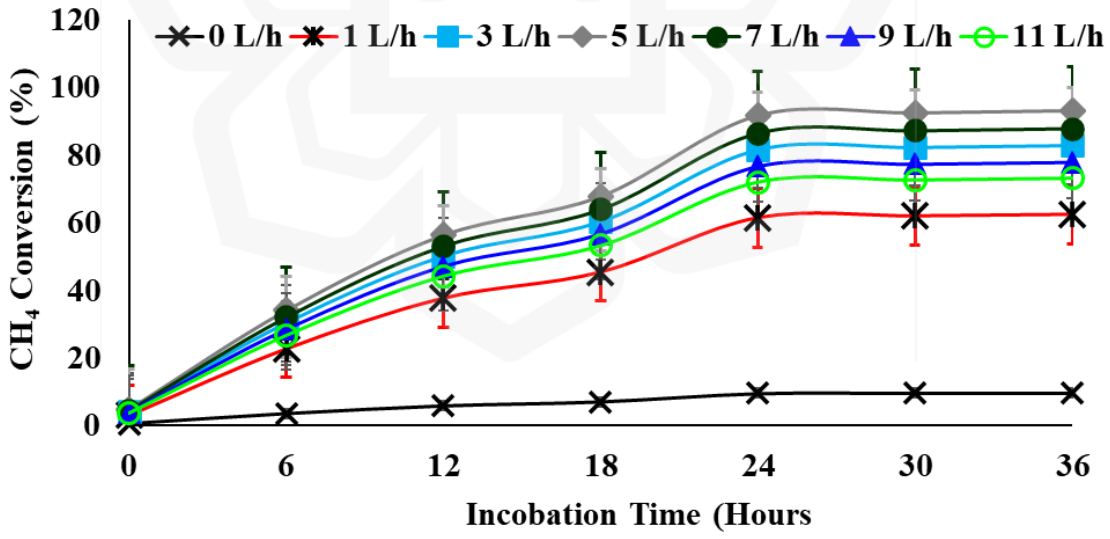

Figure 4.29: Effects on incubation time for CH_4 production by using strain TNFW-2. Other factors were fixed the inoculum dose 10mL, pH of 7, incubation time of 24 hours, basal media of 100mL, H2-CO2 of 80-20%, applied voltage at −0.9 V and room temperature 30°C (±2).

Initial condition, the conversion was very low percentage. After that flow rate was increased (up to 5 L/hour) the conversion percentage also sharply increased. Moreover, the gas flow rate from 7L/hour to 11L/hour the conversion percentage was fall down which were almost 87%, 77% and 73%, respectively. Flow rate and aqueous recycling have both been proven to have a substantial influence on MEC efficiency, with the high flow mode being the only one in which the medium + substrate was continuously fed (Lewis and Borole, 2016). Any operational environment that promotes acid degradation by the bacteria reduces the active surface area required to achieve a certain rate of current output (Ki et al., 2016). The positive and negative electrodes potentials of MEC positioned under whole cell circumstances may reduce simultaneously.

4.10.6 Optimization of the EMMs TNFW-2 Strain by FCCCD Under RSM

RSM was one of the most effective experimental techniques for process optimization. Table 4.11 listed the CH_4 production percentage of experimental and predicted response for each experimental run, six center points and 30 experimental runs were generated. The highest CH_4 production of 92.37% was achieved for run 14, and the lowest CH_4 production of 53.35% was for run 6.

The main objective for optimization process was to reveal and assess the statistical approach to find better conversion of the interaction between factors related in the CH_4 production. It can also enhance the total yield as well as reduce the cost of experiments. High pressure and short time were significant factors in CH_4 production; its assignation between H_2 and CO_2 ratio (Chen et al., 1998; Chen & Sachtler, 1998). The final regression equation attained from experimental runs; it was employed to predict the production rate.

Table 4.10: Experimental design generated by FCCCD of TNFW2 process for CH_4 conversion.

Run No.	Factor 1 A: High Flow rate (L/hour)	Factor 2 B: Short Time (Hours)	Factor 3 C: Low Flow rate (L/hour)	Factor 4 D: Long Time (Hours)	Response % CH_4 Convesion (Actual)	Response % CH_4 Convesion (Predicted)
1	**5**	**24**	**5**	**24**	**91.985**	**91.94**
2	5	24	1	36	77.16	77.01
3	8	18	3	30	68	66.12
4	11	18	3	30	64.585	63.59
5	11	12	5	24	68.495	68.61
6	11	12	1	24	53.18	53.35
7	8	18	3	30	68	66.12
8	**5**	**12**	**5**	**24**	**92.005**	**90.91**
9	5	18	3	30	77.5	79.35
10	**11**	**24**	**5**	**24**	**82**	**82.97**
11	8	18	3	30	71.13	66.12
12	11	24	1	36	66.67	67.79
13	**11**	**24**	**5**	**36**	**82.3**	**83.22**
14	**5**	**24**	**5**	**36**	**92.515**	**92.37**
15	8	18	1	30	61.34	61.16
16	8	18	3	36	70.895	71.04
17	8	12	3	30	60.5	59.61
18	8	24	3	30	68	67.19
19	11	24	1	24	66.69	67.64
20	8	18	3	30	68	66.12
21	5	12	1	36	77.175	76.23
22	11	12	5	36	69	69.03
23	8	18	3	30	69	66.12
24	8	18	5	30	76.25	76.47
25	11	12	1	36	53.66	53.67
26	5	24	1	24	76.69	76.68
27	8	18	3	30	68	66.12
28	5	12	1	24	76.69	75.73
29	**5**	**12**	**5**	**36**	**92.5**	**91.52**
30	8	18	3	24	70.76	70.66

*Bold indicates center points

The process parameters of high pressure, short conversion time, low pressure and long conversion time and their optimum points were better described in the quadratic polynomial equation. The following equation explains the process parameters in terms of coded factors in Equation 4.2.

$$Y = 67.6 - 8.2 \times \mathrm{A} + 3.38 \times \mathrm{B} + 7.66 \times \mathrm{C} + 0.19 \times \mathrm{D} + 3.33 \times \mathrm{AB} + 0.02 \times \mathrm{AC} + 0.04 \times \mathrm{AD} + 0.018 \times \mathrm{BC} - 0.04 \times \mathrm{BD} + 0.025 \times \mathrm{CD} + 4.4 \times A^2 - 2.38 \times B^2 + 2.16 \times C^2 + 4.19 \times D^2 \quad (4.2)$$

where, Y was the CH_4 conversion (%) and used variables of high gas flow rate (A), short time (B), low gas flow rate (C) and long time (D), respectively.

The formula in terms of real parameters can be utilized to forecast reaction for different degrees within each element. For each parameter, the values must be indicated in the original units. So, because variables were scaled to fit the units of each element, and the endpoint was not at the centre point of the design process, this formula should not be utilized to evaluate the quantitative influence from each parameter.

Table 4.12 summarizes the analysis of variance used to assess the comparability of the statistical approach. The model's F-value of 109.85 indicates that it was significant. An F-value this big might arise owing to noise just 0.01% of the time. Model terms with P-values less than 0.0500 were significant. In this case A, B, C, BC, A^2, B^2, D^2 were significant model terms. Values larger than 0.1 imply that the model terms were not significant. Model simplification may enhance overall model if there were numerous inconsequential customized version (except those necessary to enable hierarchy). The Lack of Fit F-value of 1.41 indicates that there was a 37.10% possibility that a big Lack of Fit F-value might develop owing to noise. A lack of fit was undesirable; designers want the model to fit. This relatively low probability (<10%) was troubling. In addition, the efficiency of the model

was demonstrated by the high value of regression co-efficient (R^2) and adjusted R^2 values were 0.9903 and 0.9813, respectively, which indicated the actual and predicted values, were found to be better correlation.

Table 4.11: Analysis of variance (ANOVA) for CO_2 conversion (Biogas upgrade)

Source	Sum of Squares	df	Mean Square	F-value	p-value	
Model	3109.76	14	222.13	109.85	< 0.0001	**significant**
A-High flow rate	1210.98	1	1210.98	598.90	< 0.0001	
B-Shor Time	205.40	1	205.40	101.58	< 0.0001	
C-Low flow rate	1054.86	1	1054.86	521.69	< 0.0001	
D-Long Time	0.6347	1	0.6347	0.3139	0.5836	
AB	177.86	1	177.86	87.96	< 0.0001	
AC	0.0058	1	0.0058	0.0029	0.9579	
AD	0.0320	1	0.0320	0.0158	0.9016	
BC	0.0054	1	0.0054	0.0027	0.9593	
BD	0.0293	1	0.0293	0.0145	0.9057	
CD	0.0108	1	0.0108	0.0053	0.9428	
A^2	50.36	1	50.36	24.91	0.0002	
B^2	14.72	1	14.72	7.28	0.0165	
C^2	12.10	1	12.10	5.99	0.0272	
D^2	45.57	1	45.57	22.54	0.0003	
Residual	30.33	15	2.02			
Lack of Fit	22.38	10	2.24	1.41	0.3710	**not significant**
Pure Error	7.95	5	1.59			
Cor Total	3140.09	29				

R^2 = 0.99, Adjusted R^2 = 0.98, C.V% = 1.96, Predicted R^2= 0.97, Adequate precision= 38

The appropriate precision was utilized to measure the signal to noise ratio; the adequate precision of 4 suggests that navigating the design parameters for statistical models may be necessary, and the model attained a ratio of 38.63. Furthermore, the coefficient of variation (CV) was a mean percentage that represents the standard deviation between

variables. The CV for the CO_2 conversion rate was 1.96; lower CV values can provide more consistent results (Liyana-Pathirana & Shahidi, 2005).

Figure 4.30 depicts the response surface curves for the interplay of components (high and low gas flow rate, short and long conversion time). The effect of high gas flow rate and short conversion time on %CH_4 production was shown in Figure 4.27 (i) and (ii). In the optimization process, the interaction of these factors was insignificant and it indicated that high gas flow rate favors CH_4 production; when conversion time increases from 8 to 11L/hour the CH_4 production was decreased from synthetic CO_2 conversion, this was good agreement with the present (Xu et al., 2003; Ruocco et al., 2022). Figures 4.30 (iii) and (iv) showed the effect of high gas flow rate and low gas flow rate on CH_4 production rate at central point of conversion time for high and low gas flow rate. The response surface curves' form indicated a favorable relationship between low and high gas flow rate. Maximum and minimum gas flow rate had different impacts on the reaction, with CH_4 yield increasing just 9% (from 83 % to 92%) from the centre position to the substantial stage. As a result, the response surface curve suggested that the ideal circumstances were taken into account in the middle point.

Figures 4.30 (v) and (vi) indicated that interaction between high gas flow rate and long conversion time. The result showed that optimum response 92% was achieved at center point. Although the interaction of the factors was insignificant but they can be act as limiting factor after alteration of factor levels to achieve maximum CH_4 production rate. Figures 4.30 (vii) and (viii) depicted the effect of low gas flow rate and short time on CH_4 generation when the gas flow rate and time were set at the middle point. Short conversion times had an exponential influence on the reaction, but low pressure had a linear effect.

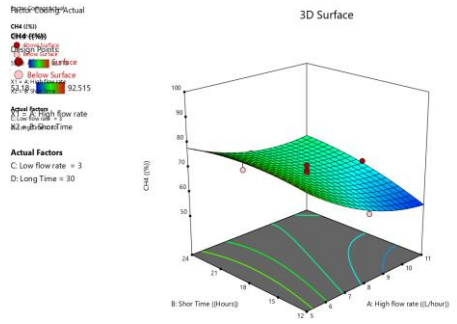

(i)

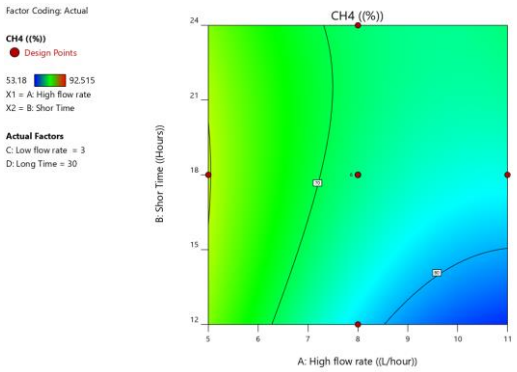

(ii)

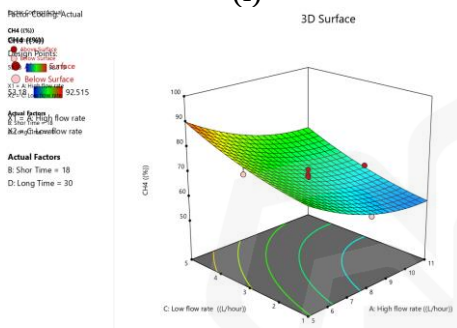

(iii)

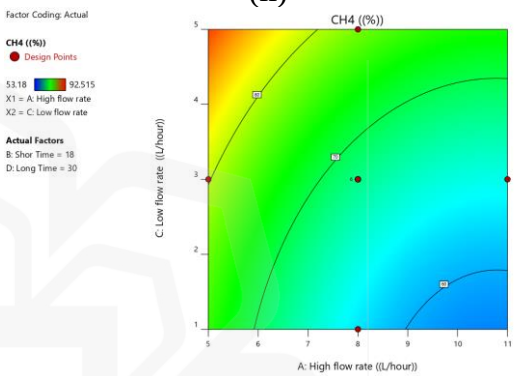

(iv)

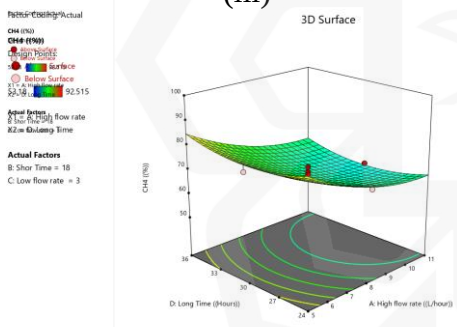

(v)

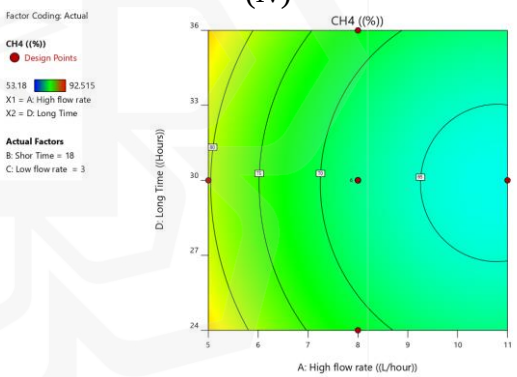

(vi)

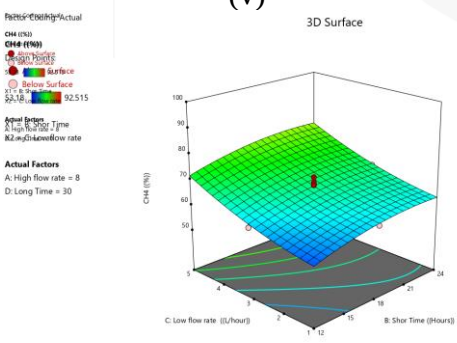

(vii)

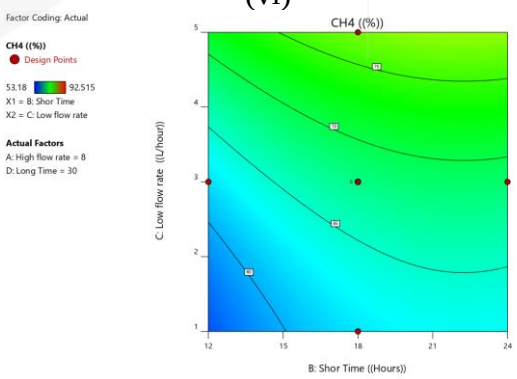

(viii)

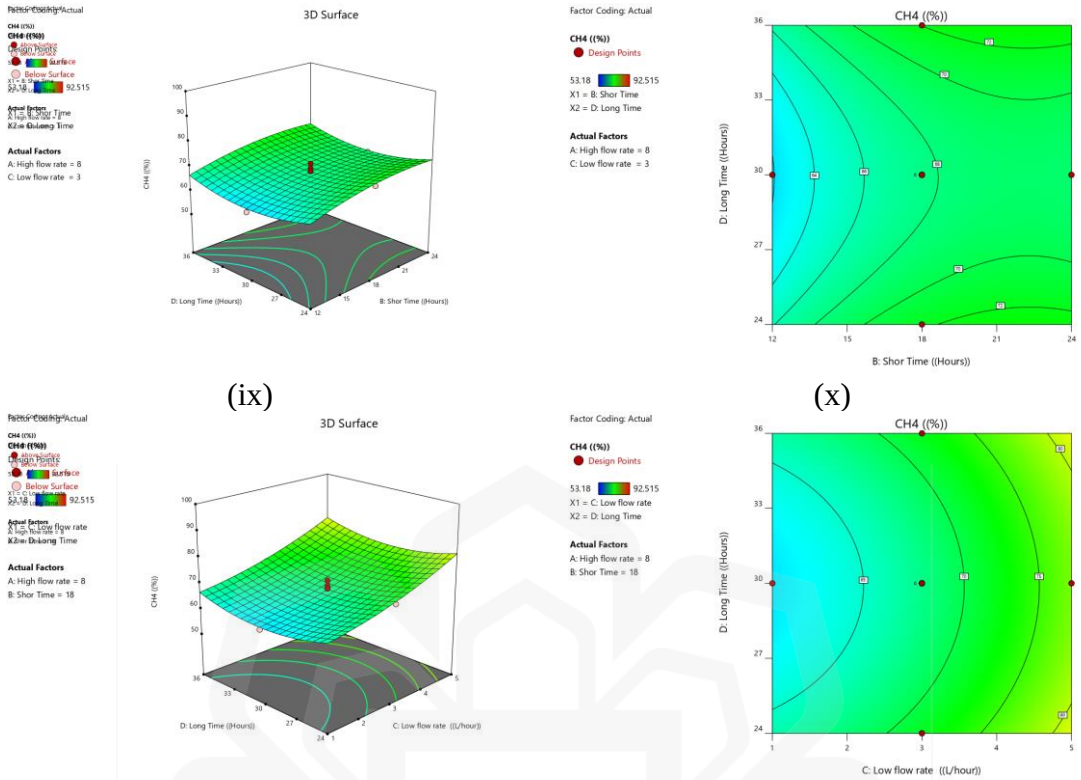

Figure 4.30: Response surface curve of the interaction effects of: (i, ii) 3D & 2D contour plot of high gas flow rate & short time; (iii, iv) 3D & 2D plots of high gas flow rate & low gas flow rate; (v, vi) 3D & 2D plots of high gas flow rate & long time; (vii, viii) 3D & 2D contour plot of low gas flow rate & short time; (ix, x) 3D & 2D plots of short time & long time; (xi, xii) 3D & 2D plots of low gas flow rate & long time on CH_4 yield percentage.

Figures 4.30 (ix) and (x) demonstrate the influence of short and long conversion times on CH_4 generation when high and low gas flow rate were placed at the main point. According to the 3D graph, optimum CH_4 generation was attained while short and long conversion times were at a high level. According to Wang Han (2022), appropriate time must have been allowed to generate electromethonogenesis for an efficient H_2/CO_2 convert CH_4 process. The similar phenomenon was found when the CH_4 process was optimized, with a maximum CH_4 generation rate of 94% recorded from 5 L/hour to 11 L/hour and conversion time extended from 30 to 36 hours (Zhang et al., 2021). The synergistic effect

of low pressure and long conversion time on CH_4 production by the EMM showed that low pressure and long conversion time were not suitable in the optimization (Figure 4.20 xi & xii). The increase the pressure and time from 1 to 5 L/hour and 12 to 24 hours were the optimum in center point.

4.10.7 Validation of the Statistical Model

Validation was a part of any optimization process to check the conformity between actual and predicted values which made a better understanding in the optimization process. Some of experiments were conducted within the level of parameters as predicted based on the high and low conditions because of the point prediction mechanism by utilize of the Design Expert software. The strategy of validation experiment was offered some solution when CH_4 production was set as maximum; hence, high and low levels were determined manually. The findings were displayed in Table 4.13 the experimental and predicted values and error percentages. Results obtained showed that the experimental response was in high similarity with the predicted values which exhibited the accuracy of the predicted models. The results demonstrated that highest CH_4 yield 92% was achieved in the run 21 and the lowest result was recorded in run 14 at 53.37%. The FCCCD method raised the conversion process where CH_4 yield was 92% (EMM dose 10mL, incubation time 24 hours, pH 7, basal media of 100mL, H_2-CO_2 of 80-20%, applied voltage at −0.95 V and room temperature 30°C (±2)) before optimization and CH_4 production of 92% (5L/hour for 24 hours and 5L/hour for 36 hours, EMM dose 10mL, pH 7, basal media of 100mL, H_2-CO_2 of 80-20%, applied voltage at −0.95 V and room temperature 30°C (±2)) was accomplished by the optimization.

Table 4.12 Validation of an experiment for CH_4 conversion optimization

Experiment No.	High gas flow rate (L/hour)	Short Conversion Time (Hours)	Low gas flow rate (L/hour	Long Conversion Time (Hours)	CH_4 Conversion %	
					Predicted	Experimental
1	8	22.48	5	36	92.06	93.65
2	8	14.76	1.07	28.52	60	58.95
3	8	12.18	4.22	25.33	70	69.08

No reports were found regarding optimization of gas flow rate and time for TNFW2 by RSM in the form of FCCCD. However, Suzuki et al., (2019) reported that different long conversion time had significant impact on charge neutralization and electromethanogenesis formation in electron transfer mechanism. The experiment was carried out to investigate H_2/CO_2 gash phase by using single chamber MEC system. The gas flow rate was high at 10L/hour for 24 hours, low pressure at 0.5L/hour for 36 hours and then allowed to H_2/CO_2 ratio 80:20 to measure the CH_4 production. In the study, resulting improvement indicated that experimental design-based response surface methodology by FCCCD was a favorable method in optimizing process factors for TNFW2 based CH_4 production.

4.11 SUMMARY OF FINDINGS FOR THE THIRD OBJECTIVE

In this study, identification, TNFW2 production and purification, characterization, EMMs strain TNFW2 stability and methanogenesis mechanisms were investigated. The EMMs strain TNFW2 was collected after 6 days of cultivation by using the optimized growth conditions mentioned section 4.8. Then the separation and purification were conducted to achieve 10mL/100mL purified EMMs strain TNFW2. Molecular identification, SEM,

TEM, chemical and elemental analysis was conducted to understand the methanogenesis mechanisms of the EMMs strain TNFW2 to CH_4 production. For molecular identification, 16S rRNA EMMs strain TNFW-2 genes were used and identified to *Methanobacterium formicicum*. Scanning electron microscopy (SEM) and the images revealed that the EMMs was irregular structure with netted texture. The EPS of *Methanobacterium formicicum* included 5.3% N, 4.1% H, and 32.1% C, according to elemental analyses. Rhamnose, fucose, mannose, galactose, glucose, glucosamine, galactosamine, and mannosamine were the primary sugar contents in the EPS recovered. The EMMs strain TNFW2 showed 92% CH_4 yield at 10mL/100mL; it showed better EMMs strain TNFW2 performance compared to others. The current study found that addition of cationic methanogenesis did not significantly enhance the CH_4 yield rate and exhibited excellent EMMs strain TNFW2 activity over a wide pH range of 4 to 9; with the maximal CH_4 production rate of 92% observed at pH 7. Overall findings revealed that, the methanogenesis mechanisms were polymer bridging and charge neutralization.

4.12 CHARACTERISTICS OF H-MECAD SYSTEM

This study was carried out to assess the H-MECAD performance of EMMs convert CO_2 by dual chamber MEC system. The control experiments were conducted without EMM. The experimental methods were described in method section 3.5.13.

4.12.1 Electron Transfer Mechanism

H-MEC technologies represent mechanisms involving the creation of electrical power or the achievement of a reduction reaction with a specific potential balance by electron

transfer between the electron acceptor and electron donor. Studies concentrate on electrode selection of materials and optimization, electrochemical structural modifications, and screening of electron transfer or inert type EMMs. Significantly, all of these methods and research were concerned with electron transport, namely membrane permeability and consumption. Thus, the fundamental ideas explain of electrochemical conversion systems and focus on intra- and extracellular electron transmission, as well as the potential electron transfer process as displayed in Figure 4.31. From Figure 4.31, it was clearly realized that the applied potential of 900mV was applied to conductive anode and cathode mixed materials such as staleness still with graphed plate (SS+GF), the hydrogen production rate (HPR) was optimum 3.5 m^3/m^3 day and the cathodic hydrogen yield rate (HYR) was 6.5 mol/mol. The HPR and HYR were minimum for used staleness still with aluminum plate (SSAL) when applied potential of 100mV and the HPR and HYR were 0.07 m^3/m^3 day and 0.5 mol/mol, respectively. However, staleness still (SS), mild steel (MS) and staleness still with mild steel (SSMS) were gradually increased HPR of 1.5 m^3/m^3 day, 1.8 m^3/m^3 day and 3.1 m^3/m^3 day and HYR of 5.1 mol/mol, 5 mol/mol and 6 mol/mol at 100mV to 900mV after that fall down of both cases. These findings indicate that polymer materials such as H-MEC of electron transfer mechanism were suitable for HPR and HYR; however, their electron transfer mechanism was improved used mixed materials. Another two hybrid catalysts of SSMS and SSAL deposits on a SSGF base at 0.9 V. These two different materials can improve electrochemical properties to drive HPR through a collaborative electronic effect, thus dropping cathode overvoltage and HYR good HPRs of 3.1 and 1.9 m^3/m^3 day as well as and high HPR of 6 mol/mol and 3mol/mol, respectively. These expressions the potential applied change of hybrid materials in being proficient to support

electrochemical performances and cathode electron transfer mechanism stability over an extended time (Yoshida et al., 2011; Wu et al., 2019; Zheng et al., 2022; Zho et al., 2022).

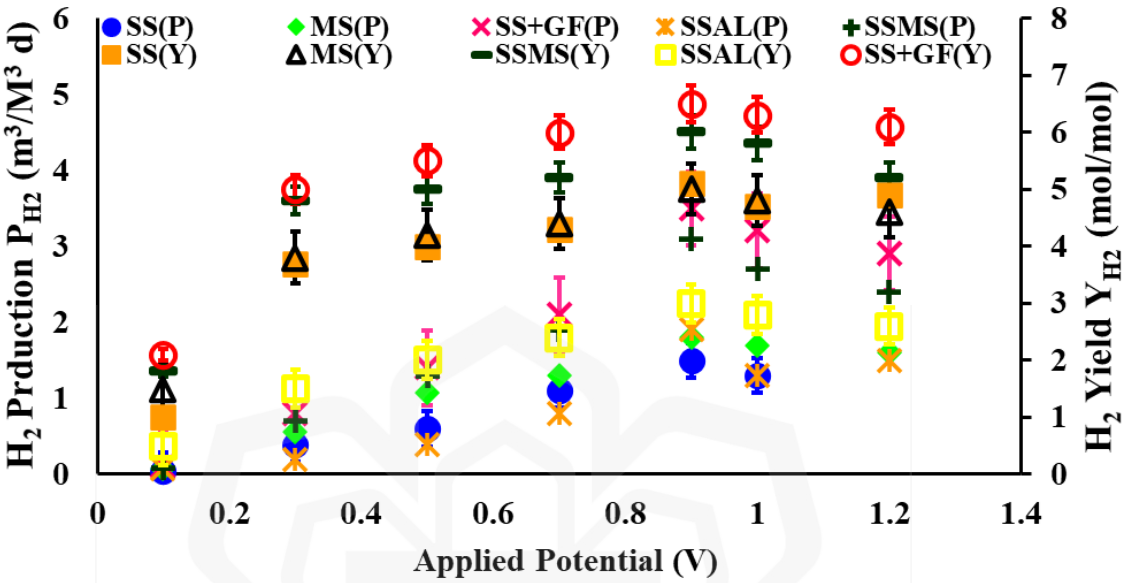

Figure 4.31: Hydrogen production rate (P_{H2}) and hydrogen yield (Y_{H2}). Other factors were fixed the inoculum dose 10ml, basal media of 100mL, H_2-CO_2 of 80-20%, and room temperature 30°C (±2).

In Figure 4.31, the maximum HPR was achieved utilizing a SS+GF catalyst. Utilizing basal medium as the substrate, the applied voltage of 1200mV was increased. The HPR was also fall drop because the EEMs can survive what why HPR and HYR day by day decrease the outperforming SS (1.1 m^3/m^3 day) MS (1.6 m^3/m^3 day), SSAL (1.5 m^3/m^3 day), SSMS (2.4 m^3/m^3 day) and SS+GF (2.9 m^3/m^3 day). The HPR was 3.5 m^3/m^3 day, which was comparable to SSGF and SSMS and almost similar. However, MS, SSAL and SSMS also shows unwarranted electron loss, a contest that remains as the search continues for novel H-MEC anode and cathode catalysts (Srikanth et al., 2011; Zho & Ci, 2019; Jayabalan et al., 2019; Park et al., 2022; Posadas et al., 2022).

4.12.2 Current Density

The current and power density curves of metal-based electrodes such AL, MS, and SS for EMMs basal medium based on different substrate were shown in Figure 4.32. H-MECs with an AL and MS anode have the lowest power and current densities, whereas those with an SS anode have the greatest. In contrast, both of electrode material have unwarranted electron loss because using acid or base based substrate. Direct electron transfer procedures, in addition to being compatible with metal-based electrodes, have a smaller loss than indirect electron transfer through transportable electron exchangers. From Figure 4.32, it was seen that the SSGF anode H-MEC involved with EMMs basal medium produced the highest current and power densities each cell was almost 531.04 mA $m^{-2}$and 477.94 mW m^{-2}, respectively. The H-MECs power densities were gradually increase from 15 to 498.96 mWm^{-2}, when applied voltage were used from 0.1V to 1V. While the current density almost similar up to 900mV after that fall down when applied voltage 1000mV. These significances establish a good combination of anode and cathode terminal between direct electron transfer mechanisms and the potential of SSGF as an anode and cathode in a H-MEC. Even for SSGF of the H-MEC based AD inoculated with *Methanobacterium formicicum* TNFW-2, the produced power densities were much advanced than the SSAL and SSMS based electrodes (Lee et al., 2022), which specifies effective compatibility of metal-based electrodes. Cu has been shown to be a competitive electron acceptor for the co-substrate when used as an anode in H-MECs. When *Geobacter* dominating strain (Wilkins et al., 2009) and *S. oneidensis* MR-1 were employed, optimum power densities of 2 and 69 mW m^{-2} were attained in Cu-anode MECs, accordingly.

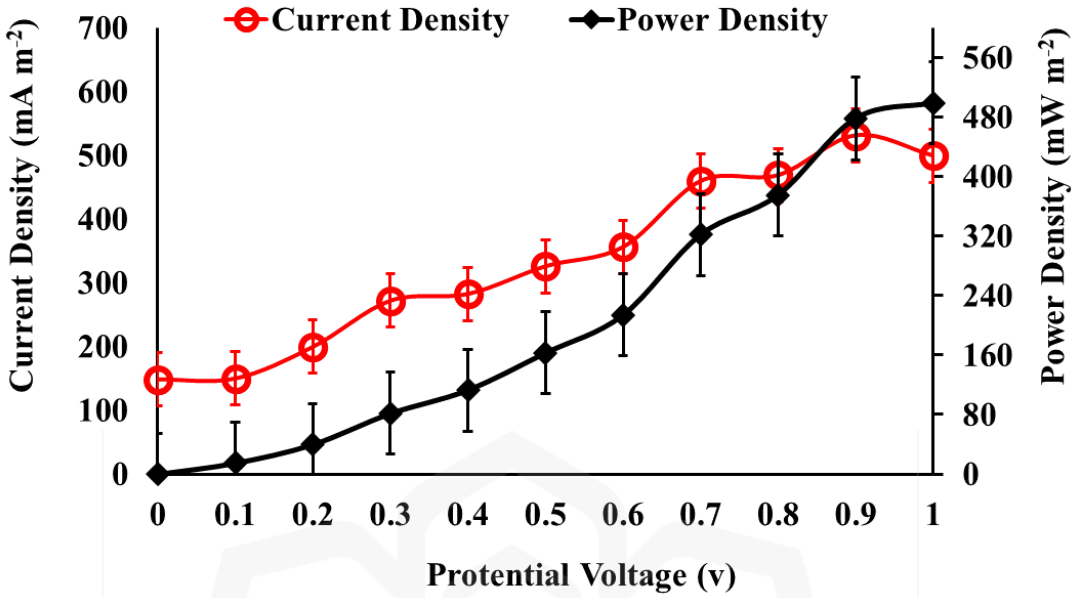

Figure 4.32: Current density influencing the performance of MECs

Toxic ion leakage and corrosion have been blamed for the poor performance (Antunes et al., 2010). Mass transfer circumstances (Tang et al., 2020), nutrient sourcing for biofilm formation (Borole et al., 2009; Zhou et al., 2013; Allam et al., 2021), hydrodynamic stability (Chaudhuri, et al., 2011), and bacteria separation by minimizing tensile force close the anode side (Tang et al., 2020; Zhou et al., 2013) all influence the desired flow speed in MECs.

4.12.3 Cyclic Voltammetry (CV)

Cyclic voltammetry (CV) was used to investigate the electrochemical capacitance characteristics of electrodes in 0.1 M H_2SO_4. Figure 4.33 depicts the typical CV plots of SSGF electrodes at different scan speeds in a visible range ranging from 200 mV to 1200 mV. As when the scan rate goes up, the engagement involving ions and electrode

decreases due to electrode resistance and the CV curve differs from selected value of -15mA to 5mA.

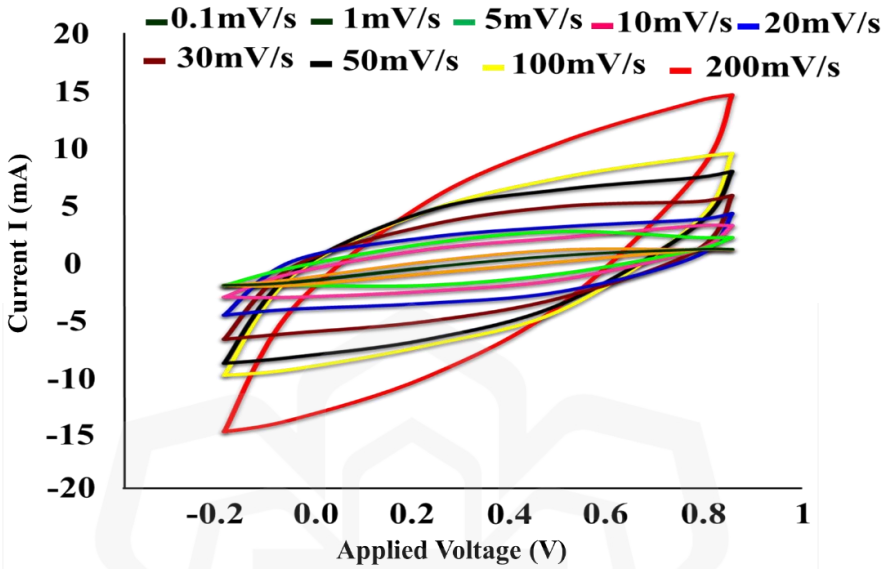

Figure 4.33: The typical CV plots of SSGF electrodes at various scan rates in potential window.

There was no discernible peak at any of the scan speeds, implying that the electrode charges and discharges at a pseudo-constant rate throughout the CV cycle. The area under the CV curve of the SSGF electrode was many orders of magnitude more than that of the electrodes, which might be attributable to increased capacitive performance, charge storage, and catalytic performance sites. The almond shape form of the CV curves implies that the capacitance was due to electrical double layer capacitance and pseudo capacitance. The redox reaction of nitrogen functional groups on SSGF produces pseudo capacitance (Lv & Wang, 2017; Harnisch et al., 2009). Furthermore, a hydrogenophilic do for seems to be for the observed methane generation in that scenario as well, and the rates were similar to those measured in this investigation such as 400 mmol CH_4 Day^1 m^2 at V = -900 mV in as well as the prior work (Cheng et al., 2009). Some experts believe that

bacteria evolved this ability to facilitate intraspecies and interspecies electron transfer (Reguera et al., 2005; Cheng et al., 2009; Boedicker, 2020).

4.13 OPTIMIZATION OF H-MECADs OPERATING PARAMETERS BY OFAT

4.13.1 Substrate Loading by Anode and Cathode Chamber of H-MEC

To make CH_4, electroactive microbe oxidizes the substrate and delivers electrons to the cathode via the anode. The ultimate CH_4 production was determined by selecting the proper substrate. Organic content and substrate loading rate were two main factors that were critical in MECs for significant CH_4 production. Based on *Methanobacterium formicicum* was cultivated in anaerobic conditions at 30°C in a baseline medium (Schauer & Ferry, 1982; Chen et al., 1999) buffered with 0.01% (vol/vol) vitamin solution (Wolin et al., 1963) and potassium phosphate which was used 20mM. The medium was added with 4mM sodium acetate and 1mM sodium sulfide to allow *Methanobacterium formicicum* to thrive. Figure 4.34 shown that the different substrate loading dose such as 50mL, 100mL, 150mL, 200mL and 250mL which was improved hydrogen production and stable microbes to convert CO_2 to CH_4. The graph compares the conversion of CO_2 in different substrate loading between 50mL and 250mL. It can be clearly seen that yield of CH_4 for different substrate loading dose was initially low and that incubation time was increased and the CH_4 yield was also gradually increased. In 100mL, the optimum CH_4 was conversion almost of 92% when incubation time was 24 hours after that sight change of CH_4 conversion when times were increased from 24 to 36 hours which was 3% of develop.

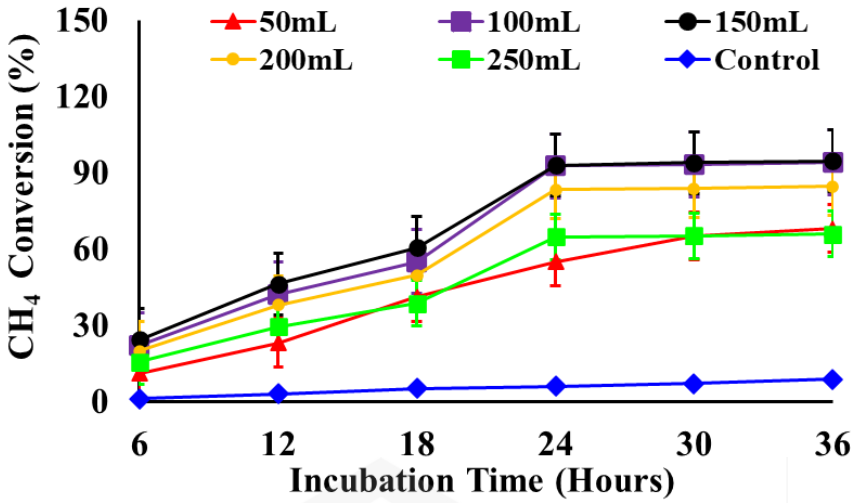

Figure 4.34: Substrate consumption and methane conversion dynamics during the incubation time. Other factors were fixed the inoculum dose of 10mL, Biogas flow rate of 5L/h, applied voltage at 0.9 V and room temperature 30°C (±2).

Other factor was fixed such as pH of 7, inoculum dose of 10mL, H_2-CO_2 of 80-20%, applied voltage at −0.9 V and room temperature 30°C (±2). In 50mL, the incubation times 6 hours to 36 hours were continued to increase of 65% at 30 hours but more steeply to 68% of CH_4 in 36 hours. In contrast, the CH_4 yield was raised gradually 6 hours to 24 hours after that stable 30 to 36 hours which were CH_4 yield of 92% and 93%, respectively. From 200mL to 250mL, the CH_4 yield was very low of 19.8% and 15.8% at times 6 hours while the incubation times of 12 to 36 hours were almost closed. Finally, it was clearly seen that the CH_4 yield then remained stable at 30 hours to 36 hours between 100mL and 150mL which point the figures began to compare to slightly decline and were dropped from 200mL to 250mL.

In all actions, CH_4 making improved until substrates were exhausted. Nevertheless, the CH_3COONa reached the turning point most quickly. Both the average CH_4 yield and substrate consumption rates were highest as show in Figure 4.34. MECs

may use any organic substrate, from basic sugars to challenging fermentable substrates including wastewater and biomass. Acetate was the most often utilized substrate in MECs, with a greater ionic conductivity of 91% (Yang et a., 2015; Kadier et al., 2016; Muddasar et al., 2022). When cultivated on formate-containing medium, *Methanobacterium formicicum* in the cells may create more extracellular polymer (ECP). Hydrogen and formate can be created as metabolites during fermentation and methanogenic breakdown of fatty acids and biofuel during methanogenesis (Crable et al., 2011; Toledo-Alarcón et al., 2018). It was challenging to determine the formate-to-hydrogen ratio generated as an advance. *Methanobacterium formicicum*, on the other hand, may undertake a positive feedback loop, namely the generation of hydrogen from formate and the gene expression of formate from hydrogen plus alkalinity. When H_2-CO_2 was used as the substrate, larger quantities of formate were seen in the medium produced significant hydroxide levels (50 to 80 mM) (Sakai & Yagishita, 2007). As a result, a high-bicarbonate buffered environment, such as that seen in many anaerobic reactors, may have been favorable for the bacteria (Lin et al., 2013).

4.13.2 pH of H-MECAD

CH_4 yields were comparable in samples with and without buffer, demonstrating that the buffers were neither limiting nor stimulating. In the condition of antibiotic, H_2/CO_2 induced moderate enhancement of methanogenesis and significant enhancement of acetogenesis at all pH levels. In the case of antibiotic, there was no discernible pH maximum for methanogenesis from H_2/CO_2, although acetogenesis was highest when buffered at pH 6.2. This might be because higher pH levels have a bigger buffer capacity,

leading for more acetic acid buildup. In the absence of antibiotic, no acetic acid was identified in H_2/CO_2 samples, and methanogenesis was considerably increased, with a clear maximum near pH of 7. Together with input voltage and temperature, pH influences CH_4 production in MECs. Because of the balanced behavior of microbes, the majority of CH_4 MECs function at pH range of 4.5 to 7 as shown in Figure 4.35. From Figure 4.35, it was clearly shown that inoculating strain TNFW-2 into media previously adjusted to various pH values by applying 1 M HCl or 1 M NaOH yielded the best pH for CH_4 yield and methanogenesis. Initially condition, the control pH was converted 8.67% of CH_4 at 36 hours.

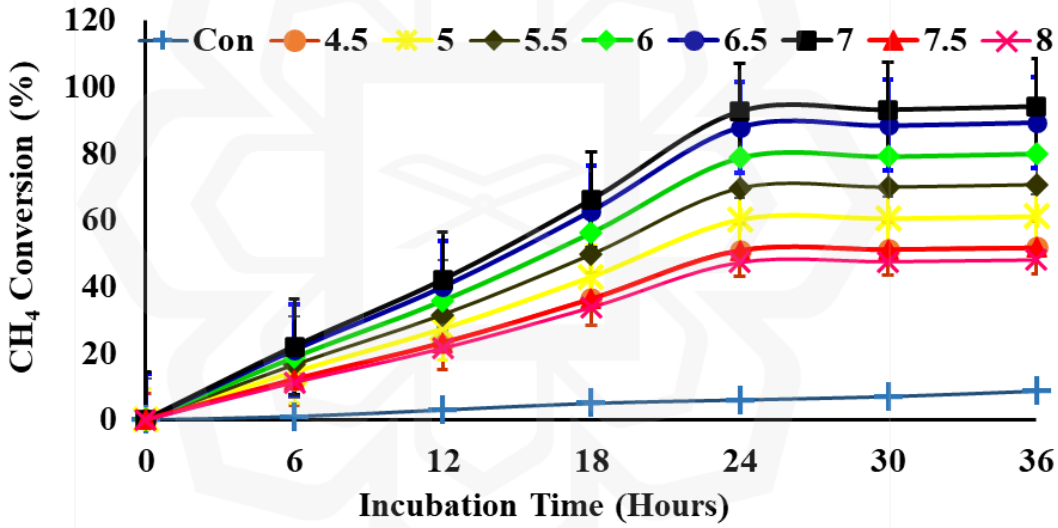

Figure 4.35: The effect of pH and incubation time for methane conversion. Other factors were fixed the substrate dose 100mL, inoculum dose of 10mL, H_2-CO_2 of 80-20%, applied voltage at −0.9 V, gas flow rate of 5L/h and room temperature 30°C (±2).

After that CH_4 output occurred within a limited pH range of 6 to 7, and the optimal pH for CH_4 yield was about 7 whereas other factor was fixed such as substrate dose 100mL, inoculum dose of 10mL, H_2-CO_2 of 80-20%, gas flow rate of 5L/h, applied voltage at 0.9 V and room temperature 30°C (±2). Acidic condition of pH 4.5 to 5.5, the CH_4 yield

was little bit low when pH was increased gradually the yield also increased. The main key of combined with H-MECs, AD explains the acidification apparatus and enables the treatment of substrates with a high influent (Satinover et al., 2020). The yield was below 50% occurred when pH 7 or above 8. The optimum pH for CH_4 yield (pH 7.0) was comparable to those of *Methanobacterium formicicum* (pH 7) (Bryant and Boone, 1987) and *Methanobacterium congolense* (pH 7.2) (Cuzin et al., 2001) and a little changed from those of *Methanobacterium alcaliphilum* (pH 8.1 to 9.1) (Worakit et al., 1986), *Methanobacterium subterraneum* (pH 7.8 to 8.8) (Kotelnikova et al., 1998) and *Methanobacterium espanolae* (pH 5.6 to 6.2) (Patel et al., 1990). This was due to the electromethanogenesis sensitivity to its surroundings; even little variations in pH would elicit modifications in bacterial metabolic (Wu et al., 2021). Many additional parameters, such as ion transport, substrate oxidation, and liquid permeability, were also linked to changes in pH, either directly or indirectly.

4.13.3 Applied Potential

One of the required physical criteria for the functioning of MECs to generate CH_4 was the electric potential or additional voltage. Changes in electric potential have a considerable influence on the growth and dispersion of electroactive microbes, as well as CH_4 formation as shown in Figure 4.36. It was critical to remember that excessive amounts of supplied electron density may be harmful to the bacterium. This study suggested the necessity to examine utilized potentials to maximize bacterial growth and promotes the activation. Gram-positive microorganisms were discovered to be the most often employed electroactive microbes in MECs paired with anaerobic digesting processes in several

studies. The tests were carried out under cathodic circumstances, with the modified electrode opportunities ranging from 100 to 1300 mV, in order to measure the outcomes of the electrical and chemical conversions catalyzed by the methanogenic microorganisms via direct electron transfer. Figure 4.36 depicts the findings of experiments performed at 900 mV with the bacterial culture. In the control (Figure 4.36), H_2 production was low, and there was no BioM generation. The absence of electrical and chemical hydrogen generation was most likely caused by the reaction's large oxidation potential at the carbon electrode. Methane gas was generated practically linearly in the presence of microbes at a rate of 91.65 % at 36 hours whereas other factors were fixed the substrate dose 100mL, inoculum dose of 10mL, H_2-CO_2 of 80-20%, pH of 7 and room temperature 30°C (±2). The hydrogen output was also relatively modest in this situation.

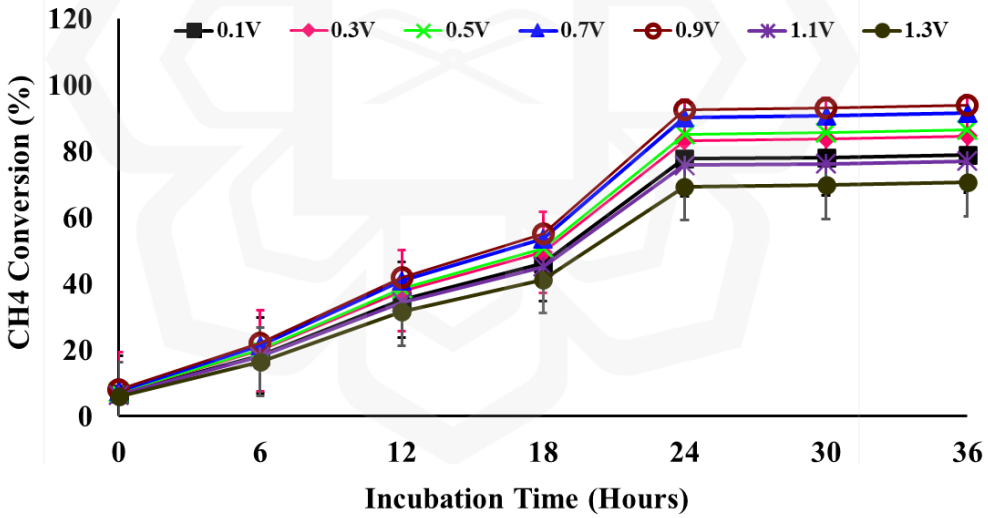

Figure 4.36: The voltage effect for CH_4 production using MEC. other factors were fixed the substrate dose 100mL, inoculum dose of 10mL, H_2-CO_2 of 80-20%, pH of 7 gas flow rate of 5 L/h and room temperature 30°C (±2).

The deflection of the determined cathodic current during in the microbiological test was likewise shown in Figure 4.36. Following a sharp increased, it remained

relatively stable at levels between 0.5 and 0.9V for the duration of 24 hours to 36 hours. The overall positive potential exchanged during the test was extremely similar to the overall electrons captured as CH_4 plus H_2, and as a result, the system's cumulative charge density efficiency (total electron regeneration) was high around of 90%, owing mostly to methane production 91.63%. As indicated in Figure 4.36, the redox reactions impact of the methanogenic microbes was evident at negative electrode potentials greater than 900 mV. Indeed, the total rate of reduced end-product formation was extremely similar to that seen in control experiments in the presence of bacteria in the range from 700 to 900 mV; however, beginning with higher negative electrode potentials than 900 mV, it was continuously greater. than in the range from 1000 to 1300mV. The CH_4 generation rate in the organisms testing was similar to that recorded in the organic and inorganic experiments when the electrode was polarized from 500 to 700 mV; however, at significantly negative voltage, the detected rate of CH_4 yield was much lower than in the biogenic studies. This was most likely owing to the quick direct conversion of generated CO_2 into CH_4 stimulated by the methanogenic culture, as evidenced by the trend of the CH_4 production rate. In abiotic experiments, no methane was produced, but in biotic studies, the rate of CH_4 synthesis improved as the electrode potential upgraded, reaching 90% at 900 mV after 24 hours.

To assess such a MEC, the influence of voltage level at the negative electrode potential improvements of -0.8 V and electrode permittivity at power supply of 0.9 V on the hydrogen yield was simulated with similar starting conditions and supplied intensity, and the consequences were depicted in Figure 4.37.

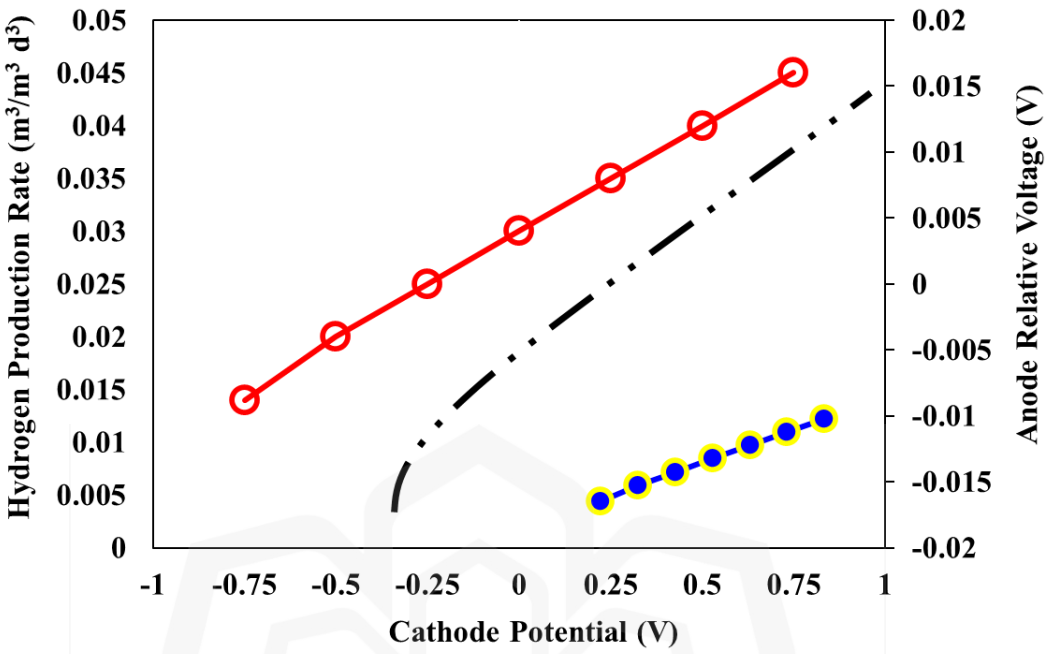

Figure 4.37: The influence of cathode potential on hydrogen generation rate and anode comparative voltage variance vs cathode potential in the H-MEC.

According to the data in this Figure, a higher hydrogen yield was measured directly at the higher electric potential and cathode surface potential, which was funded by scientific work (Hu et al., 2009); however, by influencing the implementation of an external electrical field of 0.9 V and strenuously posing the cathode surface potential, the hydrogen production rate was achieved significantly. The fundamental cause for this was the change in anode surface potential, which has a direct impact on the colony state and microbial population. The anode zone voltage was approximated at various cathode area potentials after 36 hours when the system achieved a stable state. As seen in Figure 4.37, higher cathode potentials resulted in more positive anode potentials, indicating more energy gain from increased electrogenic activity (Modestra et al., 2020). Finally, more current was available to generate H_2. Similarly, as shown in Figure 4.37 the conductive microbes at the poised

cathode potential of 900 mV contains more electrogene and less methanogens than the paused cathode potential of 0.2 V. Furthermore, under the identical beginning circumstances, the impact of cathode surface potential on the liquid bulk was so little in this simulation that after 24 hours, the ratio of CO_2/H_2 methanogens at 0.2 per 0.9 V cathode potential was 1.005 and 1 for fermentative microorganisms (Rader, 2010; Selembo et al., 2010; Perez, 2021).

4.13.4 Optimization of the H-MECADs by FCCCD under RSM

The four process parameters such as substrate loading, pH, applied potential and current density of CH_4 yield were optimized, their optimum points were maintained the rest of the experiments. Three contributing process parameters like substrate loading, pH and applied potential were selected for further optimization process to determine their optimum level for enhanced CO_2 conversion to CH_4 production. Response surface methodology (RSM) by FCCCD was employed for detecting optimum levels of the conversion process parameters. These factors were analyzed in three levels: high (+1), medium (0) and low (-1). Twenty experimental runs with six center points (0) were generated as shown in Table 4.14. The regression equation obtained from the experimental analysis and the equation was used to predict about the response for given levels of each factor. The quadratic polynomial equation provided the optimum levels of the parameters and BioM production upgrade. The model provided in terms of coded factors as given in Equation 4.3.

$$CO_2 \text{ Conversion } (Y) = 91.92 + 7.58A - 11.58B - 2.43C - 5.93AB \quad (4.3)$$
$$+1.49AC - 1.11BC - 7.31A^2 - 17.19B^2 - 3.10C^2$$

The model in respect of coded components can be utilized to predict response for different amounts per each element.

Table 4.13 Experimental design by FCCCD method for CH_4 Conversion

Run	Factor 1 A: Substrate Loading (mL)	Factor 2 B: pH	Factor 3 C: Applied Potential (mV)	Response 1 CH_4 Conversion (%)	
				Experimental	Predicted
1	100	6.5	900	86.05	86.30
2	100	7	1100	85.96	86.39
3	150	6.5	1100	89.25	89.57
4	**100**	**7**	**900**	**92**	**92.32**
5	50	6.5	1100	60	59.57
6	150	7.5	700	56.03	56.43
7	50	7.5	1100	46.01	46.07
8	150	6.5	700	89.02	89.24
9	**150**	**7**	**900**	**92.35**	**92.59**
10	50	7	900	76.25	77.02
11	**100**	**7**	**900**	**92.26**	**92.32**
12	100	7.5	900	62.89	63.15
13	50	7.5	700	56.05	56.11
14	**100**	**7**	**900**	**91.99**	**92.12**
15	100	7	900	91.98	91.99
16	**100**	**7**	**900**	**92.03**	**92.25**
17	**100**	**7**	**900**	**92.31**	**92.37**
18	100	7	700	91.56	91.98
19	50	6.5	700	65.04	65.18
20	150	7.5	1100	52.01	52.34

Bold indicates center points

The highest concentrations of the components were recorded as +1 by convention, while the low concentrations were coded as -1. By contrasting the component coefficients, the coded formula may be used to determine the comparative importance of the elements.

Table 4.15 shows how the interpretation of variance was utilized to assess the conformance of the statistical design model. The designer's F-value of 2086.43 indicates that it was significant. An F-value this big might arise owing to noise just 0.01% of the time. Model terms with P-values less than 0.0500 were significant. A, B, C, AB, AC, BC, A^2, B^2, C^2 were crucial customized version in this scenario. Values larger than 0.1000 imply that the regression coefficients were not significant. Model minimization helps enhance overall model if there were numerous inconsequential modulation scheme (except those necessary to enable hierarchical). The Lack of Fit F-value of 2.79 indicates that there was a 14.26% possibility that a big Lack of Fit F-value might develop owing to noise. A lack of fit was undesirable; researchers would like the model to fit. This minimal chance (just 10%) was concerning.

The high value of R^2 (0.9995) demonstrated that the model was significant and adjusted R^2 (0.9990) was very close to the predicted R^2 value of 0.9959 which indicating better similarity between responses from experimental and predicted value. The sufficient precision of 122.932 was larger than 4, indicating that the relative terms may be utilized to navigate the design parameters. The coefficient of variation (CV%) throughout this design was a low value of 0.68, indicating that the experimentation was more precise and adequate. Table 4.13 shows the predicted value of the linear regression.

The interactions among the parameters were illustrated by using response surface curves generated from the optimization of BioM production process. Two-dimensional (2-D) contour plots and three-dimensional (3-D) response surface plots graphically demonstrate the relationships between both the response and experimental conditions of

each parameter. A 3D curve was a simple technique to clarify depiction of component relationship in order to discover the optimal points of researched parameters (Tanyildizi et al., 2005; Bari et al., 2010).

Table 4.14: ANOVA for Quadratic model of CH_4 conversion by FCCCD

Source	Sum of Squares	df	Mean Square	F-value	p-value	
Model	5285.98	9	587.33	2086.43	< 0.0001	**significant**
A-Substrate Loading	574.72	1	574.72	2041.61	< 0.0001	
B-pH	1340.27	1	1340.27	4761.16	< 0.0001	
C-Applied Protential	58.90	1	58.90	209.25	< 0.0001	
AB	281.44	1	281.44	999.78	< 0.0001	
AC	17.67	1	17.67	62.78	< 0.0001	
BC	9.79	1	9.79	34.78	0.0002	
A^2	147.00	1	147.00	522.22	< 0.0001	
B^2	812.74	1	812.74	2887.18	< 0.0001	
C^2	26.45	1	26.45	93.96	< 0.0001	
Residual	2.82	10	0.2815			
Lack of Fit	2.07	5	0.4143	2.79	0.1426	**not significant**
Pure Error	0.7435	5	0.1487			
Cor Total	5288.80	19				

R^2 = 0.9995, Adjusted R^2 = 0.9990, CV% = 0.68, Adequate precision = 122.93; *p<0.05 indicates the model terms were significant, **p<0.0001 indicates highly significant.

The interaction between substrate loading and pH on CO_2 conversion by second order quadratic equation for optimum BioM production was exposed in Figure 4.38 (a). The contour plot as demonstrated in Figure 4.38 (b) that CO_2 to BioM was affected by biogas substrate loading and less effect on pH. The highest CO_2 to BioM of 92% was achieved when substrate dose 100mL, pH 7 and applied potential -900mV were in the center point

and other parameters were fixed such as inoculum dose of 10mL, bio gas flow rate 5L/hour incubation time 36 hours and room temperature 30°C (±2).

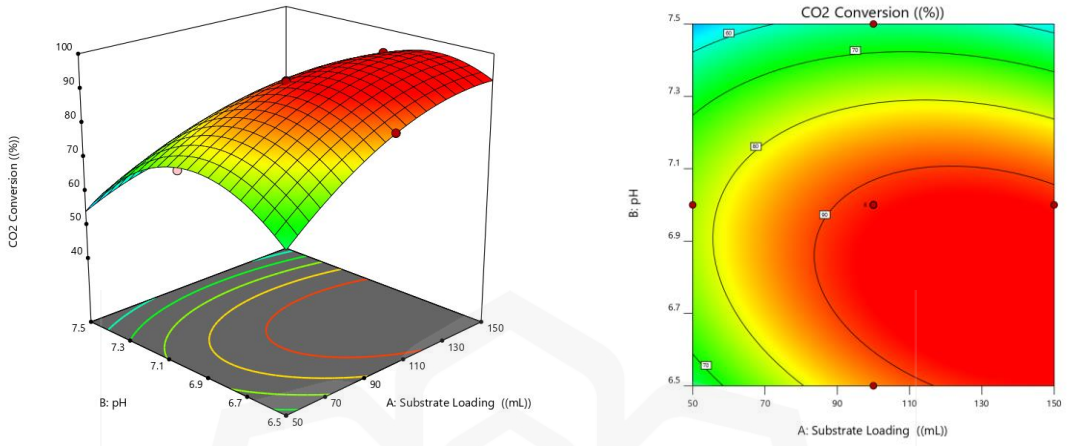

(a) (b)

Figure 4.38: Response surface curves showing the interaction effect of substrate loading and pH on CO_2 to BioM conversion (%). (a) 3D response surface plot (b) 2D contour plot.

Result showed that the less incubation time could be used for high BioM production to reduce CO_2; this was a good similarity with the findings of Al-Juboori et al., (2020) which reported that BioM production was upgraded while biogas flow rate increased from 1 to 4L/hour.

The effect of substrate loading and applied potential on CO_2 to BioM conversion showed that increased applied potential was decreased to BioM production at fixed level of biogas flow rate at 5l/hour as shown in Figure 4.39. However, the effects exhibited maximum BioM production at the center point level and response surface plot indicates that the applied potential was negative to CH_4 production.

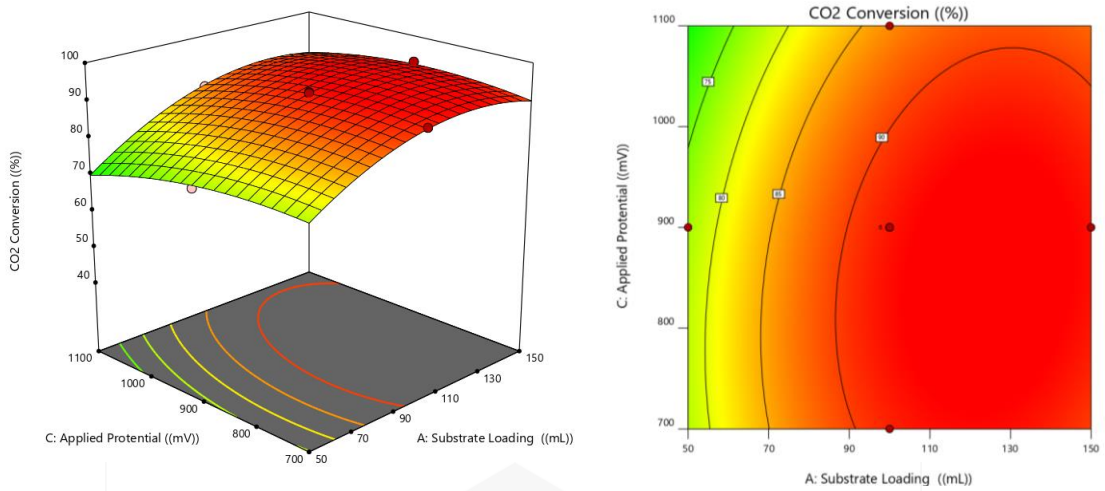

(a) (b)

Figure 4.39: Response surface plots showing the interaction between the substrate loading and applied potential on BioM production rate. (a) 3-D response surface plot (b) 2-D contour plot.

Figure 4.40 (a) and (b) exhibited the relationship between pH and CO_2 to CH_4 conversion while applied potential was located in the center. pH displayed linear outcome on the response, whereas CO_2 to BioM production exhibited asymmetrical effect on the response. pH was a significant factor because a successful BioM production as well as process cost depends on it. Marshall et al., (2012) informed that the highest CH_4 production rate of 64% was attained at pH 7 by CO_2 then production rate remained constant until 36 hours. In the study, results showed that the incubation time had a less effect for BioM production in the different dose of substrate. So, it was clear from the result that, less conversion time could be used in wide range of biogas to BioM the organic biogas and pure CO_2/H_2 ratio for the EMMs application. Zhu et al., (2004) studied the preliminary incubation time to remove CO_2 in the treatment of AD system. Result found that the incubation time had an effect for CO_2 conversion for the 36 hours then CH_4 production rate remain unchanged.

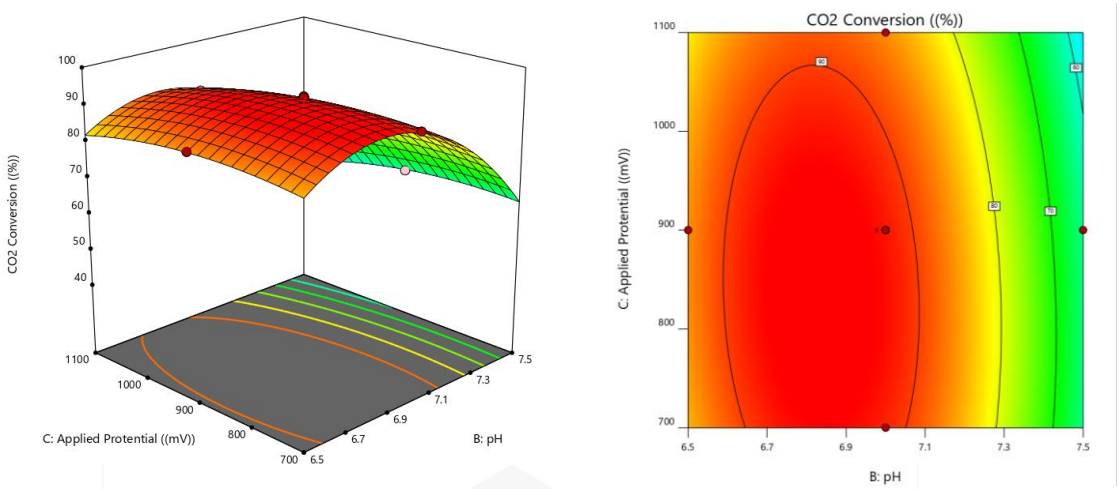

(a) (b)

Figure 4.40: Response surface plots showing the effect of pH and BioM production on the response at fixed level of applied potential. (a) 3-D response plot (b) 2-D contour plot.

In generally, applied voltage, inoculum dose and pH were chosen factors for BioM process optimization conveyed by some authors (Kadier et al., 2016; Kadier et al., 2022; Pawar et al., 2022). In the present study, the substrate concentration was chosen instead of pH factor in the optimization process. The EMMs showed above 92% CO2 convert to BioM production with a wide pH range from 4.5 to 8 have carried out in previously (see section 4.11.2). Pawer et al., (2022) reported that, pH 7, EMMS dose of 10 mL/L and applied voltage of 900mV were optimized by the RSM while production rate of 63.9% was achieved. Although, much report in the literature were not available regarding the statistical optimization of BioM production process by using EMMs dose, applied voltage and pH as process parameter.

4.13.5 Validation of the Quadratic Model

The following sets of experiment were validated as generated by the point prediction with the target of maximizing BioM production percentage as shown in Table 4.16. The good

agreement between predicted and experimental values was exhibited in the validation experiment. Standard error and less than 10% error verified the model, suggesting significant agreement between experimental and anticipated values.

Table 4.15: Validation of the quadratic model and optimized CH_4 production process for CO_2 reduction.

Substrate Loading (mL)	CO_2/H_2 flow ratio	Applied potential (mV)	CO_2 to CH_4 Conversion		Error (%)
			Experimental (%)	Predicted (%)	
100	50:50	900	92.09	92.85	0.76%
100	60:40	900	91.01	92.76	1.75%
100	70:30	900	90.07	90.89	0.82%
100	80:20	900	88.76	89.15	0.39%
100	90:10	900	81.02	82.23	1.21%

Therefore, from the validation experiments, the optimum process conditions such as 10mL of EMMs dose, pH of 7, 100mL of substrate loading, temperature of 30°C, flow rate 5L/hour, incubation time 36 hours and applied voltage of 900mV were used to convert CO_2 to CH_4, where the ratio of CO_2/H_2 such as 50:50, 60:40 and 70:30 was reduced to CO_2 almost 92%, 91% and 90% respectively. Based on the findings, the system of H-MECAD with the strain TNFW-2 was converted 92% of CO_2 and the ratio error was less than 2%.

4.14 STUDIES OF THE KINETIC PARAMETERS FOR H-MECAD

During kinetic study, the interaction of H_2 Yield, CO_2 consumption and CH_4 production were observed from basal medium based the H-MEC system. EMMs was determined as a yield of H_2 indicator of *Methanobacterium* growth as it was an important and steady component in mycelial cell walls. The H_2 content appears to be a suitable factor in the

approximation of the total sum of the BioM production and its modifications may parallel to the development of the H_2 growth. While, the CH_4 production was increased and increased EMMs growth, but decreased the CO_2 and H_2 (Shah, 2021; Rani et al., 2022). Figure 4.41 shows the result of the growth kinetic of BioM production using H-MEC system. It was obtainable that the consumption by the CO_2 flow rate and the yield of H_2 was sharply fall drop with the gradually increased of bioM together with the EMMs growth, in term of BioM, until the production reaches its highest level and after that all the three parameters progress slowly. The CO_2 and H_2 content in the conversion broth compact to 5 L/hour and 1692 mL from the initial value of 5 L/hour of CO_2 from AD based food waste and 1800mL of H_2 which was yield 10mL of EMMs with applied voltage 900mV after 36 hours of incubation time and the BioM production level was at 2820mL when the BioM production attained at the highest level. Through the progress of conversion, the CO_2 and H_2 content becomes less and the value were 1 L/hour and 102 mL after 36 hours of conversion.

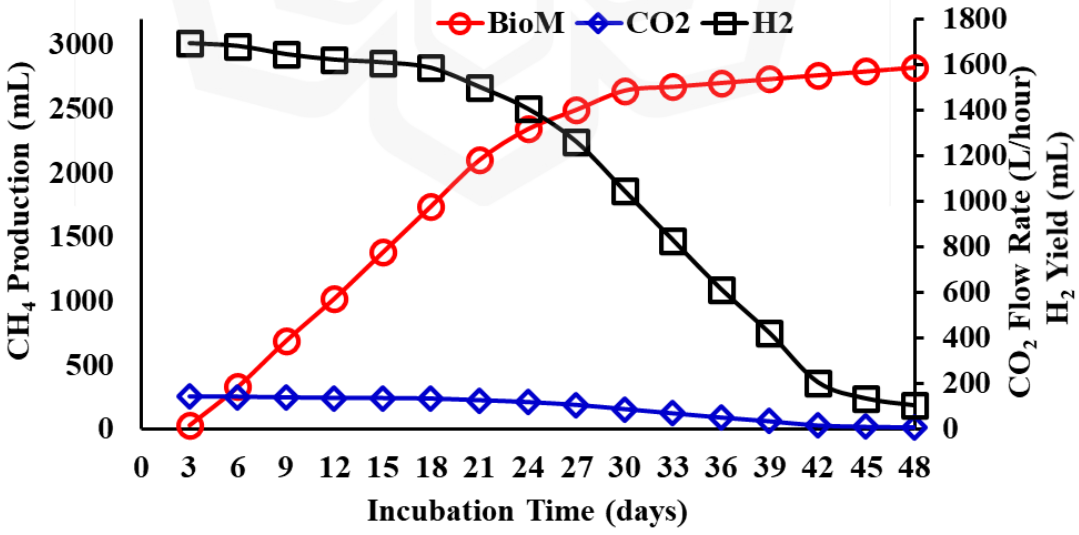

Figure 4.41: BioM production, H_2 yield and CO_2 consumption.

The H_2 growth was improved from 36 hours of 1692 mL and after that it suddenly decayed to 102 mL after 36 hours of conversion. The relationship of the C-source consumption, H_2 yield and the BioM production that was obtained during the production of BioM by *Methanobacterium formicicum* through gas phase of AD based food waste was found in agreement with the classical kinetic model of this type.

For the exponential growth phase, the particular growth rate may be computed using the Monod Equation 4.4 and Equation 4.5.

$$\text{In } X = \text{In}X_0 + \mu t \quad (4.4)$$

Assumption, $X_0 = 0$

$$\mu = \frac{InX}{t} \quad (4.5)$$

where, X was H_2 yield, Xo was initial of H_2 and t was time. The above Equation (4.5) was presented as a straight line, where the slop μ represents the specific growth rate which was change of H_2 per unit time. The exponential growth was obviously found to be linear when logarithm of the H_2 was plotted against time, which follows the Monod equation (Figure 4.42).

It was observed from the Figure 4.39 that the exponential growth occurred until 36 hours of conversion and the overall specific growth rate (μ) was estimated to be 7.43 h^{-1}. Many researchers (Amin et al., 23021) have reported on optimum BioM production a low specific growth rate (4.5 day^{-1}) using *Methanobacterium formicicum* and Wang and Liu, (2014) found the optimum bioethanol production at the lower specific growth rate (5.4 ± 0.030 day^{-1}) using Escherichia coli FBWHR in the hot-water sugar maple wood extract

hydrolysate based medium. The specific rate at substance synthesize can be calculated by using the Equation (4.5).

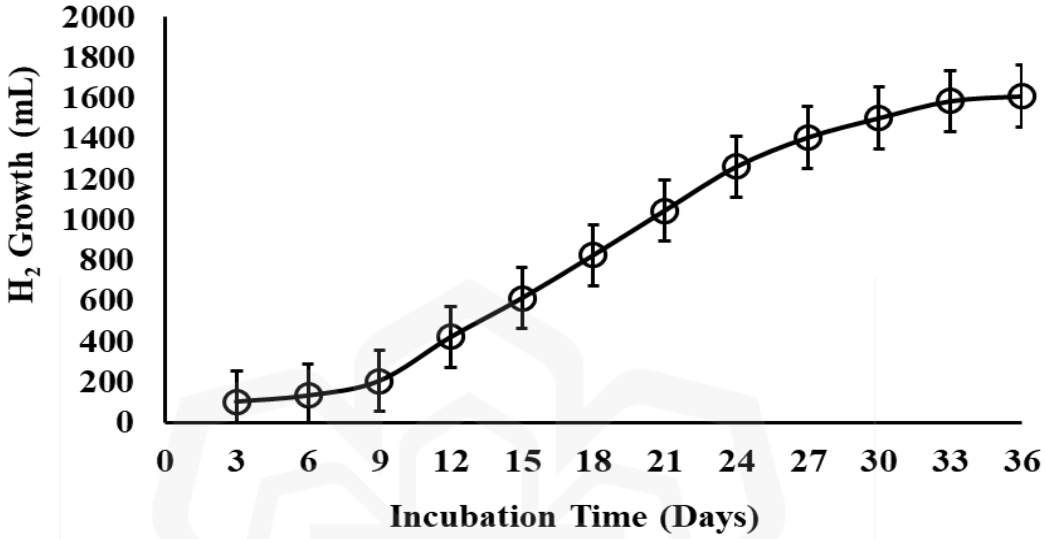

Figure 4.42: Specific rate of H_2 growth

Yp/x was the true yield of product from biomass and mp was the specific rate of product formation due to maintenance. The first term was growth associated and the second term was non-growth associated which can be neglected in this study where product formation did not occur due to maintenance. Finally, qp was the product of the theoretical yield of product from H_2 Yp/x (1.102 g g^{-1}) and a specific rate of growth μ (0.207 h^{-1}). The maximum specific rate of product formation was estimated to be about 0.239 h^{-1}. Whereas, the yield of bioethanol production based on total CO_2 consumption Yp/s (17.69 g g^{-1}), the yield of H_2 formation based on CO_2 consumption Yx/s (-10.81 g g-1), from the experimental results. Table 4.17 summarized the kinetic parameters for each linearized model (Appendix I). Model with highest coefficient of determination (R^2) were regarded as the best fit for the EMMs.

Table 4.16: Kinetic parameters for BioM production

Parameters	Units	Value	R^2
μ	h^{-1}	0.207	0.8596
$Y_{p/x}$	g g^{-1}	1.102	0.6275
$Y_{p/s}$	g g^{-1}	17.69	0.9848
$Y_{x/s}$	g g^{-1}	-10.81	0.7123

Modeling approach was a critical activity that involves adapting the simulation process to practical data acquired in specific investigations (Fdez-Guelfo et al., 2011). The correlations between CH_4 conversion and biological materials of chemically synthesized waste were first calculated using Curve Expert in this work, and the connecting curves were presented in Figure 4.41. The polynomial Regression Equation was then used to investigate the reaction mechanism of ch4 curves and the prediction of final yields (Table 4.17). The correlation coefficient (R^2) was observed to be 0.6275-0.9848.

4.14.1 Comparison between EMMs and CO_2/H_2 contains

Many of gas phase were commonly applied in the CH_4 production system for high conversion efficiency and economic feasibility in which CO_2/H_2, N_2/CO_2, N_2O/CO_2, NH_4^+/O_2 and N_2O/NH_4^+ (Sadeghi et al., 2016; Vasiliadou et al., 2022; Santos et al., 2022; Zhang et al., 2022). In the experiment, low, medium and high design level was chosen to compare the EMMs and conversion in the CH_4 production. The EMMs dosages were 5mL, 10mL, and 15mL as low, medium and high in the optimization of CH_4 production. These doses had a corresponding equivalent biogas flow rate of 50/50, 60/40 70/30, respectively.

The basal medium was used and its efficiency was compared with equivalent dose of EMMs.

The novel EMMs was applied to conversion the CO_2 in a lab scale H-MEC based AD as shown in Table 4.18; such study was not reported in literature yet. Results showed that 92% CO_2 removal was achieved at 10mL/100mL concentration of EMMs. At the same condition the organic CO_2 removal by AD based biogas was 90% which was less than that of 1.75% of gas phase (CO_2:H_2).

Table 4.17: Comparison between biogas, CO_2/H_2 ratio and EMMs on CH_4 production

Experiment No.	Gas flow rate (L/hour)	EMM Dose	BioM %	
		mg/L	H_2/CO_2	Biogas
1	5	10	92	90.85
2	5	10	92	92.08
3	5	10	92	91.24

This finding was good agreement with the findings of Gong et al., (2008) in which showed the CH4 production rate of EMMs TNFW-2 produced by *M. formicicum* showed high CO_2 of 92% direct conversion system and CO_2 removal of 92% organic compared to gas phase CO_2 and organic CO_2 which showed 91.85% & 92.08% and 92% & 92%, respectively and TNEW-2 showed slightly better CO_2 removal efficiency than the gas phase in the AD based food waste (Shahsavar et al., 2022).

4.14.2 Major Contributions and Comparison with Other Works

Microbial Electrochemical Cells (MECs) were a promising technology for energy conversion, utilizing electroactive microbes to generate electricity or produce valuable

chemicals. Various types of MECs have been studied, each employing different electroactive microbes, cathode materials, electrolytes, applied voltages, and exhibiting different levels of biomass conversion efficiency as shown in Table 4.18. For instance, a double chamber MFC (Microbial Fuel Cell) utilizing *Shewanella oneidensis sp.* as the electroactive microbes, carbon cloth as the cathode material, and sodium chloride solution as the electrolyte, achieved a biomass conversion efficiency of 75% at an applied voltage of 140mV (Xio et al., 2020).

Table 4.18: Major Contributions and Comparison with Other Works

Type of MEC	**Electroactive Microbes**	**Cathode Selection**	**Electrolyte Selection**	**Applied Voltage**	**BioM Conversion**	**Reference**
Double chamber MFCs	*Shewanella oneidensis sp*	Carbon cloth	Sodium chloride solution	140mV	75%	Xio et al., (2020)
Single Chamber MEC	*Methanosarcina sp*	Stainless steel	BFS01 medium	600mV	85%	Kadier et al.,(2022)
Single-chamber MEC	*Geobacter sp*	Graphite	Glucose Solution	600mV	63.9%	Yin et al., (2016)
Two Chamber MEC without Membrane	*Methanobrevibacter sp*.	Carbon stick	Sodium chloride solution	700mV	82%	Pawar et al., (2022)
Two Chamber MEC with Membrane	*Methanobacterium formicicum*	Stainless steel with graphite	Basal media with Yest Extract	900mV	92%	Proposed model

On the other hand, a single chamber MEC using *Methanosarcina sp*. as the electroactive microbes, stainless steel as the cathode material, and BFS01 medium as the electrolyte, demonstrated a higher biomass conversion efficiency of 85% at an applied

voltage of 600mV (Kadier et al., 2022). Another single-chamber MEC employed *Geobacter sp.* as the electroactive microbes, graphite as the cathode material, and glucose solution as the electrolyte, achieving a biomass conversion efficiency of 63.9% at an applied voltage of 600mV (Yin et al., 2016). In the case Proposed model of a two-chamber MEC with a membrane, *Methanobacterium formicicum* was used as the electroactive microbes, stainless steel with graphite as the cathode material, and a basal media with yeast extract as the electrolyte. This MEC exhibited an impressive biomass conversion efficiency of 92% at an applied voltage of 900mV. Lastly, a two-chamber MEC without a membrane utilized *Methanobrevibacter sp.* as the electroactive microbes, carbon stick as the cathode material, and sodium chloride solution as the electrolyte. It achieved a biomass conversion efficiency of 82% at an applied voltage of 700mV (Pawar et al., 2022). Overall, these studies highlight the diversity in MEC configurations and their corresponding performances, providing valuable insights for the development and optimization of microbial-based energy conversion systems.

4.15 SUMMARY OF FINDINGS OF THE FOURTH OBJECTIVE

The CH_4 production capacity in a lab scale H-MEC, anode and cathode potential analysis, optimization of conversion operating parameters by lab scale H-MEC, electron transfer mechanism, current density and CV analysis were studied in the fourth objective of this research. The H-MEC performance was investigated to reduce CO_2 from AD based food waste and calculated result were by incubation time and CO_2: H2 ratio 50:50 and 36 hours, respectively to 90% of CO_2 conversion and incubation time and CO_2/H_2 flow rate of 70:30 and 36 hours for 90% CO_2 conversion to CH_4 production, respectively by using strain

TNFW-2 *M. formicicum*. The result obtained from optimization of operating parameters indicated that the interaction and model were found to be significant $R^2 = 0.99$ and adjusted $R^2 = 0.99$ there were a good agreement between the experimental and predicted values by the model. The optimum conditions of H-MEC of food waste-based biogas upgrade by the EMMs were obtained at applied voltage 900mV, pH 7 and EMMs dose 10mL/100mL. At this optimum, the CH_4 production in terms of CO_2 removal of 92% was achieved. In the validation experiment, the biogas and EMMs were compared to CH_4 production of organic CO_2 by the H-MEC. The EMMs convert CO_2 were investigated to determine BioM and results showed that convert BioM was 92% compared to direct gas phase CO_2/H_2. Finally, the EMMs can be considered in suitable for CO_2 convert to CH_4 world. Through H-MEC based AD system, different factors such as pH, EMMs dose, incubation time, gas flow rate, applied voltage and substrate loading were found to have significant contribution toward BioM produced in Basel medium. However, the typical OFAT studies shown that incubation time, EMMs dose and organic CO_2/H_2 content were connected with high BioM produced. It was found from the kinetic study of the production of the BioM with the developed process condition that the production in this system was growth associated and the specific growth rate (μ) was estimated to be -0.207 h^{-1}, the maximum specific rate of product formation was estimated to be about 0.239 h^{-1}.

CHAPTER FIVE

CONCLUSIONS AND RECOMMENDATION

5.1 CONCLUSIONS

Biogas upgrading was the process of the converting CO_2 to methane by using EMMs. The determined biogas adjacent to 100% methane was called BioM. Biomethane (BioM) was a sustainable fuel that was formerly created by the decomposition of organic matter of bio-waste. Furthermore, the procedure requires many days to accomplish. The appearance of anaerobic microorganisms in the MES bacterial community facilitated the collection of CH_4 from the cathode chamber of MECs via CO_2 electromethanogenesis. Hybrid microbial electrochemical systems (H-MES) were an effective technique to generate energy in a stable and ecologically friendly approach. Simply said, H-MES generates electrical energy by converting chemical energy derived from food waste cellulosic materials and wastewater via the catalytic reaction utilizing a biological electrocatalyst. H-MES technology was a multidisciplinary discipline that combines electrochemical processes, nanotechnology, microorganisms, and analytical chemistry. Generally, EMMs have been employed in the convert of CH_4 from AD based organic CO_2. However, the EMMs were not so environmentally friendly and also harmful to the human being. One of the challenges of biogas upgrade was to reduce time in the H-MEC after conversion process. Therefore, this study was conducted to convert CH_4 from organic CO_2 by new EMMs which can be good replacement of bioelectrochemically (BEC) based AD system. The study on CH_4 upgrade by locally isolated EMMs consisted of ten parts, namely:

a) Isolation, purification and screening of fungi, aspergilla from bio compost and animal feed to degrade food waste and high biogas production.
b) Evaluation of setup potentiality by fungi and aspergilla using shake flask fermentation to degrade and high biogas production.
c) Again isolation, purification and screening of EMMs from food waste and anaerobic sludge to convert CO_2 to BioM production.
d) Screening of potential strains by EMMs supernatant and biomass to reduce CO_2 by Duran bottle.
e) Screening and optimization of nutrient and growth conditions of production for the EMMs strains in terms of CH_4 production activity.
f) Characterization of selected/potential strain by identification, chemical analysis, EMMs stability and EMMs performance.
g) Optimization of conversion process conditions by statistical experimental design for the potential EMMs.
h) Investigation of H-MEC characteristics of the EMMs by using a lab scale for biogas upgrading.
i) Optimization of H-MEC operating parameters in a lab scale to reduce organic CO_2 by the EMMs.
j) Kinetic study of H-MECAD can be done to evaluate the process conditions.

On this basis, the following conclusions were drawn:

1. Locally isolate six fungi strains such as TN-AF1 to TN-AF3 and TN-BC1 to TN-BC3 from bio compost and animal food was obtained. This was done with the aim to achieve better degrading capability by the microbes to increased biogas in the

food waste. High activity enzymes were improved 7.25-fold RS on enzymatic hydrolysis. Among the six strains, the supernatants of TN-AF1 and TN-BC1 were improved 7.25-fold reducing sugar on enzymatic hydrolysis and the 59.45 g/L of VS whereas TS (12.59 %), enzyme dose (79.47U/mL) and pH (5.19) and 116 g/L of reducing whereas TS (12.5%) and enzyme dose (80U/mL).

2. Enzymatic hydrolysis and anaerobic digestion (AD) were used for biogas fermentation without supplements. The optimal biogas production was achieved using specific parameters: 25% biogas inoculum, pH 7, 29 days of AD digestion, 500mL of hydrolyzed food waste, and a room temperature of 30°C (±2). The food waste hydrolysis process resulted in a promising 54.7% reduction in volatile solids within just 5 days of digestion at day 25. The biogas composition from the AD system was found to be approximately 3% hydrogen, 57% methane, and 40% carbon dioxide.
3. This study focused on isolating and characterizing two EMMs strains (TNFW-2 and NTAS-2) from anaerobic digestion (AD) using food waste and anaerobic sludge. TNFW-2, identified as *Methanobacterium formicicum*, showed the highest growth rate at 30°C and 38°C with temperature stability at 30°C. It was selected as the most potential strain for CO_2 conversion. The EMMs production was optimized for maximum CH_4 production, revealing a biopolymer with carbohydrate, protein, and glycoprotein components. The methanogenesis mechanisms were identified as polymer bridging and charge neutralization. The study also introduced a novel optimization method using Response Surface

Methodology (RSM) for gas pressure and incubation time, leading to improved CH_4 production rates.

4. In conclusion, this study focused on H-MECAD design and EMMs characteristics at a lab scale volume. The SSGF anode H-MEC with EMMs basal medium demonstrated the highest current and power densities, reaching 531.04 mA m^{-2} and 477.94 mW m^{-2}, respectively. Application of response surface methodology (RSM) for EMMs dose and biogas flow rate optimization resulted in 92% CO^2 reduction from biogas in the H-MEC system. The novel EMMs achieved 92% CO^2 removal in a lab scale H-MEC based AD, and kinetic studies indicated growth-associated production of BioM with a specific growth rate (μ) of 0.207 h^{-1} and maximum specific rate of product formation of 0.239 h^{-1}. Overall, the developed process conditions showed promising results for efficient CO_2 reduction and methane production from biogas.

5.2 MAJOR CONTRIBUTIONS

The major findings and contributions of this research provided more insight in to shortcomings in past studies on H-MECAD characteristics and performance in a lab scale for CO_2 reduction from biogas. Therefore, based on the obtained results in the entire study, the following contribution can be highlighted:

1. Cellulase and amylase were produced locally, and the enzymes exhibited high activity, resulting in a significant 7.25-fold increase in reducing sugar (RS) during enzymatic hydrolysis. The combination of enzymatic hydrolysis and anaerobic digestion (AD) was employed for biogas fermentation without the need for any

additional supplements. Biogas contained was found 3% of H_2, 52% of CH_4 and 40% of CO_2.

2. The main concern of this research was locally isolated the novel EMMs strains. The EMMs strains such as TNFW and NTAS were identified as highly potential electromethanogenic microbes for converting organic CO_2 to CH_4 production by using H-MEC. In case of mycotoxins issue, the explored strain was under an edible cellulase and amylase enzymes and EMMs thereby no toxicity concern.
3. To best of investigator's knowledge, a lab scale design and test was the first-time attempt was applied in order to determine H-MEC performance by the converting of organic CO_2 to produce BioM from AD biogas upgrade-based food waste. As a result, the H-MECAD with TNEW-2 demonstrated better CO_2 to CH_4 conversion and FW treatment capability, with a maximum conversion efficiency of 92% while the literature was found 63.9 to 85% of conversion efficiency by MEC based AD. Because seitan was a very inexpensive FW material, this research might lead the way for the development of high-performance, low-cost H-MECAD for practical applications.
4. A deep insight was provided on H-MEC process of the EMMs using RSM by a constructed lab scale two chamber to evaluate the H-MEC performance in a flowing environment. According to our knowledge, there was no literature which used to upgrade organic CO_2 to BioM by microbial EMM to increase the CH_4 property of the biogas such that stable and high continuous H-MEC process may take place.

5.3 RECOMMENDATIONS

For large scale production, limitations, commercial uses, application of the new EMMs, the following recommendations were suggested for further studies:

a. There were need for further investigations in the characterization of the structure and molecular weight of active compound from extracellular substances of new EMMs by *Methanococcus vannielii* and *Methanobacterium beijingense*.

b. In addition, strain improvement through mutagenesis technique should be carried out to enhance on its adaptability in cold condition and storage properties. *Methanobacterium formicicum* of TNFW-2 mycelia have been died while it was stored in the chiller (4-6°C).

c. The application of *Methanobacterium formicicum* of strain TNFW-2 produced myco-flocculant should be explored in the actual CO_2 conversion system and wastewater treatment plant in order to establish the green technology for sustainable development.

d. Recommended for immobilization of enzymes on supported material.

e. The lab-scale production needs further improvement in order to design a system for large pilot-scale system. Scale-up of the new product in a bioreactor by investigating process parameters such as agitation and temperature with the suitable and recommended nutrient levels for commercialization.

f. Further research is needed to scale up the HMECAD system for large-scale production and meet market demand for upgraded biomethane.

REFERENCES

Abd Ghafar, S. W. (2017). Food waste in Malaysia: trends, current practices and key challenges. Centre of Promotion Technology, MARDI, Persiaran MARDI-UPM.

Abraham, M., & Kurup, G. M. (1996). Bioconversion of tapioca (Manihot esculenta) waste and water hyacinth (Eichhornia crassipes)—Influence of various physico-chemical factors. Journal of fermentation and bioengineering, 82(3), 259-263.

Acién Fernández, F. G., González-López, C. V., Fernández Sevilla, J. M., & Molina Grima, E. (2012). Conversion of CO2 into biomass by microalgae: how realistic a contribution may it be to significant CO2 removal. Applied microbiology and biotechnology, 96(3), 577-586.

Adekunle, K. F., & Okolie, J. A. (2015). A review of biochemical process of anaerobic digestion. Advances in Bioscience and Biotechnology, 6(03), 205.

Aguilar, R., Ramırez, J. A., Garrote, G., & Vázquez, M. (2002). Kinetic study of the acid hydrolysis of sugar cane bagasse. Journal of Food Engineering, 55 (4), 309-318.

Ahamed, M. I., & Asiri, A. M. (Eds.). (2019). Applications of Ion Exchange Materials in the Environment. Springer.

Ahmad, A., Ghufran, R., & Abd. Wahid, Z. (2012). Effect of COD loading rate on an upflow anaerobic sludge blanket reactor during anaerobic digestion of palm oil mill effluent with butyrate. Journal of Environmental Engineering and Landscape Management, 20(4), 256-264.

Ai, L., Ng, S. F., & Ong, W. J. (2022). Carbon dioxide electroreduction into formic acid and ethylene: a review. Environmental Chemistry Letters, 1-58.

Akinfalabi, S. I., Rashid, U., Ngamcharussrivichai, C., & Nehdi, I. A. (2020). Synthesis of reusable biobased nano-catalyst from waste sugarcane bagasse for biodiesel production. Environmental Technology & Innovation, 18, 100788.

Alam, M. Z., Mansor, M. F., Jalal, K.C.A. (2009a). Optimization of lignin peroxidase production and its stability by Phanerochaete chrysosporium using sewage treatment plant sludge as substrate in a stirred tank bioreactor. Journal of Industrial Microbiology and Biotechnology, 36 (5), 757–764.

Alam, M., Fakhru'l-Razi, A., Abd-Aziz, S., & Molla, A. H. (2003). Optimization of compatible mixed cultures for liquid state bioconversion of municipal wastewater sludge. Water, Air, and Soil Pollution, 149(1), 113-126.

Ali, J., Sohail, A., Wang, L., Rizwan Haider, M., Mulk, S., & Pan, G. (2018). Electro-microbiology as a promising approach towards renewable energy and environmental sustainability. Energies, 11(7), 1822.

Alibardi, L., & Cossu, R. (2016). Effects of carbohydrate, protein and lipid content of organic waste on hydrogen production and fermentation products. Waste Management, 47, 69-77.

Aljuboori, A. H. R., Idris, A., Al-Joubory, H. H. R., Uemura, Y., & Abubakar, B. I. (2015). Flocculation behavior and mechanism of bioflocculant produced by Aspergillus flavus. Journal of environmental management, 150, 466-471.

Al-Juboori, O., Sher, F., Khalid, U., Niazi, M. B. K., & Chen, G. Z. (2020). Electrochemical production of sustainable hydrocarbon fuels from CO2 co-electrolysis in eutectic molten melts. ACS Sustainable Chemistry & Engineering, 8(34), 12877-12890.

Allam, F., Elnouby, M., Sabry, S. A., El-Khatib, K. M., & El-Badan, D. E. (2021). Optimization of factors affecting current generation, biofilm formation and rhamnolipid production by electroactive Pseudomonas aeruginosa FA17. International Journal of Hydrogen Energy, 46(20), 11419-11432.

Amin, F. R., Khalid, H., El-Mashad, H. M., Chen, C., Liu, G., & Zhang, R. (2021). Functions of bacteria and archaea participating in the bioconversion of organic waste for methane production. Science of The Total Environment, 763, 143007.

Andrade-Velasques, A., Dominguez-Cañedo, L., & Melgar-Lalanne, G. (2021). Growth kinetic model, antioxidant and hypoglycemic effects at different temperatures of potential probiotic Lactobacillus spp. Revista Mexicana de Ingeniería Química, 20(1), 37-49.

Angelidaki, I., Treu, L., Tsapekos, P., Luo, G., Campanaro, S., Wenzel, H., & Kougias, P. G. (2018). Biogas upgrading and utilization: Current status and perspectives. Biotechnology advances.

Antunes, R. A., Oliveira, M. C. L., Ett, G., & Ett, V. (2010). Corrosion of metal bipolar plates for PEM fuel cells: A review. International journal of hydrogen energy, 35(8), 3632-3647.

APHA. (1989). Standard methods for the examination of water and wastewater. 17th edn. American public health association, Washington, DC.

Arbour, T. J., Gilbert, B., & Banfield, J. F. (2020). Diverse microorganisms in sediment and groundwater are implicated in extracellular redox processes based on genomic analysis of bioanode communities. Frontiers in microbiology, 11, 1694.

Arelli, V., Juntupally, S., Begum, S., & Anupoju, G. R. (2020). Significance of pretreatment in enhancing the performance of dry anaerobic digestion of food waste:

an insight on full scale implementation strategy with theoretical analogy. Processes, 8(09), 1018.

Arvin, Amin, et al., "A comparative study of the anaerobic baffled reactor and an integrated anaerobic baffled reactor and microbial electrolysis cell for treatment of petrochemical wastewater." Biochemical engineering journal 144 (2019): 157-165.

Aswathy, U. S., Sukumaran, R. K., Devi, G. L., Rajasree, K. P., Singhania, R. R., & Pandey, A. (2010). Bio-ethanol from water hyacinth biomass: an evaluation of enzymatic saccharification strategy. Bioresource technology, 101(3), 925-930.

Aulenta, F., Canosa, A., Reale, P., Rossetti, S., Panero, S., & Majone, M. (2009). Microbial reductive dechlorination of trichloroethene to ethene with electrodes serving as electron donors without the external addition of redox mediators. Biotechnology and bioengineering, 103(1), 85-91.

Aulenta, F., Tocca, L., Verdini, R., Reale, P., & Majone, M. (2011). Dechlorination of trichloroethene in a continuous-flow bioelectrochemical reactor: effect of cathode potential on rate, selectivity, and electron transfer mechanisms. Environmental science & technology, 45(19), 8444-8451.

Awadalla, O. A., Metwally, A. M., Bedawy, M. Y., & Rashad, M. R. (2017). Cellulolytic activities of some filamentous fungi from soil. Egypt. J. Exp. Bio, 367-374.

Babanova, S., Hubenova, Y., & Mitov, M. (2011). Influence of artificial mediators on yeast-based fuel cell performance. Journal of bioscience and bioengineering, 112(4), 379-387.

Baek, G., Kim, J., Kim, J., & Lee, C. (2018). Role and potential of direct interspecies electron transfer in anaerobic digestion. Energies, 11(1), 107.

Bai, X., Huang, D., Chen, Y., Wang, Q., Chen, Q., Wang, N., & Xu, Q. (2022). Exploration of Fe speciation preference for aerobic methane oxidation by using isotopic Fe-modified zeolites. Chemical Engineering Journal, 140844.

Bajracharya, S., et al., 2015. Carbon dioxide reduction by mixed and pure cultures in microbial electrosynthesis using an assembly of graphite felt and stainless steel as a cathode. Bioresour. Technol. 195, 14–24.

Bajracharya, S., Sharma, M., Mohanakrishna, G., Benneton, X. D., Strik, D. P., Sarma, P. M., & Pant, D. (2016). An overview on emerging bioelectrochemical systems (BESs): technology for sustainable electricity, waste remediation, resource recovery, chemical production and beyond. Renewable Energy, 98, 153-170.

Balaban, N. P., Suleimanova, A. D., Shakirov, E. V., & Sharipova, M. R. (2018). Histidine Acid Phytases of Microbial Origin. Microbiology, 87(6), 745-756.

Balch, W. E., Fox, G. E., Magrum, L. J., Woese, C. R., & Wolfe, R. (1979). Methanogens: reevaluation of a unique biological group. Microbiological reviews, 43(2), 260-296.

Bang, C., Schilhabel, A., Weidenbach, K., Kopp, A., Goldmann, T., Gutsmann, T., & Schmitz, R. A. (2012). Effects of antimicrobial peptides on methanogenic archaea. Antimicrobial agents and chemotherapy, 56(8), 4123-4130.

Banks, C. J., Chesshire, M., Heaven, S., & Arnold, R. (2011). Anaerobic digestion of source-segregated domestic food waste: performance assessment by mass and energy balance. Bioresource technology, 102(2), 612-620.

Baranitharan, E., Khan, M. R., Prasad, D. M. R., Teo, W. F. A., Tan, G. Y. A., & Jose, R. (2015). Effect of biofilm formation on the performance of microbial fuel cell for the treatment of palm oil mill effluent. Bioprocess and biosystems engineering, 38(1), 15-24.

Barbosa, S. G., Rodrigues, T., Peixoto, L., Kuntke, P., Alves, M. M., Pereira, M. A., & Ter Heijne, A. (2019). Anaerobic biological fermentation of urine as a strategy to enhance the performance of a microbial electrolysis cell (MEC). Renewable energy, 139, 936-943.

Bari, N., Alam, Z., Muyibi, S. A., Jamal, P., & Al-Mamun, A. (2010). Statistical optimization of process parameters for the production of citric acid from oil palm empty fruit bunches. African Journal of Biotechnology, 9(4).

Basri, M. F., Yacob, S., Hassan, M. A., Shirai, Y., Wakisaka, M., Zakaria, M. R., & Phang, L. Y. (2010). Improved biogas production from palm oil mill effluent by a scaled-down anaerobic treatment process. World Journal of Microbiology and Biotechnology, 26(3), 505-514.

Batlle-Vilanova, P., Puig, S., Gonzalez-Olmos, R., Balaguer, M. D., & Colprim, J. (2016). Continuous acetate production through microbial electrosynthesis from CO2 with microbial mixed culture. Journal of Chemical Technology & Biotechnology, 91(4), 921-927.

Beg, Q. K., Sahai, V., and Gupta, R. (2003). Statistical media optimization and alkaline protease production from Bacillus mojavensis in a bioreactor. Process Biochemistry 39, 203-209.

Benck, J. D., Hellstern, T. R., Kibsgaard, J., Chakthranont, P., & Jaramillo, T. F. (2014). Catalyzing the hydrogen evolution reaction (HER) with molybdenum sulfide nanomaterials. Acs Catalysis, 4(11), 3957-3971.

Bharathiraja, B., Sudharsanaa, T., Bharghavi, A., Jayamuthunagai, J., & Praveenkumar, R. (2016). Biohydrogen and Biogas–An overview on feedstocks and enhancement process. Fuel, 185, 810-828.

Bhatia, L., Sarangi, P. K., & Nanda, S. (2022). Hydrogen production through microbial electrolysis. In Biohydrogen (pp. 175-188). Apple Academic Press.

Bhatia, R. K., Sakhuja, D., Mundhe, S., & Walia, A. (2020). Renewable energy products through bioremediation of wastewater. Sustainability, 12(18), 7501.

Bhuiyan, M. I. H., Mavinic, D. S., & Koch, F. A. (2008). Phosphorus recovery from wastewater through struvite formation in fluidized bed reactors: a sustainable approach. Water Science and Technology, 57(2), 175-181.

Blasco-Gómez, R., Batlle-Vilanova, P., Villano, M., Balaguer, M. D., Colprim, J., & Puig, S. (2017). On the edge of research and technological application: a critical review of electromethanogenesis. International journal of molecular sciences, 18(4), 874.

Bo, T., Zhu, X., Zhang, L., Tao, Y., He, X., Li, D., & Yan, Z. (2014). A new upgraded biogas production process: coupling microbial electrolysis cell and anaerobic digestion in single-chamber, barrel-shape stainless steel reactor. Electrochemistry Communications, 45, 67-70.

Boedicker, J. Q. (2020). Multispecies Microbial Communities and Synthetic Microbial Ecosystems. In Biomimetic Microengineering (pp. 61-79). CRC Press.

Boliko, M. C. (2019). FAO and the situation of food security and nutrition in the world. Journal of nutritional science and vitaminology, 65(Supplement), S4-S8.

Boone, D. R. (1987). Request for an opinion: replacement of the type strain of Methanobacterium formicicum and reinstatement of Methanobacterium bryantii sp. nov. nom. rev.(ex Balch and Wolfe, 1981) with MoH (DSM 863) as the type strain. International Journal of Systematic and Evolutionary Microbiology, 37(2), 172-173.

Boone, D. R. (2015). Methanothermobacter. Bergey's Manual of Systematics of Archaea and Bacteria, 1-8.

Boone, D. R., & Mah, R. A. (2001). Genus I. Methanobacterium. Bergey's Manual of Systematic Bacteriology,, 1, 215-218.

Borole, A. P., Hamilton, C. Y., Vishnivetskaya, T., Leak, D., & Andras, C. (2009). Improving power production in acetate-fed microbial fuel cells via enrichment of exoelectrogenic organisms in flow-through systems. Biochemical Engineering Journal, 48(1), 71-80.

Box, G.E.P., Behnken, D. W. (1960). Some new three level designs for the study of quantitative variables. Technometrics 2, 455-475.

Bradley, N. (2007). Marketing research: tools & techniques. Oxford University Press, USA.

Brown, A. E., Finnerty, G. L., Camargo-Valero, M. A., & Ross, A. B. (2020). Valorisation of macroalgae via the integration of hydrothermal carbonisation and anaerobic digestion. Bioresource Technology, 312, 123539.

Bryant, M. P., & Boone, D. R. (1987). Isolation and characterization of Methanobacterium formicicum MF. International Journal of Systematic and Evolutionary Microbiology, 37(2), 171-171.

Bryant, M. P., Wolin, E. A., Wolin, M. J., & Wolfe, R. S. (1967). Methanobacillus omelianskii, a symbiotic association of two species of bacteria. Archiv für Mikrobiologie, 59(1), 20-31.

Buitrón, G., Cardeña, R., & Arcila, J. S. (2019). Bioelectrosynthesis of methane integrated with anaerobic digestion. In Microbial Electrochemical Technology (pp. 899-919). Elsevier.

Bywater, A., Heaven, S., Zhang, Y., & Banks, C. J. (2022). Potential for Biomethanisation of CO2 from Anaerobic Digestion of Organic Wastes in the United Kingdom. Processes, 10(6), 1202.

Cai, W., Liu, W., Yang, C., Wang, L., Liang, B., Thangavel, S., ... & Wang, A. (2016). Biocathodic methanogenic community in an integrated anaerobic digestion and microbial electrolysis system for enhancement of methane production from waste sludge. ACS Sustainable Chemistry & Engineering, 4(9), 4913-4921.

Call, D., & Logan, B. E. (2008). Hydrogen production in a single chamber microbial electrolysis cell lacking a membrane. Environmental science & technology, 42(9), 3401-3406.

Cao, X., Huang, X., Liang, P., Xiao, K., Zhou, Y., Zhang, X., & Logan, B. E. (2009). A new method for water desalination using microbial desalination cells. Environmental science & technology, 43(18), 7148-7152.

Cao, Y., Hu, Y., Sun, J., & Hou, B. (2010). Explore various co-substrates for simultaneous electricity generation and Congo red degradation in air-cathode single-chamber microbial fuel cell. Bioelectrochemistry, 79(1), 71-76.

Cao, Y., Mu, H., Liu, W., Zhang, R., Guo, J., Xian, M., & Liu, H. (2019). Electricigens in the anode of microbial fuel cells: pure cultures versus mixed communities. Microbial cell factories, 18(1), 1-14.

Caresani, J. R. F., Dallegrave, A., & dos Santos, J. H. (2019). Amylases immobilization by sol–gel entrapment: application for starch hydrolysis. Journal of Sol-Gel Science and Technology, 1-12.

Carlson, L. A. (2005). Nicotinic acid: the broad-spectrum lipid drug. A 50th anniversary review. Journal of internal medicine, 258(2), 94-114.

Carmona-Martínez, A. A., Trably, E., Milferstedt, K., Lacroix, R., Etcheverry, L., & Bernet, N. (2015). Long-term continuous production of H2 in a microbial electrolysis cell (MEC) treating saline wastewater. Water research, 81, 149-156.

Castelle, C., Guiral, M., Malarte, G., Ledgham, F., Leroy, G., Brugna, M., & Giudici-Orticoni, M. T. (2008). A new iron-oxidizing/O2-reducing supercomplex spanning both inner and outer membranes, isolated from the extreme acidophile Acidithiobacillus ferrooxidans. Journal of biological chemistry, 283(38), 25803-25811.

Cerrillo, M., Viñas, M., & Bonmatí, A. (2018). Anaerobic digestion and electromethanogenic microbial electrolysis cell integrated system: Increased stability and recovery of ammonia and methane. Renewable Energy, 120, 178-189.

Cersosimo, L. M., & Wright, A. D. G. (2015). Rumen methanogens. In Rumen microbiology: From evolution to revolution (pp. 143-150). Springer, New Delhi.

Chae, K. J., Choi, M. J., Lee, J. W., Kim, K. Y., & Kim, I. S. (2009). Effect of different substrates on the performance, bacterial diversity, and bacterial viability in microbial fuel cells. Bioresource technology, 100(14), 3518-3525.

Chakraborty, S., Rene, E. R., Lens, P. N., Rintala, J., Veiga, M. C., & Kennes, C. (2020). Effect of tungsten and selenium on C1 gas bioconversion by an enriched anaerobic sludge and microbial community analysis. Chemosphere, 250, 126105.

Chanal, P. S., Chanal, D. S., & Andre, G. (1992). Cellulase production profile of Trichoderma reesei on different cellulosic substrates at various pH levels. Journal of Fermentation and Bioengineering 74,126-128.

Chandrasekhar, K., Kadier, A., Kumar, G., Nastro, R. A., & Jeevitha, V. (2018). Challenges in microbial fuel cell and future scope. In Microbial Fuel Cell (pp. 483-499). Springer, Cham.

Chaudhary, A., et al., 2000. Separation of nickel from cobalt using electrodialysis in the presence of EDTA. J. Appl. Electrochem. 30 (4), 439–445.

Chaudhuri, S., Akkerman, V. Y., & Law, C. K. (2011). Spectral formulation of turbulent flame speed with consideration of hydrodynamic instability. Physical Review E, 84(2), 026322.

Chen, B. Y., Zhang, M. M., Chang, C. T., Ding, Y., Lin, K. L., Chiou, C. S., ... & Xu, H. (2010). Assessment upon azo dye decolorization and bioelectricity generation by Proteus hauseri. Bioresource technology, 101(12), 4737-4741.

Chen, C. C., Lin, C. Y., & Chang, J. S. (2001). Kinetics of hydrogen production with continuous anaerobic cultures utilizing sucrose as the limiting substrate. Applied Microbiology and Biotechnology, 57(1-2), 56-64

Chen, G. C., & Johnson, B. R. (1983). Improved colorimetric determination of cell wall chitin in wood decay fungi. Applied and Environmental Microbiology, 46(1), 13-16.

Chen, H. Y., & Sachtler, W. M. (1998). Activity and durability of Fe/ZSM-5 catalysts for lean burn NOx reduction in the presence of water vapor. Catalysis Today, 42(1-2), 73-83.

Chen, J. M., & Hao, O. J. (1998). Microbial chromium (VI) reduction. Critical Reviews in Environmental Science and Technology, 28(3), 219-251.

Chen, M., Ma, L. Q., & Harris, W. G. (1999). Baseline concentrations of 15 trace elements in Florida surface soils (Vol. 28, No. 4, pp. 1173-1181). American Society of Agronomy, Crop Science Society of America, and Soil Science Society of America.

Chen, P., Zhang, H. B., Lin, G. D., & Tsai, K. R. (1998). Development of coking-resistant Ni-based catalyst for partial oxidation and CO2-reforming of methane to syngas. Applied Catalysis A: General, 166(2), 343-350.

Chen, Y. Y., Zhang, Y., Zhang, X., Tang, T., Luo, H., Niu, S., ... & Hu, J. S. (2017). Self-templated fabrication of MoNi4/MoO3-x nanorod arrays with dual active components for highly efficient hydrogen evolution. Advanced Materials, 29(39), 1703311.

Chen, Y., Xu, Y., Chen, L., Li, P., Zhu, S., & Shen, S. (2015). Microbial electrolysis cells with polyaniline/multi-walled carbon nanotube-modified biocathodes. Energy, 88, 377-384.

Cheng, S., & Logan, B. E. (2007). Sustainable and efficient biohydrogen production via electrohydrogenesis. Proceedings of the National Academy of Sciences, 104(47), 18871-18873.

Cheng, S., Xing, D., Call, D. F., & Logan, B. E. (2009). Direct biological conversion of electrical current into methane by electromethanogenesis. Environmental science & technology, 43(10), 3953-3958.

Choi, C., Hu, N., & Lim, B. (2014). Cadmium recovery by coupling double microbial fuel cells. Bioresource technology, 170, 361-369.

Choi, K. S., Kondaveeti, S., & Min, B. (2017). Bioelectrochemical methane (CH4) production in anaerobic digestion at different supplemental voltages. Bioresource technology, 245, 826-832.

Chopra, I., & Howe, T. G. (1978). Bacterial resistance to the tetracyclines. Microbiological reviews, 42(4), 707-724.

Chuah, S. H. W., Tseng, M. L., Wu, K. J., & Cheng, C. F. (2021). Factors influencing the adoption of sharing economy in B2B context in China: Findings from PLS-SEM and fsQCA. Resources, Conservation and Recycling, 175, 105892.

Clauwaert, P., & Verstraete, W. (2009). Methanogenesis in membraneless microbial electrolysis cells. Applied microbiology and biotechnology, 82(5), 829-836.

Clauwaert, P., Toledo, R., van der Ha, D., Crab, R., Verstraete, W., Hu, H., & Rabaey, K. (2008). Combining biocatalyzed electrolysis with anaerobic digestion. Water Science and Technology, 57(4), 575-579.

Colantonio, N., & Kim, Y. (2016). Cadmium (II) removal mechanisms in microbial electrolysis cells. Journal of hazardous materials, 311, 134-141.

Colindres, P., Yee-Madeira, H., & Reguera, E. (2010). Removal of Reactive Black 5 from aqueous solution by ozone for water reuse in textile dyeing processes. Desalination, 258(1-3), 154-158.

Comninellis, C. (1994). Electrocatalysis in the electrochemical conversion/combustion of organic pollutants for waste water treatment. Electrochimica Acta, 39(11-12), 1857-1862.

Confer, D. R., & Logan, B. E. (1997). Molecular weight distribution of hydrolysis products during the biodegradation of model macromolecules in suspended and biofilm cultures. II. Dextran and dextrin. Water Research, 31(9), 2137-2145.

Confer, D. R., & Logan, B. E. (1998). Location of protein and polysaccharide hydrolytic activity in suspended and biofilm wastewater cultures. Water Research, 32(1), 31-38.

Cookson, R. F. (1974). Determination of acidity constants. Chemical Reviews, 74(1), 5-28.

Crable, B. R., Plugge, C. M., McInerney, M. J., & Stams, A. J. (2011). Formate formation and formate conversion in biological fuels production. Enzyme Research, 2011.

Cremonez, P. A., Sampaio, S. C., Teleken, J. G., Meier, T. W., Frigo, E. P., de Rossi, E., ... & Rosa, D. M. (2020). Effect of substrate concentrations on methane and hydrogen biogas production by anaerobic digestion of a cassava starch-based polymer. Industrial crops and products, 151, 112471.

Croese, E., Pereira, M. A., Euverink, G. J. W., Stams, A. J., & Geelhoed, J. S. (2011). Analysis of the microbial community of the biocathode of a hydrogen-producing microbial electrolysis cell. Applied microbiology and biotechnology, 92(5), 1083-1093.

Cui, D., Guo, Y. Q., Cheng, H. Y., Liang, B., Kong, F. Y., Lee, H. S., & Wang, A. J. (2012). Azo dye removal in a membrane-free up-flow biocatalyzed electrolysis reactor

coupled with an aerobic bio-contact oxidation reactor. Journal of hazardous materials, 239, 257-264.

Cusick, R. D., Bryan, B., Parker, D. S., Merrill, M. D., Mehanna, M., Kiely, P. D., ... & Logan, B. E. (2011). Performance of a pilot-scale continuous flow microbial electrolysis cell fed winery wastewater. Applied microbiology and biotechnology, 89(6), 2053-2063.

Cusick, R. D., Ullery, M. L., Dempsey, B. A., & Logan, B. E. (2014). Electrochemical struvite precipitation from digestate with a fluidized bed cathode microbial electrolysis cell. water research, 54, 297-306.

Cuzin, N., Ouattara, A. S., Labat, M., & Garcia, J. L. (2001). Methanobacterium congolense sp. nov., from a methanogenic fermentation of cassava peel. International journal of systematic and evolutionary microbiology, 51(2), 489-493.

Cysneiros, D., Banks, C. J., Heaven, S., & Karatzas, K. A. G. (2012). The effect of pH control and 'hydraulic flush'on hydrolysis and Volatile Fatty Acids (VFA) production and profile in anaerobic leach bed reactors digesting a high solids content substrate. Bioresource technology, 123, 263-271.

Dai, X., Duan, N., Dong, B., & Dai, L. (2013). High-solids anaerobic co-digestion of sewage sludge and food waste in comparison with mono digestions: stability and performance. Waste Management, 33(2), 308-316.

Deb, N., Alam, M. Z., Rahman, T., Al-Khatib, M. A. F. R., Jami, M. S., & Mansor, M. F. B. (2023). Acid–Base Pretreatment and Enzymatic Hydrolysis of Palm Oil Mill Effluent in a Single Reactor System for Production of Fermentable Sugars. International Journal of Polymer Science, 2023.

Deb, N., Alam, M. Z., Rahman, T., Jami, M. S., Mansor, M. F. B., & Tajuddin, H. B. A. (2023). Anaerobic Digestion for Biomethane Production from Food Waste Pretreated by Enzymatic Hydrolysis.

Deb, N., Alam, M. Z., Rahman, T., Jami, M. S., Bt Mansor, M. F., & Tajuddin, H. B. A. (2023). Design and Analysis of a Fuel Cell and Batteries in Energy Production for Electric Vehicle. Iranian (Iranica) Journal of Energy & Environment, 14(3), 301-313.

Deb, N, M. Z. Alam, Ma An Fahmi Rashid Al-Khatib, and E. A. Ahmed. (2017). "Development of acid-base-enzyme pretreatment and hydrolysis of palm oil mill effluent for bioethanol production" Advances in Biofeedstocks and Biofuels; Volume 3: Liquid Biofuel Production, Wiley.

Deb, N., Alam, M. Z., Al-khatib, M. F. R., & Elgharbawy, A. (2019). Development of Acid-Base-Enzyme Pretreatment and Hydrolysis of Palm Oil Mill Effluent for Bioethanol Production. Liquid Biofuel Production, 197-217.Gunaseelan, V. N.

(2004). Biochemical methane potential of fruits and vegetable solid waste feedstocks. Biomass and bioenergy, 26(4), 389-399.

Deb, N. (2017). Development of Acid-Base-Enzyme Pretreatment and Hydrolysis Processes for Enhanced Bioethanol Production from Palm Oil Mill Effluent. Mater dissertation. IIUM.

Deena, S. R., Vickram, A. S., Manikandan, S., Subbaiya, R., Karmegam, N., Ravindran, B., ... & Awasthi, M. K. (2022). Enhanced biogas production from food waste and activated sludge using advanced techniques–a review. Bioresource Technology, 355, 127234.

Deepanraj, B., Sivasubramanian, V., & Jayaraj, S. (2015). Experimental and kinetic study on anaerobic digestion of food waste: The effect of total solids and pH. Journal of Renewable and Sustainable Energy, 7(6), 063104.

Deng, H., Li, X., Peng, Q., Wang, X., Chen, J., & Li, Y. (2005). Monodisperse magnetic single-crystal ferrite microspheres. Angewandte Chemie, 117(18), 2842-2845.

Desloover, J., Arends, J. B., Hennebel, T., & Rabaey, K. (2012). Operational and technical considerations for microbial electrosynthesis.

Dessì, P., Rovira-Alsina, L., Sánchez, C., Dinesh, G. K., Tong, W., Chatterjee, P., ... & Puig, S. (2021). Microbial electrosynthesis: Towards sustainable biorefineries for production of green chemicals from CO2 emissions. Biotechnology Advances, 46, 107675.

Devi, M. K., Manikandan, S., Oviyapriya, M., Selvaraj, M., Assiri, M. A., Vickram, S., ... & Awasthi, M. K. (2022). Recent advances in biogas production using Agro-Industrial Waste: A comprehensive review outlook of Techno-Economic analysis. Bioresource Technology, 127871.

Dhanariya, R., Sharma, S., Sharma, A. K., & Verma, S. (2014). A Review on Biogas Production from Food Waste. International Journal of Pharmaceutical and Chemical Sciences Issn, 3(4), Traducción mía. Retrieved from www.ijpcsonline.com

Di Lorenzo, M., Scott, K., Curtis, T. P., Katuri, K. P., & Head, I. M. (2009). Continuous feed microbial fuel cell using an air cathode and a disc anode stack for wastewater treatment. Energy & Fuels, 23(11), 5707-5716.

Dianat, F., Khodakarami, V., Hosseini, S. H., & Shakouri, H. (2022). Combining game theory concepts and system dynamics for evaluating renewable electricity development in fossil-fuel-rich countries in the Middle East and North Africa. Renewable Energy, 190, 805-821.

Díaz, E. E., Stams, A. J., Amils, R., & Sanz, J. L. (2006). Phenotypic properties and microbial diversity of methanogenic granules from a full-scale upflow anaerobic

sludge bed reactor treating brewery wastewater. Applied and environmental microbiology, 72(7), 4942-4949.

Ding, A., Yang, Y., Sun, G., & Wu, D. (2016). Impact of applied voltage on methane generation and microbial activities in an anaerobic microbial electrolysis cell (MEC). Chemical Engineering Journal, 283, 260-265.

Ding, H. B., Tan, G. Y. A., & Wang, J. Y. (2010). Caproate formation in mixed-culture fermentative hydrogen production. Bioresource technology, 101(24), 9550-9559.

Ditzig, J., Liu, H., & Logan, B. E. (2007). Production of hydrogen from domestic wastewater using a bioelectrochemically assisted microbial reactor (BEAMR). International Journal of Hydrogen Energy, 32(13), 2296-2304.

Dolfing, J., Griffioen, A., Van Neerven, A. R. W., & Zevenhuizen, L. P. T. M. (1985). Chemical and bacteriological composition of granular methanogenic sludge. Canadian Journal of Microbiology, 31(8), 744-750.

Dong, Z. S., Zhao, Y., Fan, L., Wang, Y. X., Wang, J. W., & Zhang, K. (2017). Simultaneous sulfide removal and hydrogen production in a microbial electrolysis cell. Int. J. Electrochem. Sci, 12(11), 10553-10566.

Dou, Z., Dykstra, C. M., & Pavlostathis, S. G. (2018). Bioelectrochemically assisted anaerobic digestion system for biogas upgrading and enhanced methane production. Science of the Total Environment, 633, 1012-1021.

Doyle, J. D., & Parsons, S. A. (2002). Struvite formation, control and recovery. Water research, 36(16), 3925-3940.

Dutta, J. R., Dutta P.K., Banarjee, R. (2004). Optimization of culture parameters for etracellular protease production from a newly isolate Pseudomonas sp. Using response surface and artificial neural network models. Process Biochemistry 39, 2193-2198.

Dutta, K., Tsai, C. Y., Chen, W. H., & Lin, J. G. (2014). Effect of carriers on the performance of anaerobic sequencing batch biofilm reactor treating synthetic municipal wastewater. International Biodeterioration & Biodegradation, 95, 84-88.

Dykstra, C. M., & Pavlostathis, S. G. (2017). Zero-valent iron enhances biocathodic carbon dioxide reduction to methane. Environmental Science & Technology, 51(21), 12956-12964.

Edgcomb, V. P., Leadbetter, E. R., Bourland, W., Beaudoin, D., & Bernhard, J. M. (2011). Structured multiple endosymbiosis of bacteria and archaea in a ciliate from marine sulfidic sediments: a survival mechanism in low oxygen, sulfidic sediments?. Frontiers in Microbiology, 2, 55.

El Asri, O., Fadlaoui, S., & Afilal, M. E. (2022). Applications of Microbes in Municipal Solid Waste Treatment. In Application of Microbes in Environmental and Microbial Biotechnology (pp. 587-607). Springer, Singapore.

El-araby, A., El Ghadraoui, L., & Errachidi, F. (2022). Usage of biological chitosan against the contamination of post-harvest treatment of strawberries by Aspergillus niger. Frontiers in Sustainable Food Systems, 6, 881434.

Elgharbawy, A. A., Alam, M. Z., & Salleh, H. M. (2016). Characterization of low-cost lipase by solid-state fermentation of palm kernel cake using candida cylindracea.

Escapa, A., Mateos, R., Martínez, E. J., & Blanes, J. (2016). Microbial electrolysis cells: An emerging technology for wastewater treatment and energy recovery. From laboratory to pilot plant and beyond. Renewable and Sustainable Energy Reviews, 55, 942-956.

Escapa, A., Mateos, R., Martínez, E. J., & Blanes, J. (2016). Microbial electrolysis cells: An emerging technology for wastewater treatment and energy recovery. From laboratory to pilot plant and beyond. Renewable and Sustainable Energy Reviews, 55, 942-956.

Evans, A., Strezov, V., & Evans, T. J. (2010). Sustainability considerations for electricity generation from biomass. Renewable and sustainable energy reviews, 14(5), 1419-1427.

Fahimizadeh, M., Pasbakhsh, P., Mae, L. S., Tan, J. B. L., & Raman, R. S. (2022). Multifunctional, sustainable, and biological non-ureolytic self-healing systems for cement-based materials. Engineering.

Fakhru'l-Razi, A., Alam, M., Z., Idris, A., Abd-Aziz, S., & Molla, A. H. (2002). Filamentous fungi in Indah Water Konsortium (IWK) sewage treatment plant for biological treatment of domestic wastewater sludge. Journal of Environmental Science and Health, Part A, 37(3), 309-320.

Falk, H. M., & Benz, H. (2011). Monitoring the anaerobic digestion process (Doctoral dissertation, IRC-Library, Information Resource Center der Jacobs University Bremen).

Fazeli, A., Bakhtvar, F., Jahanshaloo, L., Sidik, N. A. C., & Bayat, A. E. (2016). Malaysia ' s stand on municipal solid waste conversion to energy: A review. Renewable and Sustainable Energy Reviews, 58, 1007-1016.

Forster-Carneiro, T., Pérez, M., & Romero, L. I. (2008). Influence of total solid and inoculum contents on performance of anaerobic reactors treating food waste. Bioresource technology, 99(15), 6994-7002.

Fu, B., Jin, X., Conrad, R., Liu, H., & Liu, H. (2019). Competition between chemolithotrophic acetogenesis and hydrogenotrophic methanogenesis for exogenous H2/CO2 in anaerobically digested sludge: impact of temperature. Frontiers in microbiology, 10, 2418.

Fu, Q., He, Y., Li, Z., Li, J., Zhang, L., Zhu, X., & Liao, Q. (2022). Direct CO2 delivery with hollow stainless steel/graphene foam electrode for enhanced methane production in microbial electrosynthesis. Energy Conversion and Management, 268, 116018.

Gao, Y., Sun, D., Dang, Y., Lei, Y., Ji, J., Lv, T., ... & Holmes, D. E. (2017). Enhancing biomethanogenic treatment of fresh incineration leachate using single chambered microbial electrolysis cells. Bioresource technology, 231, 129-137.

Garcıa, A. J., Esteban, M. B., Marquez, M. C., & Ramos, P. (2005). Biodegradable municipal solid waste: Characterization and potential use as animal feedstuffs. Waste Management, 25(8), 780-787.

Gardy, J., Hassanpour, A., Lai, X., Ahmed, M. H., & Rehan, M. (2017). Biodiesel production from used cooking oil using a novel surface functionalised TiO2 nano-catalyst. Applied Catalysis B: Environmental, 207, 297-310.

Garrone, P., Melacini, M., & Perego, A. (2014). Opening the black box of food waste reduction Journal of Food Policy, 46, 129–139.

Gatto, I., Carbone, A., Saccà, A., Passalacqua, E., Oldani, C., Merlo, L., ... & Baglio, V. (2019). Increasing the stability of membrane-electrode assemblies based on Aquivion® membranes under automotive fuel cell conditions by using proper catalysts and ionomers. Journal of Electroanalytical Chemistry, 842, 59-65.

Ghose, T. K. & Sahai, V. (1979) Production of cellulases by Trichoderma reesei QM 9414 in fed-batch and continuous flow culture with cell recycle. Biotechnology and Bioengineering 21,283-296.

Ghose, T. K. (1987). Measurement of cellulase activities. Pure and applied Chemistry, 59(2), 257-268.

Gohil, A., & Nakhla, G. (2006). Treatment of Food Industry Waste by Bench-Scale Upflow Anaerobic Sludge Blanket-Anoxic-Aerobic System. Water environment research, 78(9), 974-985.

Gong, Y., Ebrahim, A., Feist, A. M., Embree, M., Zhang, T., Lovley, D., & Zengler, K. (2013). Sulfide-driven microbial electrosynthesis. Environmental science & technology, 47(1), 568-573.

Goswami, R., & Mishra, V. K. (2018). A review of design, operational conditions and applications of microbial fuel cells. Biofuels, 9(2), 203-220.

Großkopf, R., Janssen, P. H., & Liesack, W. (1998). Diversity and structure of the methanogenic community in anoxic rice paddy soil microcosms as examined by cultivation and direct 16S rRNA gene sequence retrieval. Applied and environmental microbiology, 64(3), 960-969.

Güelfo, L. F., Álvarez-Gallego, C., Márquez, D. S., & García, L. R. (2011). The effect of different pretreatments on biomethanation kinetics of industrial Organic Fraction of Municipal Solid Wastes (OFMSW). Chemical engineering journal, 171(2), 411-417.

Guilbault, G. G. (2013). Recent Developments in Enzymatic Methods for. Trace Analysis: Volume 3, 3, 31.

Gunaseelan, V. N. (1997). Anaerobic digestion of biomass for methane production: a review. Biomass and bioenergy, 13(1-2), 83-114.

Guo, X., Liu, J., & Xiao, B. (2013). Bioelectrochemical enhancement of hydrogen and methane production from the anaerobic digestion of sewage sludge in single-chamber membrane-free microbial electrolysis cells. International Journal of Hydrogen Energy, 38(3), 1342-1347.

Guo, Z., Thangavel, S., Wang, L., He, Z., Cai, W., Wang, A., & Liu, W. (2017). Efficient methane production from beer wastewater in a membraneless microbial electrolysis cell with a stacked cathode: the effect of the cathode/anode ratio on bioenergy recovery. Energy & Fuels, 31(1), 615-620.

Haddar, A., Ayed, E. B., Sila, A., Putaux, J. L., Bougatef, A., & Boufi, S. (2021). Hybrid levan–Ag/AgCl nanoparticles produced by UV-irradiation: properties, antibacterial efficiency and application in bioactive poly (vinyl alcohol) films. RSC advances, 11(62), 38990-39003.

Hales, B. A., Edwards, C., Ritchie, D. A., Hall, G., Pickup, R. W., & Saunders, J. R. (1996). Isolation and identification of methanogen-specific DNA from blanket bog peat by PCR amplification and sequence analysis. Applied and Environmental Microbiology, 62(2), 668-675.

Haltrich, D., Laussamayer, B., Steiner, W., Nidetzky, B., Kulbe, K. D. (1994). Cellulolytic and hemicellulolytic enzymes of sclerotium rolfsii: Optimization of the culture medium and enzymatic hydrolysis of lignocellulosic material. Bioresource Technology 50 (1), 43-50.

Hao, L., Michaelsen, T. Y., Singleton, C. M., Dottorini, G., Kirkegaard, R. H., Albertsen, M., ... & Dueholm, M. S. (2020). Novel syntrophic bacteria in full-scale anaerobic digesters revealed by genome-centric metatranscriptomics. The ISME Journal, 1-13.

Harada, H., Endo, G., Tohya, Y., & Momonoi, K. (1988). High rate performance and its related characteristics of granulated sludges in UASB reactors treating various wastewaters. In Proceedings of the fifth international symposium on anaerobic digestion (pp. 1011-1020). Bologna: Monduzzi editore.

Harnisch, F., Sievers, G., & Schröder, U. (2009). Tungsten carbide as electrocatalyst for the hydrogen evolution reaction in pH neutral electrolyte solutions. Applied Catalysis B: Environmental, 89(3-4), 455-458.

Hartmann, H., & Ahring, B. K. (2005). Anaerobic digestion of the organic fraction of municipal solid waste: influence of co-digestion with manure. Water research, 39(8), 1543-1552.

Haryanto, A., Hasanudin, U., Afrian, C., & Zulkarnaen, I. (2018, March). Biogas production from anaerobic codigestion of cowdung and elephant grass (Pennisetum Purpureum) using batch digester. In IOP Conference Series: Earth and Environmental Science (Vol. 141, No. 1, p. 012011). IOP Publishing.

Hashemi, S. S., Karimi, K., & Mirmohamadsadeghi, S. (2019). Hydrothermal pretreatment of safflower straw to enhance biogas production. Energy, 172, 545-554.

Haslett, N. D., Rawson, F. J., Barrière, F., Kunze, G., Pasco, N., Gooneratne, R., & Baronian, K. H. (2011). Characterisation of yeast microbial fuel cell with the yeast Arxula adeninivorans as the biocatalyst. Biosensors and Bioelectronics, 26(9), 3742-3747.

He, K., Li, W., Tang, L., Li, W., Lv, S., & Xing, D. (2022). Suppressing Methane Production to Boost High-Purity Hydrogen Production in Microbial Electrolysis Cells. Environmental Science & Technology, 56(17), 11931-11951.

Hennebel, T., Benner, J., Clauwaert, P., Vanhaecke, L., Aelterman, P., Callebaut, R., ... & Verstraete, W. (2011). Dehalogenation of environmental pollutants in microbial electrolysis cells with biogenic palladium nanoparticles. Biotechnology letters, 33(1), 89-95.

Hickey, R. F., Vanderweilen, J., & Switzenbaum, M. S. (1987). Production of trace levels of carbon monoxide during methanogenesis on acetate and methanol. Biotechnology letters, 9(1), 63-66.

Higuchi, Y., Ohashi, A., Imachi, H., & Harada, H. (2005). Hydrolytic activity of alpha-amylase in anaerobic digested sludge. Water Science and Technology, 52(1-2), 259-266.

Hilpert, R., Winter, J., Hammes, W., & Kandler, O. (1981). The sensitivity of archaebacteria to antibiotics. Zentralblatt für Bakteriologie Mikrobiologie und Hygiene: I. Abt. Originale C: Allgemeine, angewandte und ökologische Mikrobiologie, 2(1), 11-20.

Hirooka, K., & Ichihashi, O. (2013). Phosphorus recovery from artificial wastewater by microbial fuel cell and its effect on power generation. Bioresource technology, 137, 368-375.

Holl, E., Steinbrenner, J., Merkle, W., Krümpel, J., Lansing, S., Baier, U., ... & Lemmer, A. (2022). Two-stage anaerobic digestion: State of technology and perspective roles in future energy systems. Bioresource Technology, 127633.

Hong, G., Su, W., Wen, Q., & Wu, P. (2020). RAVEC: An Optimal Resource Allocation Mechanism in Vehicular MEC Systems. J. Inf. Sci. Eng., 36(4), 865-878.

Hong, S. B., Lee, M., Kim, D. H., Varga, J., Frisvad, J. C., Perrone, G., ... & Samson, R. A. (2013). Aspergillus luchuensis, an industrially important black Aspergillus in East Asia. PLoS One, 8(5), e63769.

Horikoshi, K. (1999). Alkaliphiles: some applications of their products for biotechnology. Microbiology and molecular biology reviews, 63(4), 735-750.

Horiuchi, J. I., Shimizu, T., Tada, K., Kanno, T., & Kobayashi, M. (2002). Selective production of organic acids in anaerobic acid reactor by pH control. Bioresource technology, 82(3), 209-213.

Hou, Y., Zhang, R., Luo, H., Liu, G., Kim, Y., Yu, S., & Zeng, J. (2015). Microbial electrolysis cell with spiral wound electrode for wastewater treatment and methane production. Process Biochemistry, 50(7), 1103-1109.

Hou, Y., Zhang, R., Yu, Z., Huang, L., Liu, Y., & Zhou, Z. (2017). Accelerated azo dye degradation and concurrent hydrogen production in the single-chamber photocatalytic microbial electrolysis cell. Bioresource technology, 224, 63-68.

Hu, H., Fan, Y., & Liu, H. (2009). Hydrogen production in single-chamber tubular microbial electrolysis cells using non-precious-metal catalysts. international journal of hydrogen energy, 34(20), 8535-8542.

Hu, H., Fan, Y., & Liu, H. (2010). Optimization of NiMo catalyst for hydrogen production in microbial electrolysis cells. international journal of hydrogen energy, 35(8), 3227-3233.

Huang, L., Jiang, L., Wang, Q., Quan, X., Yang, J., & Chen, L. (2014). Cobalt recovery with simultaneous methane and acetate production in biocathode microbial electrolysis cells. Chemical Engineering Journal, 253, 281-290.

Huang, Q., Li, S. G., Teng, H., Jin, Y. G., Ma, M. H., & Song, H. B. (2015). Optimizing preparation conditions for angiotensin-I-converting enzyme inhibitory peptides derived from enzymatic hydrolysates of ovalbumin. Food science and biotechnology, 24, 2193-2198.

Hungate RE (1950) The anaerobic mesophilic cellulolytic bacteria. Bacterial Rev 14: 1 - 49

Huo, E., Xin, L., & Wang, S. (2022). Thermal stability and pyrolysis mechanism of working fluids for organic Rankine cycle: A review. International Journal of Energy Research, 46(14), 19341-19356.

Hutchinson, A. J., Tokash, J. C., & Logan, B. E. (2011). Analysis of carbon fiber brush loading in anodes on startup and performance of microbial fuel cells. Journal of Power Sources, 196(22), 9213-9219.

Jadhav, D. A., Chendake, A. D., Schievano, A., & Pant, D. (2019). Suppressing methanogens and enriching electrogens in bioelectrochemical systems. Bioresource technology, 277, 148-156.

Jadhav, D.A., et al., 2019. Suppressing methanogens and enriching electrogens in bioelectrochemical systems. Bioresour. Technol. 277, 148–156.

Jafary, T., Daud, W. R. W., Ghasemi, M., Kim, B. H., Carmona-Martínez, A. A., Bakar, M. H. A., ... & Ismail, M. (2017). A comprehensive study on development of a biocathode for cleaner production of hydrogen in a microbial electrolysis cell. Journal of cleaner production, 164, 1135-1144.

Jankowska, E., Chwiałkowska, J., Stodolny, M., & Oleskowicz-Popiel, P. (2015). Effect of pH and retention time on volatile fatty acids production during mixed culture fermentation. Bioresource Technology, 190, 274-280.

Jayabalan, T., Matheswaran, M., & Mohammed, S. N. (2019). Biohydrogen production from sugar industry effluents using nickel based electrode materials in microbial electrolysis cell. International Journal of Hydrogen Energy, 44(32), 17381-17388.

Jeremiasse, A. W., Hamelers, H. V., Saakes, M., & Buisman, C. J. (2010). Ni foam cathode enables high volumetric H2 production in a microbial electrolysis cell. International Journal of Hydrogen Energy, 35(23), 12716-12723.

Jeya, M., Moon, H. J., Kim, S. H., & Lee, J. K. (2010). Conversion of woody biomass into fermentable sugars by cellulase from Agaricus arvensis. Bioresource Technology, 101(22), 8742-8749.

Jiang, Y., Su, M., Zhang, Y., Zhan, G., Tao, Y., & Li, D. (2013). Bioelectrochemical systems for simultaneously production of methane and acetate from carbon dioxide at relatively high rate. International Journal of Hydrogen Energy, 38(8), 3497-3502.

Jiménez Otero, F., Chan, C. H., & Bond, D. R. (2018). Identification of different putative outer membrane electron conduits necessary for Fe (III) citrate, Fe (III) oxide, Mn (IV) oxide, or electrode reduction by Geobacter sulfurreducens. Journal of bacteriology, 200(19), e00347-18.

Jones, S. M., & Solomon, E. I. (2015). Electron transfer and reaction mechanism of laccases. Cellular and molecular life sciences, 72, 869-883., E. I. (2015). Electron transfer and reaction mechanism of laccases. Cellular and molecular life sciences, 72, 869-883.

Joulian, C., Patel, B. K., Ollivier, B., Garcia, J. L., & Roger, P. A. (2000). Methanobacterium oryzae sp. nov., a novel methanogenic rod isolated from a Philippines ricefield. International journal of systematic and evolutionary microbiology, 50(2), 525-528.

Kadier, A., Kalil, M. S., Abdeshahian, P., Chandrasekhar, K., Mohamed, A., Azman, N. F., ... & Hamid, A. A. (2016). Recent advances and emerging challenges in microbial electrolysis cells (MECs) for microbial production of hydrogen and value-added chemicals. Renewable and Sustainable Energy Reviews, 61, 501-525.

Kadier, A., Simayi, Y., Abdeshahian, P., Azman, N. F., Chandrasekhar, K., & Kalil, M. S. (2016). A comprehensive review of microbial electrolysis cells (MEC) reactor designs and configurations for sustainable hydrogen gas production. Alexandria Engineering Journal, 55(1), 427-443.

Kadier, A., Simayi, Y., Chandrasekhar, K., Ismail, M., & Kalil, M. S. (2015). Hydrogen gas production with an electroformed Ni mesh cathode catalyst in a single-chamber microbial electrolysis cell (MEC). International Journal of Hydrogen Energy, 40(41), 14095-14103.

Kadier, A., Simayi, Y., Kalil, M. S., Abdeshahian, P., & Hamid, A. A. (2014). A review of the substrates used in microbial electrolysis cells (MECs) for producing sustainable and clean hydrogen gas. Renewable Energy, 71, 466-472.

Kadier, A., Wang, J., Chandrasekhar, K., Abdeshahian, P., Islam, M. A., Ghanbari, F., ... & Ma, P. C. (2022). Performance optimization of microbial electrolysis cell (MEC) for palm oil mill effluent (POME) wastewater treatment and sustainable Bio-H2 production using response surface methodology (RSM). International journal of hydrogen energy, 47(34), 15464-15479.

Karakashev, D., Batstone, D. J., & Angelidaki, I. (2005). Influence of environmental conditions on methanogenic compositions in anaerobic biogas reactors. Applied and environmental microbiology, 71(1), 331-338.

Karim, K., Hoffmann, R., Klasson, K. T., & Al-Dahhan, M. H. (2005). Anaerobic digestion of animal waste: Effect of mode of mixing. Water research, 39(15), 3597-3606.

Karunarathna, M. J. S., Linhart, A. N., Giammanco, G. E., Norton, A. E., Chory, J. J., Keleher, J. J., & Ostrowski, A. D. (2021). Harnessing Fe (III)–Carboxylate Photochemistry for Radical-Initiated Polymerization in Hydrogels. ACS Applied Bio Materials, 4(7), 5765-5775.

Kato Marcus, A., Torres, C. I., & Rittmann, B. E. (2007). Conduction-based modeling of the biofilm anode of a microbial fuel cell. Biotechnology and bioengineering, 98(6), 1171-1182.

Kavuma, C. (2013). Variation of Methane and Carbon dioxide Yield in a biogas plant. Department of Energy Technology, MSc, 46. Retrieved from http://www.diva-portal. org/smash /get/diva2: 604559/ FULLTEXT02

Keller, J. (2010). Bioelectrochemical systemsfrom extracellular electron transfer to biotechnological application (No. 660.62 B5).

Khan, M. Z., Nizami, A. S., Rehan, M., Ouda, O. K. M., Sultana, S., Ismail, I. M., & Shahzad, K. (2017). Microbial electrolysis cells for hydrogen production and urban wastewater treatment: A case study of Saudi Arabia. Applied energy, 185, 410-420.

Khan, M. Z., Sim, Y. L., Lin, Y. J., & Lai, K. M. (2013). Testing biological effects of hand-washing grey water for reuse in irrigation on an urban farm: a case study. Environmental technology, 34(4), 545-551.

Khan, M. Z., Singh, S., Sreekrishnan, T. R., & Ahammad, S. Z. (2014). Feasibility study on anaerobic biodegradation of azo dye reactive orange 16. RSC Advances, 4(87), 46851-46859.

Khokhar, I., Haider, M. S., Mushtaq, S., & Mukhtar, I. (2012). Isolation and screening of highly cellulolytic filamentous fungi. Journal of Applied Sciences and Environmental Management, 16(3).

Khoshnevisan, B., He, L., Xu, M., Valverde-Pérez, B., Sillman, J., Mitraka, G. C., ... & Angelidaki, I. (2022). From renewable energy to sustainable protein sources: Advancement, challenges, and future roadmaps. Renewable and Sustainable Energy Reviews, 157, 112041.

Kim, D. H., Kim, S. H., Kim, K. Y., & Shin, H. S. (2010). Experience of a pilot-scale hydrogen-producing anaerobic sequencing batch reactor (ASBR) treating food waste. International Journal of Hydrogen Energy, 35(4), 1590-1594.

Kim, J. H., Lee, J. C., & Pak, D. (2011). Feasibility of producing ethanol from food waste. Waste management, 31(9-10), 2121-2125.

Kim, J. K., Han, G. H., Oh, B. R., Chun, Y. N., Eom, C. Y., & Kim, S. W. (2008). Volumetric scale-up of a three-stage fermentation system for food waste treatment. Bioresource technology, 99(10), 4394-4399.

Kim, J. K., Oh, B. R., Chun, Y. N., & Kim, S. W. (2006). Effects of temperature and hydraulic retention time on anaerobic digestion of food waste. Journal of Bioscience and bioengineering, 102(4), 328-332.

Kim, N., Choi, Y., Jung, S., & Kim, S. (2000). Effect of initial carbon sources on the performance of microbial fuel cells containing Proteus vulgaris. Biotechnology and bioengineering, 70(1), 109-114.

Kiran, E. U., Trzcinski, A. P., & Liu, Y. (2015). Enhancing the hydrolysis and methane production potential of mixed food waste by an effective enzymatic pretreatment. Bioresource technology, 183, 47-52.

Kiran, E. U., Trzcinski, A. P., Ng, W. J., & Liu, Y. (2014). Bioconversion of food waste to energy: a review. Fuel, 134, 389-399.

Kobayashi, H., Fu, Q., Maeda, H., & Sato, K. (2017). Draft genome sequence of a novel Coriobacteriaceae sp. strain, EMTCatB1, reconstructed from the metagenome of a thermophilic electromethanogenic biocathode. Genome Announc., 5(10), e00022-17.

Kobayashi, H., Saito, N., Fu, Q., Kawaguchi, H., Vilcaez, J., Wakayama, T., ... & Sato, K. (2013). Bio-electrochemical property and phylogenetic diversity of microbial communities associated with bioelectrodes of an electromethanogenic reactor. Journal of bioscience and bioengineering, 116(1), 114-117.

Koch, C., & Harnisch, F. (2016). Is there a specific ecological niche for electroactive microorganisms?. ChemElectroChem, 3(9), 1282-1295.

Korytár, P., Janssen, H. G., Matisová, E., & Udo, A. T. (2002). Practical fast gas chromatography: methods, instrumentation and applications. TrAC Trends in Analytical Chemistry, 21(9-10), 558-572.

Kotelnikova, S., Macario, A. J., & Pedersen, K. (1998). Methanobacterium subterraneum sp. nov., a new alkaliphilic, eurythermic and halotolerant methanogen isolated from deep granitic groundwater. International journal of systematic and evolutionary microbiology, 48(2), 357-367.

Krishna, K. V., Swathi, K., Hemalatha, M., & Mohan, S. V. (2019). Bioelectrocatalyst in Microbial Electrochemical Systems and Extracellular Electron Transport. In Microbial Electrochemical Technology (pp. 117-141). Elsevier.

Krivushin, K. V., Shcherbakova, V. A., Petrovskaya, L. E., & Rivkina, E. M. (2010). Methanobacterium veterum sp. nov., from ancient Siberian permafrost. International journal of systematic and evolutionary microbiology, 60(2), 455-459.

Kumar, A. N., Reddy, C. N., & Mohan, S. V. (2015). Biomineralization of azo dye bearing wastewater in periodic discontinuous batch reactor: Effect of microaerophilic conditions on treatment efficiency. Bioresource Technology, 188, 56-64.

Kumar, G., Saratale, R. G., Kadier, A., Sivagurunathan, P., Zhen, G., Kim, S. H., & Saratale, G. D. (2017). A review on bio-electrochemical systems (BESs) for the syngas and value added biochemicals production. Chemosphere, 177, 84-92.

Kumar, P., Chandrasekhar, K., Kumari, A., Sathiyamoorthi, E., & Kim, B. S. (2018). Electro-fermentation in aid of bioenergy and biopolymers. Energies, 11(2), 343.

Kuroda, K., Yamamoto, K., Nakai, R., Hirakata, Y., Kubota, K., Nobu, M. K., & Narihiro, T. (2022). Symbiosis between Candidatus Patescibacteria and Archaea Discovered in Wastewater-Treating Bioreactors. Mbio, 13(5), e01711-22.

Lee, C. (2022). Engineering Direct Interspecies Electron Transfer for Enhanced Methanogenic Performance. In Renewable Energy Technologies for Energy Efficient Sustainable Development (pp. 23-59). Springer, Cham.

Lee, H. S., & Rittmann, B. E. (2010). Characterization of energy losses in an upflow single-chamber microbial electrolysis cell. International journal of hydrogen energy, 35(3), 920-927.

Leung, D. Y., & Wang, J. (2016). An overview on biogas generation from anaerobic digestion of food waste. International Journal of Green Energy, 13(2), 119-131.

Leung, J. Y., Zhang, S., & Connell, S. D. (2022). Is Ocean Acidification Really a Threat to Marine Calcifiers? A Systematic Review and Meta-Analysis of 980+ Studies Spanning Two Decades. Small, 18(35), 2107407.

Li, H., Opgenorth, P. H., Wernick, D. G., Rogers, S., Wu, T. Y., Higashide, W., ... & Liao, J. C. (2012). Integrated electromicrobial conversion of CO2 to higher alcohols. Science, 335(6076), 1596-1596.

Li, X., Angelidaki, I., & Zhang, Y. (2018). Salinity-gradient energy driven microbial electrosynthesis of value-added chemicals from CO2 reduction. Water research, 142, 396-404.

Li, Y., Han, D., Sommerfeld, M., & Hu, Q. (2011). Photosynthetic carbon partitioning and lipid production in the oleaginous microalga Pseudochlorococcum sp.(Chlorophyceae) under nitrogen-limited conditions. Bioresource technology, 102(1), 123-129.

Li, Y., Liu, H., Yan, F., Su, D., Wang, Y., & Zhou, H. (2017). High-calorific biogas production from anaerobic digestion of food waste using a two-phase pressurized biofilm (TPPB) system. Bioresource technology, 224, 56-62.

Li, Y., Yang, H. Y., Shen, J. Y., Mu, Y., & Yu, H. Q. (2016). Enhancement of azo dye decolourization in a MFC–MEC coupled system. Bioresource technology, 202, 93-100.

Lin, C. S. K., Pfaltzgraff, L. A., Herrero-Davila, L., Mubofu, E. B., Abderrahim, S., Clark, J. H., ... & Luque, R. (2013). Food waste as a valuable resource for the production of chemicals, materials and fuels. Current situation and global perspective. Energy & Environmental Science, 6(2), 426-464.

Lin, C., Wu, P., Liu, Y., Wong, J. W., Yong, X., Wu, X., ... & Zhou, J. (2019). Enhanced biogas production and biodegradation of phenanthrene in wastewater sludge treated anaerobic digestion reactors fitted with a bioelectrode system. Chemical Engineering Journal, 365, 1-9.

Lin, H., Williams, N., King, A., & Hu, B. (2016). Electrochemical sulfide removal by low-cost electrode materials in anaerobic digestion. Chemical Engineering Journal, 297, 180-192.

Lin, Y., Lü, F., Shao, L., & He, P. (2013). Influence of bicarbonate buffer on the methanogenetic pathway during thermophilic anaerobic digestion. Bioresource technology, 137, 245-253.

Liu, H., Chen, Y., Ye, J., Xu, H., Zhu, Z., & Xu, T. (2021). Effects of different amino acids and their configurations on methane yield and biotransformation of intermediate metabolites during anaerobic digestion. Journal of Environmental Management, 296, 113152.

Liu, H., Grot, S., & Logan, B. E. (2005). Electrochemically assisted microbial production of hydrogen from acetate. Environmental science & technology, 39(11), 4317-4320.

Liu, H., Hu, H., Chignell, J., & Fan, Y. (2010). Microbial electrolysis: novel technology for hydrogen production from biomass. Biofuels, 1(1), 129-142.

Liu, M., Yuan, Y., Zhang, L. X., Zhuang, L., Zhou, S. G., & Ni, J. R. (2010). Bioelectricity generation by a Gram-positive Corynebacterium sp. strain MFC03 under alkaline condition in microbial fuel cells. Bioresource technology, 101(6), 1807-1811.

Liu, W., Cai, W., Guo, Z., Wang, L., Yang, C., Varrone, C., & Wang, A. (2016). Microbial electrolysis contribution to anaerobic digestion of waste activated sludge, leading to accelerated methane production. Renewable Energy, 91, 334-339.

Liu, X., Wang, L., Wang, S., Cai, R., Yue, T., Yuan, Y., ... & Wang, Z. (2023). Detoxification of patulin in apple juice by enzymes and evaluation of its degradation products. Food Control, 145, 109518.

Liu, Y. P., Wang, Y. H., Wang, B. S., & Chen, Q. Y. (2014). Effect of anolyte pH and cathode Pt loading on electricity and hydrogen co-production performance of the bio-electrochemical system. International Journal of Hydrogen Energy, 39(26), 14191-14195.

Liu, Y., Xu, H. L., Yang, S. F., & Tay, J. H. (2003). Mechanisms and models for anaerobic granulation in upflow anaerobic sludge blanket reactor. Water Research, 37(3), 661-673.

Lo, Y. C., Saratale, G. D., Chen, W. M., Bai, M. D., & Chang, J. S. (2009). Isolation of cellulose-hydrolytic bacteria and applications of the cellulolytic enzymes for cellulosic biohydrogen production. Enzyme and Microbial Technology, 44(6-7), 417-425.

Logan, B. E. (2009). Exoelectrogenic bacteria that power microbial fuel cells. Nature Reviews Microbiology, 7(5), 375.

Logan, B. E., & Rabaey, K. (2012). Conversion of wastes into bioelectricity and chemicals by using microbial electrochemical technologies. Science, 337(6095), 686-690.

Logan, B. E., Call, D., Cheng, S., Hamelers, H. V., Sleutels, T. H., Jeremiasse, A. W., & Rozendal, R. A. (2008). Microbial electrolysis cells for high yield hydrogen gas production from organic matter. Environmental science & technology, 42(23), 8630-8640.

Logan, B. E., Hamelers, B., Rozendal, R., Schröder, U., Keller, J., Freguia, S., ... & Rabaey, K. (2006). Microbial fuel cells: methodology and technology. Environmental science & technology, 40(17), 5181-5192.

Long, H., Wang, S., Wu, W., & Zhang, G. (2022). The economic influence of oil shortage and the optimal strategic petroleum reserve in China. Energy Reports, 8, 9858-9870.

Lopes, W. S., Leite, V. D., & Prasad, S. (2004). Influence of inoculum on performance of anaerobic reactors for treating municipal solid waste. Bioresource technology, 94(3), 261-266.

Loukas, Y.L. (2001). A Plackett—Burnam screening design directs the efficient formulation of multicomponent DRV liposomes. Journal of Pharmaceutical and Biomedical Analysis 26 (2), 255-63.

Louro, R. O., Costa, N. L., Fernandes, A. P., Silva, A. V., Trindade, I. B., Fonseca, B. M., & Paquete, C. M. (2019). Exploring the Molecular Mechanisms of Extracellular Electron Transfer for Harnessing Reducing Power in METs: Methodologies and Approaches. In Microbial Electrochemical Technology (pp. 261-293). Elsevier.

Lowry, O. H., Rosebrough, N. J., Farr, A. L., & Randall, R. J. (1951). Protein measurement with the Folin phenol reagent. Journal of biological chemistry, 193, 265-275.

Lu, L., & Ren, Z. J. (2016). Microbial electrolysis cells for waste biorefinery: A state of the art review. Bioresource technology, 215, 254-264.

Lu, L., Ren, N., Xing, D., & Logan, B. E. (2009). Hydrogen production with effluent from an ethanol–H2-coproducing fermentation reactor using a single-chamber microbial electrolysis cell. Biosensors and Bioelectronics, 24(10), 3055-3060.

Lu, L., Ren, N., Zhao, X., Wang, H., Wu, D., & Xing, D. (2011). Hydrogen production, methanogen inhibition and microbial community structures in psychrophilic single-chamber microbial electrolysis cells. Energy & Environmental Science, 4(4), 1329-1336.

Lu, L., Xing, D., Xie, T., Ren, N., & Logan, B. E. (2010). Hydrogen production from proteins via electrohydrogenesis in microbial electrolysis cells. Biosensors and Bioelectronics, 25(12), 2690-2695.

Lu, S., Tan, G., & Zhu, X. (2020). H2 Evolution Catalysts for Microbial Electrolysis Cells. Novel Catalyst Materials for Bioelectrochemical Systems: Fundamentals and Applications, 27-43.

Lu, Y., Qin, M., Yuan, H., Abu-Reesh, I., & He, Z. (2015). When bioelectrochemical systems meet forward osmosis: accomplishing wastewater treatment and reuse through synergy. Water, 7(1), 38-50.

Lu, Y., Qin, M., Yuan, H., Abu-Reesh, I., & He, Z. (2015). When bioelectrochemical systems meet forward osmosis: accomplishing wastewater treatment and reuse through synergy. Water, 7(1), 38-50.

Luo, H., Jenkins, P. E., & Ren, Z. (2011). Concurrent desalination and hydrogen generation using microbial electrolysis and desalination cells. Environmental science & technology, 45(1), 340-344.

Luo, H., Liu, G., Zhang, R., Bai, Y., Fu, S., & Hou, Y. (2014). Heavy metal recovery combined with H2 production from artificial acid mine drainage using the microbial electrolysis cell. Journal of hazardous materials, 270, 153-159.

Luton, P. E., Wayne, J. M., Sharp, R. J., & Riley, P. W. (2002). The mcrA gene as an alternative to 16S rRNA in the phylogenetic analysis of methanogen populations in landfillbbThe GenBank accession numbers for the mcrA sequences reported in this paper are AF414034–AF414051 (see Fig. 2) and AF414007–AF414033 (environmental isolates in Fig. 3). Microbiology, 148(11), 3521-3530.

Lv, Y., & Wang, X. (2017). Nonprecious metal phosphides as catalysts for hydrogen evolution, oxygen reduction and evolution reactions. Catalysis Science & Technology, 7(17), 3676-3691.

Ma, H., Liu, W. W., Chen, X., Wu, Y. J., & Yu, Z. L. (2009). Enhanced enzymatic saccharification of rice straw by microwave pretreatment. Bioresource technology, 100(3), 1279-1284.

Ma, K., Liu, X., & Dong, X. (2005). Methanobacterium beijingense sp. nov., a novel methanogen isolated from anaerobic digesters. International Journal of Systematic and Evolutionary Microbiology, 55(1), 325-329.

Madigan, M. T., Martinko, J. M., & Parker, J. (2003). Microbial growth. Brock biology of microorganisms, 137-166.

Marcucci, M., Ciardelli, G., Matteucci, A., Ranieri, L., & Russo, M. (2002). Experimental campaigns on textile wastewater for reuse by means of different membrane processes. Desalination, 149(1-3), 137-143.

Marshall, C. W., LaBelle, E. V., & May, H. D. (2013). Production of fuels and chemicals from waste by microbiomes. Current opinion in biotechnology, 24(3), 391-397.

Marshall, C. W., Ross, D. E., Fichot, E. B., Norman, R. S., & May, H. D. (2012). Electrosynthesis of commodity chemicals by an autotrophic microbial community. Applied and environmental microbiology, 78(23), 8412-8420.

Marshall, C. W., Ross, D. E., Fichot, E. B., Norman, R. S., & May, H. D. (2013). Long-term operation of microbial electrosynthesis systems improves acetate production by autotrophic microbiomes. Environmental science & technology, 47(11), 6023-6029.

Marshall, C. W., Ross, D. E., Fichot, E. B., Norman, R. S., & May, H. D. (2012). Electrosynthesis of commodity chemicals by an autotrophic microbial community. Applied and environmental microbiology, 78(23), 8412-8420.

Marsili, E., Baron, D. B., Shikhare, I. D., Coursolle, D., Gralnick, J. A., & Bond, D. R. (2008). Shewanella secretes flavins that mediate extracellular electron transfer. Proceedings of the National Academy of Sciences, 105(10), 3968-3973.

Martínez, E. J., Sotres, A., Arenas, C. B., Blanco, D., Martínez, O., & Gómez, X. (2019). Improving Anaerobic Digestion of Sewage Sludge by Hydrogen Addition: Analysis of Microbial Populations and Process Performance. Energies, 12(7), 1228.

Maryam, L., Zohreh, H. E., Mohsen, 13. (2007). Evaluation of culture conditions for Genuine production by two Trichodenna reesei mutants under solid-state fermentation conditions. Bioresource Technology 98, 3634-3637.

Matsakas, L., Kekos, D., Loizidou, M., & Christakopoulos, P. (2014). Utilization of household food waste for the production of ethanol at high dry material content. Biotechnology for biofuels, 7(1), 1-9.

Michelin, M., Gomes, D. G., Romaní, A., Polizeli, M. D. L. T., & Teixeira, J. A. (2020). Nanocellulose production: exploring the enzymatic route and residues of pulp and paper industry. Molecules, 25(15), 3411.

Miller, G. L. (1959). Use of dinitrosalicylic acid reagent for determination of reducing sugar. Analytical chemistry, 31(3), 426-428.

Mital, K. M. (1997). Biogas systems: policies, progress and prospects. Taylor & Francis.

Mitra, G. and Wilke, C. R. (1975) Continuous cellulase production. Biotechnology and Bioengineering 17, 1-13.

Modestra, J. A., Reddy, C. N., Krishna, K. V., Min, B., & Mohan, S. V. (2020). Regulated surface potential impacts bioelectrogenic activity, interfacial electron transfer and microbial dynamics in microbial fuel cell. Renewable Energy, 149, 424-434.

Modin, O., Wang, X., Wu, X., Rauch, S., & Fedje, K. K. (2012). Bioelectrochemical recovery of Cu, Pb, Cd, and Zn from dilute solutions. Journal of hazardous materials, 235, 291-297.

Mohan, S. V., Chiranjeevi, P., & Mohanakrishna, G. (2012). A rapid and simple protocol for evaluating biohydrogen production potential (BHP) of wastewater with simultaneous process optimization. international journal of hydrogen energy, 37(4), 3130-3141.

Mohan, S. V., Mohanakrishna, G., Raghavulu, S. V., & Sarma, P. N. (2007). Enhancing biohydrogen production from chemical wastewater treatment in anaerobic sequencing batch biofilm reactor (AnSBBR) by bioaugmenting with selectively enriched kanamycin resistant anaerobic mixed consortia. International Journal of Hydrogen Energy, 32(15), 3284-3292.

Mohan, S., & Jagadeesan, K. (2013). Production of biogas by using food waste. International journal of engineering research and application, 3(4), 390-394.

Mohanakrishna, G., Vanbroekhoven, K., & Pant, D. (2018). Impact of dissolved carbon dioxide concentration on the process parameters during its conversion to acetate through microbial electrosynthesis. Reaction Chemistry & Engineering, 3(3), 371-378.

Mohapatra, R. K., Padhi, D., Sen, R., & Nayak, M. (2022). Bio-inspired CO2 capture and utilization by microalgae for bioenergy feedstock production: A greener approach for environmental protection. Bioresource Technology Reports, 101116.

Molino, A., Nanna, F., Ding, Y., Bikson, B., & Braccio, G. (2013). Biomethane production by anaerobic digestion of organic waste. Fuel, 103, 1003-1009.

Montpart, N., Rago, L., Baeza, J. A., & Guisasola, A. (2015). Hydrogen production in single chamber microbial electrolysis cells with different complex substrates. Water research, 68, 601-615.

Moon, H. C., & Song, I. S. (2011). Enzymatic hydrolysis of food waste and methane production using UASB bioreactor. International Journal of Green Energy, 8(3), 361-371.

Morais, B. P., Martins, V., Martins, G., Castro, A. R., Alves, M. M., Pereira, M. A., & Cavaleiro, A. J. (2021). Hydrocarbon toxicity towards hydrogenotrophic methanogens in oily waste streams. Energies, 14(16), 4830.

Moreno, R., San-Martín, M. I., Escapa, A., & Morán, A. (2016). Domestic wastewater treatment in parallel with methane production in a microbial electrolysis cell. Renewable Energy, 93, 442-448.

Morita, M., & Sasaki, K. (2012). Factors influencing the degradation of garbage in methanogenic bioreactors and impacts on biogas formation. Applied microbiology and biotechnology, 94(3), 575-582.

Moussa, S. B., Maurin, G., Gabrielli, C., & Amor, M. B. (2006). Electrochemical precipitation of struvite. Electrochemical and Solid-State Letters, 9(6), C97.

Mu, Y., Rabaey, K., Rozendal, R. A., Yuan, Z., & Keller, J. (2009). Decolorization of azo dyes in bioelectrochemical systems. Environmental science & technology, 43(13), 5137-5143.

Muddasar, M., Liaquat, R., Aslam, A., Ur Rahman, M. Z., Abdullah, A., Khoja, A. H., ... & Bahadar, A. (2022). Performance efficiency comparison of microbial electrolysis cells for sustainable production of biohydrogen—A comprehensive review. International Journal of Energy Research, 46(5), 5625-5645.

Muñoz, R., Meier, L., Diaz, I., & Jeison, D. (2015). A review on the state-of-the-art of physical/chemical and biological technologies for biogas upgrading. Reviews in Environmental Science and Bio/Technology, 14(4), 727-759.

Najafpour, G., Younesi, H., & Ismail, K. S. K. (2004). Ethanol fermentation in an immobilized cell reactor using Saccharomyces cerevisiae. Bioresource Technology, 92 (3), 251-260.

Nakamura, R., Kai, F., Okamoto, A., & Hashimoto, K. (2013). Mechanisms of long-distance extracellular electron transfer of metal-reducing bacteria mediated by nanocolloidal semiconductive iron oxides. Journal of Materials Chemistry A, 1(16), 5148-5157.

Nam, J. Y., Yates, M. D., Zaybak, Z., & Logan, B. E. (2014). Examination of protein degradation in continuous flow, microbial electrolysis cells treating fermentation wastewater. Bioresource technology, 171, 182-186.

Nasir, I. M., Ghazi, T. I. M., & Omar, R. (2012). Production of biogas from solid organic wastes through anaerobic digestion: a review. Applied microbiology and biotechnology, 95(2), 321-329.

Naveena, B. J., Altaf, M., Bhadriah, K. (2005). Selection of medium components by Plackett–Burman design for production of L (+) lactic acid by Lactobacillus amylophilus GV6 in SSF using wheat bran. Bioresource Technology 96 (4), 485-90.

Neves, L., Ribeiro, R., Oliveira, R., & Alves, M. M. (2006). Enhancement of methane production from barley waste. Biomass and Bioenergy, 30(6), 599-603.

Nevin, K. P., Woodard, T. L., Franks, A. E., Summers, Z. M., & Lovley, D. R. (2010). Microbial electrosynthesis: feeding microbes electricity to convert carbon dioxide and water to multicarbon extracellular organic compounds. MBio, 1(2).

Nguyen, V. K., Chaudhary, D. K., Dahal, R. H., Trinh, N. H., Kim, J., Chang, S. W., ... & Nguyen, D. D. (2021). Review on pretreatment techniques to improve anaerobic digestion of sewage sludge. Fuel, 285, 119105.

Nielsen, S. S. (2010). Phenol-sulfuric acid method for total carbohydrates. In Food analysis laboratory manual (pp. 47-53). Springer, Boston, MA.

Nimje, V. R., Chen, C. Y., Chen, C. C., Chen, H. R., Tseng, M. J., Jean, J. S., & Chang, Y. F. (2011). Glycerol degradation in single-chamber microbial fuel cells. Bioresource technology, 102(3), 2629-2634.

Nimje, V. R., Chen, C. Y., Chen, C. C., Jean, J. S., Reddy, A. S., Fan, C. W., ... & Chen, J. L. (2009). Stable and high energy generation by a strain of Bacillus subtilis in a microbial fuel cell. Journal of Power Sources, 190(2), 258-263.

Niranjane, A. P., Madhou, P., Stevenson, T.W. (2007). The effect of carbohydrate carbon sources on the production of cellulase by Phlebia gigantean. Enzyme and Microbial Technology 40, 1464-1468.

O'Connor, F. M., Johnson, B. T., Jamil, O., Andrews, T., Mulcahy, J. P., & Manners, J. (2022). Apportionment of the Pre-Industrial to Present-Day Climate Forcing by Methane Using UKESM1: The Role of the Cloud Radiative Effect. Journal of Advances in Modeling Earth Systems, 14(10), e2022MS002991.

Oh, Y. K., Kim, S. H., Kim, M. S., & Park, S. (2004). Thermophilic biohydrogen production from glucose with trickling biofilter. Biotechnology and bioengineering, 88(6), 690-698.

Okeh, O. C., Onwosi, C. O., & Odibo, F. J. C. (2014). Biogas production from rice husks generated from various rice mills in Ebonyi State, Nigeria. Renewable Energy, 62, 204-208.

Oladoja, N. A., Unuabonah, E. I., Amuda, O. S., & Kolawole, O. M. (2017). Polysaccharides as a green and sustainable resources for water and wastewater treatment. Springer.

Oliveira, S. C., Oliveira, R. C., Tacin, M. V., & Gattás, E. A. (2016). Kinetic Modeling and Optimization of a Batch Ethanol Fermentation Process. Journal of Bioprocessing & Biotechniques, 2016.

Özek, G., Ishmuratova, M., Tabanca, N., Radwan, M. M., Göger, F., Özek, T., ... & Can Başer, K. H. (2012). One-step multiple component isolation from the oil of C rinitaria tatarica (Less.) S ojak by preparative capillary gas chromatography with characterization by spectroscopic and spectrometric techniques and evaluation of biological activity. Journal of separation science, 35(5-6), 650-660.

Pal, P., Singh, N., Kaur, P., Kaur, A., Virdi, A. S., & Parmar, N. (2016). Comparison of composition, protein, pasting, and phenolic compounds of brown rice and germinated brown rice from different cultivars. Cereal Chemistry, 93(6), 584-592.

Pan, L., Ren, Y., Cui, F., & Xu, Q. (2009). Viability and differentiation of neural precursors on hyaluronic acid hydrogel scaffold. Journal of Neuroscience Research, 87(14), 3207-3220.

Pant, D., Singh, A., Van Bogaert, G., Gallego, Y. A., Diels, L., & Vanbroekhoven, K. (2011). An introduction to the life cycle assessment (LCA) of bioelectrochemical systems (BES) for sustainable energy and product generation: relevance and key aspects. Renewable and Sustainable Energy Reviews, 15(2), 1305-1313.

Pant, D., Singh, A., Van Bogaert, G., Olsen, S. I., Nigam, P. S., Diels, L., & Vanbroekhoven, K. (2012). Bioelectrochemical systems (BES) for sustainable energy production and product recovery from organic wastes and industrial wastewaters. Rsc Advances, 2(4), 1248-1263.

Pant, D., Van Bogaert, G., Diels, L., & Vanbroekhoven, K. (2010). A review of the substrates used in microbial fuel cells (MFCs) for sustainable energy production. Bioresource technology, 101(6), 1533-1543.

Parawira, W., Murto, M., Read, J. S., & Mattiasson, B. (2005). Profile of hydrolases and biogas production during two-stage mesophilic anaerobic digestion of solid potato waste. Process Biochemistry, 40(9), 2945-2952.

Paritosh, K., Kushwaha, S. K., Yadav, M., Pareek, N., Chawade, A., & Vivekanand, V. (2017). Food waste to energy: an overview of sustainable approaches for food waste management and nutrient recycling. BioMed research international, 2017.

Park, J., Lee, B., Tian, D., & Jun, H. (2018). Bioelectrochemical enhancement of methane production from highly concentrated food waste in a combined anaerobic digester and microbial electrolysis cell. Bioresource technology, 247, 226-233.

Park, S. G., Rajesh, P. P., Sim, Y. U., Jadhav, D. A., Noori, M. T., Kim, D. H., ... & Chae, K. J. (2022). Addressing scale-up challenges and enhancement in performance of hydrogen-producing microbial electrolysis cell through electrode modifications. Energy Reports, 8, 2726-2746.

Park, S. G., Rhee, C., Jadhav, D. A., Eisa, T., Al-Mayyahi, R. B., Shin, S. G., ... & Chae, K. J. (2023). Tailoring a highly conductive and super-hydrophilic electrode for biocatalytic performance of microbial electrolysis cells. Science of The Total Environment, 856, 159105.

Parthasarathi, R., Sun, J., Dutta, T., Sun, N., Pattathil, S., Murthy Konda, N. V. S. N., ... & Singh, S. (2016). Activation of lignocellulosic biomass for higher sugar yields using aqueous ionic liquid at low severity process conditions. Biotechnology for biofuels, 9(1), 1-13.

Pasupuleti, S. B., Srikanth, S., Mohan, S. V., & Pant, D. (2015). Development of exoelectrogenic bioanode and study on feasibility of hydrogen production using abiotic VITO-CoRE™ and VITO-CASE™ electrodes in a single chamber microbial electrolysis cell (MEC) at low current densities. Bioresource technology, 195, 131-138.

Patel, G. B., Sprott, G. D., & Fein, J. E. (1990). Isolation and characterization of Methanobacterium espanolae sp. nov., a mesophilic, moderately acidiphilic methanogen. International Journal of Systematic and Evolutionary Microbiology, 40(1), 12-18.

Patel, M. S., & Roche, T. E. (1990). Molecular biology and biochemistry of pyruvate dehydrogenase complexes 1. The FASEB Journal, 4(14), 3224-3233.

Pavi, S., Kramer, L. E., Gomes, L. P., & Miranda, L. A. S. (2017). Biogas production from co-digestion of organic fraction of municipal solid waste and fruit and vegetable waste. Bioresource technology, 228, 362-367.

Pawar, A. A., Karthic, A., Lee, S., Pandit, S., & Jung, S. P. (2022). Microbial electrolysis cells for electromethanogenesis: Materials, configurations and operations. Environmental Engineering Research, 27(1).

Pegler, D. N. (1983). The genus Lentinus. Kew Bull Addit Ser, 10, 1-281.

Peng, H., Zhao, Z., Xiao, H., Yang, Y., Zhao, H., & Zhang, Y. (2019). A strategy for enhancing anaerobic digestion of waste activated sludge: Driving anodic oxidation by adding nitrate into microbial electrolysis cell. Journal of Environmental Sciences, 81, 34-42.

Perez, D. (2021). Operation of Microbial Electrolysis Cells for Methane Production (Doctoral dissertation, Auckland University of Technology).

Pérez-Elvira, S. I., Diez, P. N., & Fdz-Polanco, F. (2006). Sludge minimisation technologies. Reviews in Environmental Science and Bio/Technology, 5(4), 375-398.

Pérez-Rodríguez, N., García-Bernet, D., & Domínguez, J. M. (2017). Extrusion and enzymatic hydrolysis as pretreatments on corn cob for biogas production. Renewable Energy, 107, 597-603.

Perona-Vico, E., Blasco-Gómez, R., Colprim, J., Puig, S., & Bañeras, L. (2019). [NiFe]-hydrogenases are constitutively expressed in an enriched Methanobacterium sp. population during electromethanogenesis. PloS one, 14(4), e0215029.

Perrone, G., Stea, G., Epifani, F., Varga, J., Frisvad, J. C., & Samson, R. A. (2011). Aspergillus niger contains the cryptic phylogenetic species A. awamori. Fungal biology, 115(11), 1138-1150.

Persson, M. (2003). Evaluation of upgrading techniques for biogas. Report SGC, 142.

Pham, T. H., Rabaey, K., Aelterman, P., Clauwaert, P., De Schamphelaire, L., Boon, N., & Verstraete, W. (2006). Microbial fuel cells in relation to conventional anaerobic digestion technology. Engineering in Life Sciences, 6(3), 285-292.

Pham, V. H. T., Ahn, J. Y., Ro, Y. H., Ravindran, B., Kim, J. S., Chang, S. W., ... & Chung, W. J. (2022). The efficiency of potential food waste-degrading bacteria under harsh conditions. Journal of Applied Microbiology, 132(1), 340-350.

Pinck, S., Ostormujof, L. M., Teychené, S., & Erable, B. (2020). Microfluidic Microbial Bioelectrochemical Systems: An Integrated Investigation Platform for a More Fundamental Understanding of Electroactive Bacterial Biofilms. Microorganisms, 8(11), 1841.

Pinto, F. C. J., Lima, D. B. D., Agustini, B. C., Dallagassa, C. B., Shimabukuro, M. F., Chimelli, M., & Bonfim, T. M. B. (2012). Morphological and molecular identification of filamentous fungi isolated from cosmetic powders. Brazilian Archives of Biology and Technology, 55(6), 897-901.

Plackett, Rt., Burman, J. P. (1946). The design of optimum multifactor experiments. Biometrika 33, 305-25.

Poh, P. E., & Chong, M. F. (2010). Biomethanation of Palm Oil Mill Effluent (POME) with a thermophilic mixed culture cultivated using POME as a substrate. Chemical Engineering Journal, 164(1), 146-154.

Poi, A. (1985). Studies on a lab-scale fluidized bed reactor: fundamental studies of surface attachment by Klebsiella oxytoca. University of New South Wales.

Posadas-Hernández, M., García-Rojas, J. L., Khamkure, S., García-Sánchez, L., Gutierrez-Macías, T., Morales-Morales, C., & Estrada-Arriaga, E. B. (2022). Enhanced biohydrogen production in a membraneless single-chamber microbial electrolysis cell during high-strength wastewater treatment: Effect of electrode materials and configurations. International Journal of Hydrogen Energy.

Pour, F. H., & Makkawi, Y. T. (2021). A review of post-consumption food waste management and its potentials for biofuel production. Energy Reports, 7, 7759-7784.

Prasad, D., Arun, S., Murugesan, M., Padmanaban, S., Satyanarayanan, R. S., Berchmans, S., & Yegnaraman, V. (2007). Direct electron transfer with yeast cells and construction of a mediatorless microbial fuel cell. Biosensors and Bioelectronics, 22(11), 2604-2610.

Premier, G. C., Kim, J. R., Michie, I., Dinsdale, R. M., & Guwy, A. J. (2011). Automatic control of load increases power and efficiency in a microbial fuel cell. Journal of Power Sources, 196(4), 2013-2019.

Qu, Y., Xiao, C., Workie, E., Zhang, J., He, Y., & Tong, Y. W. (2021). Bioelectrochemical enhancement of methanogenic metabolism in Anaerobic digestion of food waste under salt stress conditions. ACS Sustainable Chemistry & Engineering, 9(40), 13526-13535.

Rabaey, K., & Rozendal, R. A. (2010). Microbial electrosynthesis—revisiting the electrical route for microbial production. Nature Reviews Microbiology, 8(10), 706.

Rabii, A., Aldin, S., Dahman, Y., & Elbeshbishy, E. (2019). A review on anaerobic co-digestion with a focus on the microbial populations and the effect of multi-stage digester configuration. Energies, 12(6), 1106.

Rachbauer, L., Voitl, G., Bochmann, G., & Fuchs, W. (2016). Biological biogas upgrading capacity of a hydrogenotrophic community in a trickle-bed reactor. Applied Energy, 180, 483-490.

Rader, G. K., & Logan, B. E. (2010). Multi-electrode continuous flow microbial electrolysis cell for biogas production from acetate. international journal of hydrogen energy, 35(17), 8848-8854.

Raghavulu, S. V., Goud, R. K., Sarma, P. N., & Mohan, S. V. (2011). Saccharomyces cerevisiae as anodic biocatalyst for power generation in biofuel cell: influence of redox condition and substrate load. Bioresource technology, 102(3), 2751-2757.

Rambla, F. J., Garrigues, S., & De La Guardia, M. (1997). PLS-NIR determination of total sugar, glucose, fructose and sucrose in aqueous solutions of fruit juices. Analytica Chimica Acta, 344(1-2), 41-53.

Ramesh, S. T., Jayanthi, S., & Gandhimathi, R. (2008). Feasibility study on anaerobic digestion of garbage using lime pretreatment. Jr. of Industrial Pollution Control, 24, 123-128.

Rampelotto, P. H. (2013). Extremophiles and extreme environments. Life, 3(3), 482-485.

Rani, P., Bishnoi, K., Bishnoi, N. R., Kumar, D., & Singh, A. (2022). Biohydrogen Production Technologies: Past, Present, and Future Perspective. In Biomass, Bioenergy & Bioeconomy (pp. 185-205). Springer, Singapore.

Rashid, M. A., Jabloun, M., Andersen, M. N., Zhang, X., & Olesen, J. E. (2019). Climate change is expected to increase yield and water use efficiency of wheat in the North China Plain. Agricultural Water Management, 222, 193-203.

Rashid, U., Anwar, F., Ashraf, M., Saleem, M., & Yusup, S. (2011). Application of response surface methodology for optimizing transesterification of Moringa oleifera oil: Biodiesel production. Energy conversion and Management, 52(8-9), 3034-3042.

Reguera, G., McCarthy, K. D., Mehta, T., Nicoll, J. S., Tuominen, M. T., & Lovley, D. R. (2005). Extracellular electron transfer via microbial nanowires. Nature, 435(7045), 1098-1101.

Rehan, M., Nizami, A. S., Shahzad, K., Ouda, O. K. M., Ismail, I. M. I., Almeelbi, T., ... & Demirbas, A. (2016). Pyrolytic liquid fuel: a source of renewable electricity generation in Makkah. Energy Sources, Part A: Recovery, Utilization, and Environmental Effects, 38(17), 2598-2603.

Ren, Y., Wang, T., & Wang, J. (2011). Characterization of biohydrogen production by co-fermentation of glucose and xylose [J]. CIESC Journal, 9.

Reshmy, R., Philip, E., Madhavan, A., Sirohi, R., Pugazhendhi, A., Binod, P., ... & Sindhu, R. (2022). Lignocellulose in future biorefineries: Strategies for cost-effective production of biomaterials and bioenergy. Bioresource Technology, 344, 126241.

Riaz, M., Rashid, M. H., Sawyer, L., Akhtar, S., Javed, M. R., Nadeem, H., & Wear, M. (2012). Physiochemical properties and kinetics of glucoamylase produced from deoxy-D-glucose resistant mutant of Aspergillus niger for soluble starch hydrolysis. Food chemistry, 130(1), 24-30.

Riccaboni, A., Neri, E., Trovarelli, F., & Pulselli, R. M. (2021). Sustainability-oriented research and innovation in 'farm to fork'value chains. Current Opinion in Food Science, 42, 102-112.

Richardson, D. J., Butt, J. N., Fredrickson, J. K., Zachara, J. M., Shi, L., Edwards, M. J., ... & Clarke, T. A. (2012). The 'porin–cytochrome'model for microbe-to-mineral electron transfer. Molecular microbiology, 85(2), 201-212.

Rosenberg, E., DeLong, E. F., Lory, S., Stackebrandt, E., & Thompson, F. (Eds.). (2014). The prokaryotes: other major lineages of Bacteria and the Archaea.

Rotaru, A. E., Shrestha, P. M., Liu, F., Markovaite, B., Chen, S., Nevin, K. P., & Lovley, D. R. (2014). Direct interspecies electron transfer between Geobacter metallireducens and Methanosarcina barkeri. Applied and environmental microbiology, 80(15), 4599-4605.

Rovira-Alsina, L., Romans-Casas, M., Balaguer, M. D., & Puig, S. (2022). Thermodynamic approach to foresee experimental CO2 reduction to organic compounds. Bioresource Technology, 354, 127181.

Roycroft, E., Fitzgibbon, M. M., Cruz, A. G., O'Meara, M., Downes, R. F., & O'Toole, R. F. (2016). Cluster Analysis of Mycobacterium tuberculosis using Whole Genome Sequencing (WGS): The Irish Mycobacteria Reference Laboratory (IMRL) Experience. In ASM Microbe 2016.

Rozendal, R. A., Hamelers, H. V., Euverink, G. J., Metz, S. J., & Buisman, C. J. (2006). Principle and perspectives of hydrogen production through biocatalyzed electrolysis. International journal of hydrogen energy, 31(12), 1632-1640.

Rozendal, R. A., Hamelers, H. V., Molenkamp, R. J., & Buisman, C. J. (2007). Performance of single chamber biocatalyzed electrolysis with different types of ion exchange membranes. Water research, 41(9), 1984-1994.

Rozendal, R. A., Hamelers, H. V., Rabaey, K., Keller, J., & Buisman, C. J. (2008). Towards practical implementation of bioelectrochemical wastewater treatment. Trends in biotechnology, 26(8), 450-459.

Rozendal, R. A., Leone, E., Keller, J., & Rabaey, K. (2009). Efficient hydrogen peroxide generation from organic matter in a bioelectrochemical system. Electrochemistry Communications, 11(9), 1752-1755.

Rozendal, R.A., et al., 2007. Performance of single chamber biocatalyzed electrolysis with different types of ion exchange membranes. Water Res. 41 (9), 1984–1994.

Rozenfeld, S., Ouaknin Hirsch, L., Gandu, B., Farber, R., Schechter, A., & Cahan, R. (2019). Improvement of Microbial Electrolysis Cell Activity by Using Anode Based on Combined Plasma-Pretreated Carbon Cloth and Stainless Steel. Energies, 12(10), 1968.

Ruocco, C., Cortese, M., Martino, M., & Palma, V. (2022). Fuel grade bioethanol reforming in a fluidized bed reactor over highly durable Pt-Ni/CeO2-SiO2 catalysts. Chemical Engineering and Processing-Process Intensification, 174, 108888.orted, Pt-promoted iron Fischer–Tropsch catalysts. Topics in catalysis, 26(1), 55-71.

Sadeghi, N., Sharifnia, S., & Arabi, M. S. (2016). A porphyrin-based metal organic framework for high rate photoreduction of CO2 to CH4 in gas phase. Journal of CO2 Utilization, 16, 450-457.

Sadhukhan, J., Lloyd, J. R., Scott, K., Premier, G. C., Eileen, H. Y., Curtis, T., & Head, I. M. (2016). A critical review of integration analysis of microbial electrosynthesis (MES) systems with waste biorefineries for the production of biofuel and chemical from reuse of CO2. Renewable and Sustainable Energy Reviews, 56, 116-132.

Saha, B. C., & Cotta, M. A. (2008). Lime pretreatment, enzymatic saccharification and fermentation of rice hulls to ethanol. Biomass and Bioenergy, 32(10), 971-977.

Sakai, S., & Yagishita, T. (2007). Microbial production of hydrogen and ethanol from glycerol-containing wastes discharged from a biodiesel fuel production plant in a bioelectrochemical reactor with thionine. Biotechnology and bioengineering, 98(2), 340-348.

Sakthi, S. S., Kanchana, D., Saranraj, P., & Usharani, G. (2012). Evaluation of amylase activity of the amylolytic fungi Aspergillus niger using cassava as substrate. Int J Appl Microbiol Sci, 1, 24-34.

Salihu, A., & Alam, M. Z. (2016). Pretreatment methods of organic wastes for biogas production. J. Appl. Sci, 16(3), 124-137.

Salihu, A., Alam, M. Z., AbdulKarim, M. I., & Salleh, H. M. (2011). Optimization of lipase production by Candida cylindracea in palm oil mill effluent based medium using statistical experimental design. Journal of Molecular Catalysis B: Enzymatic, 69 (1), 66-73.

Samuels, G. J., Ismaiel, A., Mulaw, T. B., Szakacs, G., Druzhinina, I. S., Kubicek, C. P., & Jaklitsch, W. M. (2012). The Longibrachiatum Clade of Trichoderma: a revision with new species. Fungal diversity, 55(1), 77-108.

Sangeetha, T., Guo, Z., Liu, W., Cui, M., Yang, C., Wang, L., & Wang, A. (2016). Cathode material as an influencing factor on beer wastewater treatment and methane production in a novel integrated upflow microbial electrolysis cell (Upflow-MEC). International Journal of Hydrogen Energy, 41(4), 2189-2196.

Santoro, C., Arbizzani, C., Erable, B., & Ieropoulos, I. (2017). Microbial fuel cells: from fundamentals to applications. A review. Journal of power sources, 356, 225-244.

Santos, D. M., Sequeira, C. A., & Figueiredo, J. L. (2013). Hydrogen production by alkaline water electrolysis. Química Nova, 36, 1176-1193.

Santos, J. S., Fereidooni, M., Marquez, V., Arumugam, M., Tahir, M., Praserthdam, S., & Praserthdam, P. (2022). Single-step fabrication of highly stable amorphous TiO2

nanotubes arrays (am-TNTA) for stimulating gas-phase photoreduction of CO2 to methane. Chemosphere, 289, 133170.

Santos, T. C., Silva, M. A., Morgado, L., Dantas, J. M., & Salgueiro, C. A. (2015). Diving into the redox properties of Geobacter sulfurreducens cytochromes: a model for extracellular electron transfer. Dalton Transactions, 44(20), 9335-9344.

Sasaki, K., Hirano, S. I., Morita, M., Sasaki, D., Matsumoto, N., Ohmura, N., & Igarashi, Y. (2011). Bioelectrochemical system accelerates microbial growth and degradation of filter paper. Applied microbiology and biotechnology, 89(2), 449-455.

Satinover, S. J., Rodriguez, M., Campa, M. F., Hazen, T. C., & Borole, A. P. (2020). Performance and community structure dynamics of microbial electrolysis cells operated on multiple complex feedstocks. Biotechnology for biofuels, 13(1), 1-21.

Savla, N., Guin, M., Pandit, S., Malik, H., Khilari, S., Mathuriya, A. S., ... & Jung, S. P. (2022). Recent advancements in the cathodic catalyst for the hydrogen evolution reaction in microbial electrolytic cells. International Journal of Hydrogen Energy, 47(34), 15333-15356.

Savvas, S., Donnelly, J., Patterson, T., Dinsdale, R., & Esteves, S. R. (2017). Closed nutrient recycling via microbial catabolism in an eco-engineered self regenerating mixed anaerobic microbiome for hydrogenotrophic methanogenesis. Bioresource technology, 227, 93-101.

Schauer, N. L., & Ferry, J. G. (1982). Properties of formate dehydrogenase in Methanobacterium formicicum. Journal of bacteriology, 150(1), 1-7.

Schink, B. (1997). Energetics of syntrophic cooperation in methanogenic degradation. Microbiology and molecular biology reviews, 61(2), 262-280.

Segrè, A., & Falasconi, L. (2011). Il libro nero dello spreco in Italia: il cibo (Vol. 12). Edizioni Ambiente.

Seifert, A. H., Rittmann, S., & Herwig, C. (2014). Analysis of process related factors to increase volumetric productivity and quality of biomethane with Methanothermobacter marburgensis. Applied Energy, 132, 155-162.

Selembo, P. A. (2010). Microbial electrolysis cells: Hydrogen production from glycerol and alternative cathode materials.

Selembo, P. A., Merrill, M. D., & Logan, B. E. (2009). The use of stainless steel and nickel alloys as low-cost cathodes in microbial electrolysis cells. Journal of power sources, 190(2), 271-278.

Selembo, P. A., Merrill, M. D., & Logan, B. E. (2010). Hydrogen production with nickel powder cathode catalysts in microbial electrolysis cells. international journal of hydrogen energy, 35(2), 428-437.

Selembo, P. A., Perez, J. M., Lloyd, W. A., & Logan, B. E. (2009). High hydrogen production from glycerol or glucose by electrohydrogenesis using microbial electrolysis cells. international journal of hydrogen energy, 34(13), 5373-5381.

Sen, M., & Dastidar, M. G. (2010). Chromium removal using various biosorbents. Journal of Environmental Health Science & Engineering, 7(3), 182-190.

Shah, M. P. (Ed.). (2021). Biological Treatment of Industrial Wastewater (Vol. 5). Royal Society of Chemistry.

Shahsavari, S., Shokri, Z., & Bagheri, G. (2022). Food-Based Waste for Energy. In Energy from Waste (pp. 115-127). CRC Press.

Sharma, A., & Rawal, N. (2022). Ranking of Municipal Wastewater Treatment Alternatives Using Analytical Network Process Technique. In Environmental Degradation: Monitoring, Assessment and Treatment Technologies (pp. 15-32). Springer, Cham.

Sharma, A., Kuthiala, T., Thakur, K., Thatai, K. S., Singh, G., Kumar, P., & Arya, S. K. (2022). Kitchen waste: Sustainable bioconversion to value-added product and economic challenges. Biomass Conversion and Biorefinery, 1-22.

Sharma, S. K., Kalra, K. L., & Grewal, H. S. (2002). Enzymatic saccharification of pretreated sunflower stalks. Biomass and Bioenergy, 23(3), 237-243.

Shkil, H., Schulte, A., Guschin, D. A., & Schuhmann, W. (2011). Electron Transfer between Genetically Modified Hansenula polymorpha Yeast Cells and Electrode Surfaces via Os-complex modified Redox Polymers. ChemPhysChem, 12(4), 806-813.

Shlimon, A. G., Friedrich, M. W., Niemann, H., Ramsing, N. B., & Finster, K. (2004). Methanobacterium aarhusense sp. nov., a novel methanogen isolated from a marine sediment (Aarhus Bay, Denmark). International journal of systematic and evolutionary microbiology, 54(3), 759-763.

Siegert, M., Li, X. F., Yates, M. D., & Logan, B. E. (2015). The presence of hydrogenotrophic methanogens in the inoculum improves methane gas production in microbial electrolysis cells. Frontiers in microbiology, 5, 778.

Siegert, M., Yates, M. D., Call, D. F., Zhu, X., Spormann, A., & Logan, B. E. (2014). Comparison of nonprecious metal cathode materials for methane production by electromethanogenesis. ACS sustainable chemistry & engineering, 2(4), 910-917.

Siegert, M., Yates, M. D., Spormann, A. M., & Logan, B. E. (2015). Methanobacterium dominates biocathodic archaeal communities in methanogenic microbial electrolysis cells. ACS sustainable chemistry & engineering, 3(7), 1668-1676.

Simankova, M. V., Kotsyurbenko, O. R., Lueders, T., Nozhevnikova, A. N., Wagner, B., Conrad, R., & Friedrich, M. W. (2003). Isolation and characterization of new strains of methanogens from cold terrestrial habitats. Systematic and Applied Microbiology, 26(2), 312-318.

Singer, R. (1986). The Agaricales in Modern Taxonomy-4th Edifion.

Sleutels, T. H., Lodder, R., Hamelers, H. V., & Buisman, C. J. (2009). Improved performance of porous bio-anodes in microbial electrolysis cells by enhancing mass and charge transport. international journal of hydrogen energy, 34(24), 9655-9661.

Sleutels, T.H.J.A., et al., 2009b. Ion transport resistance in microbial electrolysis cells with anion and cation exchange membranes. Int. J. Hydrogen Energy 34 (9), 3612–3620.

Sly, L. I., Blackall, L. L., Kraat, P. C., Tian-Shen, T., & Sangkhobol, V. (1986). The use of second derivative plots for the determination of mol% guanine plus cytosine of DNA by the thermal denaturation method. Journal of microbiological methods, 5(3-4), 139-156.

Smith, P. H., & Hungate, R. E. (1958). Isolation and characterization of Methanobacterium ruminantium n. sp. Journal of Bacteriology, 75(6), 713-718.

Song, Y., Lee, Y. G., Lee, D. S., Nguyen, D. T., & Bae, H. J. (2022). Utilization of bamboo biomass as a biofuels feedstocks: Process optimization with yeast immobilization and the sequential fermentation of glucose and xylose. Fuel, 307, 121892.

Spiess, S., Conde, A. S., Kucera, J., Novak, D., Thallner, S., Kieberger, N., ... & Haberbauer, M. (2022). Bioelectrochemical methanation by utilization of steel mill off-gas in a two-chamber microbial electrolysis cell. Frontiers in Bioengineering and Biotechnology, 10.

Sravan, J. S., Butti, S. K., Sarkar, O., & Mohan, S. V. (2019). Electrofermentation: chemicals and fuels. In Microbial Electrochemical Technology (pp. 723-737). Elsevier.

Sravan, J. S., Tharak, A., & Mohan, S. V. (2021). Status of biogas production and biogas upgrading: A global scenario. In Emerging technologies and biological systems for biogas upgrading (pp. 3-26). Academic Press.

Srikanth, S., Pavani, T., Sarma, P. N., & Mohan, S. V. (2011). Synergistic interaction of biocatalyst with bio-anode as a function of electrode materials. International journal of hydrogen energy, 36(3), 2271-2280.

Steinbusch, K. J., Hamelers, H. V., Schaap, J. D., Kampman, C., & Buisman, C. J. (2010). Bioelectrochemical ethanol production through mediated acetate reduction by mixed cultures. Environmental science & technology, 44(1), 513-517.

Stoknes, K., Scholwin, F., Krzesiński, W., Wojciechowska, E., & Jasińska, A. (2016). Efficiency of a novel "Food to waste to food" system including anaerobic digestion of food waste and cultivation of vegetables on digestate in a bubble-insulated greenhouse. Waste management, 56, 466-476.

Strazzera, G., Battista, F., Garcia, N. H., Frison, N., & Bolzonella, D. (2018). Volatile fatty acids production from food wastes for biorefinery platforms: A review. Journal of Environmental Management, 226, 278-288.

Strik, D. P., Timmers, R. A., Helder, M., Steinbusch, K. J., Hamelers, H. V., & Buisman, C. J. (2011). Microbial solar cells: applying photosynthetic and electrochemically active organisms. Trends in biotechnology, 29(1), 41-49.

Stumm, W., & Morgan, J. J. (2012). Aquatic chemistry: chemical equilibria and rates in natural waters (Vol. 126). John Wiley & Sons.

Sugnaux, M., Happe, M., Cachelin, C. P., Gasperini, A., Blatter, M., & Fischer, F. (2017). Cathode deposits favor methane generation in microbial electrolysis cell. Chemical Engineering Journal, 324, 228-236.

Sun, J., Hu, Y. Y., Bi, Z., & Cao, Y. Q. (2009). Simultaneous decolorization of azo dye and bioelectricity generation using a microfiltration membrane air-cathode single-chamber microbial fuel cell. Bioresource Technology, 100(13), 3185-3192.

Sun, M., Sheng, G. P., Mu, Z. X., Liu, X. W., Chen, Y. Z., Wang, H. L., & Yu, H. Q. (2009). Manipulating the hydrogen production from acetate in a microbial electrolysis cell–microbial fuel cell-coupled system. Journal of Power Sources, 191(2), 338-343.

Sun, R., Zhou, A., Jia, J., Liang, Q., Liu, Q., Xing, D., & Ren, N. (2015). Characterization of methane production and microbial community shifts during waste activated sludge degradation in microbial electrolysis cells. Bioresource technology, 175, 68-74.

Sun, Y., Alimohammadi, F., Zhang, D., & Guo, G. (2017). Enabling colloidal synthesis of edge-oriented MoS2 with expanded interlayer spacing for enhanced HER catalysis. Nano letters, 17(3), 1963-1969.

Suzuki, K., Owen, R., Yui, A., Ando, S., Kudo, Y., Yasuike, K., ... & Futamata, H. (2019). Novel Energy Production: Conversion of Organic Compounds to Electricity by Microbial Extracellular Electron Transfer Mechanisms. In Green Science and Technology (pp. 1-13). CRC Press.

Syaichurrozi, I., Rusdi, R., Hidayat, T., & Bustomi, A. (2016). Kinetics studies impact of initial pH and addition of yeast Saccharomyces cerevisiae on biogas production from tofu wastewater in Indonesia. International Journal of Engineering, 29(8), 1037-1046.

Tabssum, F., & Ali, S. S. (2018). Screening of Pectinase Producing Gram Positive Bacteria: Isolation and Characterization. Punjab University Journal of Zoology, 33(1), 11-15.

Taiwo, A. M. (2011). Composting as A Sustainable Waste Management Technique in Developing. Journal of Environmental Science and Technology, 4(2), 93-102.

Tamura, K., Dudley, J., Nei, M., & Kumar, S. (2007). MEGA4: molecular evolutionary genetics analysis (MEGA) software version 4.0. Molecular biology and evolution, 24(8), 1596-1599.

Tandukar, M., Huber, S. J., Onodera, T., & Pavlostathis, S. G. (2009). Biological chromium (VI) reduction in the cathode of a microbial fuel cell. Environmental science & technology, 43(21), 8159-8165.

Tang, R. C. O., Jang, J. H., Lan, T. H., Wu, J. C., Yan, W. M., Sangeetha, T., & Ong, Z. C. (2020). Review on design factors of microbial fuel cells using Buckingham's Pi Theorem. Renewable and Sustainable Energy Reviews, 130, 109878.

Tang, X., Alavi, S., & Herald, T. J. (2008). Effects of plasticizers on the structure and properties of starch–clay nanocomposite films. Carbohydrate Polymers, 74(3), 552-558.

Tang, Y. Q., Koike, Y., Liu, K., An, M. Z., Morimura, S., Wu, X. L., & Kida, K. (2008). Ethanol production from kitchen waste using the flocculating yeast Saccharomyces cerevisiae strain KF-7. Biomass and Bioenergy, 32(11), 1037-1045.

Tanyildizi, M. S., Özer, D., & Elibol, M. (2005). Optimization of α-amylase production by Bacillus sp. using response surface methodology. Process biochemistry, 40(7), 2291-2296.

Tartakovsky, B., Manuel, M. F., Wang, H., & Guiot, S. R. (2009). High rate membrane-less microbial electrolysis cell for continuous hydrogen production. International Journal of Hydrogen Energy, 34(2), 672-677.

Tashyrev, O., Hovorukha, V., Havryliuk, O., Sioma, I., Gladka, G., Kalinichenko, O., ... & Ivanov, Y. (2022). Spatial Succession for Degradation of Solid Multicomponent Food Waste and Purification of Toxic Leachate with the Obtaining of Biohydrogen and Biomethane. Energies, 15(3), 911.

Tee, P. F., Abdullah, M. O., Tan, I. A., Amin, M. A., Nolasco-Hipolito, C., & Bujang, K. (2017). Effects of temperature on wastewater treatment in an affordable microbial

fuel cell-adsorption hybrid system. Journal of environmental chemical engineering, 5(1), 178-188.

Thiele, J. H., & Zeikus, J. G. (1988). Control of interspecies electron flow during anaerobic digestion: significance of formate transfer versus hydrogen transfer during syntrophic methanogenesis in flocs. Applied and environmental microbiology, 54(1), 20-29.

Timur, S., Haghighi, B., Tkac, J., Pazarlıoğlu, N., Telefoncu, A., & Gorton, L. (2007). Electrical wiring of Pseudomonas putida and Pseudomonas fluorescens with osmium redox polymers. Bioelectrochemistry, 71(1), 38-45.

Toledo-Alarcón, J., Capson-Tojo, G., Marone, A., Paillet, F., Júnior, A. D. N. F., Chatellard, L., ... & Trably, E. (2018). Basics of bio-hydrogen production by dark fermentation. In Bioreactors for microbial biomass and energy conversion (pp. 199-220). Springer, Singapore.

Tongco, J. V., Kim, S., Oh, B. R., Heo, S. Y., Lee, J., & Hwang, S. (2020). Enhancement of Hydrolysis and Biogas Production of Primary Sludge by Use of Mixtures of Protease and Lipase. Biotechnology and Bioprocess Engineering, 25(1), 132-140.

Torino, M. I., Taranto, M. P., Sesma, F., & De Valdez, G. F. (2001). Heterofermentative pattern and exopolysaccharide production by Lactobacillus helveticus ATCC 15807 in response to environmental pH. Journal of Applied Microbiology, 91(5), 846-852.

Torres, C. I., Kato Marcus, A., & Rittmann, B. E. (2007). Kinetics of consumption of fermentation products by anode-respiring bacteria. Applied microbiology and biotechnology, 77(3), 689-697.

Torres, C. I., Krajmalnik-Brown, R., Parameswaran, P., Marcus, A. K., Wanger, G., Gorby, Y. A., & Rittmann, B. E. (2009). Selecting anode-respiring bacteria based on anode potential: phylogenetic, electrochemical, and microscopic characterization. Environmental science & technology, 43(24), 9519-9524.

Tront, J. M., Fortner, J. D., Plötze, M., Hughes, J. B., & Puzrin, A. M. (2008). Microbial fuel cell biosensor for in situ assessment of microbial activity. Biosensors and Bioelectronics, 24(4), 586-590.

Ukonu, C. U. (2011). Optimization of biogas production using combinations of saw dust and cow dung in a batch anaerobic digestion bioreactor. Master's, University of Nigeria, Nsukka, Nigeria.

Van Eerten-Jansen, M. C., Heijne, A. T., Buisman, C. J., & Hamelers, H. V. (2012). Microbial electrolysis cells for production of methane from CO2: long-term performance and perspectives. International Journal of Energy Research, 36(6), 809-819.

Van Steendam, C., Smets, I., Skerlos, S., & Raskin, L. (2019). Improving anaerobic digestion via direct interspecies electron transfer requires development of suitable characterization methods. Current opinion in biotechnology, 57, 183-190.

Van Wyk, J. P. H., Mogale, M. A., & Moroka, K. S. (1999). Bioconversion of waste paper materials to sugars: An application illustrating the environmental benefit of enzymes. Biochemical Education, 27(4), 227-228.

Varanasi, J. L., Veerubhotla, R., Pandit, S., & Das, D. (2019). Biohydrogen production using microbial electrolysis cell: recent advances and future prospects. Microbial electrochemical technology, 843-869.

Vasiliadou, I. A., Kalogiannis, A., Spyridonidis, A., Katsaounis, A., & Stamatelatou, K. (2022). Effect of applied potential on the performance of an electroactive methanogenic biocathode used for bioelectrochemical CO2 reduction to CH4. Journal of Chemical Technology & Biotechnology, 97(3), 643-652.

Veiga, M. C., Jain, M. K., Wu, W., Hollingsworth, R. I., & Zeikus, J. G. (1997). Composition and role of extracellular polymers in methanogenic granules. Applied and Environmental Microbiology, 63(2), 403-407.

Veldhoen, A. B., Plugge, C. M., Stams, A. J. M., & Buisman, C. J. N. (2013). Microbial Community Analysis of a Methane-Producing Biocathode in a bioelectrochemical System. Archaea: an international microbiological journal.

Venkataraman, A., Rosenbaum, M., Arends, J. B., Halitschke, R., & Angenent, L. T. (2010). Quorum sensing regulates electric current generation of Pseudomonas aeruginosa PA14 in bioelectrochemical systems. Electrochemistry Communications, 12(3), 459-462.

Véras, I. C., Silva, F. A., Ferrão-Gonzales, A. D., & Moreau, V. H. (2011). One-step enzymatic production of fatty acid ethyl ester from high-acidity waste feedstocks in solvent-free media. Bioresource technology, 102(20), 9653-9658.

Vida, V., Kovács, T. Z., Nagy, A. S., Madai, H., & Bittner, B. (2022). Food waste in EU countries. Applied Studies in Agribusiness and Commerce, 16(2).

Villano, M., Monaco, G., Aulenta, F., & Majone, M. (2011). Electrochemically assisted methane production in a biofilm reactor. Journal of Power Sources, 196(22), 9467-9472.

Vladimirov, M. G., Ryzhkov, Y. F., Alekseev, V. A., Bogdanovskaya, V. A., Otroshchenko, V. A., & Kritsky, M. S. (2004). Electrochemical reduction of carbon dioxide on pyrite as a pathway for abiogenic formation of organic molecules. Origins of Life and Evolution of the Biosphere, 34(4), 347-360.

Vu, H. T., & Min, B. (2019). Integration of submersible microbial fuel cell in anaerobic digestion for enhanced production of methane and current at varying glucose levels. International Journal of Hydrogen Energy, 44(14), 7574-7582.

Wagner, R. C. (2012). Methane production and methanogenic communities in microbial electrolysis cells, anodic potential influence on microbial fuel cells, and a method to entrap microbes on an electrode. The Pennsylvania State University.

Wagner, R. C., Regan, J. M., Oh, S. E., Zuo, Y., & Logan, B. E. (2009). Hydrogen and methane production from swine wastewater using microbial electrolysis cells. water research, 43(5), 1480-1488.

Wainaina, S., Lukitawesa, Kumar Awasthi, M., & Taherzadeh, M. J. (2019). Bioengineering of anaerobic digestion for volatile fatty acids, hydrogen or methane production: A critical review. Bioengineered, 10(1), 437-458.

Walker, A. L., & Walker Jr, C. W. (2006). Biological fuel cell and an application as a reserve power source. Journal of Power Sources, 160(1), 123-129.

Wang, A., Liu, W., Cheng, S., Xing, D., Zhou, J., & Logan, B. E. (2009). Source of methane and methods to control its formation in single chamber microbial electrolysis cells. international journal of hydrogen energy, 34(9), 3653-3658.

Wang, A., Sun, D., Cao, G., Wang, H., Ren, N., Wu, W. M., & Logan, B. E. (2011). Integrated hydrogen production process from cellulose by combining dark fermentation, microbial fuel cells, and a microbial electrolysis cell. Bioresource Technology, 102(5), 4137-4143.

Wang, C., Wang, C., Liu, J., Han, Z., Xu, Q., Xu, X., & Zhu, L. (2020). Role of magnetite in methanogenic degradation of different substances. Bioresource Technology, 314, 123720.

Wang, L., Hao, J., Wang, C., Li, Y., & Yang, Q. (2022). Carbohydrate-to-protein ratio regulates hydrolysis and acidogenesis processes during volatile fatty acids production. Bioresource Technology, 355, 127266.

Wang, Q., & Han, L. (2022). Hydrogen production. In Handbook of Climate Change Mitigation and Adaptation (pp. 1855-1900). Cham: Springer International Publishing.

Wang, X., Cheng, S., Feng, Y., Merrill, M. D., Saito, T., & Logan, B. E. (2009). Use of carbon mesh anodes and the effect of different pretreatment methods on power production in microbial fuel cells. Environmental science & technology, 43(17), 6870-6874.

Wang, Y., & Liu, S. (2014). Kinetic modeling of ethanol batch fermentation by Escherichia coli FBWHR using hot-water sugar maple wood extract hydrolyzate as substrate. Energies, 7(12), 8411-8426.

Wang, Y., Zhang, J., & Zhang, L. (2022). An active and pH-responsive film developed by sodium carboxymethyl cellulose/polyvinyl alcohol doped with rose anthocyanin extracts. Food Chemistry, 373, 131367.

Wasserfallen, A., Nölling, J., Pfister, P., Reeve, J., & De Macario, E. C. (2000). Phylogenetic analysis of 18 thermophilic Methanobacterium isolates supports the proposals to create a new genus, Methanothermobacter gen. nov., and to reclassify several isolates in three species, Methanothermobacter thermautotrophicus comb. nov., Methanothermobacter wolfeii comb. nov., and Methanothermobacter marburgensis sp. nov. International Journal of Systematic and Evolutionary Microbiology, 50(1), 43-53.

Weber, R. S., & Ramasamy, K. K. (2020). Electrochemical oxidation of lignin and waste plastic. ACS omega, 5(43), 27735-27740.

Weiland, P. (2010). Biogas production: current state and perspectives. Applied microbiology and biotechnology, 85(4), 849-860.

Weld, R. J., Glithero, N., & Pasco, N. (2011). Escherichia coli knock-out mutants with altered electron transfer activity in the Micredox® assay and in microbial fuel cells. International Journal of Environmental and Analytical Chemistry, 91(2), 138-149.

Wellinger, A., Murphy, J. D., & Baxter, D. (Eds.). (2013). The biogas handbook: science, production and applications. Elsevier.

Wen, Z., Liao, W. (2005). Chen S. Production of cellulase by Trichoderma reesei from dairy manure. Bioresource Technology. 96, 491-499.

Wilkins, M. J., VerBerkmoes, N. C., Williams, K. H., Callister, S. J., Mouser, P. J., Elifantz, H., ... & Banfield, J. F. (2009). Proteogenomic monitoring of Geobacter physiology during stimulated uranium bioremediation. Applied and environmental microbiology, 75(20), 6591-6599.

Wolin, E. A., Wolin, M., & Wolfe, R. S. (1963). Formation of methane by bacterial extracts. Journal of Biological Chemistry, 238(8), 2882-2886.

Worakit, S., Boone, D. R., Mah, R. A., Abdel-Samie, M. E., & El-Halwagi, M. M. (1986). Methanobacterium alcaliphilum sp. nov., an H2-utilizing methanogen that grows at high pH values. International Journal of Systematic and Evolutionary Microbiology, 36(3), 380-382.

Wu, F., Yang, H., Bai, Y., & Wu, C. (2019). Paving the path toward reliable cathode materials for aluminum-ion batteries. Advanced Materials, 31(16), 1806510.

Wu, L., Wei, W., Song, L., Woźniak-Karczewska, M., Chrzanowski, Ł., & Ni, B. J. (2021). Upgrading biogas produced in anaerobic digestion: Biological removal and bioconversion of CO2 in biogas. Renewable and Sustainable Energy Reviews, 150, 111448.

Wu, W. M., Hickey, R. F., & Zeikus, J. G. (1991). Characterization of metabolic performance of methanogenic granules treating brewery wastewater: role of sulfate-reducing bacteria. Applied and Environmental Microbiology, 57(12), 3438-3449.

Wu, W. M., Jain, M. K., & Zeikus, J. G. (1996). Formation of fatty acid-degrading, anaerobic granules by defined species. Applied and Environmental Microbiology, 62(6), 2037-2044.

Wu, Y., Wang, S., Liang, D., & Li, N. (2020). Conductive materials in anaerobic digestion: From mechanism to application. Bioresource technology, 298, 122403.

Wünschiers, R., & Lindblad, P. (2002). Hydrogen in education—a biological approach. International journal of hydrogen energy, 27(11-12), 1131-1140.

Wyman, V., Henríquez, J., Palma, C., & Carvajal, A. (2018). Lignocellulosic waste valorisation strategy through enzyme and biogas production. Bioresource technology, 247, 402-411.

Xafenias, N., & Mapelli, V. (2014). Performance and bacterial enrichment of bioelectrochemical systems during methane and acetate production. international journal of hydrogen energy, 39(36), 21864-21875.

Xafenias, N., Anunobi, M. O., & Mapelli, V. (2015). Electrochemical startup increases 1, 3-propanediol titers in mixed-culture glycerol fermentations. Process Biochemistry, 50(10), 1499-1508.

Xia, T., Jiang, X., Deng, L., Yang, M., & Chen, X. (2021). Albumin-based dynamic double cross-linked hydrogel with self-healing property for antimicrobial application. Colloids and Surfaces B: Biointerfaces, 208, 112042.

Xia, X., Cao, X. X., Liang, P., Huang, X., Yang, S. P., & Zhao, G. G. (2010). Electricity generation from glucose by a Klebsiella sp. in microbial fuel cells. Applied microbiology and biotechnology, 87(1), 383-390.

Xiao, L., Liu, F., Lichtfouse, E., Zhang, P., Feng, D., & Li, F. (2020). Methane production by acetate dismutation stimulated by Shewanella oneidensis and carbon materials: An alternative to classical CO2 reduction. Chemical Engineering Journal, 389, 124469.

Xu, C. P., Kim, S. W., Hwang, Hi, Choi, J. W., Yun, J. W. (2003). Optimization of submerged culture conditions for mycelial growth and exo-biopolymer production by Paecilomyces tenuipes C240. Process Biochemistry 38, 1025-1030.

Xu, J., Bartholomew, C. H., Sudweeks, J., & Eggett, D. L. (2003). Design, synthesis, and catalytic properties of silica-supp

Xu, S. Y., Lam, H. P., Karthikeyan, O. P., & Wong, J. W. (2011). Optimization of food waste hydrolysis in leach bed coupled with methanogenic reactor: effect of pH and bulking agent. Bioresource technology, 102(4), 3702-3708.

Xu, S., Fu, B., Zhang, L., & Liu, H. (2015). Bioconversion of H2/CO2 by acetogen enriched cultures for acetate and ethanol production: the impact of pH. World Journal of Microbiology and Biotechnology, 31(6), 941-950.

Xu, X. J., Wang, W. Q., Chen, C., Xie, P., Liu, W. Z., Zhou, X., ... & Ren, N. Q. (2020). The effect of PBS on methane production in combined MEC-AD system fed with alkaline pretreated sewage sludge. Renewable Energy, 152, 229-236.

Yan, C., Liu, Y., Cui, X., Cao, L., Xiong, J., Zhang, Q., ... & Ruan, R. (2022). Improving the efficiency of anaerobic digestion: Domesticated paddy soil microbes enhance the hydrolytic acidification of rice straw and pig manure. Bioresource Technology, 345, 126570.

Yang, L., Huang, Y., Zhao, M., Huang, Z., Miao, H., Xu, Z., & Ruan, W. (2015). Enhancing biogas generation performance from food wastes by high-solids thermophilic anaerobic digestion: Effect of pH adjustment. International Biodeterioration & Biodegradation, 105, 153-159.

Yang, N., Hafez, H., & Nakhla, G. (2015). Impact of volatile fatty acids on microbial electrolysis cell performance. Bioresource technology, 193, 449-455.

Yang, S., Liu, Y., Wu, N., Zhang, Y., Svoronos, S., & Pullammanappallil, P. (2019). Low-cost, Arduino-based, portable device for measurement of methane composition in biogas. Renewable Energy, 138, 224-229.

Yang, Y., & McCarty, P. L. (1998). Competition for hydrogen within a chlorinated solvent dehalogenating anaerobic mixed culture. Environmental Science & Technology, 32(22), 3591-3597.

Yasri, N., Roberts, E. P., & Gunasekaran, S. (2019). The electrochemical perspective of bioelectrocatalytic activities in microbial electrolysis and microbial fuel cells. Energy Reports, 5, 1116-1136.

Ye, N. F., Lü, F., Shao, L. M., Godon, J. J., & He, P. J. (2007). Bacterial community dynamics and product distribution during pH-adjusted fermentation of vegetable wastes. Journal of Applied Microbiology, 103(4), 1055-1065.

Yee, M. O., Deutzmann, J., Spormann, A., & Rotaru, A. E. (2020). Cultivating electroactive microbes—from field to bench. Nanotechnology, 31(17), 174003.

Yin, Q., Zhu, X., Zhan, G., Bo, T., Yang, Y., Tao, Y.,& Yan, Z. (2016). Enhanced methane production in an anaerobic digestion and microbial electrolysis cell coupled system with co-cultivation of Geobacter and Methanosarcina. Journal of environmental sciences, 42, 210-214.

Yoshida, K., Nakamura, M., Kazue, Y., Tachikawa, N., Tsuzuki, S., Seki, S., & Watanabe, M. (2011). Oxidative-stability enhancement and charge transport mechanism in glyme–lithium salt equimolar complexes. Journal of the American Chemical Society, 133(33), 13121-13129.

Youn, J. H., & Shin, H. S. (2005). Comparative performance between temperaturephased and conventional mesophilic two-phased processes in terms of anaerobically produced bioenergy from food waste. Waste management & research, 23(1), 32-38.

Youngblut, N. D., Reischer, G. H., Dauser, S., Walzer, C., Stalder, G., Farnleitner, A. H., & Ley, R. E. (2020). Strong influence of vertebrate host phylogeny on gut archaeal diversity. BioRxiv.

Yuan, Y., Ahmed, J., Zhou, L., Zhao, B., & Kim, S. (2011). Carbon nanoparticles-assisted mediator-less microbial fuel cells using Proteus vulgaris. Biosensors and Bioelectronics, 27(1), 106-112.

Yusoff, M. S., Kamaruddin, M. A., Hanif, M. H. M., Norashiddin, F. A., Shadi, A. M. H., Wang, L. K., & Wang, M. H. S. (2022). Solid Waste Management in the Tourism Industry. In Solid Waste Engineering and Management (pp. 1-54). Springer, Cham.

Zabranska, J., & Pokorna, D. (2018). Bioconversion of carbon dioxide to methane using hydrogen and hydrogenotrophic methanogens. Biotechnology advances, 36(3), 707-720.

Zakaria, B. S., Guo, H., Kim, Y., & Dhar, B. R. (2022). Molecular biology and modeling analysis reveal functional roles of propionate to acetate ratios on microbial syntrophy and competition in electro-assisted anaerobic digestion. Water Research, 216, 118335.

Zealand, A. M., Roskilly, A. P., & Graham, D. W. (2017). Effect of feeding frequency and organic loading rate on biomethane production in the anaerobic digestion of rice straw. Applied Energy, 207, 156-165.

Zeng, F., Wu, Y., Bo, L., Zhang, L., Liu, W., & Zhu, Y. (2020). Coupling of electricity generation and denitrification in three-phase single-chamber MFCs in high-salt conditions. Bioelectrochemistry, 133, 107481.

Zeppilli, M., Cristiani, L., Dell'Armi, E., & Majone, M. (2020). Bioelectromethanogenesis reaction in a tubular Microbial Electrolysis Cell (MEC) for biogas upgrading. Renewable Energy, 158, 23-31.

Zeppilli, M., Villano, M., Aulenta, F., Lampis, S., Vallini, G., & Majone, M. (2015). Effect of the anode feeding composition on the performance of a continuous-flow methane-producing microbial electrolysis cell. Environmental Science and Pollution Research, 22(10), 7349-7360.

Zhang, C., Su, H., Baeyens, J., & Tan, T. (2014). Reviewing the anaerobic digestion of food waste for biogas production. Renewable and Sustainable Energy Reviews, 38, 383-392.

Zhang, C., Xiao, G., Peng, L., Su, H., & Tan, T. (2013). The anaerobic co-digestion of food waste and cattle manure. Bioresource technology, 129, 170-176.

Zhang, F., Zhang, W., Qian, D. K., Dai, K., van Loosdrecht, M. C., & Zeng, R. J. (2019). Synergetic alginate conversion by a microbial consortium of hydrolytic bacteria and methanogens. Water research, 163, 114892.

Zhang, G., Cui, Y., & Kucernak, A. (2022). Real-Time In Situ Monitoring of CO2 Electroreduction in the Liquid and Gas Phases by Coupled Mass Spectrometry and Localized Electrochemistry. ACS catalysis, 12, 6180-6190.

Zhang, H., Sun, Z., & Hu, Y. H. (2021). Steam reforming of methane: Current states of catalyst design and process upgrading. Renewable and Sustainable Energy Reviews, 149, 111330.

Zhang, J., Loh, K. C., Li, W., Lim, J. W., Dai, Y., & Tong, Y. W. (2017). Three-stage anaerobic digester for food waste. Applied energy, 194, 287-295.

Zhang, L., Zhou, S., Zhuang, L., Li, W., Zhang, J., Lu, N., & Deng, L. (2008). Microbial fuel cell based on Klebsiella pneumoniae biofilm. Electrochemistry communications, 10(10), 1641-1643.

Zhang, R., El-Mashad, H. M., Hartman, K., Wang, F., Liu, G., Choate, C., & Gamble, P. (2007). Characterization of food waste as feedstock for anaerobic digestion. Bioresource technology, 98(4), 929-935.

Zhang, T., Mao, C., Zhai, N., Wang, X., & Yang, G. (2015). Influence of initial pH on thermophilic anaerobic co-digestion of swine manure and maize stalk. Waste Management, 35, 119-126.

Zhang, Y. X., Tang, L. Z., Deng, Y. F., & Zhan, S. Z. (2016). Synthesis and electrocatalytic function for hydrogen generation of cobalt and nickel complexes supported by phenylenediamine ligand. Inorganic Chemistry Communications, 72, 100-104.

Zhang, Z., Lu, X., Niu, C., Cai, T., Wang, N., Han, Y., & Zhen, G. (2022). Clarifying catalytic behaviors and electron transfer routes of electroactive biofilm during bioelectroconversion of CO2 to CH4. Fuel, 310, 122450.

Zhang, Z., Song, Y., Zheng, S., Zhen, G., Lu, X., Kobayashi, T., & Bakonyi, P. (2019). Electro-conversion of carbon dioxide (CO2) to low-carbon methane by bioelectromethanogenesis process in microbial electrolysis cells: The current status and future perspective. Bioresource technology, 279, 339-349.

Zhao, D., Armutlulu, A., Chen, Q., & Xie, R. (2022). Enhanced ciprofloxacin degradation by electrochemical activation of persulfate using iron decorated carbon membrane cathode: promoting direct single electron transfer to produce 1O2. Chemical Engineering Journal, 437, 135264.

Zhao, H., Jones, C. L., Baker, G. A., Xia, S., Olubajo, O., & Person, V. N. (2009). Regenerating cellulose from ionic liquids for an accelerated enzymatic hydrolysis. Journal of biotechnology, 139(1), 47-54.

Zhao, J., Li, Y., & Dong, R. (2021). Recent progress towards in-situ biogas upgrading technologies. Science of The Total Environment, 800, 149667.

Zhao, K., Xue, P. J., & Gu, G. Y. (2008). Study on Determination of Reducing Sugar Content Using 3, 5-Dinitrosalicylic Acid Method [J]. Food Science, 8, 128.

Zhao, W., & Ci, S. (2019). Nanomaterials as electrode materials of microbial electrolysis cells for hydrogen generation. In Nanomaterials for the removal of pollutants and resource reutilization (pp. 213-242). Elsevier.

Zhao, Y., Boone, D. R., Mah, R. A., Boone, J. E., & Xun, L. (1989). Isolation and characterization of Methanocorpusculum labreanum sp. nov. from the LaBrea Tar Pits. International Journal of Systematic and Evolutionary Microbiology, 39(1), 10-13.

Zhen, G., Kobayashi, T., Lu, X., & Xu, K. (2015). Understanding methane bioelectrosynthesis from carbon dioxide in a two-chamber microbial electrolysis cells (MECs) containing a carbon biocathode. Bioresource technology, 186, 141-148.

Zhen, G., Lu, X., Kobayashi, T., Kumar, G., & Xu, K. (2016). Promoted electromethanosynthesis in a two-chamber microbial electrolysis cells (MECs) containing a hybrid biocathode covered with graphite felt (GF). Chemical Engineering Journal, 284, 1146-1155.

Zheng, Z., Jing, J., Yang, Z., Sang, J., Guo, L., Mi, W., & Peng, S. (2022). Stability evaluation and quantitative analysis of filmy cathode in solid oxide fuel cells under operating conditions. International Journal of Hydrogen Energy.

Zhi, Z., Pan, Y., Lu, X., Zhen, G., Zhao, Y., Zhu, X., & Zhao, T. (2019). Electrically regulating co-fermentation of sewage sludge and food waste towards promoting biomethane production and mass reduction. Bioresource technology, 279, 218-227.

Zhou, M., Wang, H., Hassett, D. J., & Gu, T. (2013). Recent advances in microbial fuel cells (MFCs) and microbial electrolysis cells (MECs) for wastewater treatment, bioenergy and bioproducts. Journal of Chemical Technology & Biotechnology, 88(4), 508-518.

Zhou, M., Yang, J., Wang, H., Jin, T., Xu, D., & Gu, T. (2013). Microbial fuel cells and microbial electrolysis cells for the production of bioelectricity and biomaterials. Environmental technology, 34(13-14), 1915-1928.

Zhu, D. Y., Lau, L., Liu, S. H., Wei, J. S., & Lu, Y. M. (2004). Activation of cAMP-response-element-binding protein (CREB) after focal cerebral ischemia stimulates neurogenesis in the adult dentate gyrus. Proceedings of the National Academy of Sciences, 101(25), 9453-9457.

Zinatizadeh, A. A. L., Mohamed, A. R., Abdullah, A. Z., Mashitah, M. D., Isa, M. H., & Najafpour, G. D. (2006). Process modeling and analysis of palm oil mill effluent treatment in an up-flow anaerobic sludge fixed film bioreactor using response surface methodology (RSM). Water Research, 40(17), 3193-3208.

List of Publications

Submission Journal Papers:

1. Rahman, T., Alam, M. Z., and **Deb, N.** (2023). Electrostatic Method based on High Contain of Biohydrogen Production System. **IIUM, Patern.** (accepted)
2. **Deb, N.,** Alam, M. Z., Rahman, T., Jami, M. S., Mansor, M. F. B., & Tajuddin, H. B. A. (2023). Isolation, Purification and Characterization of Electromethanoganic Microbes Strain for Carbon Conversion. **Nature Cell Biology**. (Submitted)
3. **Deb, N.,** Alam, M. Z., Rahman, T., Jami, M. S., & Tajuddin, H. B. A. (2023). Isolation and Characterization of Potential Hydrolytic Fungal Strain for Sugar Production from Food Waste. **Microbial Open**. (Submitted).
4. **Deb, N.,** Alam, M. Z., Rahman, T., Jami, M. S., & Tajuddin, H. B. A. (2023). Design, Materials and Operations of a Hybrid System Microbial Electrolysis Cells for Electromethanogenesis, **Energy Advance.** (Submitted).
5. **Deb, N.,** Alam, M. Z., Rahman, T., Jami, M. S., & Tajuddin, H. B. A. (2023). An Overview on Hybrid MEC with AD for High Content of Chemicals Production, Waste Remediation, Energy Valorization, Resource Recovery, and Beyond, Journal of Electrochemical Energy Conversion and Storage. (Submitted)
6. **Deb, N.,** Alam, M. Z., Rahman, T., Jami, M. S., and Mansor, M. F. (2023). "Anaerobic Biodigestion based Optimizing Potential Hydrolytic Enzyme for Bioenergy Production from Food Waste" Journal of King Saud University - Engineering Sciences. (Submitted)
7. **Deb, N.,** Alam, M. Z., Rahman, T., Jami, M. S., & Tajuddin, H. B. A. (2023). Enzymatic Hydrolysis for Methane Production from hydrolysate Food Waste. ICME2023. (Accepted)
8. **Deb, N.,** Alam, M. Z., Rahman, T., Al-Khatib, M. F. R., Jami, M. S., and Mansor, M. F. (2023). "A Single Reactor System for Simultaneous Pretreatment and Fermentation of POME For Bioethanol Production". Biofuel. (Submitted)
9. **Deb, N.,** Rahman, T., Alam, M. Z., and Motakabber, S. M. A. (2023). "Design and Analysis of Energy Management Systems for a Hybrid Power System of Electric Vehicle". Energy. (Submitted)
10. **Deb, N.,** M. Z. Alam, Ma An Fahmi Rashid Al-Khatib, and E. A. Ahmed. (2018). Statistical Optimization of A Single Bioreactor for Bioethanol Production From Palm Oil Mill Effluent Based On Acid-Base-Enzyme Pretreatment and Hydrolysis Processes by Using Saccharomyces Cerevisiae", Energy & Fuels. (Submitted)
11. Samihah, S., M. Z. Alam and **Deb. N** "Optimization of Operational Parameters of Composter For Food Waste Composting Process", Journal of Chemical Engineering Research Updates (JCEU). (Under rewview)

Published Papers

12. **Deb, N.,** Alam, M. Z., Rahman, T., Al-Khatib, M. A. F. R., Jami, M. S., & Mansor, M. F. B. (2023). Acid–Base Pretreatment and Enzymatic Hydrolysis of Palm Oil Mill Effluent in a Single Reactor System for Production of Fermentable Sugars. International Journal of Polymer Science, 2023.
13. **Deb, N.,** Alam, M. Z., Rahman, T., Jami, M. S., Mansor, M. F. B., & Tajuddin, H. B. A. (2023). Anaerobic Digestion for Biomethane Production from Food Waste Pretreated by Enzymatic Hydrolysis. Journal of Biotechnology Research, 9(1), 6-20.
14. **Deb, N.,** Alam, M. Z., Rahman, T., Jami, M. S., Bt Mansor, M. F., & Tajuddin, H. B. A. (2023). Design and Analysis of a Fuel Cell and Batteries in Energy Production for Electric Vehicle. Iranian (Iranica) Journal of Energy & Environment, 14(3), 301-313.
15. Rahman, T., Alam, M. Z., **Deb, N.,** & Kamal, R. (2022). Mathematical modeling of an oscillation criteria based on second order linear difference equations using fuel cell system for electric vehicle. Journal of Interdisciplinary Mathematics, 25(7), 2039-2051.
16. **Deb, N.,** Alam, M. Z., Al-khatib, M. F. R., & Elgharbawy, A. (2019). Development of Acid-Base-Enzyme Pretreatment and Hydrolysis of Palm Oil Mill Effluent for Bioethanol Production. Liquid Biofuel Production, 197-217.
17. Alam, M. Z., Elgharbawy, A. A., Riyadi, F., **Deb, N.,** & Islam, M. T. (2022). Domestic and Industrial Waste as Renewable Resources for Biofuel Production. Utilization of Waste for The Generation of Value-Added Products, 99.
18. Alam, M. Z., & Dev, N. (2020). Solid State Bioreactor for Food Waste Composting Process: Process Optimization. Journal of Energy and Environment. 12(2), 1-6.
19. **Deb, N,** M. Z. Alam, Ma An Fahmi Rashid Al-Khatib, and E. A. Ahmed. (2017). "Development of acid-base-enzyme pretreatment and hydrolysis of palm oil mill effluent for bioethanol production" Advances in Biofeedstocks and Biofuels; Volume 3: Liquid Biofuel Production, Wiley.

Awards& Recognition

20. 01 May 2019, Gold Medal: International Invention, Innovation & Technology Exhibition, (ITEX'19). MINDS - International level.

APPENDIX A

A.1 List of Some of the Chemical Used

Chemicals	Company
3,5 Dinitrosalicylic Acid	Sigma,USA
Acetylacetone	Merck, Germany
Yeast extract	FS chemical (Australia)
Glucose (Anhydrous)	Merck, Germany
Sucrose	Merck Germany
Malt extract	FS chemical (Australia)
Citric Acid Monohydrate	R&M Chemical, UK
COD HR Reagent (300-1500 mg/Ml)	HACH, USA
Total Nitrogen Persulfate Reagent Powder Pillow	HACH, USA
Ethanol 95%	Kollin, UK
Soluble starch	HmbG Chemical, Germany
Kaolin powder	R&M Chemical, UK
Poly aluminium chloride (PAC)	R&M Chemical, UK
Aluminium sulfate [$Al_2(SO_4)_3$]	R&M Chemical, UK
Hydrochloric Acid (HCl)	Merck Germany
$CuSO_4.5H_2O$	Merck Germany
Phenol	R&M Chemical, UK
Folin-Ciocalteu reagent	Sigma, USA
Ehrlich reagent	Merck Germany
Potassium Dichromate	The Science Company, USA
Potato Dextrose Agar (PDA)	OXOID Ltd, England
Sodium Hydroxide (NaOH), Na_2CO_3	R & M chemicals, UK
Calcium chloride ($CaCl_2$)	HmbG Chemicals
Magnesium chloride ($MgCl_2$)	ChemAR -SYSTERM

Iron (II) sulphate ($FeSO_4$)	HmbG Chemicals
Sodium Potassium Tartrate (Rochelle Salt)	FS chemicals (Australia)
Sodium Sulphite	R & M chemicals
Sulfuric Acid (H_2SO_4)	Fisher scientific, UK
Bovine serum albumin (BSA)	Merck, Germany
Glucosamine hydrochloride	Merck, Germany
Sodium acetate buffer	HmbG Chemicals
ABTS	Merck, Germany
TN Hydroxide Digestion Reagent vial	HACH, USA
Nessler reagent	HACH, USA
Hydrogen per oxide (H_2O_2)	Bendosen laboratory chemicals
Copper sulphate ($CuSO_4$,5 H_2O)	HmbG Chemicals

APPENDIX B

B.1 List of Some of the Equipment Used

Equipment Name	Model	Functions
Autoclave	Hirayama,HV-110,HVE-50	Sterilization process
-20°C freezer	MDF-U531 (SANYO)	Sample storage
Freeze dryer	2.5L-84°C Benchtop, Labconco	Drying after purified the sample
Automatic ice machine	AF100AS-E (Scotsman Frimount)	Rapid cooling process
Biological safety cabinet (Laminar air flow)	CFM 4 (ERLA)	Plate culturing, sub-culturing & inoculum preparation
Centrifuge machine	F-45-12-11 Eppendorf 5804	Separation process to obtain supernatant
Chiller (4°C)	LAW-CHAIN LDS102	Storage of fungal culture, inoculum, supernatant, buffer & other consumables
Dryer	FDD 720 (PROTECH)	Drying of glassware & other materials
Hot plate & magnetic stirrer	EMS-HP-7000 (ERLA)	Stirring for homogenous mixing
Incubator	Memmert	fungal culture incubation
Compound biological Microscope with Digital Camera	National DC5-163 Digital	Observe cell, spore and morphology of isolated strains at ×10, ×40 and ×100 magnification
Oven	Memmert	Drying of samples
pH meter	METTLER TOLEDO, PB-10 Sartorius	pH measurement
Rotary Shaker (Open Hood)	SK-71	Fungal entrapment treatment, myco-flocculant production and inoculum preparation
Rotary Shaker (Temperature Control)	Infrors HT Ecotron	Myco-flocculant stability
Vortex mixer	EVM-600 (ERLA)	Mixing of analytical solutions

Water bath	ISOTEMP 220, Fisher Scientific	Incubation during chemical analysis
Weighing Balance	B204-S METTLER TOLEDO	Chemical & sample measurements
Equipment Name	**Model**	**Functions**
Vacuum pump	DOA-P104-BN	Filter the sample
Double beam spectrophotometer	ANTHELIE Junior, Advance 5	Measuring absorbance of chemical analysis
Muffle furnace 500^{o}C	BIBBY Stuart	Analysis of Total volatile solids
HACH laboratory spectrophotometer	HACH DR/2400	Analysis of COD, Total nitrogen
HACH COD digester	DRB200	COD analysis
FTIR	FTIR-Spectrum 400	Functional groups analysis
Zetasizer Nano ZS	Nano ZS, Malvern Instruments Ltd., United Kingdom	Measurement of zeta potential
Particle size analyser	Mastersizer 1000, USA Malvern Instruments Ltd.,	Particles size analysis of treated and untreated kaolin & river water samples
Portable Turbidity meter	2100Q HACH,USA	Measurement of turbidity of kaolin suspension and river water samples
Flocculator/ Jar apparatus	SW6, UK	All flocculation test
CHNS/O Elemental analyzer	Perkin Elmer CHNS/O Elemental analyzer Series II	Elemental analysis of purified myco-flocculant
Field Scanning Electron Microscopy (FSEM)	JEOL JSM-6700F	Images analysis for purified sample, kaolin particles and flocculated kaolin samples
Cylindrical glass settling column	Bio lab technical services (001516378-K)	Investigation of settling characteristics of treated and raw kaolin suspension & river water

APPENDIX C

Identification services

1st Molecular Diagnostic Lab in Bangladesh

C.1 SDS-PAGE image

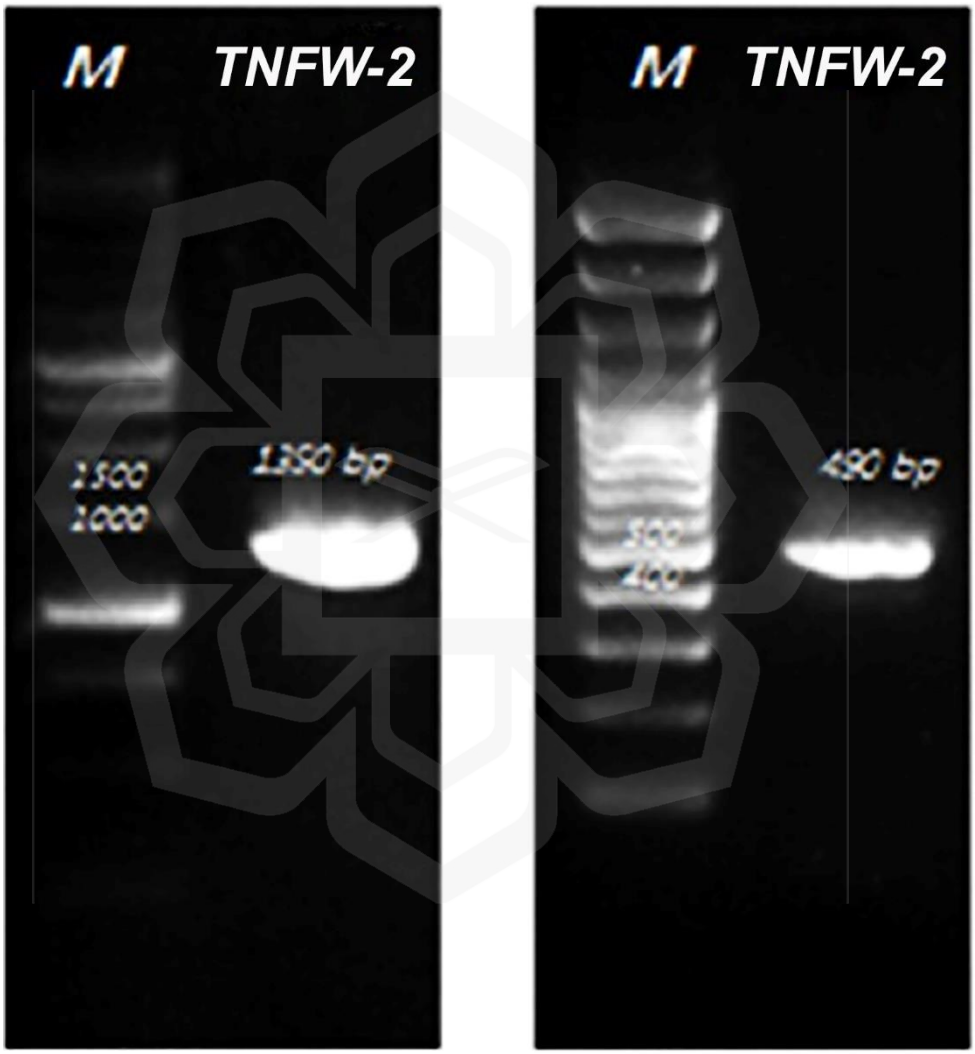

Fractionated DNA bands image of TNFW-2 by SDS-PAGE technique. Agarose gel electrophoresis of PCR products of strain TNFW-2 (A: 16S rRNA gene and B: mcrA gene

C.2 Nucleotide sequences (Base pairs) of TNFW-2

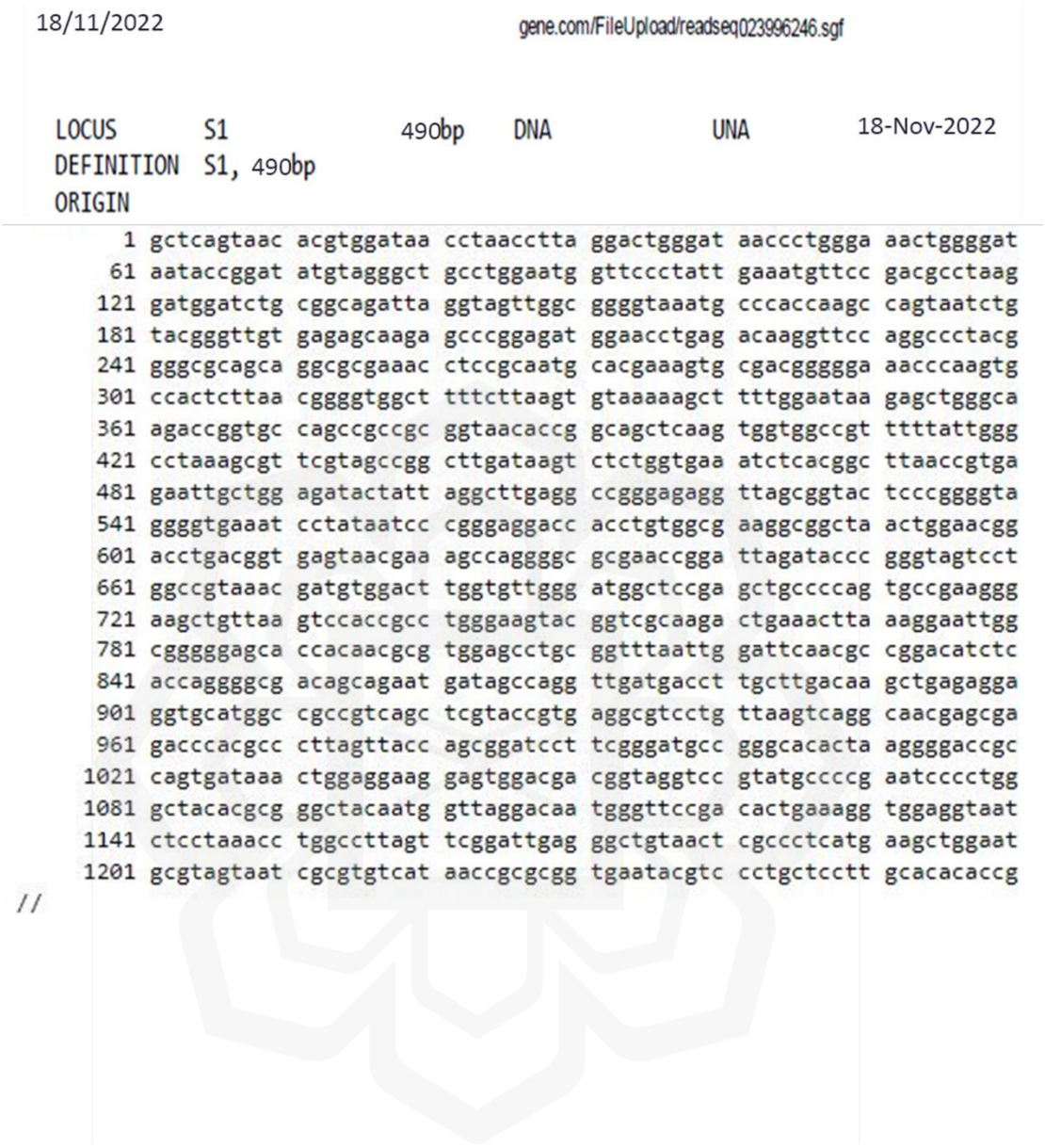

18/11/2022 gene.com/FileUpload/readseq023996246.sgf

LOCUS S1 490bp DNA UNA 18-Nov-2022
DEFINITION S1, 490bp
ORIGIN

```
      1 gctcagtaac acgtggataa cctaacctta ggactgggat aaccctggga aactggggat
     61 aataccggat atgtagggct gcctggaatg gttccctatt gaaatgttcc gacgcctaag
    121 gatggatctg cggcagatta ggtagttggc ggggtaaatg cccaccaagc cagtaatctg
    181 tacgggttgt gagagcaaga gcccggagat ggaacctgag acaaggttcc aggccctacg
    241 gggcgcagca ggcgcgaaac ctccgcaatg cacgaaagtg cgacgggggа aacccaagtg
    301 ccactcttaa cggggtggct tttcttaagt gtaaaaagct tttggaataa gagctgggca
    361 agaccggtgc cagccgccgc ggtaacaccg gcagctcaag tggtggccgt ttttattggg
    421 cctaaagcgt tcgtagccgg cttgataagt ctctggtgaa atctcacggc ttaaccgtga
    481 gaattgctgg agatactatt aggcttgagg ccgggagagg ttagcggtac tcccggggta
    541 ggggtgaaat cctataatcc cgggaggacc acctgtggcg aaggcggcta actggaacgg
    601 acctgacggt gagtaacgaa agccaggggc gcgaaccgga ttagataccc gggtagtcct
    661 ggccgtaaac gatgtggact tggtgttggg atggctccga gctgccccag tgccgaaggg
    721 aagctgttaa gtccaccgcc tgggaagtac ggtcgcaaga ctgaaactta aaggaattgg
    781 cgggggagca ccacaacgcg tggagcctgc ggtttaattg gattcaacgc cggacatctc
    841 accaggggcg acagcagaat gatagccagg ttgatgacct tgcttgacaa gctgagagga
    901 ggtgcatggc cgccgtcagc tcgtaccgtg aggcgtcctg ttaagtcagg caacgagcga
    961 gacccacgcc cttagttacc agcggatcct tcgggatgcc gggcacacta aggggaccgc
   1021 cagtgataaa ctggaggaag gagtggacga cggtaggtcc gtatgccccg aatcccctgg
   1081 gctacacgcg ggctacaatg gttaggacaa tgggttccga cactgaaagg tggaggtaat
   1141 ctcctaaacc tggccttagt tcggattgag ggctgtaact cgccctcatg aagctggaat
   1201 gcgtagtaat cgcgtgtcat aaccgcgcgg tgaatacgtc cctgctcctt gcacacaccg
//
```

APPENDIX D

D.1 DETERMINATION OF CHEMICAL OXYGEN DEMAND (COD)

Hach DR 2400 spectrophotometer was used to analyze the concentration of COD of the treated sample. The range for the spectrophotometer was 1500 mg/L hence every sample needs to be diluted before they can be analyzed. The high range COD vial was used in this analysis because the concentration of COD of POME was very high and need to be diluted. Hach DBR 200 COD digestion reactor was preheated to 150 ℃ before the vial can be placed in it. 2 mL of diluted sample was pipetted into the COD vial and it was called as prepared sample. Meanwhile, another vial was added with 2 mL of deionized water and act as blank. Both of the vials were cap tightly and rinse with deionized water and wipe with clean paper towel. Both vials were invert gently to mix, placed in the reactor and heated for 2 hours. Then, the vials were cooled to room temperature before the COD concentration can be read using Hach DR 2400 spectrophotometer.

D.2 Determination of Hemicellulose, Cellulose and Lignin

The serial fractionation of lignocellulosics was perpetrated according to Datta (1981) with small variations. 1g of the sample was suspended in 100 ml distilled water, preserved at 100°C for 2 hours in a water bath and filtered on a were crucible. Then, the residue was dried at 90°C till constant weigh and loss was considered as water soluble part. After that, 100 ml of 0.5 M H_2SO_4 was taken and dried residue was suspended with this, kept in a water bath at 100°C for 2 hours. The substances were filtered, dried and weighed as defined

as like as first step and weight loss was considered as hemicellulose content. For cellulose and lignin determinations, the above dried residue was added in 10 ml of 72% (v/v) H2SO4. After that, kept for 1 hour at 30°C on a rotary shaker at 200 rpm. The mixture was diluted up to 4% (v/v) of H2SO4 and autoclaved at 1.06 kg/cm2 for 40 min. The contents were filtered, dried and weighed. The weight loss was represented as cellulose, and the left-over residue was deliberated as lignin.

D.3 Moisture Content (MC) = $\frac{Wo - Wf}{Wo} \times 100$

Wo = Original Weight of cruscible and sample
Wf = Weight of cruscible and sample after oven dry at 105ºC for 24 hours.

APPENDIX E

The most common method for cellulase enzyme detection was the DNS (dinitrosalicylic acid) assay. It works as follows:

- Prepare a solution of the cellulase enzyme and substrate (e.g. cellulose or carboxymethylcellulose).
- Incubate the mixture at optimal temperature and pH for enzyme activity.
- Add DNS reagent and boil the mixture to convert reducing sugars produced by cellulase into 3,5-dinitrosalicylic acid.
- Cool the solution and measure the absorbance at 540 nm.
- Compare the absorbance of the test solution to a reference solution with known reducing sugar concentration to determine the cellulase activity.

Another commonly used method was the high-performance liquid chromatography (HPLC) assay, which separates and quantifies reducing sugars produced by cellulase by passing the reaction mixture through a column and measuring the peak areas of the sugars.

E.1 ESTIMATION OF REDUCING SUGAR

The estimation of reducing sugars was a common method to determine the number of sugars that can reduce a compound such as Fehling's solution or Tollens' reagent to a metal complex. The most common method for reducing sugar estimation was the DNS (dinitrosalicylic acid) assay, which works as follows:

- Prepare a solution of the sample (e.g. fruit juice, honey, or a hydrolysate from a polysaccharide) and add DNS reagent.
- Boil the mixture to convert reducing sugars into 3,5-dinitrosalicylic acid.
- Cool the solution and measure the absorbance at 540 nm.
- Compare the absorbance of the test solution to a standard solution with known reducing sugar concentration to determine the amount of reducing sugars in the sample.

Another commonly used method was the Lane-Eynon (LE) assay, which measures the reducing power of the sample by monitoring the production of a colored product (potassium ferricyanide). The absorbance of the colored product was proportional to the amount of reducing sugars present in the sample. To prepare a reducing sugar graph was follow these steps:

1. Choose a reducing sugar to study (e.g. glucose, fructose, lactose).
2. Prepare a sugar solution of known concentration.
3. Add a few drops of the sugar solution to a test tube and add an equal volume of Benedict's solution.
4. Heat the test tube gently until the solution turns orange, green, yellow, or brick red, which indicates the presence of reducing sugars.
5. Repeat steps 2 to 4 with different concentrations of sugar solution to obtain a series of results.
6. Plot the results on a graph with sugar concentration on the x-axis and the color change on the y-axis.

7. Interpret the graph to determine the relationship between the concentration of reducing sugars and the color change.

Note: Benedict's solution was a reagent used to test for the presence of reducing sugars.

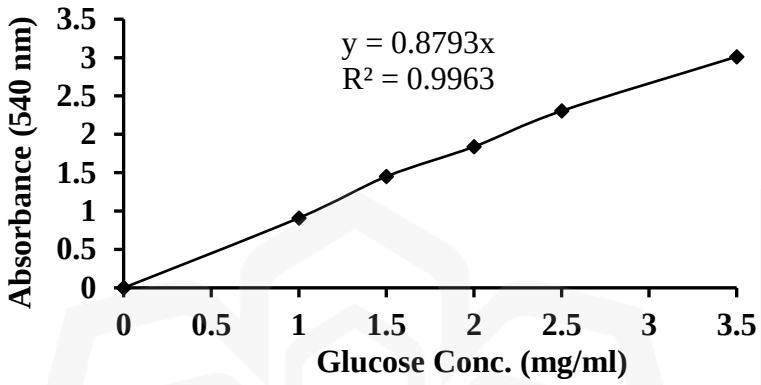

Calculations:

$$\textbf{Reducing sugar (mg/ml)}, \quad \boldsymbol{X} = \frac{\boldsymbol{absorbance\ (Y)}}{\mathbf{0.8793}}$$

E.2 DETERMINATION OF CELLULASE ENZYME ACTIVITY

To prepare a glucose standard curve was follow these steps:

1. Obtain a stock solution of glucose, with a known concentration (e.g. 10 mM).
2. Prepare a series of glucose solutions of different concentrations by diluting the stock solution with water.
3. Use a spectrophotometer to measure the absorbance of each glucose solution at a specific wavelength (e.g. 340 nm).
4. Plot the absorbance values on the y-axis and the glucose concentration on the x-axis to obtain a standard curve.
5. Draw a best-fit line through the data points.

6. Use the standard curve to determine the concentration of an unknown glucose solution by measuring its absorbance and finding the corresponding concentration on the curve.

Note: A spectrophotometer was a device used to measure the absorption of light by a sample, which can be used to determine the concentration of a substance in solution.

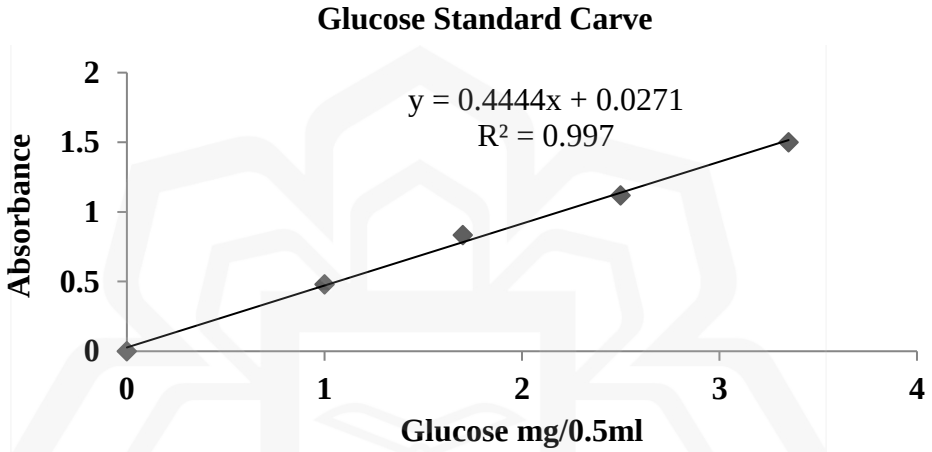

Calculation the dilution factor for 2 mg of glucose by drawing the following curve

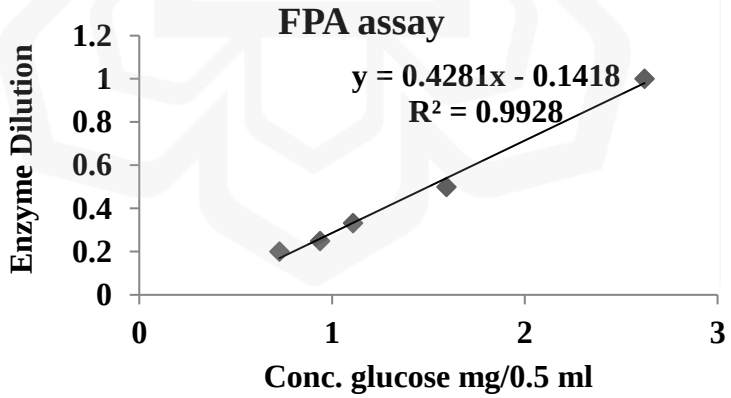

Calculations:

$$\text{Cellulase Acitivity } = \frac{0.37}{Enzymeconcentration\ to\ release\ 2.0\ mg\ glucose} \times \frac{units}{ml}$$

$$\text{Cellulase Acitivity } = \frac{0.37}{0.012} \times \frac{units}{ml}$$

= 61.97 FPU/ml

Calculation the dilution factor for 0.5 mg of glucose by drawing the following curve

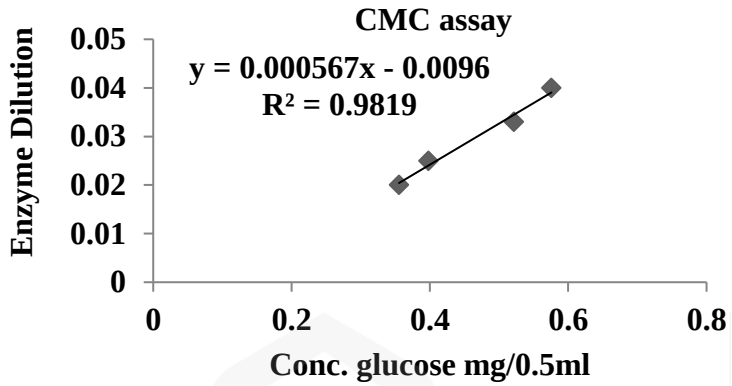

Calculations:

$$\text{Cellulase Acitivity} = \frac{0.185}{Enzymeconcentration\ to\ release\ 0.5\ mg\ glucose} \times \frac{units}{ml}$$

$$\text{Cellulase Acitivity} = \frac{0.185}{0.000567} \times \frac{units}{ml}$$

=326.27 U/ml (CMC assay)

APPENDIX F

Calculations of TS:

$$\text{TS (w/v)} = \frac{(W_2 - W_1) * 1000}{V} \times 1000$$

$$= \frac{1.85}{10} \times 1000$$

= 185 mg/ml

Calculations of VS:

$$\text{VS (w/v)} = \frac{(W_1 - W_2)}{W_1} \times 100$$

$$= \frac{1.362}{10} \times 100$$

= 13.62%

Calculations of Hemicellulose:

$$\text{Hemicellulose (\%)} = 1 - \frac{W_3 - W_2}{W_1} \times 100$$

$$= (1 - 0.98) \times 100$$

= 1.19 % w/w

Calculations of Cellulose:

$$\text{Cellulose (\%)} = 1 - \frac{W_3 - W_2}{W_1} \times 100$$

$$= (1 - \frac{2.472}{2.573}) \times 100$$

= 3.7 % w/w

Calculations of lignin:

$$\text{Lignin (\%)} = 100 - (W_1 + W_2 + W_3)$$

$$= 0.57 \text{ \% w/w}$$

Estimation of Soluble Protein

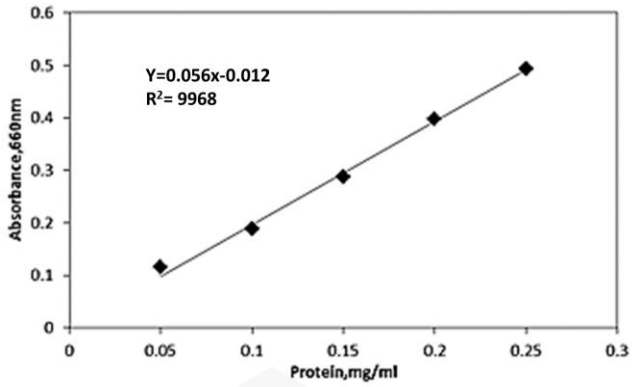

The equation from the standard curve was, y = 0.056x

Where y = absorbance, x = protein, mg

So, y = 0.056x

2.994 = 0.054x

x = $\frac{2.994}{.056}$ = 53.46429 mg/ml X 2 (dilution factor) = 106.9285714g/L =9.7%

D.3 Estimation of Total Carbohydrates

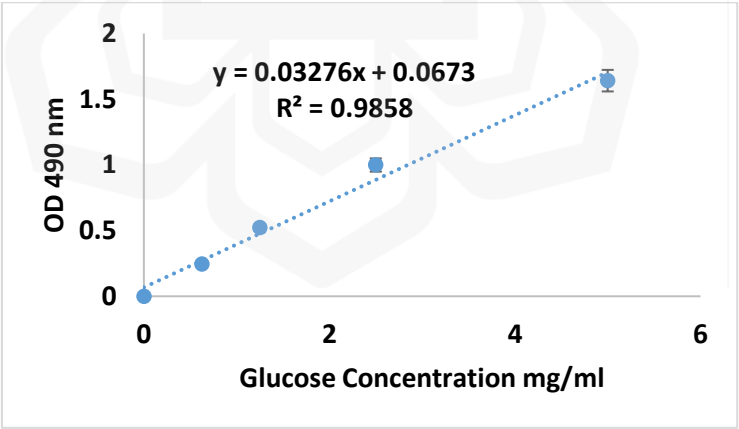

y = 5.4855x

2.223 = 0.03276x

x = $\frac{0.261}{0.03276}$ = 67.86 mg/ml X 5 (Dilution factor) = 339.29 mg/ml = 25.4%

APPENDIX G

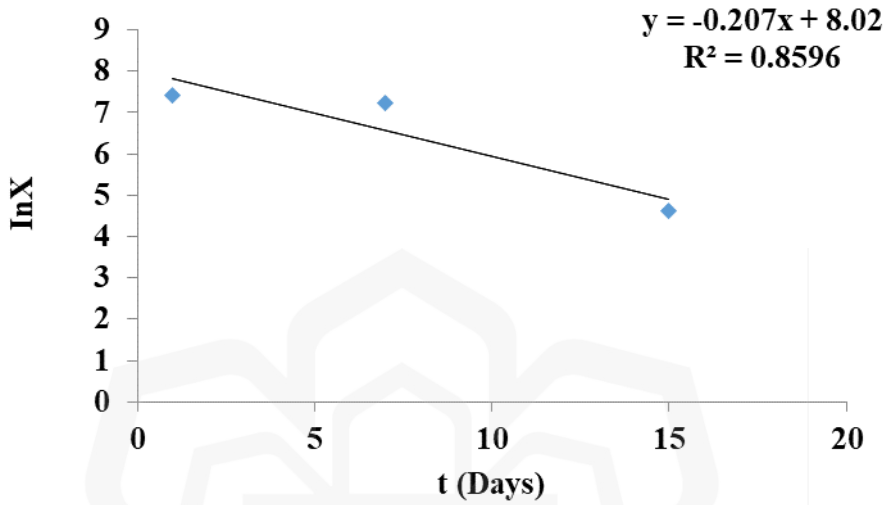

Kinetic models of the specific growth rate (μ)

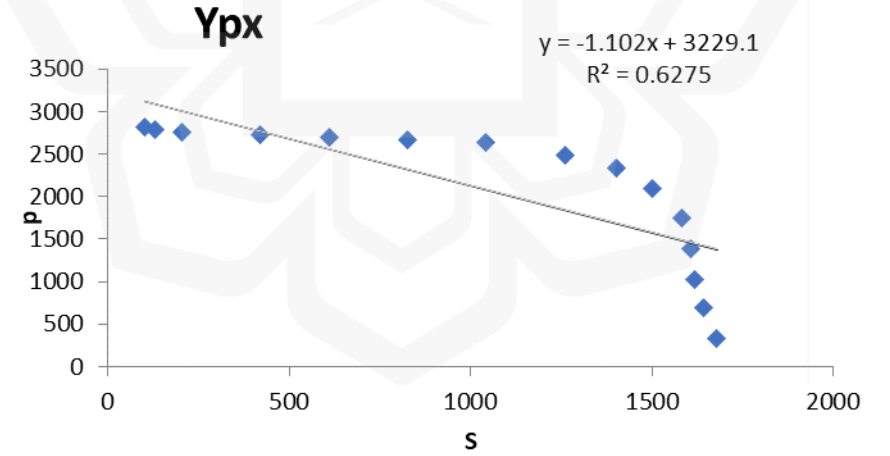

Kinetic models of the yield of product from biomass ($Y_{p/x}$)

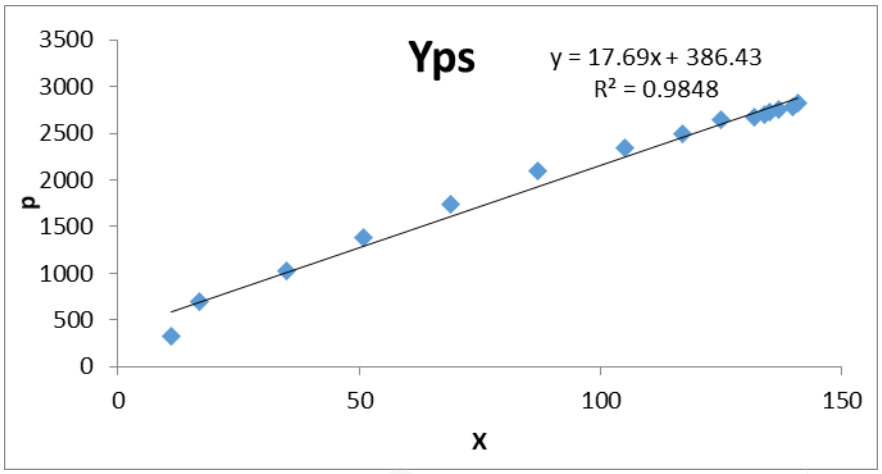

Kinetic models of the yield of bioethanol production based on total reducing sugar consumption ($Y_{p/s}$)

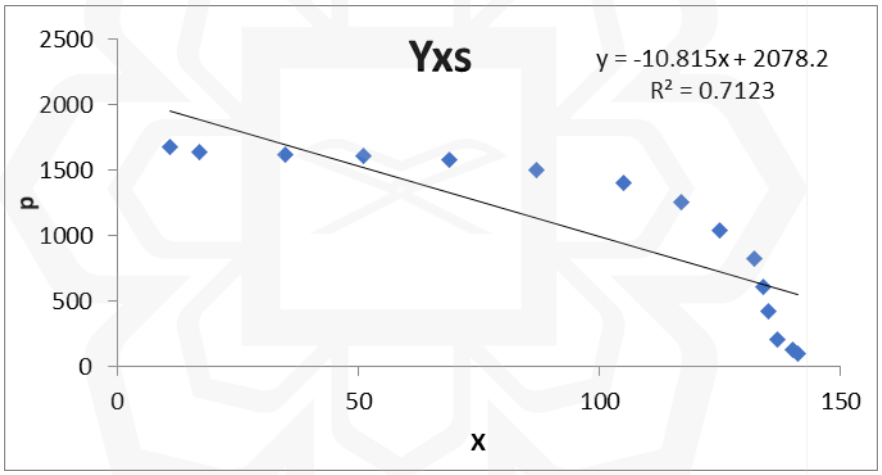

Kinetic models of the yield of biomass formation based on reducing sugar consumption ($Y_{x/s}$)

APPENDIX H

H.1 MQ8 Hydrogen Gas Sensor Matlab code

```
const int AOUTpin=0;
const int DOUTpin=8;
const int ledPin=13;
int limit;
int value;
void setup() {
Serial.begin(115200);
pinMode(DOUTpin, INPUT);
pinMode(ledPin, OUTPUT);
}
void loop()
{
value= analogRead(AOUTpin);
limit= digitalRead(DOUTpin);
Serial.print("Hydrogen value: ");
Serial.println(value);
Serial.print("Limit:");
Serial.print(limit);
delay(100);
if (limit == HIGH){
digitalWrite(ledPin, HIGH);
}
else{
digitalWrite(ledPin, LOW);
}
}
```

H.2 MQ135 CH4 Gas Sensor Matlab Code

```
/*
 * Interfacing MQ135 Gas Senor with Arduino
 * Author: Ashish
 * Website: www.circuitdigest.com
 * Date: 11-11-2020
```

```
 */
// The load resistance on the board
#define RLOAD 22.0
#include "MQ135.h"
#include <SPI.h>
#include <Adafruit_GFX.h>
#include <Adafruit_SSD1306.h>
#define SCREEN_WIDTH 128 // OLED display width, in pixels
#define SCREEN_HEIGHT 64 // OLED display height, in pixels
// Declaration for SSD1306 display connected using software SPI (default case):
#define OLED_MOSI   9
#define OLED_CLK   10
#define OLED_DC    11
#define OLED_CS    12
#define OLED_RESET 13
Adafruit_SSD1306 display(SCREEN_WIDTH, SCREEN_HEIGHT,
  OLED_MOSI, OLED_CLK, OLED_DC, OLED_RESET, OLED_CS);
MQ135 gasSensor = MQ135(A0);
int val;
int sensorPin = A0;
int sensorValue = 0;
void setup() {
  Serial.begin(9600);
  pinMode(sensorPin, INPUT);
  display.begin(SSD1306_SWITCHCAPVCC);
  display.clearDisplay();
  display.display();
}
```

```
void loop() {
  val = analogRead(A0);
  Serial.print ("raw = ");
  Serial.println (val);
 // float zero = gasSensor.getRZero();
 // Serial.print ("rzero: ");
  //Serial.println (zero);
  float ppm = gasSensor.getPPM();
  Serial.print ("ppm: ");
  Serial.println (ppm);
  display.setTextSize(2);
  display.setTextColor(WHITE);
  display.setCursor(18,43);
  display.println("CO2");
  display.setCursor(63,43);
  display.println("(PPM)");
  display.setTextSize(2);
  display.setCursor(28,5);
  display.println(ppm);
  display.display();
  display.clearDisplay();
  delay(2000);
}
```

H.4 MQ4 CO_2 Sensor - Analog Output Arduino

```
/* MQ4 Sensor - Analog Output Example
* Prints out methane concentration in PPM to serial monitor
* by R. Pelayo
*
```

```
* From TeachMeMicro (www.teachmemicro.com/arduino-mq4-methane-sensor
*
* Date Created: 09/11/2020
*/
const byte MQ4_Pin = A0; //MQ4 A0 pin
const int R_0 = 945; //Change this to your own R0 measurements

void setup() {
  Serial.begin(9600);
}

void loop() {
  Serial.println(getMethanePPM());
}

/*
* getMethanePPM returns a float value in PPM of methane concentration
*/
float getMethanePPM(){
  float a0 = analogRead(A0); // get raw reading from sensor
  float v_o = a0 * 5 / 1023; // convert reading to volts
  float R_S = (5-v_o) * 1000 / v_o; // apply formula for getting RS
  float PPM = pow(R_S/R_0,-2.95) * 1000; //apply formula for getting PPM
  return PPM; // return PPM value to calling function
}
```

APPENDIX I

I.1 Cellulase enzyme inoculum preparation

Cellulolytic enzyme inoculum can be prepared as follows:

- Grow a cellulolytic microorganism, such as Trichoderma reesei or Penicillium funiculosum, in a suitable medium that supports the growth and production of cellulolytic enzymes.
- Harvest the cells from the culture using centrifugation or filtration.
- Resuspend the cells in a buffer solution, such as citrate-phosphate buffer or sodium acetate buffer, at the desired concentration.
- Store the inoculum in a refrigerator at 4°C until ready to use.
- Before use, activate the inoculum by incubating it at a suitable temperature (e.g. 30-35°C) and pH (e.g. 5.0-5.5) for a period of time that allows for adequate enzyme production.

I.2 Liquid culture media for cellulase enzyme production

Culture media were produced from a mixture of sugarcane bagasse (C), wheat bran (W), and soybean bran (S), with the following dry mass (w:w) compositions: W(100); WCS(80:10:10) (80:10:10). To minimize microbial development, sugarcane bagasse in natura (Usina Iracema, Iracemápolis, So Paulo, Brazil) with 50% moisture on a wet basis was held at 20°C (Roussos et al., 1991). Following the addition of the spore suspension and a salt solution, the sugarcane bagasse was dried at 50 °C to 6% moisture in order to modify

the starting moisture of the crop to 60%. The granulometry of dried sugarcane bagasse was acquired by sifting and selecting the fraction maintained between 10 and 20 mesh to construct the culture medium. "Anaconda Industrial e Agrcola de Cereais" (So Paulo, Brazil) supplied wheat bran at 13% moisture on a wet basis, and "Coama Agroindustrial Cooperativa" (Paraná, Brazil) supplied soybean bran at 11% moisture. The two varieties of bran were maintained at room temperature because low moisture prevents microbial growth. They were dried after usage to enable for additional moisture adjustment with the addition of the spore suspension and a salt solution, to an initial value of 60 or 80% on a wet basis. Both bran kinds were sieved between 8 and 20 mesh.

I.3 Solid-state cultures for cellulase enzyme production

Solid-state cultures were formed in 500 mL Erlenmeyer flasks with 7 g of culture medium plus a salt solution and sterilized by autoclaving at 121°C for 20 minutes before inoculation with a sufficient amount of the spore suspension to achieve 107 spores/gdm. The initial moisture was adjusted using a salt solution (Urbánszki et al., 2000): 5 g/L KH_2PO_4; 5 g/L $(NH_4)_2SO_4$; 1 g/L $MgSO_4 \cdot 7H_2O$; 1 g/L NaCl; 5 mg/L $FeSO_4 \cdot 7H_2O$; 1.6 mg/L $MnSO_4$; 3.45 mg/L $ZnSO_4 \cdot 7H_2O$; and 2.0 mg/L $CoCl_2 \cdot 6H_2O$. The flasks were incubated for 120 hours at 30 °C (all fungi except *Myceliophthora thermophila* M77) or 45 °C (*Myceliophthora thermophila* M77). Except for cultures containing soybean bran, which were prepared in triplicate, all cultivations were done in duplicate, from the spore suspension to the cultures. From the first through the third day, and after five days of cultivation, samples were taken once a day.

I.4 Preparation of inoculum for amylase enzyme

The organism was grown in a 250 ml Erlenmeyer flask with 100 ml of Czapek-Dox broth containing 30 g/l sucrose, 3 sodium nitrate, 1 K_2HPO_4, 1 $MgSO_4$, 0.5 KCl, 0.5 $FeSO_4$, trace; agar, 15. The medium was inoculated with Czapek-Dox agar slants and incubated in a shaker (200 rpm) at 30 °C for 3 days before being used for fermentation.

I.4 Submerged fermentation (SmF)

Submerged fermentation was carried out in 250 ml Erlenmeyer flasks containing 100 ml of fermentation medium. The composition of the medium contained the following g/l of distilled water. L-Glutamic acid, 0.3; NH_4NO_2, 1.4; K_2HPO_4, 2.0; $CaCl_2$, 2.0; $MgSO_4$, 0.3; protease peptone, 7.5; $FeSO_4$, 5.0; $MnSO_4$, 1.6; $ZnSO_4$, 1.4; tween 80, 20 % (v/v); coir waste, 30. The medium was sterilized by autoclaving at 121°C for 15 min. Each flask was inoculated with 1ml of the above said inoculum. The cultures were incubated on a rotary shaker (120 rpm) at 30°C for 72 h.

I.5 Solid state fermentation (SSF)

Solid state fermentation was carried out in 250 ml Erlenmeyer flasks that contained 10 g of coir waste and 15 ml of distilled water (moistening agent). The flasks were sterilized at 121°C for 15 min and cooled to room temperature. About 1ml of inoculum was added, mixed well and incubated at 30°C in a humidified incubator for 96 h. The flasks were periodically mixed by gentle shaking.

I.6 Extraction and concentration of cellulase and amylase

The method described by Baig and Saleem (2012) was adopted for cellulase extraction with slight modification. Culturing of the *A. niger* was performed in 250-ml Erlenmeyer flasks containing 100 ml of medium. The medium composition (in gl^{-1}) used for growth and enzyme induction was determined and it composed of *A. hypogaea* shells, 1–5%; $(NH_4)_2SO_4$, 1.4; KH_2PO_4, 1; $MgSO_4 \cdot 7H_2O$, 0.6; $CaCl_2.2H_2O$, 0.4; $FeSO_4 \cdot 7H_2O$, 0.05; $MnSO_4.H_2O$, 0.1; $ZnSO_4.7H_2O$, 0.14; $CoCl_2.6H_2O$, 0.37 and protease peptone, 0.75. Inocula size was 105 spores' ml^{-1}. Flasks were shaken on an orbital shaker at 120 rpm for 7 days at 30 °C. The culture supernatant and pellet (mycelia mat) were separated by filtration. Supernatant was discarded and 1 g of pellet was re-suspended in 100 ml of 0.05M citrate buffer (pH 4.8) and homogenized with hand grinder and kept in an ice bath. This supernatant was taken as crude enzyme solution and concentrated to five-folds by citrate buffer. Optimum fermentation conditions of 120 h, pH of 4 ±2, temperature of 40 ±10°C, substrate concentration of 1–5%, inoculum size of 10–13 × 105 CFU/ml and in the presence of protease peptone as nitrogen source.

To produce cellulase enzyme:

- Isolate microorganisms with cellulase producing ability
- Grow the microorganisms in a suitable fermentation media
- Optimize conditions such as temperature, pH, and substrate concentration to enhance cellulase production
- Harvest and purify the enzyme using methods such as centrifugation, dialysis, and chromatography

To analyze cellulase:

- Determine the activity of the enzyme using a substrate such as carboxymethyl cellulose or filter paper
- Measure the rate of product formation and calculate the specific activity of the enzyme
- Characterize the enzyme using techniques such as SDS-PAGE, Western blotting, and mass spectrometry
- Determine the optimum pH and temperature for activity
- Study the effects of inhibitors and activators on enzyme activity.

APPENDIX J

J.1 Electromethanogenesis microorganism's detection

Methanogens were highly sensitive to oxygen and must be grown and isolated under strict anaerobic condition as well as in from before the media. The procedures for preparing medium and substrate solutions, as well as the culturing processes, were adapted from Hungate (1950), as modified by Balch et al (1979). Table 3.1 shows that the chemicals (per liter distilled water) were enrichment culture and separation, as reported by Zhao et al., (1989).

Table J.1: Basal medium culture composition

Culture Media (pH 7)			**Agar (pH 6.8)**		
Parameters	**Units**	**Values**	**Parameters**	**Units**	**Values**
Sodium formate	mM	50	Sodium formate	g	15
Trypticase peptone	g	2	Sodium acetate	g	1.5
yeast extract	g	2	Trypticase peptone	g	2
$NaHCO_3$	g	5	yeast extract	g	2
NH_4Cl	g	1	$NaHCO_3$	g	1
K_2HPO_4	g	0.4	NH_4Cl	g	1
KH_2PO_4	g	1	K_2HPO_4	g	0.4
$MgCl_{2.}\,6H_2O$	g	0.1	KH_2PO_4	g	0.2
L-cysteine hydrochloride	g	0.5	$MgCl_{2.}\,6H_2O$	g	0.1
$Na_2S.9H_2O$	g	0.2	NaCl	g	0.8
			L-cysteine hydrochloride	g	0.5
			$Na_2S.9H_2O$	g	0.2
			Agar	g	150

Liquid Medium (pH 7.2), the liquid medium was utilized for characterization of the isolate contained 1000mL of deionized water, 0.34 g of sodium acetate, 2 g of Trypticase peptone, 2 g of yeast extract, 0.4 g of K_2HPO_4, 2.5 g of NaCl, 3.8 g of $NaHCO_4$, 1 g of NH_4Cl, 0.1 g of $MgCl_2.6H_2O$, 0.1 g of $CaCl_2.2H_2O_4$, 0.5 g of L-cysteine hydrochloride, 0.25 g of $Na_2S.9H_2O_4$, 1 mg of resazurin and 10 ml of a trace mineral solution. The medium was supplemented with sterile, O_2-free stock solutions. Normally, they were autoclaved, but antibiotic solutions were made fresh in O_2-free water and sterilized by filtering (Zhao et al., 1989).